M-PM-F5

LYS480 AND LYS501 OF THE α-SUBUNIT OF NA,K-ATPASE HAVE DIFFERENT MICROENVIRONMENTS. ((Sylvia Daoud, Svetlana Lutsenko and **Jack H. Kaplan**)) Department of Biochemistry and Molecular Biology, OHSU, Portland, OR 97201.

Lys501 in the ATP-binding domain of the Na,K-ATPase was shown to have a unique reactivity towards FITC and other aromatic isothiocyanates and it was preferentially labeled when treated with these reagents. Chemical modification of Na,K-ATPase with a positively charged analog of FITC (TRITC) results in the labeling of the α-subunit of the Na pump, however, surprisingly, the target of modification in this case is exclusively Lys480. TRITC-labeled peptide was identified by N-terminal amino-acid sequencing of the fluorescently labeled fragment, obtained after cyanogen bromide cleavage of the α-subunit of Na-pump. Unlike modification with FITC, NIPI or SITS labeling of Na,K-ATPase with TRITC is ligand-independent. Experiments on double labeling of the Na,K-ATPase with FITC and TRITC showed that preincubation of Na-pump with FITC did not prevent incorporation of TRITC, suggesting that these two reagents do not share the same binding pocket and probably both Lys480 and Lys501 are exposed at the surface of the α-subunit. Our data also indicate that the microenvironments of Lys480 and Lys501 differ significantly inspite of the close location of these residues in the primary sequence of the α-subunit. Supported by NIH R01 HL30315 and R01 GM39500 to JHK.

M-PM-F6

KINETIC INVESTIGATIONS OF CONFORMATIONAL CHANGES OF THE NA^+, K^+-ATPASE. ((D.J. Kane, K. Fendler, E. Grell, E. Bamberg, K. Taniguchi, J.P. Froehlich and **R. J. Clarke**)) Max-Planck-Institute for Biophysics, Frankfurt am Main, Germany; Hokkaido University, Sapporo, Japan; NIA, NIH, Baltimore, MD 21204, USA.

Widely varying rate constants, between 25 and 200 s^{-1}, have been reported for the rate-determining step of the Na^+ translocation sequence of the Na^+, K^+-ATPase cycle under similar experimental conditions using different experimental methods and diffierent probes. In order to clarify this situation, we have investigated the kinetics of the Na^+-related partial reactions of the pig kidney enzyme via electrical bilayer measurements after the photochemical release of ATP and via fluorescence stopped-flow mixing using the probes RH 421 and BIPM. Results obtained from all of these methods were consistent with a rate constant of about 200 s^{-1} at pH 7.5 and 24°C. The fluoresence signals were pH-dependent, decreasing in rate from 200 s^{-1} at pH 7.5 to around 80 s^{-1} at pH 6.2. It was found that concentrations of the probe RH 421 in the micromolar range inhibit the Na^+-related partial reactions of the enzyme. Previously reported lower values of the rate constant can be attributed to 1) underestimation of the dissociation constant of ATP for its high affinity binding site, 2) neglect of the effects of caged ATP, and 3) the use of inhibiting concentrations of RH 421. The ATP concentration dependence of the observed rate constant yielded an ATP dissociation constant of 10 μM. All of the results are consistent with the assumption of two major enzyme conformations inherent in the Albers-Post model of the Na^+, K^+-ATPase mechanism.

M-PM-F7

EXPRESSION OF NA/K-ATPASE ALPHA SUBUNIT ISOFORMS DURING NEURONAL DIFFERENTIATION AND MATURATION. ((Y. Choi*, L.C. Williamson^, E.A. Neale^,, T.D. Copeland#, M. Takahashi@, **M.W. McEnery***)) *Dept. of Physiology and Biophysics, Case Western Reserve Univ. Sch. of Med., Cleveland, OH 44106, ^Lab. Dev. Neurobiol., NICHD, NIH, #ABL-Basic Research Program, NCI-Frederick Cancer Research and Development Center, Frederick, MD 21702, and @Mitsubishi-Kasei Institute, Tokyo, Japan.

A monoclonal antibody (mAb 9A7) identifies all three isoforms of Na/K-ATPase alpha subunit by western blotting, immunohistochemical localization and immunoaffinity purification. As mAb 9A7 reacts with an epitope conserved in all three isoforms, it is a valuable reagent to investigate and compare the relative level of expression of the alpha1, alpha2 and alpha3 isoforms in a given tissue. The primary focus of these experiments is the temporal pattern of expression of Na/K-ATPase alpha subunit isoforms in developing rat brain, differentiating human neuroblastoma cell lines (IMR32 cells), and primary spinal cord neurons obtained from embryonic mice. The results of these experiments using mAb 9A7 in conjunction with characterized antibodies specific for the three alpha subunit isoforms, indicate tissue-dependent differences in the alpha subunit isoforms expressed throughout *in vitro* differentiation. Specifically, while the alpha3 isoform is expressed in each of these neuronal tissues, the presence of a second alpha isoform appears to be a hallmark of particular tissue. These results are significant as they establish a framework to understand the normal expression pattern of Na/K-ATPase in primary spinal cord neurons in culture and permit us in future studies to determine if perturbations in Na/K-ATPase expression occurs in response to agents which inhibit or enhance the process of spinal cord maturation.

M-PM-F8

HYPOTONIC SWELLING ALTERS THE VOLTAGE-DEPENDENCE OF THE NA^+-K^+ PUMP IN CARDIAC MYOCYTES.((N.L.Bewick, H. H. Rasmussen and D. W. Whalley))Cardiology Department, Royal North Shore Hospital, St Leonards, NSW, Australia 2065. (Spon. by D. Whalley).

The cardiac Na^+-K^+ pump is stimulated by cell swelling during exposure to hypotonic solutions. Since cell swelling is known to alter the voltage-dependence of stretch-sensitive ion channels we examined the effect of hypotonicity on the voltage-dependence of the pump. Myocytes were voltage-clamped at -40 mV with patch-pipettes containing 10 mM Na^+. Swelling was induced by superfusion with hypotonic Tyrode's solution (240 mosM/L) containing 105 mM Na^+. Isotonic solutions (300 mosM/L) were identical to the hypotonic superfusates apart from the addition of 70 mM sucrose. We recorded steady-state currents elicited by test potentials (V_m) from -100 to + 60 mV. Na^+-K^+ pump current (I_p) was defined as the ouabain (100 μM) induced shift in holding current. I_p was recorded from myocytes superfused with isotonic solution (n=6,○) and hypotonic solution (n=6,● see fig). The data at each V_m is normalised relative to I_p recorded at V_m of 0 mV. The slope of the I_p-V_m relationship was significantly less steep for myocytes exposed to hypotonic solutions. Stimulation of the insulin receptor tyrosine kinase (TK) reduces the I_p-V_m relationship of the pump. We examined the effect of tyrphostin A25 (tyr A25, 100 μM), a specific inhibitor of TK. Tyr A25 eliminated the effect of hypotonicity on the slope of the I_p-V_m relationship. We conclude that the I_p-V_m relationship is regulated via a TK dependent mechanism in osmotically swollen cells.

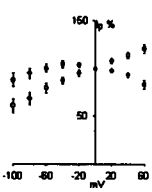

K CHANNELS: GATING

M-Pos1

CONTRIBUTIONS OF L1 AND L2 HEPTAD LEUCINES TO STABILIZATION OF THE OPEN STATE IN *SHAKER B* K^+ CHANNELS. ((**M. Hermosura**, M. Andres, J. Lu, J. Starkus and M. Rayner)) Bekesy Lab of Neurobiology, PBRC, University of Hawaii, Honolulu, HI.

Using thermodynamic analysis of a pseudo first-order deactivation-reactivation reaction, we have previously shown that mutations of the L1 heptad leucine in the S4 segment reduce open state stability in inactivation-removed *Shaker B* K+ channels (Andres et al.,1996 *Biophys.J.*, Abstr.; Rayner et al.,1996 *Biophys.J.*,Abstr).

We now extend this study to include effects at the L2 site and double mutations at both L1-L2 sites. Specifically, we have looked at effects of L to F and L to V substitutions at each site (ie., F1, V1, F2, and V2), plus that of the combined F1V2 double mutant. Observed ΔΔG shifts relative to wild-type were: **+1.3** for F1, **+2.0** for V1, **+1.8** for F2,**+2.3** for V2, and **+3.5** for F1V2. Since the observed F1V2 shift is not significantly different from the calculated total for F1 and V2 (**+3.6**) we conclude that hydrophobic interactions due to L1 and L2 act in a parallel and additive manner in stabilizing the open state. Moreover, effects from each site appear quantitatively similar as seen from ΔΔG shifts of **+2.0** for V1, **+2.3** for V2 and **+1.3** for F1 and **+1.8** for F2, suggesting similar interaction mechanisms at these sites.

Supported by NIH grant RO1 NS21151 and by awards from the American Heart Association (Hawaii Affiliate).

M-Pos2

ANOMALOUS CONDUCTION IN *SHAKER* B K^+ CHANNELS: CONDUCTION IN "NON-CONDUCTING" MUTANTS WITH MODIFIED S4 SEGMENTS. ((**M. Henteleff**, H. Bao, A. Hakeem, J. Starkus and M. Rayner)) Bekesy Lab. of Neurobiology, PBRC, Univ of Hawaii, Honolulu, HI.

In N-terminus deleted *Shaker* B channels, the W434F pore domain mutation typically prevents permeation by potassium ions. We describe here S4 mutations which modify the action of W434F, such that K^+ currents remain although channel gating becomes voltage-insensitive.

In a series of S4 mutants with multiple charge-neutralizations, we find voltage-sensitive gating with parameters similar to channels with unmodified S4 segments. In mutants from this series in which either charges 1 and 2 or charges 1, 4 and 7 were neutralized, addition of W434F resulted in maintained K^+ currents in which conductance is unaffected by changes in membrane potential between -160 and +100 mV. However, back mutation from glutamine to arginine at the 1st charge site restores both normal voltage-sensitive gating and the expected "non-conducting" behavior of the W434F mutation.

We conclude that the W434 residue normally interacts both with the permeation pathway and with charges towards the N-terminus end of the S4 segment. The W434 residue may thus be a significant component of the mechanism by which channels are "gated" into conducting or non-conducting states by S4 movement.

Supported by NIH grant RO1 NS21151 and by awards from the American Heart Association (Hawaii Affiliate).

M-Pos3

ANOMALOUS INACTIVATION OF A Kv1.3 MUTANT ((G.Panyi and C. Deutsch)). Dept of Physiology, University of Pennsylvania, Phila., PA 19104 and Dept of Biophysics, University Medical School of Debrecen, Debrecen, Hungary.

Kv1.3, the predominant K^+ channel in T lymphocytes, inactivates by a C-type mechanism. The binding of both extracellular tetraethylammonium (TEA) and extracellular K^+ slow inactivation. This effect of TEA has been attributed to the inability of TEA-blocked channels to inactivate. Histidine 399 (H399), located at the extracellular mouth of the channel, directly participates in binding extracellular TEA (Kavanaugh et al., 1991). This binding site is located 17.1± 0.02 % (n=7) into the membrane electric field. A H399Y mutation confers high sensitivity for TEA blockade. We have characterized these channels heterologously expressed in CTLL-2. TEA and tetrapropylammonium (TPrA) are fast blockers of H399Y. Inactivation is biphasic, accelerated by elevated extracellular $[K^+]$ and extracellular TEA and TPrA, in contrast to the operational definition of C-type inactivation. The binding site for TEA is 10.3±0.02 % (n=12) into the membrane electric field. The dose-dependence of channel blockade and of the inactivation time-constants occurred over the same concentration range for both TEA (K_i=0.22±0.02 mM, n=12) and TPrA (K_i=13.3±0.9 mM, n=6), indicating that the same binding site is involved in both channel block and modulation of inactivation. Our results are consistent with a physical model in which four subunits are brought into closer proximity by the coordination of the channel with an alkylammonium ion at a relatively superficial distance in the electric field. (Supp. GM 52302, and FO5 TWO 5079).

M-Pos4

K^+ CHANNEL INTER-SUBUNIT INTERACTIONS. ((**Z.F. Sheng**, W. Skach, V. Santarelli, and C. Deutsch)). Dept. of Physiology and Dept. of Molecular and Cellular Engineering, University of Pennsylvania; Dept. of Physiology, Jefferson Medical College, Philadelphia, PA 19104-6085.

Using an N-terminally deleted mutant (Kv1.3($T1^-$)), we have previously shown that sites in the central core of Kv1.3 may serve as intersubunit association sites (Tu et al., J. Biol. Chem. 271: 18904-18911, 1996). Moreover, there are suppression sites in the central core that interact with specific Kv1.3 peptide fragments to inhibit expressed Kv1.3 ($T1^-$) current, and these sites are promiscuous across voltage-gated K^+ channel subfamilies. To elucidate the mechanism whereby Kv1.3 peptide fragments suppress Kv1.3 ($T1^-$) current, we have studied the ability of peptide fragments containing the transmembrane segments S1, S1-S2, or S1-S2-S3 to associate with the Kv1.3 ($T1^-$) polypeptide subunit *in vitro*. Co-immunoprecipitation experiments were carried out using an antibody to the C-terminus of Kv1.3 as well as an anti-myc antibody directed at myc-labeled peptide fragments. From these experiments, as well as from carbonate extraction experiments, we conclude that 1) efficient association correlates with efficient integration of both proteins into the membrane, 2) association takes place mainly in a membrane compartment, 3) membrane-dependent association requires co-translation, and 4) association is necessary but not sufficient to cause suppression of expressed current. (Supp. GM 52302 and CA 01614).

M-Pos5

ION PERMEATION PREVENTS GATING CHARGE IMMOBILIZATION IN VOLTAGE-DEPENDENT hKv1.5 CHANNELS. ((**F.S.P. Chen** and D.Fedida)) Queen's University, Kingston, ON, Canada K7L 3N6

Gating currents of hKv1.5 channels have been measured using high levels of heterologous channel expression in human embryonic kidney cells (HEK-293). These currents were measured under whole-cell voltage clamp. The mean series resistance was 5.6 ± 0.4 MΩ (mean ± SEM, n=39) and cell capacitance was 19.9 ± 1.4 pF (n=39). Leak subtraction using a P/6 protocol was routinely employed. In order to record gating currents in the absence of ionic current, 140 mM N-methyl-D-glucamine (NMG) was used to replace all of the cations inside and outside the cell. In other experiments, we obtained a limited ion flux by the inclusion of 130 mM CsCl in the pipette filling solution and 5 mM CsCl in the bath. Off-gating currents were recorded at the reversal potential to prevent contamination by Cs tail currents. The off-gating currents in NMG were typical of those seen by others (Stefani et al. 1994. *Biophys. J.* 66:996-1010), with immobilization of off-gating charge occurring after more depolarized voltage prepulses. Immobilization consisted of a decrease in the peak off-gating current from a maximum at a prepulse of -10 mV to 40.8 ± 2.1% (n=5) of maximum at a prepulse of +60 mV. When held at a constant potential of +60 mV for increasing lengths of time, the off-gating currents showed a slowing in the return of charge. The time constant of decay of the off-gating current in NMG increased from 0.29 ± 0.02 ms (n=5) at 0.25 ms to 1.13 ± 0.07 ms (n=5) at 7.25 ms, whereas in Cs, it only increased from 0.30 ± 0.04 ms (n=4) at 0.15 ms to 0.57 ± 0.04 ms (n=4) at 7.05 ms. For longer pulses up to 458 ms, the off-gating charge (found by integrating the off-gating current for 20 ms) decreased to 27.6 ± 12.2% (n=8) of maximum in NMG and only 94.9 ± 5.1% (n=4) of maximum in Cs. For a non-conducting mutant in the presence of Cs, there was no ion flux and the gating currents were similar to those seen in NMG. We suggest that gating charge immobilization occurs when gating currents are measured without ion permeation through the channel.
(Supported by the Heart and Stroke Foundation of Ontario and MRC Canada)

M-Pos6

MUTATION OF A SINGLE AMINO ACID IN HUMAN BRAIN K^+ CHANNEL Kv1.4 ALTERS GATING AND INCREASES 4-AP SENSITIVITY BY TWO ORDERS OF MAGNITUDE. ((**S.I.V. Judge**, M.J. Monteiro and C.T. Bever)) Research and Neurology Services, VA Medical Center, Dept. of Neurology, Univ. of Maryland School of Medicine, and Medical Biotechnology Center of the Maryland Biotechnology Institute, Baltimore, MD 21201. (Spon. by J.Z. Yeh).

The Kv1.4 rapidly inactivating A type K^+ channel is known to be blocked by mM concentrations of 4-aminopyridine (4-AP). This laboratory isolated, from a human fetal brain library, a K^+ channel clone (clone 1a) that exhibits nearly complete sequence homology with human Kv1.4. To examine the role of codon 478 in 4-AP sensitivity, the single amino acid at this location was mutated from leucine to phenylalanine (L478F). The resulting channel, L478F, showed a dramatic increase in 4-AP sensitivity. Half block was seen at 790 ± 28.28 μM (n = 4) in the wild-type (wt) channels, and at 1.98 ± 0.23 μM (n = 2) in the mutated L478F channels, with complete block between 1-2 mM in wt and 5-10 μM in L478F. Both channels exhibited nearly identical rapid activation kinetics, with time-to-half-peak at +40 mV of 80.91 ± 2.21 ms (n = 22) in wt, and 80.83 ± 1.75 ms (n = 16) in L478F. These channels exhibited distinctly different rates of current inactivation, with a time constant of inactivation at +40 mV of 40.20 ± 23.25 ms (n = 16) in wt and 224.78 ± 149.76 ms (n = 15) in L478F. Current activated in wt channels around -40 mV (-41.11 ± 10.79 mV; n = 18), while approximately a 20 mV depolarizing shift was seen in L478F (-23.33 ± 7.79 mV; n = 12). Supported by grants from the VA, NMSS, and NIH.

M-Pos7

BARIUM BINDING TO THE C-TYPE INACTIVATED STATE IN *SHAKER* -IR K^+ CHANNELS. ((**C. Basso**[*] and R. Latorre[‡])) Dpto. de Biologia, Univ. de Chile and Centro de Estudios Cientificos de Santiago. Santiago, Chile.

Two types of inactivation are present in *Shaker* K^+ channels: N-type inactivation and C-type inactivation. The C-type inactivation involves amino acid residues in the pore region and in the S6 segment. In C-type inactivation there is a local rearrangement and a constriction of the channel at the outer mouth of the pore.

We have tested pore accessibility using Ba^{2+} as a probe in an attempt to define where the hindrance to the ion passage resides and what is the extend of the conformational change of the *Shaker*-IR K^+ pore during the C-type inactivation. The extend of Ba^{2+} binding in the C-inactivated state was tested by applying a test pulse of 0 mV from a holding voltage of -100 mV, right after repolarization. Extracellular Ba^{2+} is able to bind to K^+ channels in the C-inactivated state, by interacting with a site in the pore. The binding is 1:1 and it has an apparent dissociation constant at 0mV, K(0) = 3.97 mM. The Ba^{2+} site in the C-inactivated state do not sense the electrical field, unlike the Ba^{2+} site in the close state that senses a 25 % of the electrical field. These results were verified in a *Shaker*-IR D447E T449V mutant, that present a C-type inactivation more complete than the wild-type channel.

Our results indicated that the conformational rearrangement when channels move from close to the C inactivated state involves a movement, relative to the electrical field, of the pore region that conform the Ba^{2+} site.

Supported by Fundación Andes[*], FNI 2950008[*], FNI 1940227[‡] and Cátedra Presidencial[‡].

M-Pos8

GATING KINETICS OF THE RAT Kv2.1 POTASSIUM CHANNEL EXPRESSED IN *XENOPUS* OOCYTES. ((**Kathryn G. Klemic**[*], Char-Chang Shieh[‡], Glenn E. Kirsch[*‡], and Stephen W. Jones[*])) [*]Department of Physiology and Biophysics, and [‡]Rammelkamp Center for Research, Case Western Reserve University, Cleveland, OH 44106.

Kv2.1 channels have been the subject of extensive mutational analysis, but their gating kinetics have not been thoroughly described at the macroscopic level. We recorded outward ionic currents from cell-attached patches on *Xenopus* oocytes, and gating currents from inside-out patches, using only impermeant ions in the pipet solution. Charge movement occured at more negative voltages than channel opening (Q-V, $V_{½}$=-20 mV, z=1.6e_0; G-V, $V_{½}$=7.3 mV, z=2.3e_0; the G-V was better fit by the sum of 2 Boltzmanns). The time course of activation was sigmoidal, approximated by an exponential raised to a power of <3. Deactivation changed e-fold for 44 mV, with τ ~4 ms at -90 mV. Following the initial delay, activation was nearly independent of voltage above +60 mV (τ ~11 ms), and was much slower than the ON gating current (τ ~2 ms at +50 mV). The τ for OFF gating current at -90 mV was comparable to the ionic current, or slightly slower following steps to voltages where most channels opened. Currents decayed little during ~100 ms depolarizations, but steps to intermediate voltages reduced the current evoked by subsequent depolarization, suggestive of inactivation from 'partially activated' closed states. Differences from *Shaker* (Kv1) include slower kinetics, less sigmoidal activation, and less steep G-V and Q-V curves.

M-Pos9

SHAKER B K CHANNELS FALL INTO A REMARKABLY STABLE NONCONDUCTING (POSSIBLY CLOSED) STATE AFTER ACTIVATION IN ZERO K^+ SOLUTIONS ((F. Gómez-Lagunas)). Instituto de Biotecnologia: UNAM. Cuernavaca, Mor. México. (Spon. by M. Hiriart).

Shaker B K^+ channels expressed in Sf9 cells where studied under whole-cell patch clamp with, zero K^+, Na^+ or NMG-containing solutions at both sides of the membrane.

In the absence of K^+ ions, the K^+ conductance collapses when the channels go through repeated gating cycles. The drop of the conductance is not reverted just by adding K^+ to the external solution. Moreover, at -80 mV or hyperpolarized potential the conductance never recovers. The drop of the conductance is prevented if the channels are kept closed while they are in zero K^+.

The collapse of the conductance depends on the number of depolarizing pulses delivered in zero K^+, but not on the frequency of pulsing (1 to 0.002 Hz).

TEA, K^+, Rb^+, Cs^+ and NH_4^+ impede the drop of the conductance, by binding to a site probably located toward the extracellular side of the pore.

The collapse of the conductance is also prevented by depolarized holding potentials.

The K^+ conductance recovers completely after long lasting (seconds to minutes) depolarizations.

This work was supported by DGPA IN-206994.

M-Pos10

SIMULTANEOUS NEUTRALIZATION OF FOUR VOLTAGE SENSING RESIDUES IN SHAKER K^+ CHANNELS REDUCES THE APPARENT GATING CHARGE PER CHANNEL BY ABOUT 80 %. ((S. -A. Seoh, D. M. Papazian, and F. Bezanilla)) Dep. of Physiology, UCLA School of Medicine, Los Angeles, CA 90095

In Shaker K^+ channels, single neutralization mutations at positions E293 in S2 and R365, R368, and R371 in S4 reduce the gating charge per channel from 13 e_0 to 6~8 e_0 (Seoh et al., 1996, *Neuron* 16:1159-1167). We have now neutralized two, three, or four charges simultaneously and estimated the remaining charge per channel (z, in units of e_0) using limiting slope procedures. The ionic currents induced by slow voltage ramps or steady state ionic currents were obtained with cut-open oocyte voltage clamp or macropatch techniques at very negative membrane potentials to estimate limiting slopes at low P_o. The constructs with combined neutralization mutations were E293Q+R368N, R368N+R371Q, E293Q+R368N+R371Q, R365Q+R368N+R371Q (or R365Q+R368N+R371Q with T449Y to remove part of the prominent resting slow inactivation), and E293Q+R365Q+R368N+R371Q all in the ShB-IR background. Each construct produced voltage-dependent potassium currents. The z value in all these mutant channels was 5~6 e_0 except for E293Q+R365Q+R368N+R371Q channel in which the z value was only 2~3 e_0. The data indicate that only the simultaneous neutralization of *all four* residues E293 in S2 and R365, R368, and R371 in S4 removes ~80 % of the nonlinear gating charge movements while double or triple mutant combinations remove only 50~60 %. The leftover charge in the quadruple-mutant channel could come from one or more of the remaining charged residues in transmembrane segments. Possible candidates include D310 and D316 in S3, and R377 in S4. It is interesting to note that the single neutralization at D316 reduced the charge per channel by ~2 e_0 (Seoh et al., 1996). The value of z represents the product of the charge times the fraction of the field traversed. Therefore these results indicate that charged residues contribute to the voltage sensor either as moving charges or by shaping the electric field where other gating charges move, or both. Supported by NIH grants GM30376 and GM43459.

M-Pos11

THE NOVEL ROLE OF THE N-TERMINUS IN CONTROLLING THE VOLTAGE-DEPENDENT GATING BEHAVIOR OF THE POTASSIUM CHANNEL KAT1. ((**I. Marten** and T. Hoshi)) Dept. of Physiology and Biophysics, The University of Iowa, Iowa City, IA 52242.

The transmembrane core segments, in particular the S4 domain, are thought to primarily determine the voltage-dependent gating of potassium channels. However, we found that the gating of the voltage-dependent potassium channel KAT1 also depends on the putative cytoplasmic N- and C-terminal channel regions. While the C-terminus is important for voltage sensing (gating charge movement), the N-terminus mainly affects the apparent threshold voltage of activation. To study the potential interaction of the N-terminus with the putative voltage sensing S4 domain in channel gating, we introduced mutations in the S4 domain and/or the N-terminus of KAT1. The removal of a positively charged residue in the S4 domain altered the voltage dependence of KAT1: In the R176S channel, the gating charge movement was reduced and the half activation voltage ($V_{1/2}$) shifted to a more positive voltage. In contrast, the N-terminal deletion Δ20-34 did not markedly affect the gating charge movement but caused a faster deactivation of KAT1 resulting in a more negative half-activation voltage. As expected from the opposite effect of the R176S and the Δ20-34 mutation on $V_{1/2}$, the half activation voltage was totally restored in the double mutant channel R176S:Δ20-34. However, the number of gating charges required for the steady state activation was also partially restored by the double mutation. Our results suggest an interaction between the N-terminus and the S4 domain of KAT1 enabling the control of the voltage-sensing gating process by the N-terminal domain. (Supported by HFSP, NIH)

M-Pos12

EXTERNAL POTASSIUM AND RUBIDIUM SLOW DOWN THE 'OFF' GATING CHARGE MOVEMENT OF NON-CONDUCTING SHAKER K^+ CHANNEL.

((Andrey Loboda & Clay M. Armstrong)) University of Pennsylvania, Neuroscience Program and Department of Physiology, PA 19104.

It is known that K^+ channels close more slowly in the presence of external K^+ and Rb^+ (Swenson and Armstrong, 1981). We studied the action of these ions on gating charge movement in the non-conducting W434F mutant of Shaker K^+ channel. It was found that concentrations as low as 30 mM K^+ and 10 mM Rb^+ in an external solution containing predominantly Na^+ and 2-10 mM Ca^{2+} can markedly decrease the rate of gating charge return following depolarizing pulses more positive than -40 mV. The kinetics and amplitude of 'ON' gating currents and 'OFF' gating currents after smaller depolarizations are not modified by extracellular Rb^+ and K^+. It was also found that extracellular Ba^{2+} is very potent in counteracting these effects of K^+ and Rb^+ (see Hurst et al., Biophysical Society Abstracts, 1996), whereas extracellular calcium is not effective in concentrations up to 15mM.

Apparently even in a non-conducting mutant K^+ and Rb^+ can occupy a site in the external end of the channel and thus modify gating behavior after depolarizations that are large enough to open the channels.

M-Pos13

PARAMETER OPTIMIZATION OF GATING MODELS FOR *SHAKER* K^+ CHANNELS BASED ON NON-IDEAL VOLTAGE-CLAMP DATA.

((**Rüdiger Steffan**, Christian Hennesthal, and Stefan H. Heinemann)) Max-Planck-Gesellschaft, AG Molekulare & zelluläre Biophysik, Drackendorfer Straße 1, D-07747 Jena, Germany.

Gating currents of voltage dependent ion channels provide valuable information for the development of kinetic models for ion channel function. In particular for the recording of gating currents, possible limitations of the voltage clamp, such as the true voltage profile and distributed low-pass filters, have to be considered carefully. During the recording of gating currents from *Shaker* K^+ channels additional problems may arise due to over-compensation of gating currents acquired during the collection of reference leak currents (Heinemann et al., 1992, Meth. Enzym., 207: 353). Procedures which automatically account for such limitations were implemented into software for the optimization of parameter sets describing kinetic gating models. The methods were applied to two-electrode voltage-clamp recordings from *Xenopus* oocytes which were injected with mRNA coding for *Shaker* Δ2-30 W434F•T449R. Due to limited clamp speed and endogenous current components at extreme potentials, which limited the voltage range suited for the collection of P/n leak sweeps, consideration of the non-ideal nature of the data was particularly important. As an initial example, the parameters of the TR-model for *Shaker* gating (McCormack et al., 1994, Neuron, 12: 301) were optimized for data sets obtained at pH 7.2 and pH 5.0, in the absence and presence of 4-aminopyridin.

M-Pos14

PHOSPHORYLATION OF KV2.1 K^+ CHANNELS ALTERS VOLTAGE-DEPENDENCE OF ACTIVATION. (**H. Murakoshi**, G. Shi and J. S. Trimmer) Department of Biochemistry and Cell Biology, SUNY at Stony Brook, Stony Brook, NY 11794-5215.

Among all voltage-dependent K+ channels, Kv2.1 (853 amino acids) has the longest (440 amino acids) C-terminus, in which are found many potential phosphorylation sites. Previously (JBC 269:23204), we showed that when expressed in COS-1 cells wild-type Kv2.1 was constitutively phosphorylated on serine. A truncation mutant, ΔC318, lacking the last 318 amino acids of the C-terminus of Kv2.1, was phosphorylated to a lesser degree. Here the effects of phosphorylation on the activation of Kv2.1 and ΔC318 were investigated using the whole cell patch clamp. The $V_{1/2}$ for the activation of Kv2.1 (+2 mV) was shifted to the positive compared to ΔC318 (-6 mV), while no differences in macroscopic kinetics were observed. However, after intracellular application of alkaline phosphatase, expected to remove phosphates from cytoplasmic sites, there was little difference in $V_{1/2}$ between Kv2.1 (-18 mV) and ΔC318 (-16 mV). By comparison, heat-inactivated phosphatase had no effect. This suggests the difference in $V_{1/2}$ between Kv2.1 and ΔC318 is due to differences in phosphorylation rather than a gross conformational change caused by the truncation. We also examined the activation properties of two other Kv2.1 C-terminal truncation mutants, ΔC60 and ΔC187, which lack the last 60 and 187 amino acids, respectively. The $V_{1/2}$ for ΔC60 was similar to that for Kv2.1, whereas ΔC187 was similar to ΔC318. These results suggest that some, but not all, of the constitutive phosphorylation sites responsible for the differences in the $V_{1/2}$ of these different forms of Kv2.1 lie in the region between amino acids 667 and 793 near the distal end of the C-terminus.

M-Pos15

INACTIVATION OF Kv4.1 K^+ CHANNELS IN CELL-FREE INSIDE-OUT PATCHES. ((**M. Covarrubias** and E.J. Beck)) Dept. Pathology, Anatomy and Cell Biology, Jefferson Medical College, Philadelphia, PA 19107.

Shal K^+ channels appear to inactivate by mechanisms that differ from those known in Shaker K^+ channels (Jerng and Covarrubias, Biophys. J., in press). We have extended our previous studies to cell-attached and inside-out patches from Xenopus oocytes. We found that upon patch excision Kv4.1 outward K^+ currents ran down slowly ($\tau_{run\text{-}down}$ = 73±36 s) and macroscopic current inactivation is simultaneously accelerated. Although the sum of at least three exponential terms was necessary to describe macroscopic inactivation of Kv4.1 in cell-attached patches (or whole-oocytes), in inside-out patches the sum of two exponential terms was generally sufficient. In fact, currents from inside-out patches did not exhibit the slowest time constant observed with cell-attached patches and closely resembled Kv4.1 currents heterologously expressed in mammalian cells (Table below). The effects of patch excision could be partially reversed by cramming the patch into the oocyte. We are currently investigating the nature of the cytoplasmic factors that regulate the slow inactivation process. Supported by NIH grant NS32337 (M.C.).

Kv4.1 decay (+50 mV)	τf (ms)	τi (ms)	τs (ms)
Cell-Attached	18±4	66±22	222±47
Inside-Out	20±6	83±19	
NIH-3T3/HEK-293	11±1	73±10	

M-Pos16

ROLE OF CHARGES ON EXTRACELLULAR LOOPS IN THE VOLTAGE-DEPENDENCE OF GATING OF Kv1.4. ((G-N Tseng, J Xia and M Jiang)) Dept of Pharmacology, Columbia U., New York, NY 10032.

Surface charges on the extracellular loops connecting transmembrane domains of channel proteins may influence surface potential and thus affect the apparent voltage-dependence of channel gating. Their impact may depend on their locations relative to the voltage-sensor of the channel (S4). We altered the net charges on the extracellular loops of Kv1.4 and examined the effects on $V_{0.5}$ of activation. Adding 8 positive charges to the loop connecting S1 and S2 (8+S1S2) shifted the mean $V_{0.5}$ by +25 mV (n=6). Adding 4 positive charges to the S3S4 loop shifted mean $V_{0.5}$ more (+40 mV, n=4). Adding 4 negative charges to the S1S2 loop (4-S1S2) did not shift $V_{0.5}$, while adding 4 negative charges to the S3S4 loop (4+S3S4) shifted $V_{0.5}$ by -20 mV (n=5). These shifts in $V_{0.5}$ were mainly due to mutation-induced alterations in the external surface potential because screen -ing surface potential by elevating $[Mg^{2+}]_o$ in -duced different degrees of positive shift in $V_{0.5}$ (4-S3S4 > WT > 4+S3S4, 8+S1S2, Fig) so that at 65 mM $[Mg^{2+}]_o$ the differences in $V_{0.5}$ were markedly reduced. We conclude that surface charges on the extracellular loops are a contributing factor to the voltage-dependence of channel activation.

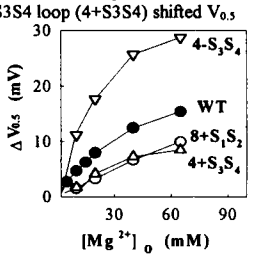

M-Pos17

ANOMALOUS CONDUCTION IN C-TYPE INACTIVATED *SHAKER* POTASSIUM CHANNELS.

((**Stefan H. Heinemann**[1], John G. Starkus[1,2], and Martin D. Rayner[2]))
1: Max-Planck-Gesellschaft, AG Molekulare & zelluläre Biophysik, Jena, Germany. 2: Békésy Lab. of Neurobiology, PBRC, Univ. Hawaii, Honolulu, HI.

In *Shaker* B channels with deleted N-terminal ends, C-type inactivation during test pulses is readily visible when external K^+ is removed (López-Barneo et al., Rec. & Chan., 1, 61-71, 1993). Using external Na^+ (or Li^+) as the permeant ion, we have studied the effects of C-type inactivation in the presence or absence of internal K^+ ions. After removal of internal K^+, development of C-type inactivation apparently increases the tail current magnitude, and markedly slows tail current kinetics (see Figure). Returning < 1 mM of internal K^+ greatly reduces the slowing of the tail currents. In both the presence and absence of internal K^+, the rate of gating charge return, measured from the recovery of Ig_{ON} in douple-pulse experiments, parallels the tail current kinetics. Since large inward currents occur well before significant recovery from C-type inactivation is observed, we conclude that at least one long-lived, C-type inactivated, state must be capable of conducting Na^+ and Li^+ ions in the absence of internal K^+.

Tail currents from inside-out recordings at -100 mV; depolarizing pulses to +20 mV, i.e. close to the estimated reversal potential for Na^+, were applied for 2, 18, 34, and 66 ms. Ext. solution (in mM): 115 NaCl, 1.8 $CaCl_2$; int. solution: 77 TrisCl, 38 NaCl, 1.8 EGTA.

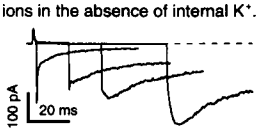

M-Pos18

THE EFFECTS OF K^+ DEPLETION FROM A PUTATIVE DIFFUSION-LIMITED SPACE: IMPLICATIONS FOR hKv1.5 ((C. Parker*, J. Anderson*, E. Salinas+, and D. Fedida*)) *Department of Physiology, Queen's University, Kingston, Canada K7L 3N6, and +Inst. de Fisiologia, BUAP, Puebla, Mexico

Under whole-cell recording (WCR) conditions in stably transfected cell lines, hKv1.5 behaves as a delayed rectifier, with fast activation kinetics and slow inactivation. This slow inactivation occurs over a period of 10 to 20 s, and is thought to be a result of C-type inactivation. Similar results are also observed in inside-out (I/O) patches from the same expression systems. However, when recording from cell-attached (C/A) patches, hKv1.5 activates with kinetics that are similar to WCR and I/O recording configurations, but relaxes within 10 ms to a steady-state level. The magnitude of the steady-state C/A current (I_{ss}) can be modulated by changes in the concentration of external bath K^+ ($[K^+]_{bath}$), despite the fact that the channels in the patch are exposed to a constant pipette $[K^+]$ of 5 mM. For example, relative to peak current (I_{peak}) at a pipette potential of -150 mV, I_{ss} was 9.1±5.8%, 20.1±8.7%, and 40.3±3.0% in 2, 5, and 10 mM $[K^+]_{bath}$, respectively (n=3, ±SEM). I_{peak} was not significantly changed over this range of $[K^+]_{bath}$. Evidence suggests that this phenomenon occurs as a result of a local depletion of K^+ from a putative diffusion-limited space adjacent to the inner surface of the plasma membrane. Depletion occurs as a result of outward K^+ conductance through hKv1.5. As the K^+ within this space depletes during a test pulse, the driving force for K^+ is reduced, resulting in the observed relaxation of current. Furthermore, the membrane that is adjacent to the pipette but exposed to the bath apparently depolarizes, allowing activation of adjacent membrane channels, which effectively clamps the intracellular K^+ in the restricted space to that of the bath, explaining why increasing $[K^+]_{bath}$ results in an increased steady-state current. (Scale bars: 200 pA, 20 ms).

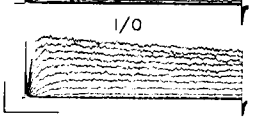

M-Pos19

ROLE OF THE S4 SEGMENT IN THE CALCIUM-DEPENDENT POTASSIUM CHANNEL, *hSLO*. ((**F. Díaz***, P. Meera§, L. Toro§, E. Stefani§, and R. Latorre*,†))
*Dpto. de Biologia, Universidad de Chile, †Centro de Estudios Cientificos de Santiago, Santiago, Chile; and §Dept. of Anesthesiology, UCLA, CA 90025 USA.

In voltage-dependent ion channels, a voltage sensor is responsible for coupling the electric field to pore opening. The experimental evidence strongly suggest that the fourth putative transmembrane segment (S4) is part the voltage sensor in Na^+ and K^+ channels. Combining site-directed mutagenesis of the S4 sequence of a Ca^{2+}-dependent K^+ channel cloned from human myometrium (*hslo*; Wallner et al 1995, Receptors & Channels 3:185-199) and electrophysiological measurements, we found that voltage-dependent activation involves the S4 segment. Of six residues tested, three significantly contribute to the channel voltage dependence: R207, R210, and R213. Neutralization of these residues had two major effects: i. it decreased the slope of the Po-V curves from 1.62 ± 0.22 e_o for wild type *hslo* (WT) to 0.70 ± 0.16 e_o for R210Q and to 0.58 ± 0.08 e_o for R213Q; and ii. it dramatically modified the close-open equilibrium, changing the half maximum activation potential ($V_{0.5}$) from 95 ± 9 mV (WT) to -74 ± 30 mV for R207Q ($[Ca^{2+}]$ = 0.63 μM). $V_{0.5}$ changed from -18 ± 33 mV for WT to 100 ± 38 mV for R210Q and to 114 ± 13 mV for R213Q ($[Ca^{2+}]$ = 103 μM). The results are incompatible with the hypothesis that in these channels voltage dependence is a consequence of solely a voltage-dependent Ca^{2+} binding. Calcium appears to be acting by decreasing the energy necessary to displace the voltage sensor in the electric field.

Supported by grants: FNI 2950028 (FD); FNI 1940227 & Cátedra Presidencial (RL); NIH HL54970 (LT) and NIH GM50550 (ES).

M-Pos20

ADDITIONAL EVIDENCE FOR THE MOLECULAR DETERMINANT OF β-SUBUNIT REGULATION IN MAXI K_{Ca} CHANNELS. ((**P. Meera**, M. Wallner and L. Toro)) Anesthesiology Dept., UCLA, Los Angeles, CA 90095-1778, USA

Large conductance voltage- and Ca^{2+}- sensitive K (MaxiK) channels have an accessory β-subunit which leads to a dramatic increase in the voltage/Ca^{2+} sensitivity. This β-subunit has two membrane spanning regions separated by an extracellular loop. We have previously shown by comparing multiple sequence alignments with hydrophobicity plots that MaxiK channel α-subunits have a unique hydrophobic segment (S0) at the N-terminus. This segment is in addition to the six putative transmembrane segments (S1-S6) usually found in voltage dependent ion channels. This idea was supported by normal functional expression of signal sequence fusions. We now show further evidence for the transmembrane nature of this unique S0 region, using in-vitro translation experiments. Moreover, in-vitro N-linked glycosylation of S0 indicates that the N-terminus is exoplasmic. The S0 region is essential for channel function, but can be expressed as a separable domain. The functional role of S0 and the exoplasmic N-terminus is to confer responsiveness to the α subunit for regulation by its β subunit. In previous studies, chimeric exchange of 41 N-terminal amino acids, including S0, from the human MaxiK channel to the Drosophila homologue transferred β-subunit regulation to the otherwise unresponsive Drosophila channel. With additional chimeric constructs, we now show that both the exoplasmic N-terminus and S0 are necessary for β-subunit modulation. We propose a new model in which MaxiK channels have a seventh transmembrane segment and an exoplasmic N-terminus, which are essential for β-subunit modulation. (Supported by NIH grant HL54970, LT is an AHA Established Investigator).

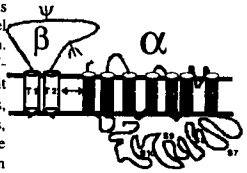

M-Pos21

INACTIVATING BK CHANNELS (BK_i): HETEROMULTIMERS OF INACTIVATION-COMPETENT AND NONINACTIVATING SUBUNITS. ((**J.P. Ding** & C.J. Lingle)) Dept. Anesth., Wash. Univ. Sch. Med., St. Louis, MO 63110. Spon. by C.J. Lingle.

Most BK channels in rat chromaffin cells exhibit rapid inactivation, which can be removed by cytosolic trypsin. Here, we suggest that BK_i channels contain up to four independent, inactivation domains (IDs), but that, on average, most BK_i channels contain only 2-3 IDs. Channels with less than four IDs per channel are heteromultimers of inactivation-competent subunits (each containing a single ID) and noninactivating subunits. Inactivation-competent subunits are relatively resistant to blockade by charybdotoxin (CTX).

First, whole-cell BK current was activated by depolarizing voltage steps with 10 μM pipette Ca^{2+}. Trypsin introduction into cells gradually slowed inactivation and increased the fraction of steady-state BK current (f_∞). The relationship between the fractional slowing of inactivation and the increase in f_∞ was most consistent with an initial value of 2-3 IDs per channel, with a limiting value of up to 4 IDs per channel. Cells with slower initial inactivation rates have fewer IDs per channel as defined by trypsin digestion. Second, the frequency of occurrence of BK_i and noninactivating BK_n channels was examined in patches in which total BK channel number could be defined. Although rare, BK_n frequency was consistent with random mixing of two types of subunits with about 2-3 IDs per channel. Patches with more slowly inactivating BK_i channels were more likely to have at least one BK_n channel. Third, the CTX sensitivity of BK_i current was variable, but weaker sensitivity to CTX was correlated with faster inactivation rates. Furthermore, reduction of BK_i current by CTX was associated with an increase in inactivation rate of the remaining BK_i current, consistent with the idea that CTX preferentially blocks those channels with more noninactivating subunits. Thus, three independent lines of evidence argue that BK_i channels are heteromultimers of inactivation-competent (but CTX-resistant) BK_i subunits and noninactivating (but CTX-sensitive) BK_n subunits. We can not infer whether IDs are intrinsic to BK_i subunits or only selectively associate with them.

M-Pos22

COUPLING OF CHARGE MOVEMENT AND PORE OPENING IN A HUMAN MAXI K CHANNEL (*HSLO*). ((**F. Noceti**, M. Ottolia, M. Wallner, R. Latorre, E. Stefani and L. Toro)) Depts. of Anesthesiology and Physiology, UCLA, Los Angeles, CA 90095-1778. (Spon. by L. Toro)

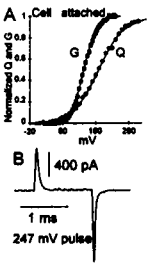

We studied the coupling between gating and ionic currents of a Maxi K channel (*hslo*) and determined the number of effective charges per channel. We used Cs^+ to measure ionic currents, and tetraethylammonium to isolate gating currents (**B**). **A** shows G-V and Q-V curves of *hslo* expressed in oocytes. At negative voltages, a small amount of charge moves prior to pore opening, indicating the presence of closed states prior to the open states. These initial closed states agree with the "Cole-Moore" shift in the ionic current. With further depolarization, in contrast to other voltage gated ion channels, the G-V curve crosses the Q-V curve and charge movement follows pore opening. Raising internal Ca^{2+} shifts both curves to the left. These results indicate that the channel transits through closed states before opening and that open transitions also carry charge. We normalized both the number of channels and the amount of charge per membrane capacity measured in 3-6 giant patches of the same cell; we obtained 4.4 ± 0.8 charges/channel (± SD, 3 cells). This number is consistent with less charged residues in the *hslo* as compared to other voltage gated ion channels of the S4 superfamily. (Supported by NIH GM 53303. L. Toro is an EI of the AHA).

M-Pos23

KINETIC SCHEMES DERIVED FROM Q-MATRIX FITTING OF TWO-DIMENSIONAL DWELL-TIME DISTRIBUTIONS SUGGEST GATING MECHANISMS FOR *dSlo* AND *mSlo* BK CHANNELS. ((**B.L. Moss**, S.D. Silberberg*, B.S. Rothberg, R.A. Bello and K.L. Magleby**)) Department of Physiology and Biophysics, University of Miami School of Medicine, Miami, FL 33101 and *Department of Life Sciences, Ben-Gurion University of the Negev, Beer-Sheva, 84105, Israel.

While considerable progress has been made in developing kinetic schemes that describe the gating behavior of native large-conductance calcium-activated potassium (BK) channels, less is known about the kinetics of cloned BK channels. This study develops kinetic models that can account for the calcium-dependent gating of cloned BK channels from *Drosophila* (*dSlo*) and mouse (*mSlo*). Currents were recorded using the inside-out configuration of the patch clamp technique from single *dSlo* and *mSlo* channels expressed in *Xenopus* oocytes. Durations of adjacent open and closed intervals were measured, and the interval pairs were log-binned to generate two-dimensional (2-D) dwell-time distributions. The 2-D distributions were then fitted with sums of 2-D exponential components to estimate the minimum numbers of open and closed states. 2-D Q-matrix fitting was then used to determine the most likely set of rate constants for different kinetic schemes and to rank these schemes. Fitting a 2-D distribution distinguishes models that are not separable by 1-D methods because 2-D fitting forces the kinetic scheme to account for correlations between adjacent interval durations. The 2-D distributions were well-described by kinetic schemes with 3-4 open states and 5-7 closed states. These schemes suggest differences in gating for *dSlo* and *mSlo* channels. Supported by grants from the **NIH, **MDA, *US-Israel BSF, and *Israeli MSA.

K CHANNELS: PERMEATION/PORE MODELS

M-Pos24

STRUCTURAL MODELS OF *SHAKER* K^+ CHANNELS IN CLOSED, OPEN, AND INACTIVATED CONFORMATIONS
((S.R. Durell and H.R. Guy)) LMMB, NCI, NIH, Bethesda, MD 20892-5677

In our latest generation of models of Kv channels, all transmembrane segments are α helices, except for the latter part of P, P2 (see sideview of 2 subunits below). In the outer half of the membrane, each subunit has a cylindrical bundle of 7 helices (S1-S6 and P1) with S4 in the middle. Four of these subunits assemble so that S1-S3 are exposed to the lipid. The relatively elongated P2 segments form the ion selective portion of the pore in the center of the tetramer. When the channel is open, S4 spans only the outer half of the membrane. All its positively charged side chains form salt bridges with negatively charged side chains of surrounding segments. The inner portion of the permeation pore is formed by the more hydrophobic surface of L45 and the C-terminal half of S6. 'Gating pores' or clefts are formed through the inner half of the membrane within each subunit parallel to a large central permeation pore. These clefts are lined by very polar residues from S2, S3, and L45. In the open conformation, L382, L385, and L389 on L45 pack next to L396, L399, and L403 on S5. The C-terminal half of S6 is postulated to be the 'activation gate'that blocks the closed channel, the L45 segment is postulated to be a 'latch' that swings inwardly when the channel closes and thus prevents opening of the gate, and S4 is postulated to be the 'voltage sensor' that moves outwardly during activation by the 'helical screw' mechanism and that pulls the latch to its open position. An NMR structure of the RAW3 'inactivation ball' (see abstract by Antz, *et. al.*) was docked into the intracellular end of the open channel conformation.

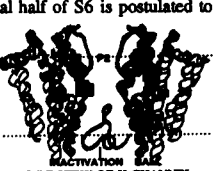

SIDE VIEW OF K CHANNEL

M-Pos25

STRUCTURAL MODELS OF HOMOLOGOUS ION CHANNEL FAMILIES: HERG, AKT1, Kir, TWIK, AND CYCLIC NUCLEOTIDE-GATED CHANNELS
((Y. Hao, S.R. Durell, and H.R. Guy)) LMMB, NCI, NIH, Bethesda, MD 20892

Structural models of Kv channels that are based on many experimental results and on a series of modeling criteria (see abstract by Durell and Guy) were extended to other distantly related ion channel families that have several known sequences within each family. These include channels that have S1-S6 segments (plant AKT1, EAG family, cyclic nucleotide-gated) and those that have only M1-P-M2 transmembrane segments (Kir and TWIK channels). In spite of very little sequence identity between these families, they can all be folded in a similar manner that satisfies our modeling criteria. In addition to having similar backbone structures, the models have the following features in common. The molecular structure of the putative ion selective region is similar in all K^+ families. Almost all of the residues that are poorly conserved within each family are exposed to lipid or water on the exterior of the protein. Residues that are highly conserved within each family usually interact with other residues that are also highly conserved. Most of the charged residues in the transmembrane region form salt bridges. The TWIK channels have two M1-P-M2 segments within each monomer. Based on our criteria of clustering residues on the basis of how well they are conserved, we postulate that these channels have a closed conformation which, unlike the putative open conformation, does not have a pseudo-four-fold symmetry; rather, the two repeats within a monomer are related by a pseudo-two-fold symmetry and the two monomers are related by two-fold symmetry.

M-Pos26

VOLTAGE-GATED POTASSIUM CHANNELS: MOLECULAR MODELS OF THE PORE-LINING REGION AND THEIR INTERACTIONS WITH WATER AND IONS.

((I.D. Kerr, K. Ranatunga and M.S.P. Sansom)) Laboratory of Molecular Biophysics, University of Oxford, Oxford, OX1 3QU, UK.

The pore-lining region of voltage-gated potassium (Kv) channels is primarily formed by four identical H5 segments, one from each subunit. Residues within the adjacent transmembrane (TM) segments, S5 and S6, have also been identified as pore-lining. We are attempting to produce objective molecular models of the pore of Kv channels which integrate the substantial body of site-directed mutagenesis data that has accumulated over the past decade. Mutagenesis data have been interpreted as a set of topological and orientational restraints for each residue, identifying 42 possible configurations of β-barrel and 24 possible configurations of α-helix bundle which have been explored as potential Kv channel pore-region models. These restraints have been employed to produce over 1300 models of the core $(H5)_4$ region. We have ranked our families of β-barrel models and α-helix bundle models according to their agreement with the biochemical data, and according to their predicted conductance values. The highest-ranking models have been refined by inclusion of TIP3P water within the pore region. We describe the extension to our highest-ranking models by the incorporation of the adjacent TM segments S5 and S6 as a surrounding α-helix bundle, and by the incorporation of the entire TM region (ie segments S1-S6). We also describe extended simulations of water with Kv channel pores and simulations of pore:ion interactions.

This work is supported by the Wellcome Trust.

M-Pos27

USING STICHODACTYLA TOXIN TO MAP THE TOPOLOGY OF THE LYMPHOCYTE POTASSIUM CHANNEL Kv1.3 ((**K. Kalman**, J. Aiyar, C.-L. Lee, M. W. Pennington*, G. A. Gutman+, and K. G. Chandy)) Department of Physiology and Biophysics, and +Department of Microbiology and Molecular Genetics, University of California, Irvine CA 92697, and *Bachem Bioscience Inc., 3700 Horizon Dr., King of Prussia PA 19406.

The voltage-gated potassium (Kv) channel, Kv1.3, plays an important role in lymphocyte proliferation, and several agents that block this channel also act as immunosuppressants. We have recently used the channel binding surface of the scorpion toxin Charybdotoxin (ChTX) to probe the structure of the external vestibule of the Kv1.3 channel pore (Aiyar et al., Neuron 15:1169, 1995).

A newly described toxin, ShK, from the sea anemone *Stichodactyla helianthus*, has been shown to block Kv1.3 with high affinity (Kd=30pM). The solution structure of this toxin has recently been solved and shown to be very different from those of the scorpion toxins. Although several residues on the toxin have been identified that are critical for function (R11, Y23, K22), the channel residues with which they interact remain unknown, and the orientation with which the toxin binds to the channel is presently unclear. We have used complementary mutagenesis coupled with thermodynamic mutant cycle analysis to identify energetic coupling between ShK-K22 and Kv1.3-Y400 (ΔG=2.3kcal/mol for Kv1.3-WT:Y400V and Shk-WT:K22E). Our results also show that substitution of K22 with the non-natural amino acid ornithine, which is similar to but shorter than lysine, facilitates strong interaction with a residue higher up in the vestibule, namely H404. These findings suggest that K22 of ShK may protrude into the channel pore and interact with Y400 in the ion conduction pathway, in a manner similar to the interaction of K27 in ChTX with Kv1.3. Further channel-toxin interactions are under investigation. (Supported by USPHS grant AI24783)

M-Pos28

SODIUM PERMEATION THROUGH POTASSIUM CHANNELS: COMPETITION OR CONFORMATIONAL CHANGE? ((**S. J. Korn**, L. Kiss, D. Immke, J. J. LoTurco)) Physiology and Neurobiology, University of Connecticut, Storrs, CT 06269

K^+ channels are highly selective for K^+ over Na^+, with P_{Na}/P_K near 0.01. Upon removal of K^+, Na^+ conducts well through the cloned K^+ channel, Kv2.1. Addition of low $[K^+]$ inhibited the ability of Na^+ to conduct, which suggested that K^+ prevented Na^+ from conducting through Kv2.1 by a competitive mechanism. Removal of K^+ also resulted in a loss of both internal and external TEA sensitivity in Kv2.1, which suggested that the pore conformation changed upon removal of K^+. Addition of $[K^+]$ that blocked Na^+ conductance restored TEA binding. This finding left us with two alternative hypotheses: 1) that Na^+ conductance was prevented by a competitive binding interaction in the pore, and that the simultaneous conformational change near the TEA binding sites was unrelated to Na^+ conducting ability or 2) that the conformational change associated with loss of TEA binding was required for Na^+ to conduct, and the competitive interaction between Na^+ and K^+ was an indirect result of the effect of K^+ on channel conformation. We expressed a chimera that consisted of the P region, S5-P linker and P-S6 linker from Kv1.3 (which does not conduct Na^+) inserted into Kv2.1.Upon removal of K^+, Na^+ conducted well through this channel, and Na^+ conductance was inhibited by low $[K^+]$ (~100μM-1 mM). External application of 20 mM TEA inhibited K^+ currents and Na^+ currents virtually identically. Pending complete concentration response curves, these data suggest that a conformational change near the external TEA binding site is not necessary for Na^+ to conduct through K^+ channels. *We thank Rod MacKinnon for the chimera described. Supported by NSF and UC Res.Found.*

M-Pos29

SNDTT: A NOVEL OPEN-CHANNEL BLOCKER OF KV1 CHANNELS. ((**M.W. Brock**, C. Mathes, and W.F. Gilly)) Department of Biology, Hopkins Marine Station, Stanford University, Pacific Grove, CA 93950.

We have previously reported a DTT-dependent speeding of Kv inactivation by NO donors (Soc. Neurosci. Abs. 21(3):1753). Recent work in our lab suggests this effect is not mediated through the action of NO on channels, but through direct open-channel block by S-nitrosodithiothreitol (SNDTT), which unlike most open channel blockers of Kv channels, is not charged. We used whole-cell voltage-clamp recordings from squid giant fiber lobe neurons and HEK293, CHO, and Sf9 cells expressing various Kv cDNAs to address the nature and specificity of this block. S-nitrosylated thiols were synthesized in physiological solutions by combining various ratios of $NaNO_2$ and thiol at low pH. In Sf9 cells infected with a ShBΔ-recombinant baculovirus, externally applied S-nitrosodithio-DL-threitol (3:1 NO_2:DTT) produces a reversible, time-dependent open-channel block (Kd < 80 μM) that decreases over time (τ=514s) as SNDTT oxidizes. Bath-applied SNDTT also produced block in cell-attached patches, suggesting it is membrane permeant. No time dependent block was seen with DTT or $NaNO_2$ alone, NO• and NO⁻ donors, or the SNDTT breakdown products NH_2OH, N_2O, and oxidized DTT. A 1:1 NO_2:DTT reaction product produced block with a Kd 7.7 fold higher than that of the 3:1 product, suggesting doubly nitrosylated SNDTT is the blocking species. The structurally similar S-nitrosylated monothiols SN-1-thioglycerol and SN-2-mercaptoethanol did not produce block. Block does not require channel cysteines, as a cysteine-less ShBΔ mutant (Borland et al., Biophys. J. 66:694-699) was blocked by SNDTT. SNDTT specifically blocked Kv1 subfamily channels, producing reversible time-dependent open-channel block in SqKv1.1, ShB, and mammalian Kv1.1-1.6, but not in mammalian Kv2.1, 3.1, and 4.2. Recovery from block was not accelerated by high external K+ as has been seen with charged open-channel blockers that act internally. Preliminary data suggest that SNDTT block is stereo-selective, with the D-enantiomer blocking with greater affinity than the L-enantiomer. (rKv's were gifts of J.S. Trimmer, SUNY Stony Brook)

M-Pos30

EFFECTIVE SURFACE CHARGES ON SHAKER K CHANNELS ARE LOCATED ON THE S5-P LOOP ((**F. Elinder** and P. Århem)) The Nobel Institute for Neurophysiology, Karolinska Institutet, S-171 77 Stockholm, Sweden.

Cations have been proposed to affect voltage-gated ion channels by screening fixed negative surface charges. A central question is where these charges are located. A previous study of different K channel clones suggests that either the net charge of all the extracellular peptide loops of the channel protein, or that of the loop between segment S5 and the poreforming region P, constitutes the effective surface charges (Elinder et al, 1996, J. Gen. Physiol; in press). To separate between these two alternatives we are investigating channels with deviating charge profiles. A preliminary investigation of the xKv1.1 channel suggests that the S5-P loop is the main determinant. In the present study, we have investigated the effect of strontium on Shaker K channels expressed in *Xenopus* oocytes with a two-electrode voltage clamp technique. The experiments showed that the voltage dependence of the channel parameters were shifted equally much along the voltage axis, suggesting a pure screening mechanism. The steady-state activation curve was shifted 10.8 ± 1.6 mV (n=5), the time-constant vs. potential curve 10.2 ± 2.3 mV (n=5) and the steady-state inactivation curve 10 mV (n=1). These shifts suggest a surface charge density of 0.28 elementary charges per nm^2. This density is incompatible with the view that the S5-P loop is the main surface charge determinant. However, it is fully compatible with the hypothesis that the first five amino acids of this loop constitute the main determinant. Taken together, the studies clearly suggest that the charge of the first five amino acids on the S5-P loop determine the effective surface charge density of K channels.

M-Pos31

MULTIPLE CONDUCTANCE LEVELS IN SHAKER B POTASSIUM CHANNELS ((V. Corvalan, C. Toman and R. Aldrich)). Department of Molecular and Cellular Physiology and Howard Hughes Medical Institute. Stanford University, Stanford CA 94305.

We used mean-variance histograms (Patlak, 1993, *Biophys. J.* 65:29-42) to analyze single channel recordings of Shaker B (Δ6-46) potassium channels expressed in *Xenopus* oocytes. Single Shaker B (Δ6-46) currents exhibited three distinct conductance levels. On cell attached patches, these levels had slope conductance of 5 pS, 3.33 pS and 1.66 pS at positive potentials and with 2 mM K^+ in the pipette solution. The high conductance level was the most frequently observed in cell attached patches, which was reached more than 80% of the time when the channel was open. Upon patch excision, the conductance ratios remained constant (i.e. 1, 2/3 and 1/3). However, we observed a change in the frequency distribution of the mean current shifting from the high conductance level to the middle and low conductance levels. This time-dependent change in the frequency distribution of the conductance levels varied among patches, and it was greatly accelerated by using constant perfusion. These results suggest that multiple conductance levels in Shaker B channels are regulated by intracellular processes that are not present or are rapidly exhausted in inside-out patches. We are currently studying the role of channel phosphorylation on the modulation of the conductance levels.

M-Pos32

A COMPUTER MODEL OF MULTI-ION BARIUM BLOCK OF A MAXI K+ CHANNEL.
((**Y.Sohma**, A.Harris*, C.J.C.Wardle*, B.E.Argent, M.A.Gray)) Dept. Physiol. Sci., Univ. Med. Sch., Newcastle upon Tyne NE2 4HH, U.K.; *Inst. Mole. Med., John Radcliffe Hosp., Oxford OX3 9DU, U.K.

Our previous experiments (*Biophys.J.* **70**:1316-1325,1996; *Biophys.J.* **70**:A192,1996) have shown that the maxi-K^+ channel from human vas deferens epithelial cells shows novel blocking kinetics induced by Ba^{2+} applied from either the external or internal face of the channel. Using ext. Ba^{2+} we identified a "flickering blocking" site located deep within the channel pore and a "slow blocking" site located close to the extracellular mouth of the channel. A "fast flickering blocking" site was also identified with int. Ba^{2+} in addition to the classical "slow block" site. These results are consistent with the channel possessing multiple binding sites for Ba^{2+} and imply that current models of barium block are inadequate. Indeed an analysis of the voltage-dependence of the dissociation constants from the different Ba^{2+} binding sites, indicate that a single binding site is unlikely to underlie the classical Ba^{2+}-induced "slow block". In order to understand the mechanism of this unique blockade we have developed a computer simulation based on a 4-state cyclic equilibrium of Ba^{2+} binding to an open channel. The model incorporates two single occupancy Ba^{2+} binding sites, connected to a "slow" double occupancy state. The simulation could reproduce the kinetics of extracellular Ba^{2+} block correctly, although it suggested that an additional fast type of block overlapping the channels natural closing events (k_{off} : 1000 sec^{-1}) should also be present, which we subsequently confirmed experimentally. The model provides evidence that the extracellular "slow block" could be caused by double occupancy of this new fast site and the "flickering block" site. (supported by the MRC and the CFT (UK)).

M-Pos33

CONSTRUCTION AND PURIFICATION OF RECOMBINANT NOXIUSTOXIN: A TOOL FOR PROBING THE ELECTROSTATIC STRUCTURE OF MAXI-K CHANNELS.
((**K.M. Gianglacomo** and T.J. Mullmann)) Dept. of Biochem., Temple Medical School, Phila., PA 19140

K+ channel toxins from the venoms of scorpions exhibit striking differences in their electrostatic structures that may contribute to binding specificity. Noxiustoxin (NxTX), a low affinity blocker of maxi-K channels, has a highly uniform distribution of charge that is distinct from other more selective maxi-K channel toxins. To examine how the electrostatic structure of NxTX controls its relative binding affinity for the maxi-K channel, we constructed a gene encoding for NxTX. This NxTX gene was than ligated into a pGEMEX-derived expression vector. The resulting construct encoded the fusion protein Sal I-T7 gene9-factor Xa-NxTX-Hind III. Transformation of this vector into *E. coli* (BL21[DE3]) resulted in an expression system that yielded large amounts of the NxTX fusion protein. After DEAE chromatography, the NxTX fusion protein was oxidized to form disulfide bonds, cleaved with TPCK-trypsin and purified by cation exchange chromatography and reverse phase (RP) C18 HPLC. The purified recombinant NxTX (rNxTX) is identical to chemically synthesized NxTX with respect to its elution profile by RP C18 HPLC. The purified rNxTX and native NxTX exhibited similar potency for block of single maxi-K channels incorporated into planar lipid bilayers (IC_{50} ~300 nM). In addition, the average block times for native and recombinant toxins were similar, ~4 ms. This work, in combination with mutagenesis of rNxTX, provides a system for examining how the electrostatic structure of rNxTX controls its binding kinetics and specificity.

M-Pos34

SEQUENCE-SPECIFIC ASSIGNMENTS AND SECONDARY STRUCTURE DETERMINATION OF A TOXIN FROM *PANDINUS IMPERATOR* (PiTX-Kβ) USING NMR SPECTROSCOPY.
((**T. Tenenholz**†, K. Klenk†, R.S. Rogowski*, J.H. Collins†, T.A. Gustafson*, M.P. Blaustein*, and D.J. Weber†)) Departments of Biological Chemistry† and Physiology*, University of Maryland School of Medicine, Baltimore, MD 21201.

PiTX-Kβ, a 35 residue peptide, is a member of the Charybdotoxin family of scorpion toxins, which can be used to characterize potassium ion channels. PiTX-Kβ differs from PiTx-Kα, another peptide derived from *Pandinus Imperator*, by only one residue (E7P), yet its affinity is 7-fold lower. In order to understand this change in affinity, structural studies of PiTx-Kβ were performed using 2D NMR spectroscopy. To this end, a PiTX-Kβ fusion protein was prepared in *E.Coli* containing an overexpression plasmid under the control of a T7 promoter. Milligram quantities of fully functional PiTX-Kβ were purified (>99%) after proteolytic cleavage of the fusion protein with enterokinase. Two-dimensional NOESY, DQF-COSY, TOCSY, and ROESY NMR experiments were then used to determine the sequence-specific backbone and sidechain proton assignments and secondary structure of PiTX-Kβ. These studies showed that PiTX-Kβ has a helix, (residues 7-18), and two β-strands (βI: 23-25; βII: 30-32) which form a small antiparallel β-sheet. The secondary structures of PiTx-Kβ and PiTx-Kα are nearly identical. Thus, differences in the three-dimensional structures and/or side-chain placements are necessary to explain their varying affinities for the rapidly inactivating, Ca^{++}-independent potassium channel.

M-Pos35

PURIFICATION, CHARACTERIZATION, BIOSYNTHESIS AND RADIOIODINATION OF HONGOTOXIN$_1$, A NOVEL K^+ CHANNEL BLOCKING COMPONENT OF *CENTRUROIDES LIMBATUS* VENOM
((**A.Koschak**[1], R.O.Koch[1], M.Emberger[1] G.J.Kaczorowski[2], M.L.Garcia[2] and H.G.Knaus[1]))
[1]Inst.Bioch.Pharmacology, A-6020 Innsbruck, Austria, [2]Merck Research Laboratories, Rahway, NJ, 07065. (Spon. by R.J.Leonard)

A family of five novel peptidyl inhibitors of *Shaker*-type (K_v1) K^+ channels, which were termed hongotoxins (HgTX's), has been purified to homogeneity from venom of the scorpion *Centruroides limbatus*. The complete primary amino acid sequence of one of the peptides ($HgTX_1$) has been determined. To demonstrate the identity of the purified toxin, $HgTX_1$ was expressed in *E.coli* as part of a fusion protein. Recombinant $HgTX_1$ displays identical properties as the native peptide. It inhibits [^{125}I]MgTX binding to rat brain synaptosomal, HEK-$K_v1.2$ and HEK-$K_v1.3$ membranes with IC_{50} values of 0.1, 0.09 and 0.07 pM, respectively. Since baseline separation of monoiodo-Tyr-37-$HgTX_1$ from wild-type $HgTX_1$ could not be achieved, we constructed a $HgTX_1$ double mutant ($HgTX_1$-A19Y/Y37F) and iodinated this peptide. Wild-type $HgTX_1$, $HgTX_1$-A19Y/Y37F, as well as monoiodinated $HgTX_1$-A19Y/Y37F display identical affinities as inhibitors of [^{125}I]MgTX binding to rat brain membranes (IC_{50} values ≈ 0.3 pM). Moreover, [^{125}I]$HgTX_1$-A19Y/Y37F binds to membrane-bound neuronal K_v1 channels with a K_d value of 0.15 pM and a B_{max} value of 0.9 pmoles/mg of protein. To determine its specificty with respect to homotetrameric K_v1 channels, radioligand binding studies to HEK-$K_v1.1$-$K_v1.6$ membranes were performed. The peptide binds with sub-pM affinities to $K_v1.1$, $K_v1.2$ and $K_v1.3$, with lower affinity to $K_v1.6$, and does not interact with $K_v1.4$ and $K_v1.5$. The HgTX's represent novel and useful tools to investigate subclasses of voltage-gated K^+ channels.

REGULATION OF ION CHANNELS I

M-Pos36

CONTROL OF GLUR6 RECEPTOR ACTIVATION BY PKA AND CALCINEURIN.
((**Stephen F. Traynelis** and Philip Wahl)) Dept. of Pharmacology, Emory University, Atlanta GA 30322-3090 and Novo Nordisk A/S, Bagsvaerd, Denmark, DK-2880.

Glutamate receptors comprised of the GluR6 subunit activate and desensitize rapidly in response to the endogenous agonist glutamate, and are widely expressed in the CNS throughout development. Whereas estimates of agonist affinity have been made for these and many other receptors, few attempts have been made to assess glutamate efficacy. We have used non-stationary variance analysis to measure the probability that a channel is open at the peak of the response ($Popen_{PEAK}$) for homomeric GluR6 receptors in excised membrane patches obtained from transiently transfected HEK 293 cells. Glutamate (3-10 mM) was rapidly applied using the liquid filament method, and multiple responses recorded at an interval that ensured full recovery from desensitization (12-15s). Inclusion of the catalytic subunit of PKA (125-250 U/ml) in our pipette solution increased $Popen_{PEAK}$ to 0.85±0.04, nearly the maximum predicted from the burst structure (0.95; n=13 patches). By contrast, calcineurin (0.2 U/ml) reduced $Popen_{PEAK}$ to 0.49+0.04 (n=7). Both PKA and calcineurin did not alter the response time course or desensitization kinetics. The calcineurin co-activators calmodulin (10 μg/ml) and Ca^{2+} (200 nM) had little effect on $Popen_{PEAK}$ by themselves (n=8). Analysis of simulated macroscopic currents with properties similar to recombinant GluR6 suggested our 95% confidence interval (v=9) is about 10% for a $Popen_{PEAK}$ value of 0.5, and decreased with increasing $Popen_{PEAK}$. These results suggest that PKA and calcineurin co-localized at A-kinase anchor proteins in neurons can exert opposing actions on GluR6. This finding holds important implications for synaptic plasticity, signal processing, and stochastic resonance in neural networks.

This work was generously supported by The John Merck Fund and Novo Nordisk A/S

M-Pos37

ANTAGONISM BETWEEN GLUTAMATE RECEPTOR AND TRANSPORTER IN ACTIVATING LARGE CONDUCTANCE ANION CHANNELS: POSSIBLE ROLE OF INTRACELLULAR pH.
((**E. Scemes**, R. Dermietzel and D.C. Spray)). Dept. Physiology, USP, Brazil; Dept Anatomy, Univ. Regensburg, Germany and Dept. Neuroscience, AECOM, NY, USA.

We have previously found that *d*- but not *l*-glutamate induces large conductance (300-400 pS) anion channel (**LCAC**) activity in cell-attached patches of astrocytes and that **LCAC** activity could be induced by *l*-glutamate when the Na^+/glutamate cotransporter was inhibited (Scemes, E. & Spray, D.C. *Biophys. J., 70(2):*A70, 1996; *FESBE*, A19.061, 1996). We have now investigated the possibility that intracellular acidification induced by *l*-glutamate would prevent channel activation by measuring astrocyte intracellular pH variations induced by *d*- and *l*-glutamate and by measuring channel activity in excised patches exposed to pH 7.4 - 6.5. BCECF loaded astrocytes (pH 7.26; N=160) were acidified to pH 6.58 (N=50) when exposed to 100 μM *l*-glutamate and to pH 6.88 (N=56) when exposed to 100 μM *d*-glutamate. Intracellular acidification induced by *l*-glutamate in the presence of the glutamate transport blocker was reduced to levels (pH 6.82; N=52) similar to those induced by *d*-glutamate. The frequency of patches with channel activity decreased from 30% (4 of 13 cells) to 8% (1 of 13 cells) when pH was lowered from 7.4 to 6.5. At pH 7.0, **LCAC** activity could be recorded in 20% (3 of 15) of the patches, but activity was only transient. These results are consistent with the hypothesis that intracellular acidification induced by the glutamate transporter may counteract receptor mediated **LCAC** activation.
Research supported by FAPESP to E.S.

M-Pos38

ROLE OF G PROTEINS IN α-ADRENERGIC INHIBITION OF THE β-ADRENERGICALLY ACTIVATED Cl^- CURRENT IN CARDIAC MYOCYTES.
((**L.C. Hool**, L.M. Oleksa and R.D. Harvey)) Department of Physiology and Biophysics, Case Western Reserve University, Cleveland, OH 44106-4970.

Using the whole-cell patch-clamp technique, we found that the α-adrenergic receptor antagonist prazosin decreased the EC_{50} for activation of the Cl^- current by the combined α/β receptor agonist norepinephrine (NE) in control, but not in pertussis toxin (PTX)-treated myocytes. This suggests that the α-adrenergic inhibition of β-adrenergic responses is mediated through a PTX-sensitive G protein. However, PTX pretreatment also increased the sensitivity to the selective β-adrenergic receptor agonist isoproterenol (Iso; EC_{50} 5.0 nM vs 1.4 nM in PTX-treated), indicating that PTX treatment may be altering the response to NE exclusively by enhancing the sensitivity of β-adrenergic receptors. Consistent with this hypothesis, the selective α-adrenergic agonist methoxamine could still inhibit the Cl^- current activated by 30 nM Iso in PTX-treated myocytes but the sensitivity to methoxamine was significantly decreased (EC_{50} 8.3 μM vs 284 μM in PTX-treated). This suggests that the effects of PTX on α-adrenergic responses can actually be explained by changes in the sensitivity to β-adrenergic stimulation. To verify a role for a G protein in mediating the α-adrenergic response, we examined the effect of methoxamine on the Cl^- current activated in cells dialyzed with the non-hydrolyzable GTP analogue GTPγS. Pre-exposure to methoxamine resulted in an attenuated response upon subsequent exposure to Iso alone. We conclude that the α-adrenergic inhibition of β-adrenergic responses involves a G protein that is PTX-insensitive.

M-Pos39

REGULATION OF Ca^{2+}-DEPENDENT Cl^- CHANNELS BY CALMODULIN-DEPENDENT PROTEIN KINASE II IN VASCULAR MYOCYTES
((**N. Leblanc** and M.-A. Lupien)) Montréal Heart Institute, and Department of Physiology, U. Montréal, Montréal (Québec), CANADA H1T 1C8.

Ca^{2+}-dependent Cl^- channels ($I_{Cl(Ca)}$) have been identified in vascular smooth muscle cells of several vascular beds. Although $I_{Cl(Ca)}$ channels can be activated by a variety of stimuli, the exact mechanism linking intracellular Ca^{2+} mobilization and $I_{Cl(Ca)}$ remains unclear. The purpose of our study was to evaluate the possibility that activation of $I_{Cl(Ca)}$ by $[Ca^{2+}]_i$ may be indirect, involving a phosphorylation step mediated by calmodulin-dependent protein kinase II (CamKII). Macroscopic $I_{Cl(Ca)}$ currents were recorded in rabbit portal vein myocytes in response to depolarizing steps that evoked $I_{Ca(L)}$ in conditions that suppressed K^+ channels. As shown in panel A of the figure, 5 μM KN-93, a specific inhibitor of CamKII (K_i = 370 nM), induced a slow inhibition ($T_{½}$ > 5 min) of the slowly decaying $I_{Cl(Ca)}$ tail current upon repolarization to the holding potential (39% block; 11 min) while having little effect on $I_{Ca(L)}$. In a different cell, the inactive analog compound, KN-92, produced little effect on $I_{Cl(Ca)}$ tail currents (panel B; 11 min) even though $I_{Ca(L)}$ decreased by 26% These results are consistent with the idea that $I_{Cl(Ca)}$ may be directly or indirectly regulated by CamKII-dependent phosphorylation. Supported by MRC and QHSF.

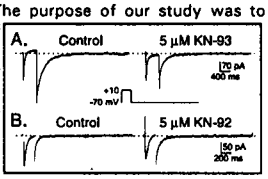

M-Pos40

ROLE OF THE SECOND NUCLEOTIDE-BINDING FOLD IN THE FUNCTION OF CFTR CHLORIDE CHANNEL.
((**Bryan Zerhusen** and Jianjie Ma)) Department of Physiology and Biophysics, Case Western Reserve University School of Medicine, Cleveland, OH 44106.

Opening and closing of the CFTR chloride channel are coupled to the hydrolysis of intracellular ATP, which requires coordinated interactions among the regulatory (R) domain and the two nucleotide-binding folds (NBF1 and NBF2), and the two NBFs seem to have different roles in the gating of the CFTR channel. To study the function of NBF2, and its interaction with the R domain in the regulation of the CFTR channel, two deletion mutants of human epithelial CFTR were constructed: **ΔNBF2, and ΔR-ΔNBF2**. The portions deleted in R and NBF2 correspond to amino acid residues 708 to 835, and 1185 to 1349. The ΔNBF2 and ΔR-ΔNBF2 proteins were expressed in HEK 293 cells, and their single channel functions were examined in the lipid bilayer system. Immunoblot analyses showed that ΔNBF2 had a molecular weight of ~110 kDa, and ΔR-ΔNBF2 had a molecular weight of ~95 kDa, which is consistent with the core-glycosylated form of CFTR proteins. With the microsomal membranes isolated from HEK 293 cells transfected with ΔR-ΔNBF2, functional CFTR chloride channels were measured. But different from the wild type CFTR channel, the ΔR-ΔNBF2 channels existed predominantly in the subconductance states (~3 pS). We are currently in the process of characterizing the function and regulation of the ΔNBF2 and ΔR-ΔNBF2 CFTR channels. Supported by NIH and CFF.

M-Pos41

EXOGENOUS R DOMAIN PROTEIN, WHEN PHOSPHORYLATED, INCREASES ACTIVITY OF THE R DOMAIN DELETION MUTANT OF CFTR CHLORIDE CHANNEL.
((Jiying Zhao, Jason Tasch*, Junxia Xie, Pamela B. Davis*, and **Jianjie Ma**)) Dept. of Physiology and Biophysics, and Pediatrics*, Case Western Reserve University. (Spon. by T. Gerken)

We have shown previously that the exogenous R domain protein (RDP, encoded by exon 13 and 84 base pairs of exon 14) interacted specifically with the wild type CFTR molecule and inhibited the chloride conductance in a phosphorylation-dependent manner. Only the unphosphorylated RDP is capable of blocking the CFTR channel (Ma et al., *JBC* **271:** 7351-7356). To further examine the mechanism of this interaction, we tested the effect of RDP on an R domain deletion mutant of CFTR, **ΔR(708-835)**, using the lipid bilayer reconstitution system. Unlike the wt-CFTR channel, addition of unphosphorylated RDP to the intracellular solution did not change activity of the ΔR(708-835)-CFTR channel. However, when phosphorylated, RDP enhanced the activity of the ΔR(708-835)-CFTR channel (Po=0.107±0.018, control; 0.192±0.019, +P-RDP). The results suggest a possible physical interaction between the R domain and the nucleotide-binding folds (NBFs) in the intact CFTR molecule. The unphosphorylated RDP could compete with the endogenous R domain in the wt-CFTR for interaction with the NBFs, and the phosphorylated RDP could take the place of the endogenous R domain in the ΔR(708-835)-CFTR, which regulate the rate of ATP hydrolysis at the NBFs, and thus the opening and closing transitions of the CFTR channel.

M-Pos42

NOVEL SUBUNIT COMPOSITION IN A RENAL EPITHELIAL K_{ATP} CHANNEL (Kir 1.1+CFTR)
((**A. Ruknudin**[1,3], D. H. Schulze[1], S. K. Sullivan, W.J. Lederer[2,3] and P. A. Welling[2])) Departments of [1]Microbiology & Immunology, [2]Physiology [3]Molecular Biology & Biophysics, Univ. Maryland at Baltimore, Baltimore. MD. 21201, USA.

ATP-sensitive K channels (K_{ATP}) in pancreatic beta-islet cells and cardiac myocytes appear to be comprised of homologous but different subunits. The common architecture in these cells, consisting of an inward-rectifier K channel (Kir 6.1 or 6.2) and a much larger ATP-binding cassette subunit (SUR 1 or 2), predicts a similar multimeric motif for other functionally distinct K_{ATP} channels. Observations, that kidney lacks either Kir 6.2, SUR1 or SUR2 expression but exhibits K_{ATP} channels with a very low affinity to either ATP or sulfonylurea agents, suggest a unique subunit composition for K_{ATP} channels in kidney. Based on co-expression pattern of Kir and ATP-binding cassette proteins along the nephron with K_{ATP} channels, we considered the possibility that the 20-25 pS K_{ATP} channel in the distal nephron is comprised of ROMK1 (Kir1.1a) and the ATP-binding cassette protein, CFTR. As determined by patch-clamp analysis in excised-inside out patches of *Xenopus* oocytes, both Kir1.1a and Kir1.1b (ROMK2) exhibited a high open probability and a single channel conductance of ~36 pS. Furthermore, using the 'oil-gate' for rapid solution exchange, no inhibition of either Kir1.1a or Kir1.1b activity by cytoplasmic ATP (up to 5 mM MgATP) or glibenclamide (up to 100 μM) was observed. When Kir 1.1a was co-expressed with CFTR, a unique smaller conductance K channel similar to the native K_{ATP} (12-26 pS) was observed. This channel had K-selectivity (P_K/P_{Cl} ~100:1 or P_K/P_{Na} 20:1) like Kir1.1a and exhibited a high open probability. In contrast to Kir 1.1 channels but similar to the renal epithelial K_{ATP} channel, the unique K channel was reversibly inhibited by glibenclamide with a Ki of 33 μM. Most importantly, the small conductance channel was inhibited by the cytoplasmic application of ATP (5 mM MgATP), the hallmark of K_{ATP}. Reminiscent of the distal nephron K_{ATP} channel, these observations demonstrate that CFTR interacts with Kir1.1 (1) to modify single channel conductance and (2) to confer both ATP and sulfonylurea sensitivity. Moreover, the modified properties of Kir1.1 by CFTR in excised membrane patches are most consistent with direct protein-protein interaction and heteroligomerization, rather than indirect interaction.

M-Pos43

CHANGES IN THE EXPRESSION OF THE SARCOLEMMAL SODIUM CHANNEL SUBTYPES IN RAT VENTRICLE AFTER MYOCARDIAL INFARCTION.
((**B. Huang**, M. Gidh-Jain, P. Jain, N. El-Sherif)) Division of Cardiology, VAMC Brooklyn and SUNY Health Science Center, Brooklyn, NY 11209. (Spon. By M. Boutjdir)

Following myocardial infarction (MI), the non-infarcted myocardium undergoes extensive architectural and physiological alterations. The latter include prolongation of action potential duration (APD), the molecular basis of which is currently under investigation. In cardiac myocytes the sodium channel (NaCh) contributes to the plateau phase of APD. The alterations in NaCh subtype expression in post-infarction hypertrophied left ventricular (LV) myocardium, were examined in female Sprague Dawley rats which underwent left coronary artery ligation (MI, n=6) or sham operation (S, n=6). Three weeks later, total LV myocardial RNA from both groups was analyzed by RNase protection assay (RPA) using cRNA probes derived from the variable region of the first cytoplasmic loop of NaCh subtypes I, IIIb and rHI. Thus, a protected band in this assay indicated the presence of a corresponding isoform of each subtype. RNA from isolated myocytes was also subjected to the RPA to eliminate contamination of non-myocytes. RNA from neonatal myocardium was used for comparison. *Results*: Two protected bands corresponding to NaCh I isoforms were observed: NaCh I (230bp) and NaCh Ia (190bp) in adult myocardium and myocytes. Only NaCh Ia was detected in neonatal LV. The expression of NaCh Ia was increased in the MI group compared to S (0.48±0.06 MI vs. 0.37±0.03 S; p<0.03). There was no significant difference in the expression of NaCh I and rHI between the MI and S groups, and the expression of NaCh III and its isoforms was undetectable in both groups. The existence of NaCh I subtype in the myocardium was also confirmed by RNase protection assay by using isolated myocyte RNA. *Conclusion*: This is the first study to indicate that there is differential expression of NaCh subtypes in hypertrophied left ventricular myocardium following MI. NaCh Ia may play a role in the APD prolongation in MI and in neonatal rats.

M-Pos44

CALCIUM TRANSIENTS INDUCED BY INTRACELLULAR ALKALINIZATION IN MOUSE SPERMATOGENIC CELLS. ((**C. M. Santi**, A. Darszon and A. Hernández-Cruz.)) Instituto de Fisiología Celular and Instituto de Biotecnología, UNAM, México.

Intracellular alkalinization and rises of intracellular [Ca^{2+}] are important during capacitation and the acrosome reaction in mammalian sperm. Also, a Ca^{2+} channel modulated by intracellular pH (pHi) participates in the sea urchin sperm acrosome reaction. Here, we analyze by fura-2 and BCECF single cell spectrofluorometry the effects of controlled intracellular alkalinizations of spermatogenic cells acutely dissociated from mouse adult testis. Cells were loaded by incubation with 1 μM fura-2-AM or 10 μM BCECF-AM. Ca^{2+} transients were recorded by alternating 340/380 nm illumination, and pHi fluctuations were recorded as changes in BCECF fluorescence at 505 nm excitation. Progressively higher resting [Ca^{2+}] were found in cells at more advanced stages of maturation: pachytene spermatocytes: 56.5±7.2 nM (n=10); round spermatids: 122.2±13.8 nM (n=19); condensed spermatids: 200.2±46.3 nM (n=5). Brief applications of 25 mM NH_4Cl increased pHi by about 0.5 units and produced an initial drop of intracellular [Ca^{2+}] followed by a 2-3 fold [Ca^{2+}] rise. These Ca^{2+} transients are produced by Ca^{2+} influx since they are abolished in the absence of external Ca^{2+}. No significant contribution of intracellular Ca^{2+} release was detected. Alkalinization-induced Ca^{2+} influx was inhibited by Ni^{2+} 0.2 and 1 mM, but was insensitive to nifedipine at concentrations up to 20 μM. This Ca^{2+} pathway was also permeable to Sr^{2+}, Ba^{2+} and Mn^{2+}. All cells responded quickly to NH_4Cl application (half rise time of BCECF signals ranged from 2.4±0.2 to 4.5±0.4 s and decayed with time constants ranging from 8.9± 0.73 to 9.9±0.89 s). In contrast, Ca^{2+} transients had significantly slower kinetics (half rise times ranged from 9.8±1.6 to 15.3±2.9 s and decay time constants from 12.9±2.9 to 24.6±8.2 s) and potentiated with repeated NH_4Cl applications. This potentiation gradually obliterated the initial [Ca^{2+}] drop. The nature of this novel pH-dependent Ca^{2+} permeation pathway present in mammalian male germ cells is currently under investigation. *Supported by grants from DGAPA, CONACyT (México) and Howard Hughes Medical Institute.*

M-Pos45

ELECTROPHYSIOLOGICAL EVIDENCE FOR INTEGRIN MODULATION OF CALCIUM CHANNELS IN RAT ARTERIOLAR SMOOTH MUSCLE. ((**X. Wu**, G.A. Meininger, G.E. Davis, J.E. Mogford, S.H. Platts and M.J. Davis)) Depts. of Medical Physiology and Pathology and Laboratory Medicine, Texas A&M University Health Science Center, College Station, TX 77843-1114.

Integrin receptors, a family of transmembrane heterodimeric proteins, provide a functional linkage between the cell interior and extracellular matrix (ECM). Recent experimental evidence indicates that integrin receptors can play an important role in signal transduction. Integrin-binding peptides have been shown to cause relaxation of arterioles (Mogford et al., Circ Res 79:821, 1996) through an interaction with the $\alpha_v\beta_3$ integrin receptor. We hypothesized that vascular smooth muscle (VSM) calcium channels were involved in this response. Single VSM cells were enzymatically digested from rat cremaster muscle arterioles and studied using patch clamp techniques. Ba^{2+} currents were measured in single VSM cells before and after application of soluble or bound (coated beads) fibronectin (FN), cRGD peptide, β_3 antibody (F11) or non-specific antibody. Soluble FN, F11 and cRGD caused a 20-50% reduction in Ba^{2+} current within 1 min; this effect was not reversed after washout. However, FN-coated beads resulted in a 20-40% elevation in calcium current 10 min after bead attachment to cells, followed by a spontaneous return to control levels. A non-specific antibody (either soluble or bound) had no effect on Ba^{2+} current, nor did beads alone, suggesting that changes in current were not the result of mechanical stimulation or non-specific interaction with protein on the beads. The data suggest that (1) integrins may be linked to L-type Ca^{2+} channels in VSM, and (2) soluble and bound ECM components mediate integrin-dependent changes in VSM Ca^{2+} current by different mechanisms. (Supported by NIH HL-45602 and HL-33324)

M-Pos46

NO-MEDIATED MUSCARINIC MODULATION OF I_{Ca} IN EARLY CARDIOMYOCYTES DERIVED FROM EMBRYONIC STEM CELLS ((G.J. JI, **B.K. FLEISCHMANN**, M.C. WELLNER AND J. HESCHELER)) Institute of Neurophysiology, University of Cologne, Robert-Kochstr. 39, 50931 Cologne, FRG.

Cardiomyocytes differentiated from pluripotent embryonic stem (ES) cells provide a new model of cardiac differentiation in vitro. We have previously shown that cells of the late stage (7+9-12 days) express a normal subset of ionic channels; in contrast, cells of the early stage (7+2-4 days) express mainly voltage dependent calcium currents (I_{Ca}) and outward rectifier K^+ currents. In the present study we investigated the modulation of I_{Ca} by the muscarinic agonist carbachol (Cch) in cells of the early stage. Single cardiomyocytes were obtained by enzymatic dissociation of embryo-like aggregates of the ES cell line D3. Spontaneously beating cardiomyocytes of the early stage were used for patch-clamp recordings in the whole cell configuration. Current clamp recordings showed a complete arrest of the spontaneous activity in most of the cells without hyperpolarization upon application of Cch (1μM) (n=17). These findings suggested, that Cch might decrease I_{Ca} and block the action potentials. To investigate this hypothesis, voltage clamp experiments were performed with 3.6 mM Ca^{2+} in the bath solution. The cells were held at a potential of -50 mV and 20 ms lasting depolarizations to 0 mV were applied. The current density in early cells was 15.7±1.5 pA/pF (n=47) and the application of Cch depressed basal I_{Ca} in 72% of cells by 62±3 %. This effect was absent after incubation of cells with PTX (1 μg/ml, 24h). Moreover the Cch induced depression of I_{Ca} could not be observed in most of the cells incubated with the NOS inhibitor L-NMMA (200 μM, 20 min) or in presence of the selective inhibitor of the soluble guanylyl cyclase, ODQ (20 μM). The non selective PDE inhibitor IBMX (100 μM) prevented the Cch induced decrease of I_{Ca} in 92% of cells. Superfusion of cells with the PDE 2 inhibitor, ENHA (30 μM), also blocked the muscarinic effect in 85% of cells. We propose that in early cardiomyocytes Cch modulates basal I_{Ca} through the NO-cGMP pathway and cGMP dependent PDE's.

M-Pos47

PHARMACOLOGICAL CHARACTERIZATION OF THE RECEPTORS INVOLVED IN THE β-ADRENERGIC STIMULATION OF L-TYPE Ca CURRENT IN FROG VENTRICULAR MYOCYTES. ((V. A. **Skeberdis**, **J. Jurevicius** and R. Fischmeister)) INSERM U-446, Univ. Paris-Sud, 92296 Châtenay-Malabry, France.

Cardiac myocytes possess both β1- and β2-adrenergic receptors. To get some insights into the respective contribution of β1- and β2-receptors in the effect of catecholamines in frog heart, we examined the effects of several β1- and β2-receptor antagonists (ICI 118551 (ICI, β2), xamoterol (XAM, β1-partial agonist), metoprolol (MET, β1)) in the presence of different β1- and β2-receptor agonists (zinterol (ZIN, β2), dobutamine (DOB, β1), salbutamol (SAL, β2), noradrenaline (NOR, β1) and isoprenaline (ISO, non selective)) on the L-type Ca current (I_{Ca}) in whole-cell patch-clamped frog ventricular myocytes. The main results are as follows: 1) XAM alone had no effect on I_{Ca}; 2) EC_{50} for the agonists used were (nM): ZIN, 2.2 < ISO, 20 < SAL, 290 < NOR, 420 < DOB, 2400; 3) whatever the agonist used to stimulate I_{Ca}, each antagonist acted with a similar K_B (nM): ICI (3.7, 3.0, 1.5) < XAM (60, 58, 61) < MET (207, 609, 456) in the presence of ISO, DOB or SAL, respectively; 4) a Schild coefficient of 1 was obtained for each set of competition curves. The rank orders of potency for β-adrenoceptor agonists and antagonists suggest that the receptors involved in the stimulation of I_{Ca} are essentially of the β2 subtype and that β1-adrenoceptors may not be functionally coupled to L-type Ca channels in frog ventricle.

M-Pos48

METHYLENE BLUE IS A MUSCARINIC ANTAGONIST IN RAT CARDIAC MYOCYTES. ((N. Abi Gerges, T. Eschenhagen, L. Hove-Madsen, **P.-F. Méry** and **R. Fischmeister**)) INSERM U446, Univ. Paris-Sud, 92296 Châtenay-Malabry, France. (spon. by R. Ventura-Clapier)

Methylene blue (MB), a guanylyl cyclase inhibitor, was shown recently to antagonize the inhibition by acetylcholine (ACh) of the isoprenaline (ISO) stimulation of the L-type Ca^{2+} current (I_{Ca}) in cardiac myocytes. Here, we examined the mechanism of action of MB in isolated rat ventricular myocytes using the whole cell patch clamp technique. The stimulation of I_{Ca} by ISO (0.01-1 μM) was reduced by ACh (1-10 μM, n=25) but was unaffected by MB (30 μM, n=5). However, MB antagonized the inhibitory effect of ACh on ISO-stimulated I_{Ca} (n=6). Surprisingly, ODQ (10 μM), another guanylyl cyclase inhibitor, did not mimic the effect of MB (n=9). Moreover, MB had no effect on the muscarinic inhibition of I_{Ca} when dialyzed inside the myocytes (n=10). In rat atrial myocytes, MB (3-30 μM) also antagonized the activation by ACh of the muscarinic K^+ current $I_{K(ACh)}$ (n=4). However, MB had little effect on $I_{K(ACh)}$ when the current increased in an agonist independent manner, upon replacement of internal GTP by GTPγS or GppNHp. Binding experiments were performed in rat ventricular membranes to examine a possible action of MB on the muscarinic receptor. MB (0.1-10 μM) displaced the QNB specific binding in a competitive manner. This binding site had a M2 footprint since QNB was displaced by AF-DX116 in the nM range and by pirenzepine in the μM range of concentrations. We conclude that MB acts as a competitive antagonist of the cardiac muscarinic receptor.

M-Pos49

THE NO-SENSITIVE GUANYLYL CYCLASE DOES NOT PARTICIPATE IN THE MUSCARINIC REGULATION OF RAT CARDIAC Ca^{2+} CURRENT. ((N. Abi Gerges, **P.-F. Méry** and R. Fischmeister)) INSERM U446, Univ. Paris-Sud, 92296 Châtenay-Malabry, France. (spon. by V. Veksler)

Recent evidence suggest that acetylcholine (ACh)-mediated inhibition of the cardiac L-type Ca^{2+} current (I_{Ca}) involves a nitric oxide (NO)-dependent stimulation of guanylyl cyclase. Here, we used the whole-cell patch-clamp technique to re-examine the effect of ACh on I_{Ca} in rat ventricular myocytes. While ACh (1-10 μM) inhibited the isoprenaline (ISO 0.01-1 μM)-stimulation of I_{Ca}, we found that ACh (0.01-10μM), unlike cGMP, had no inhibitory effect on I_{Ca} after internal dialysis with cAMP (10-50 μM, n=3-5). Moreover, ACh (1 μM) still antagonized the ISO-response when the myocytes were exposed to 10 μM ODQ (n=6) or dialyzed with 30 μM methylene blue (n=3), two guanylyl cyclase inhibitors. Surprisingly, basal I_{Ca} or I_{Ca} stimulated by ISO (10-100 nM) or cAMP (10-50 μM), was also found to be insensitive to NO-donors such as SNAP, SNP or SIN-1 (1-100 μM, n=3-4). When the internal medium was preserved using the perforated patch configuration (nystatin 200 μg/ml), SNAP (100 μM) also failed to modify the ISO (0.01-0.1μM)-stimulated I_{Ca} (n=4). We conclude that, unlike in frog ventricular myocytes (Méry *et al.*, *J. Biol. Chem.* **268**, 26286-26295, 1993), the NO-sensitive guanylyl cyclase is not efficiently coupled to L-type Ca^{2+} channels in rat ventricular myocytes. However, like in frog myocytes (Méry *et al.*, *Am. J. Physiol.* 270, H1178-H1188, 1996), we found that this mechanism does not participate in the muscarinic regulation of I_{Ca} in rat cardiac myocytes.

M-Pos50

$G_{s\alpha}$ ENHANCEMENT OF L-TYPE CALCIUM CHANNELS THROUGH AN ADENYLYL CYCLASE INDEPENDENT PATHWAY. ((A.S. Lader[1], Y. Ishikawa[2], J. Tomlinson[3], C.J. Homcy[3], D.E. Vatner[4], S.F. Vatner[4] and H.F. Cantiello[1])) 1. Renal Unit, Massachusetts General Hospital East, Charlestown, MA 02129; Brigham & Women's Hospital, Boston, MA 02115; 3. Cor Therapeutics, Inc., San Francisco, CA 94080; 4. The New England Regional Primate Research Center, Southborough, MA 01772

The α subunit of the heterotrimeric G_s protein ($G_{s\alpha}$) is crucial for β-adrenergic signal transduction in the heart. One consequence of β-adrenergic stimulation is an increase in L-type calcium currents (I_{Ca}). G_s protein-regulation of I_{Ca}, however, may be controlled through adenylyl cyclase (AC) independent pathways. In this study, the regulatory role of $G_{s\alpha}$ on cardiac I_{Ca} was assessed by applying patch-clamp techniques to neonatal cardiac myocytes from transgenic mice overexpressing $G_{s\alpha}$ (Gaudin et al., *J. Clin. Invest.* 95:1676, 1995). In transgenic mice expressing $G_{s\alpha}$, peak I_{Ca} was increased (-845 ± 155 pA/cell, n=19), as compared to either wild type controls (-224 ± 45 pA/cell, n=20), or $G_{s\alpha}$ non-expressing transgenic littermates (-313 ± 58 pA/cell, n =19). The peak activation voltage shifted from -5.5 ± 3.4 mV (n= 20) in the control myocytes to -25.3 ± 3.0 mV (n = 19, p<0.05) in the transgenic myocytes. To further assess whether $G_{s\alpha}$ regulation of Ica is independent of AC, I_{Ca} were obtained from wild type controls dialyzed with activated $G_{s\alpha}$ ($G_{s\alpha}$-GTPγS, 180 nM) with and without protein kinase A inhibitor (PKI, 5.6 μM). The peak I_{Ca} for myocytes dialyzed with $G_{s\alpha}$-GTPγS alone was -510 ± 110 pA/cell (n=4), thus statistically similar to $G_{s\alpha}$-transgenic mice. This was further confirmed by the peak activation voltage of -22.5 ± 2.5 mV (n=4), also statistically similar to the $G_{s\alpha}$-transgenic mice. The myocytes dialyzed with $G_{s\alpha}$-GTPγS and PKI had a peak I_{Ca} of -580 ± 132 pA/cell (n=5) at -18.0 ± 7.4 mV. The data indicate that $G_{s\alpha}$ enhances I_{Ca} and facilitates the activation potential through an AC-independent pathway.

M-Pos51

L-TYPE Ca^{2+} CURRENTS IN VENTRICULAR MYOCYTES FROM MICE OVEREXPRESSING $ß_2$-ADRENOCEPTORS. ((**U. Ravens**, I. Trebeß, H. Himmel, E. Wettwer, M.C. Michel*))
Inst. für Pharmakologie & *Abt. Nieren- u. Hochdruckkrankheiten, Univ. Essen, Germany.

Heart muscle of mice overexpressing the $ß_2$-adrenoceptor contracts with maximum force in the absence of ß-agonists, and this has been explained by the existence of an active form of unoccupied receptors. Since activation of adrenoceptors enhances L-type I_{Ca}, we hypothesize that increased I_{Ca} may contribute to the elevated contractile state. Overexpression of $ß_2$-adrenoceptors was confirmed by radioligand binding studies. In ventricular myocytes from adult transgenic (TG) and control mice, I_{Ca} was studied with the whole cell patch clamp technique (K^+ replaced with Cs^+; 0.6-2 mM $[Ca^{2+}]_o$; V_h -80 mV, 50 ms prepulse to -40 mV for I_{Na} inactivation, test pulse 350 ms, frequency 0.2 Hz). In 2 mM Ca^{2+}, I_{Ca} activated at -30 mV and peaked at +20 mV, peak current density was 4.22±0.32 pA/pF in TG (n=13/7, [myocytes/animals]) and 5.26±0.59 pA/pF in controls (n= 12/4; difference not significant). In myocytes from control animals, $V_{0.5}$ of steady-state inactivation was -24.9±1.8 mV, the slope factor was -4.0±0.02 mV (n=7/6). I_{Ca} increased in response to 1-10 μM isopreналine in 25 of 29 control but only in 3 of 11 transgenic cells. We conclude that overexpression in $ß_2$-adrenoceptors is not accompanied by increased I_{Ca}, and that other pathways must be responsible for the enhanced contractile state.

M-Pos52

A SINGLE AMINO ACID IN THE LOOP I-II OF THE α_1 SUBUNIT OF THE CALCIUM CHANNEL AS A MAJOR DETERMINANT OF THE INACTIVATION PROPERTIES OF THE RBA AND RBCII CALCIUM CHANNEL SUBTYPE. ((**S. Herlitze**, G.H. Hockerman, T. Scheuer and W.A. Catterall)) Dept. of Pharmacology, U. of Washington, Seattle, WA 98195-7280.

The sequence motif QxxER has been decribed to be involved in the interaction between G-protein βγ subunits and different target proteins such as adenylyl cyclase 2 or β-adrenergic receptor kinase 1. This motif is present in rbA and rbB Ca^{2+} channel α_1 subunits, which are modulated by G-proteins, but not in the non-modulated rbCII α_1 subunit, in which the arginine (R) within the QxxER motif is replaced by a glutamate (E). The QxxER motif is located in the intracellular loop connecting domains I and II of the α_1 subunit and also lies within the binding site of the Ca^{2+} channel β subunit. To analyze the effects of the amino acid at this position in rbA and rbCII α_1 subunits, wild type and mutant α_1 subunits (rbA R/E and rbCII E/R) were transiently transfected into tsA 201 cells with the β_{1b} and $\alpha_2\delta$ Ca^{2+} channel subunits. The R to E exchange in the rbA channel did not abolish G-protein modulation but had dramatic effects on channel inactivation. Steady-state inactivation was shifted to more positive potential and inactivation kinetics were slowed dramatically. The resulting currents were similar to those due to expression of the rbCII channel. Alternatively, when the rbCII channel with the reverse QxxEE to R exchange was expressed, inactivation kinetics were speeded, but there was little efffect on the steady-state inactivation. These results argue that a single amino acid within the loop I-II of the Ca^{2+} channel α_1 subunit plays a major role in the inactivation behavior of the rbA and rbCII channel subtype. Supported by NIH Grant POIHL44948 (WAC) and Deutsche Forschungsgemeinschaft.

M-Pos53

SPLICE VARIANTS OF MOUSE AND HUMAN α_{1E} Ca^{2+} CHANNEL SUBUNIT AND SOMATOSTATIN INDUCED MODULATION OF HUMAN α_{1E} TRANSFECTED IN HEK293 CELLS.

((**T. Schneider**, A. Pereverzev, M. Henry, R. Vajna, S. Olyschläger, H. Grabsch, G. Mehrke, J. Hescheler)) Inst. Neurophysiology, University of Köln, Robert-Koch-Str. 39, D-50931 Köln, Germany. (Spon. by T. Schneider)

The human α_{1E} subunit has been cloned as a shorter (α_{1E}-*sh*, Williams et al., 1994) and a longer splice variant (α_{1E}-*lo*), which mainly differ by a 129 bp insertion in the 3'-end/C-terminus. The expression pattern of α_{1E}-*sh* and α_{1E}-*lo* was investigated in an *in vitro* differentiation system (embryoid bodies), using RT-PCR and single cell RT-PCR. More fragments from α_{1E} splice variants (II/III linker and C-terminus) were amplified from mouse brain and human cerebellum, revealing *in vivo* variability of α_{1E} transcripts.
In stably transfected HEK293 cell lines the expression and modulation of α_{1E}-*lo* was investigated. Inward currents were reduced in amplitude and exhibited a slowing of activation and inactivation after stimulation of the cells with somatostatin (SST) or with carbachol, ATP or adenosine. The SST mediated inhibition of α_{1E} mediated Ca^{2+} current was reduced after preincubating with pertussis toxin (PTX). Internal perfusion of the cells with the G-protein inactivating agent GDP-β-S or the permanent activation with GTP-γ-S also decreased the SST effect. This indicates that modulation of the α_{1E} mediated Ca^{2+} current in stably transfected HEK293 cells is possible via endogenous SST receptor and involves pertussis toxin sensitive G-proteins.

M-Pos54

Modulation of Ca^{2+} Channel Currents by Cyclic Nucleotides in Smooth Muscle Cells from Rabbit Portal Vein
((**V. Ruiz-Velasco**, J.R. Hume, and K.D. Keef)) Department of Physiology and Cell Biology, University of Nevada, Reno, NV 89557.

Cyclic nucleotides are known to modulate L-type Ca^{2+} channel activity in vascular smooth muscle cells (VSMC) but the mechanism underlying the effects of PKA and PKG remains controversial. The purpose of the present study was to investigate the role of the PKA and PKG pathways in modulation of Ca^{2+} channel currents employing the whole-cell patch-clamp technique (20-22°C). Peak inward Ba^{2+} (5 mM) currents were elicited by voltage steps to +10 mV for 200 ms from a holding potential of -60 mV every 20 sec. Both 8-Br-cAMP (0.1 mM) and the adenylate cyclase activator, forskolin (1 μM), increased Ba^{2+} currents whereas the inactive analogue, 1,9-dideoxyforskolin, inhibited Ba^{2+} currents. In contrast, 8-Br-cGMP (0.1 mM) and 8-Br-cAMP (1 mM) both inhibited Ba^{2+} currents. In the presence of the selective cGMP kinase inhibitor Rp-8-Br-cGMPS (15 μM), 8-Br-cGMP (0.1 mM) enhanced Ba^{2+} currents. These results suggest that VSMC Ca^{2+} channel currents are inhibited by cGMP-dependent protein kinase and enhanced by cAMP-dependent protein kinase, and that following blockade of cGMP-dependent protein kinase, cGMP may enhance Ca^{2+} channel currents via activation of cAMP-dependent protein kinase. The results further suggest that forskolin may have additional inhibitory effects on Ca^{2+} channel currents which are independent of cAMP. Supported by AHA Nevada Affiliate, HL40399 and HL 49254.

M-Pos55

IDENTIFICATION OF THE PROTEIN KINASE C ISOFORMS PRESENT IN HUMAN HEART. ((**H-G Shin, K.T. Murray**)) Department of Pharmacology, Vanderbilt University, Nashville TN 37232 (Spon. by K.T. Murray)

Studies of functional modulation of ion channels by protein kinases have often reported inconsistent results depending on the cellular expression system utilized. One possible explanation for these discrepancies could be the heterogenous expression of protein kinase in different cell systems. For example, isoforms of protein kinase C (PKC) are expressed in a cell-specific manner. To understand the relevance of ion channel regulation by kinases, it is useful to determine the kinase isoforms present in the native cells from which the ion channel is derived. Effects of PKC activation on human cardiac voltage-gated sodium channel (hH1) have been studied previously demonstrating a significant reduction of current amplitude without much change in the voltage-dependence of channel gating or kinetics. To determine what types of PKC isoforms are present in human heart, Western blotting was performed on human heart homogenates using isoform-specific antibodies. Initial results suggest that PKC-α, βI, βII, and ζ were detected whereas PKC-γ, δ, ε, and η were not. Studies using antibodies against different isotope sites have thus far confirmed PKC-α, βI and βII expression in human heart. Experiments are underway to confirm the identity of PKC isoforms localized to ventricular myocytes. Effects of human cardiac-specific PKC isoforms on hH1 modulation then will be investigated.

M-Pos56

EFFECTS OF A CONSERVED N-GLYCOSYLATION IN EXPRESSION AND FUNCTION OF A CYCLIC NUCLEOTIDE-GATED CHANNEL .

((C.-S. Park, H.H. Lim, and S.-H. Rho)) Dept. of Life Science, Kwangju Institute of Science and Technology, Kwangju, 506-303, Korea.

Cyclic nucleotide-gated (CNG) channels cloned in various tissues contain one or more consensus N-glycosylation sequences in the small extracellular loop connecting S5 trans-membrane domain and the pore-region. Intrigued by their evolutionary conservation and the proximity to the ion conduction pathway, we studied the significances of the N-glycosylation in channel's expression and function. The glycosylation site of the bovine retinal CNG channel, Asn327, was mutagenized to Ser and the mutant channels were expressed in *Xenopus* oocyte. Immunoblot analysis showed that the oocytes injected with N327S mutant message produced a single protein band co-migrating with the smaller size of wild type protein and with the single band found in the tunicamycin-treated wild type channel. However, the expression level of mutant protein was found to be comparable to that of wild type. The mutant channel was functionally active and the macroscopic characteristics of the channel current were not significantly altered compared to the wild type. The expression pattern of the wild type and the mutant channels are currently studied in PC-12 cells for the possible role of N-glycosylation in intracellular targeting.

M-Pos57

NUCLEOTIDE-ACTIVATED CATION CURRENTS IN RAT RETINAL PIGMENT EPITHELIAL CELLS

((J.S. RYAN AND **M.E.M. KELLY***)) Departments of Pharmacology and Ophthalmology*, Dalhousie University, Canada, B3H 4H7.

We used patch-clamp recording techniques to investigate purinergic-activated currents in rat retinal pigment epithelial (RPE) cells. Using 140 mM K^+-aspartate in the pipette and 140 mM NaCl Ringers, rat RPE possessed both inward and outward K^+ currents. Puffer application of 100 μM adenosine triphosphate (ATP) induced an inward current measured at - 60 mV (206 ± 25 pA; n = 35). This current desensitized in the continued presence of agonist and recovered ~ 3 min. after withdrawal of the agonist. The current-voltage relationship showed inward rectification and reversed close to 0 mV. Replacement of extracellular sodium with choline significantly reduced the ATP-induced inward current (27 ± 7%; n = 3) suggesting the activation of a cation conductance. The current elicited by ATP was almost completely insensitive (9.5% block in 2/5 cells tested) to the common P_{2x} receptor antagonist suramin (100 μM). Adenosine A receptors did not appear to be involved in mediating ATP-induced currents in RPE cells, as adenosine (100 μM) did not produce any detectable response (n = 9). Inward currents were, however, elicited at -60 mV (75 ± 10 pA; n = 4) by puffer application of the pyrimidine derivative, uridine triphosphate (UTP; 100 μM). These results demonstrate for the first time the existence of purinoceptor-regulated ion channels in rat RPE cells. Our evidence showing current activation in response to both ATP and UTP may indicate the involvement of P_{2U} nucleotide receptors. Supported by NSERC OGP0121657.

M-Pos58

COOPERATIVE CHANNEL GATING IN MULTICHANNEL PATCHES.

((S. Harju, J. D. Wesley and K. Manivannan)) Dept. of Chemistry and Physics, Southeastern Louisiana University (SLU), Hammond, LA 70402. (Spon. Yi Liu)

Most of the analysis of single channel data presented in the literature assumes independently acting identical ion channels. However, although many channels act independently, there is evidence for interacting channels suggesting a cooperative behavior of gating. We analyze multichannel data from chloride channels and potassium channels using previously reported model-*independent* methods.[1,2] We first apply some simple tests based on binomial distributions to the steady state probabilities and check for any non-independent gating. We then extend our data analysis by utilizing a recently formulated stochastic Markovian model that involves only two parameters.[3] Our analysis using such a simple model is a first step toward understanding the salient features of cooperative channel gating. Determination of the parameters characterizing cooperative gating behavior may have far-reaching implications for modelling, and our understanding, of membrane function, drug action, and electrical conduction.

Work supported by the Louisiana Education Quality Support Fund (1995-98)-RD-A-21 and SLU Faculty Development Grant to K.M.

[1]Manivannan et al., 1992, *Biophys. J.* **61**:216-227.
[2]Ramanan et al., 1992, *J. Neurosci. Meth.* **42**:91-103.
[3]Manivannan et al., 1996, *Bull. of Math. Biol.* **58**(1):141-174.

M-Pos59

DUAL-WAVELENGTH RATIOMETRIC FLUORESCENCE MEASUREMENT OF TRANSMEMBRANE POTENTIAL AND INTRAMEMBRANE DIPOLE POTENTIAL IN SINGLE N1E-115 NEUROBLASTOMA CELLS

((**Jing Zhang**, Robert M. Davidson*, Mei-de Wei, Leslie M. Loew)) Department of Physiology, University of Connecticut Health Center, Farmington 06030, and *Basic Science Division, New York University College of Dentistry, 345 E. 24th Street, New York, NY 10012.

A previous dual-wavelength ratio imaging study from our lab has shown that the fluorescent potentiometric dye 1-(3-sulfonatopropyl)-4-[β[2-(di-n-octylamino)-6-naphthyl]vinyl]pyridinium betaine (di-8-ANEPPS) can be used to measure the intramembrane dipole potential and transmembrane potential in artificial bilayers, both of which contribute to intramembrane electric fields. In the present study, we use the whole cell patch clamp technique to accurately calibrate the ratio against transmembrane potential in single N1E-115 neuroblastoma cells. After a whole-cell patch was obtained, the membrane potential was clamped to a level varying from -100mV to 60mV and a pair of images was taken with excitation wavelengths of 440nm and 530nm respectively. After the correction of the flat-field and background, the ratio of the membrane fluorescence (R) was calculated and normalized. Using this method, we have found that the R value changes about 14% per 100mV transmembrane potential, which correlates well with the result (12% per 100mV change) using the potassium/valinomycin calibration method. When treated with 200μM 6-ketocholestanol (6-KC), a well-known modulator of intramembrane dipole potential, the R value started increasing from 10min after the treatment and did not reach equilibrium within 60min in 5 cells. Considering that the dye was 8-fold more sensitive to intramembrane dipole potential than to the transmembrane potential, based on the model membrane studies, the dipole potential of the cell membrane increased ~20mV, ~63mV, and ~94mV at 20min, 40min, and 60min respectively. The combination of whole cell patch clamp and ratio imaging therefore provides a powerful approach toward investigation of intramembrane electric fields and their effects on ion channels. (Supported by NIH Grant GM35063)

M-Pos60

INACTIVATION PROPERTIES OF VOLUME-REGULATED ANION CURRENT (VRAC) ARE INDEPENDENT OF ICLN.

((I. Levitan, M. D.Hubert, M. Hofreiter and S.S. Garber) Allegheny University of Health Science, Philadelphia, PA 19127).

Activation of VRAC by cell swelling initiates volume regulatory decrease in a variety of cell types. A characteristic feature of VRAC is voltage-dependent inactivation. Inactivation properties vary among the cell types: inactivation develops at voltages >40 mV, >60 mV and >80 mV in T84, myeloma and TSA cells respectively. The molecular identity of VRAC is uncertain. I_{Cln}, a 235 amino acid protein may be a VRAC regulator protein or VRAC itself. In this study we have addressed whether I_{Cln} is responsible for the inactivation properties of VRAC. I_{Cln} was isolated from T84 or myeloma cells and expressed in TSA cells. If I_{Cln} was responsible for the inactivation properties of VRAC, expression of T84 or myeloma-derived I_{Cln} in TSA cells should result in altering VRAC inactivation properties in the host cell. Total RNA was isolated from myeloma and T84 cell lines. Reverse transcription followed by PCR was used to generate I_{Cln} cDNA from either cell line. cDNAs were then subcloned into pCRIII for further analysis. I_{Cln} from T84 or myeloma cells was expressed in TSA cells using Ca2+ phosphate transfection procedure. Co-expression of I_{Cln} and green fluorescent protein was used in order to identify individual TSA cells that were successfully transfected. VRAC was activated by exposing the cells to a mild osmotic gradient. Expression of I_{Cln} from either source in TSA cells induced an increase in the activation rate of VRAC in response to an osmotic gradient. Inactivation properties of the current were not affected. This result indicates that I_{Cln} is not responsible for the inactivation properties of VRAC.

M-Pos61

POLYAMINE-INDUCED MODULATION OF BACTERIAL PORINS: COMPARISON BETWEEN OMPC & OMPF. ((**R. Iyer** and A. H. Delcour)) Dept. of Biology, University of Houston, Houston, TX 77204.

Polyamines are a class of positively charged polybasic compounds found in a wide variety of cell types. Patch-clamp experiments show that all four polyamines inhibit *E. coli* porin activity in a voltage-dependent manner, promoting higher frequency, longer durations and often the cooperativity of closing events. Modulation is accompanied by a loss in the number of active channels, reducing the total current through the patch. In addition, we show that OmpF appears to be more sensitive to polyamines compared to OmpC, with the effect being more drastic with spermine. Even the rate of perfusion of the polyamine has a strong influence on the reduction in the number of active channels. Usually a slow perfusion (~8 min.) leads to more reduction compared to a faster (~1-2 min.) one. Preliminary experiments show that polyamines may be able to modulate these channels from either side of the membrane. The comparison of the effects evoked by spermine and cadaverine suggest that these 2 compounds differ in the induced pattern of closing activity. In conclusion, all 4 polyamines appear to be effective modulators of porins and may be associated with this function *in vivo*. (Supported by NIH grant AI34905)

M-Pos62

THE GEOMETRY OF THE WATER LUMEN OF COLICIN IA ION CHANNELS IN PLANAR LIPID BILAYERS. ((**O.V.Krasilnikov**, J.B. Da Cruz, L.N.Yuldasheva, W.A Varanda and R.A. Nogueira)) Dept. Biophysics and Radiobiology, UFPE, 50670-901, Recife, PE, Brazil.

To evaluate the inner structure of the water lumen of Colicin Ia ion channels (including a possible constriction and its localization) a new approach was worked out. The method is based on the determination of channel filling by different non-electrolyte molecules through each side of the ion channel. Our results show that the water lumen of the Colicin Ia channel has a funnel-like structure with a small *trans*-entrance, with a diameter around 1.0 nm, and a large *cis*-entrance, with a diameter of approximately 1.84 nm. A constriction with a diameter of approximately 0.68 nm is shown to be located close to the *trans*-entrance of the channel. Application of the method in patch clamp studies of single ion channels is discussed.

M-Pos63

ESTIMATE OF THE PORE SIZE OF THE LARGE MECHANOSENSITIVE ION CHANNEL (MscL) OF *ESHERICHIA COLI*. ((**C. Cruickshank**, R.F. Minchin, A.C. Le Dain and B. Martinac)) Dept. of Pharmacology, University of Western Australia, Nedlands, WA 6907, Australia. (Spon. by A.C. Le Dain)

We used large organic cations such as spermine, BMBB[1] and poly-L-lysines (PLL) to probe the size of the channel pore of the large-conductance mechanosensitive ion channel (MscL) of *E. coli*. The isolated recombinant MscL protein was reconstituted into artificial liposomes[2] and examined for function by the patch-clamp technique. Neither 100 µM spermine (~15 Å), 100 µM BMBB (~30 Å) nor 100 µM PLL-19 (~25 Å) significantly reduced the conductance of the channel. At the same concentration, PLL's ≥37 Å in diameter blocked the channel by reducing its conductance to ~30 % of control. In parallel, we calculated the pore size of the MscL using (i) its conductance[3] and (ii) the recently proposed homohexameric model of the MscL in which each of the monomers contains two membrane-spanning α-helices[4]. The calculated pore size corresponding to the channel conductance of 3.8 nS in 200 KCl was 42 Å, whereas the estimated pore size obtained from the model was 34 Å. All three approaches were in good agreement, resulting in an average pore size of the MscL channel of approximately 37 Å. We also investigated whether polyamines permeated the channel. Under control conditions (symmetric 10mM KCl, 40mM $MgCl_2$, 5 mM HEPES, pH 7.2) the conductance was 0.90 ± 0.01 nS. With 100 mM polyamine added to the bath solution, the conductance significantly increased (putrescine: 1.6 ± 0.1 nS, cadaverine: 1.6 ± 0.1 nS, spermine: 1.9 ± 0.1 nS). In addition, an anionic analogue of cadaverine, succinate, also increased channel conductance (1.4 ± 0.1 nS). The increase in MscL conductance indicates that these ions permeate the channel, which is consistent with our estimate of the pore size.

(1) BMBB is 1,1'-bis[3-(1-methyl-[4,4'-bipyridium]-1-yl)-propyl]-4,4'-bipyridium.
(2) Häse *et al.* (1995) *J. Biol. Chem.* 270(32): 18329-18334.
(3) Hille (1992) *Ionic Channels of Excitable Membranes* Sunderland: Sinauer.
(4) Blount *et al.* (1996) *EMBO J.* 15 in press.

M-Pos64

MscL, a Large Conductance Bacterial Mechano-Sensitive Channel, Is a Pre-Assembled Homohexamer. ((**Sergei I. Sukharev**,* Paul Blount,* Matthew J. Schroeder,* Darrell R. McCaslin‡ and Ching Kung*†)) *Laboratory of Molecular Biology, Departments of †Genetics and ‡Biochemistry, University of Wisconsin, Madison, WI 53706.

One of several hypotheses for the mechanism of channel modulation by mechanical stress states that membrane tension favors the insertion of new subunits into a multimeric channel, thus affecting channel conductance (Opsahl and Webb, *Biophys. J.* 66:71). In the present biochemical study of multimeric MscL channels we address the question of whether MscL complexes are pre-formed and contain a fixed number of subunits. Consistent with our recent studies (Blount et al., *EMBO J.* 15:4798), the functional expression of double and triple tandems of MscL subunits linked in a single ORF, and the SDS-PAGE patterns of *in situ* cross-linked products of wild-type MscL and the tandems suggested a hexameric channel assembly. Size-exclusion experiments show that MscL, extracted from non-stressed native membranes by a mild detergent, emerges as a sharp peak of uniform particles much heavier then a monomer. Independently, the molecular weight of purified 6His-tagged MscL complexes, assayed by both size-exclusion and analytical centrifugation was consistent with the hexamerization. Because no monomeric MscL subunits were found in membranes or membrane extracts, we conclude that MscL gates by a conformational transition in a pre-assembled complex, but not by a recruitment of new subunits. (Supported by NASA NAGW-4934; NIH GM47856; PB is a DOE-energy biosciences fellow of the Life Sciences Research Foundation).

M-Pos65

CALCIUM CHANNELS IN *ESCHERICHIA COLI* CHEMOTAXIS ((**Jia-Qiang He** and Julius Adler)) Departments of Biochemistry and Genetics, University of Wisconsin-Madison, Madison, WI 53706

The concentration of intracellular free-calcium ions in *Escherichia coli*, measured by fluorescent calcium dye indicators, briefly increases or decreases when repellents or attrantants, respectively, are added to the bacteria (L. S. Tisa and J. Adler, Proc. Natl. Acad. Sci. USA 1995, 92:10777-10781). The chemotaxis was inhibited by a calcium channel blocker, ω-conotoxin (L. S. Tisa, B. M. Olivera, and J. Adler, J Bacteriol. 1993, 175:1235-1238). By use of the patch-clamp technique, it has now been observered that the whole-cell calcium currents in giant protoplasts of *E. coli* could be inhibited by 1.3 x 10^{-7}M ω-conotoxin, but there was no effect of other calcium channel agents, 10^{-6}M nifedipine (antagonist) and 1.4 x 10^{-6}M Bay K 8644 (agonist). The preliminary data suggest that there probably exist voltage-gated calcium channels at the inner membrane of *E. coli*. The role of calcium channels in *E. coli* chemotaxis is being determined and will be discussed.

M-Pos66

EFFECT OF POINT MUTATIONS ON THE PROPERTIES OF THE AEROLYSIN CHANNEL. ((**C. Lesieur**[1], J.T. Buckley[2], G.van der Goot[1], and F. Pattus[3])) [1]Dept. of Biochemistry, Univ. of Geneva, Geneva CH1211; [2]Dept.of Biochem. and Microbiol., Univ. of Victoria, V8W3P6 Canada; [3]ESBS, UPR 9050, CNRS, Illkirch, F67400. (Spon. by S. Edelstein).

Aerolysin is a pore-forming toxin secreted by the Gram negative bacteria, *Aeromonas hydrophila*. The toxin is responsible for the pathogenicity of this organism in mammals. The protein is secreted as an inactive dimer called proaerolysin. Proteolytic removal of a C-terminal fragment is necessary for the subsequent activation. The toxin then binds to a receptor on the surface of the target cell, leading to the formation of a heptameric transmembrane channel that induces cell lysis. According to the model of the heptameric form of the toxin, domain III forms the mouth of the channel and domain IV the channel itself. In order to challenge the model and to obtain more structural data about the transmembrane portion of aerolysin, the effects of point mutations in domain III have been analyzed. Lysine 229 (K229), a charged residue buried in the interior of the protein was changed to either glutamine (Q: polar) or leucine (L: apolar). The studies of these mutants in planar lipid bilayers showed that the mutations affected the aerolysin channels in several ways. The channels formed by the two mutants fluctuated in contrast to those formed by the wild-type protein, suggesting a possible role for K229 in controling channel opening and closing. Moreover, K229L induced the formation of channels that were no longer sensitive to negative voltages. However, voltage gating for K229Q was not affected. These observations suggest that K229 is in the voltage sensing area of the toxin. The capacity to form channels was strongly inhibited by both mutations. Parallel studies showed that the mutations affect both the insertion and the preceding oligomerization step.

M-Pos67

PROBING THE VDAC CHANNEL BY EXAMINING THE pH DEPENDENCE OF ITS SELECTIVITY AND THE OPEN-CHANNEL CURRENT NOISE ((**T.K.Rostovtseva**[1], T. T. Liu[2], M.Colombini[2], and S.M.Bezrukov[1])) LSB/DCRT, NIH, Bethesda, MD 20982[1]; Dept. of Zoology, Univ. of Maryland, College Park, MD 20742[2]

When reconstituted into planar phospholipid membranes, the mitochondrial channel,VDAC, forms highly-conductive and voltage-gated channels. Its properties are highly conserved irrespective of source. However, the pH dependence of the ion selectivity is different for VDAC isolated from *N. crassa* as compared to the yeast, *S. cerevisiae*. The change occurs in a range consistent with histidine titration. It was previously shown (*Phys.Rev.Lett.* 70, 2352 (1993) and *Biophys.J.* 69, 94 (1995)) that reversible ionization of amino acid residues inside the channel's aqueous pore is a source of measurable noise. The noise amplitude is determined by the number of ionizable residues, their pK, their kinetic parameters, and their position in the pore. The current noise of the open channel as a function of bulk solution pH was studied. It was found that the low-frequency open channel noise is different in two VDAC channels. While noise from VDAC from *Neurospora* channel exhibits a clear peak at pH 6.0, this peak is absent in the case of VDAC from the yeast. This dramatic change is consistent with the pH dependence of ion selectivity and should reflect the inferred differences in number and/or location of histidine residues lining the walls of the pore.

M-Pos68

THE GATING PROCESS OF VDAC AS PROBED BY USING BIOTIN STREPTAVIDIN SYSTEM. ((**J.Song**[1], M.Forte[2], Blachly-Dyson[2] and M.Colombini[1])) 1 Dept. Of Zool., Univ. Of Maryland, College Park, MD 20742. 2 Vollum Institute, Oregon Health Sciences Univ., Portland, OR 97201- 3098

VDAC, a channel in the mitochondrial outer membrane, has two gating processes one at positive and one at negative potentials. We carried out these experiments to test the proposed working model that the channel is a barrel and closure involves the translocation of portions of the wall of the barrel out of the membrane to the surface. After substitution of specific amino acids of N.*crassa* VDAC with cysteine residues followed by biotinylation, the channels were reconstituted into planar phospholipid membranes. When the cys was introduced into the appropriate part of the sensor region, addition of streptavidin to the right side of the membrane trapped the channel in a closed state and stopped the gating processes (by binding to the biotinylated cys). In this way, some of the sensor region has been identified. This is also consistent with the proposal that the sensor moves out of , not into, the channel during the closing processes. In addition, the binding of streptavidin to the cys from one side of the membrane stopped both of the gating processes. This indicated either that the same residue was involved in both of the gating processes, or that there is only one sensor for the two gating processes. In most cases, only addition of streptavidin to the right side had the effect, while the addition to the other side had no effect. Thus the biotinylated site reached the surface in only one of the closed conformation. Furthermore, simultaneous biotinylation at two sites was used to assess if both sites were on the same side or opposite side of the membrane. (Supported by NIH grant GM35759)

M-Pos69

CHARACTERISTICS OF BACTERIALLY EXPRESSED VDAC: ROLE OF THE N-TERMINUS IN CHANNEL GATING. ((**D.A. Koppel**, K.W. Kinnally, C.A. Mannella)) The Wadsworth Center, Empire State Plaza, Albany NY 12201-0509; Department of Biomedical Sciences, University at Albany, SUNY.

VDAC genes from *S. cerevisiae* and *N. crassa* (scVDAC and ncVDAC; gifts of M. Forte, Oregon Health Sciences Univ) have been expressed in *E. coli*. Both bacterially expressed proteins are similar to their mitochondrial counterparts in terms of channel-forming activity (in phospholipid bilayers) and far-UV circular dichroism spectra. In LDAO at pH 6-8, ncVDAC is very soluble (>5 mg/ml) and displays a CD spectrum indicating high β-sheet content. ScVDAC is less soluble (2 mg/ml) and it's CD spectrum is like that of ncVDAC at pH 4.0, (Shao et al.,1996, *Biophys. J.* 71:778) consistent with a lower β-sheet content. The presence of a 20-residue, his_6-containing extension at the N-terminus of both proteins causes a small change in CD spectra and no change in channel function. Conversely, truncation of the first 8 residues of scVDAC does not significantly alter CD spectra but results in channels that exhibit voltage-independent current transitions that flicker rapidly. Popp et al. (1996, *J. Biol. Chem.* 271;13593) have shown that replacing residues 2-12 of ncVDAC with a 12-residue, his_6-containing segment also results in a channel that flickers rapidly but displays voltage-dependent closure. Thus, it appears that one or more residues in the region 2-8 are important for stabilizing the open state of VDAC, and that shortening (but not lengthening) the N-terminal region of the polypeptide causes loss of voltage dependence. (Supported by NSF grant MCB-9506113.)

M-Pos70

A COMPARISON OF THE PEPTIDE-SENSITIVE CHANNELS OF THE INNER AND OUTER MEMBRANES OF MITOCHONDRIA FROM VDACless YEAST. ((C. Muro[1], M.L. Campo[1], E. Blachly-Dyson[2], M. Forte[2], T.A. Lohret[3] and K.W. Kinnally[3])) [1]Dpto. de Bioquimica, Univ. de Extremadura, 10071 Caceres, Spain, [2]Vollum Inst., Oregon Health Sciences Univ., Portland, OR 97201-3098; Div. Molecular Medicine, Wadsworth Center, Albany, NY 12201

Mitochondria were isolated from yeast strains in which each of the two genes encoding VDAC proteins were eliminated. The inner and outer membranes were purified and reconstituted by fusion with liposomes. The conductances measured by patch clamp techniques indicate that similar high conductance channel activities exist in the inner and outer membranes of mitochondria, which correspond to MCC (multiple conductance channel) and PSC (peptide sensitive channel) respectively. MCC and PSC have similar peak conductances, transition sizes and cation-selectivity. Furthermore the presequence peptide, yCOX-IV, induces a rapid flickering between the open, half open and closed states in both activites. The peptide-induced flickering of both MCC and PSC is reversed by washing with trypsin. Our results indicate MCC and PSC are very similar but neither activties are affected by deletion of VDAC in this reconstituted system. A comparison of the effects of other peptides is underway.
(Supported by D.G.I.C.Y.T. PB95-0456, Junta de Extremadura-Fondo Social Europeo EIA 94-11 (C.M. & M.L.C.), NIH #GM35759 (E.B.-D. & M.F.) and NSF MCB 9513439 (T.A.L. & K.W.K.)

M-Pos71

PATCH-CLAMP STUDIES OF THE EFFECT OF BCL-2 OVEREXPRESSION ON MCC ACTIVITY IN HUMAN FIBROBLASTS ((**R.C. Murphy**[1,2], M. King[3], J.J. Diwan[2] and K.W. Kinnally[1])) [1]Molecular Medicine, The Wadsworth Center, Empire State Plaza, Albany NY 12201-0509; University at Albany, SUNY, Albany, NY, [2]Biology, Rensselaer Polytechnic Inst., Troy, NY, [3]College of Physicians and Surgeons of Columbia Univ., New York, NY

MCC is a very high conductance channel located in the inner mitochondrial membrane. While originally described in mouse and rat mitochondria, its activity has also been observed in mitochondria from human fibroblasts and osteosarcoma cell lines. Data regarding preparation of mitochondria from these tissue culture cell lines will be presented.
Recent studies of others implicate a role for mitochondria and its calcium induced permeability transition in programmed cell death. One candidate for the pore that causes this transition is MCC due to it's the large pore size and pharmacology. Bcl-2 is a protooncogene that suppresses programmed cell death. Data concerning the frequency of MCC in patches of mitoplasts from parental and Bcl-2 *overexpressing* fibroblasts will be presented. (Supported by a grant from the NSF MCB-9513439.)

M-Pos72

MODULATION OF A YEAST MITOCHONDRIA INNER MEMBRANE CHANNEL BY MATRIX NUCLEOTIDES. ((C. Ballarin, A. Bertoli and **M. C. Sorgato**)) Università degli Studi di Padova, Dipartimento di Chimica Biologica, Via Trieste 75, 35121 Padova, Italy.

The inner membrane of yeast mitochondria has been shown to contain at least two distinct channel activities, having in common a preferential anionic selectivity (P_{Cl}/P_K ranging between 3 and 4), but otherwise displaying different electrophysiologic features (1). We previously studied the effects of ATP on one of these channels, which has a unitary conductance of about 45 pS (in simmetrical 150 mM KCl) and is only slightly voltage dependent. We demonstrated that ATP acts from the matrix side by blocking channel activity in a voltage dependent way with an IC_{50} of 0.24 mM at physiological (negative) potentials. We now present evidence that sub-maximal ATP concentrations apparently lower the single channel conductance as well, and that other molecules may be involved in channel modulation. Up to 2 mM, cAMP, although it does not considerably decrease neither open probability nor unitary conductance, protects channel activity from ATP inhibition. Indeed, with the membrane inner side exposed to approx. 2 mM cAMP, 3 mM ATP induces only a partial block, thus suggesting a possible competitive binding of the nucleotides to the same site(s). Consistent with this hypothesis, increasing cAMP concentrations (in the range of 0.1-2 mM) result in a progressive and apparently incomplete removal of a 1.5 mM ATP pre-induced block of the currents. In a similar fashion, ADP, which generates a less prominent inhibition of the channel activity, also seems to prevent, in the same concentration range, the total block of the currents induced by ATP. Taken together these results offer an intriguing insight into the regulation mechanisms of the inner membrane channels of yeast mitochondria.

1. Ballarin C. and Sorgato M.C. (1995) J. Biol. Chem. 270, 19262-19268

M-Pos73

SULFONYLUREA RECEPTOR – K^+ CHANNEL COUPLING IN THE MITOCHONDRIAL K_{ATP} CHANNEL. ((K. D. Garlid, M. Jaburek, V. Yarov-Yarovoy and P. Paucek)) Dept. of Chem., Biochem. and Mol. Biol., Oregon Graduate Institute, P.O. Box 91000, Portland, OR 97291-1000.

MitoK_{ATP} functions as an intracellular drug receptor and may be the site of action for the cardioprotective effects of K^+ channel openers (KCO) (Garlid et al., J. Biol. Chem. **271**, 8796-8799, 1996). Glyburide has been shown *in vivo* to prevent cardioprotection by KCOs; however, it has been difficult to demonstrate glyburide effects in isolated, respiring mitochondria. Thus, glyburide inhibits K^+ flux ($K_{1/2}$ = 30 μM) in the ***non-physiological open state*** (no Mg^{2+} or ATP); however, this is *not* due to inhibition of mitoK_{ATP}, because glyburide ≥ 20 μM strongly inhibits respiration. We now report that glyburide is a selective inhibitor of K^+ flux ($K_{1/2}$ = 3 μM) in the ***pharmacological open state*** (Mg^{2+}, ATP, and KCO such as cromakalim and diazoxide). 5-Hydroxydecanoic acid was similarly ineffective in the non-physiological open state, and effective ($K_{1/2}$ = 70 μM) in the pharmacological open state. MitoK_{ATP} is composed of a 55-kD K^+ channel coupled to a 63-kD sulfonylurea receptor (mitoSUR), which was identified by BODIPY-Fl glyburide photolabeling (Garlid et al., Biophys. J. **70**, A311, 1996). Our results demonstrate that mitoSUR reacts with glyburide in a manner depending on the presence of mitoSUR ligands and also support a role for mitoK_{ATP} in cardioprotection. (Supported by NIH grant GM 31086.)

M-Pos74

SULFONYLUREA RECEPTOR OF THE MITOCHONDRIAL K_{ATP} CHANNEL ((Petr Paucek, Vladimir Yarov-Yarovoy and Keith D. Garlid)) Department of Chemistry, Biochemistry and Molecular Biology, Oregon Graduate Institute of Science and Technology, P.O. Box 91000, Portland, OR 97291-1000

The mitochochondrial K_{ATP} channel (mitoK_{ATP}) is inhibited by glyburide and activated by potassium channel openers and may be a pharmacologically important receptor for these drugs (Garlid *et* al. J. Biol. Chem. **271**, 8796-8799, 1996). We report tentative identification of the sulfonylurea receptor that regulates mitoK_{ATP}. Inner mitochondrial membranes were photolabeled with 50 nM ***BODIPY-Fl glyburide***, solubilized with detergent and fractionated on DEAE-cellulose. The active fraction was the only one exhibiting labeling that was displaced by 1 μM glyburide. This fraction was further analyzed by preparative SDS-PAGE. In three independent experiments, a single protein at 63 kD was labeled with the fluorescent probe. Based on our previous work, the mitoK_{ATP} appears to be a heteromultimer consisting of an inward-rectifying K^+ channel (mitoKIR) and a regulatory sulfonylurea receptor (mitoSUR). (Supported by NIH grant GM 31086 and AHA grant to P.P.)

M-Pos75

EFFECTS OF SIGNAL AND NON-SIGNAL PEPTIDES ON MITOCHONDRIAL PERMEABILITY. ((**Yuliya E. Kushnareva**[1], K.W. Kinnally[2] and P.M. Sokolove[1])) [1]Dept. Pharmacol., Univ. MD Med. Schl., Baltimore, MD, [2]Molecular Medicine, Wadsworth Center, NYS Dept. of Health, Albany, NY.

We have recently reported that the signal peptide of *N. crassa* cytochrome oxidase subunit IV (pCoxIV) increases the permeability of isolated rat liver mitochondria [*Arch. Biochem. Biophys.* (1996) in press]. That study has been extended to include an additional 12 peptides with the following results. (1) All signal peptides tested (yeast $CoxIV_{1-13}$, $yCoxIV_{1-22}$, $yCoxVI_{1-20}$, bovine $CoxIV_{1-13}$), except yF1-ATPase β-$subuit_{1-19}$, increased permeability, as indicated by mitochondrial swelling. (2) Two non-signal peptides, a scrambled version of the yCoxIV 13-mer (scrIV) and pAT III, also induced swelling. (3) SMS1, SynB2, and three peptides from the *N. crassa* voltage-dependent, anion-selective channel all failed to elicit swelling. (4) Swelling induced by signal peptides was dependent on membrane potential; that induced by scrIV and pAT III was not. (5) The relative efficacies of the peptides in inducing both a permeability increase in liver mitochondria and flicker blockade of the multiple conductance channel (MCC) of proteoliposomes containing inner membranes from yeast mitochondria were the same. These data support the hypothesis that the MCC is involved in protein import and possibly in the mitochondrial permeability transition. In addition, they suggest that enhancement of mitochondrial permeability by signal sequences requires characteristics beyond positive charge and the ability to form α-helices. [Support: Amer. Heart Assoc. (#94007080) and NSF (MCB117658)]

M-Pos76

AGING EFFECTS ON THE MITOCHONDRIAL PERMEABILITY TRANSITION (PT). ((**Aya Sultan** and P.M. Sokolove)) Department of Pharmacology, University of Maryland Medical School, Baltimore, MD.

Mitochondria containing Ca^{2+} can be induced by a variety of experimental conditions to undergo a PT; the inner mitochondrial membrane becomes non-selectively permeable to solutes smaller than 1500 Da. This increased permeability is believed to reflect the opening of a pore. In rats, aging has been reported to produce a marked decrease in net mitochondrial Ca^{2+} uptake [Alemany et al. *Exp. Gerontol.* (1988) **23**: 25]. This finding would be consistent with increased Ca^{2+} release through the PT, possibly reflecting a transition that occurred more readily and/or a larger pore size. The PT was followed, in isolated liver mitochondria from rats of different age groups, by means of mitochondrial swelling measured as a decrease in apparent absorbance at 540 nm. We examined the dependence of the rate of swelling on trigger concentration when the PT was induced by P_i + Ca^{2+} or by butylated hydroxytoluene (BHT). The method of Pfeiffer et al. [*J. Biol. Chem.* (1995) **270**: 4923], based on the ability of polyethylene glycols of different average molecular weights to prevent mitochondrial swelling, was used to determine the size of the PT pore. Our results indicate that: (1) Whether the PT was triggered by P_i + Ca^{2+} or by BHT, the concentration of triggering agent required to produce a given swelling rate decreased with increasing rat age. (2) When the pore was induced by 5mM P_i and 50μM Ca^{2+}, pore size increased significantly with increasing rat age. These observations are consistent with the hypothesis that, as mammals age, their mitochondria become more sensitive to the PT. Furthermore, intrinsic pore properties may also change as a result of aging. [Supported by American Heart Association (#94007080)]

M-Pos77

VIRAL-INDUCED PERMEABILITY TRANSITION PORE IN MITOCHONDRIA. (Ljubava D. Zorova[1], Boris F. Krasnikov[2], Alevtina E. Kuzminova[2], Eugeny N. Dobrov[1], Dmitry B. Zorov[2]). [1]Biol. Faculty and [2]A. N. Belozersky Inst., Moscow State University, Moscow 119899, Moscow, Russia (Spon. by W. Tivol).

Recent evidence supports a role for the mitochondrial permeability transition pore (PTP) in programmed cellular death (Zamzami et al., *J. Exp. Med.* 183, 1-12, 1996). We suggest that apoptotic events can be triggered by a viral infection associated with PTP opening. There are numerous reports of a specific interaction of a viral particles with mitochondria (i.e. Harrison and Roberts, *J. Gen. Virol.* 3, 121-4, 1968). In this study, we focused on the aspect of functional changes in mitochondria induced by their interaction with viruses. Our model system was isolated rat liver mitochondria and tobacco mosaic virus (TMV). We found that in a presence of P_i (but without added Ca^{2+}), TMV increases respiration, collapses $\Delta\Psi$, induces the release of accumulated Ca^{2+} and promotes high amplitude swelling of mitochondria in a manner similar to that ascribed to the calcium-induced opening of PTP. TMV components (RNA or protein monomers and disks) and inactivated TMV did not induce PTP opening. The viral-induced effects were prevented by specific inhibitors of PTP, *e.g.*, cyclosporine A or EGTA. We present a model in which Ca^{2+} tightly bound to the viral particle opens the PTP. The calcium released upon binding of viral particles to the outer membrane, is transported into the mitochondria (possibly through the calcium uniporter) thus inducing PTP opening. (Supported by Russian Foundation of Basic Research, grants #96-04-49384 and #96-04-50940.)

M-Pos78

HYPOXIA MAKES MITOCHONDRIA MORE SENSITIVE TO PERMEABILITY TRANSITION PORE OPENING. (Alevtina E. Kuzminova, Boris F. Krasnikov, and Dmitry B Zorov). Dept. Bioenergetics, A.N. Belozersky Institute Physico-Chem. Biol., Moscow State University, Moscow, 119899, Russia. (Spon. by D. Carpenter)

The permeability transition pore (PTP) strongly depends on the redox state of the mitochondria and O_2 is important in this process. Many mitochondrial functions strongly depend on O_2 - the lack of it results in rapid depolarization and release of accumulated ions when the proton pump is blocked. Since many functions (*i.e.*, $\Delta\Psi$) depend on O_2, it is difficult to isolate the O_2 dependence of PTP opening. We maintained the $\Delta\Psi$ constant by supplying the system with an electron acceptor, ferricyanide. Under these conditions, the respiratory chain was oxidized even when the terminal part of the respiratory chain was blocked either by a lack of O_2 (physical hypoxia) or the presence of cyanide (chemical hypoxia). Four parameters were simultaneously measured in isolated rat liver mitochondria: respiration, Ca^{2+} fluxes, membrane potential and swelling. PTP was induced in energized mitochondria by the addition of Ca^{2+} in the presence of P_i. Low pO_2 in the incubation medium was reached by bubbling with nitrogen, consumption by respiring mitochondria and the addition of glucose+glucose oxidase. The Ca^{2+} concentration needed to open the PTP was lower than in control with both chemical and physical hypoxia. At the lowest O_2 concentrations (physical hypoxia established by the glucose/glucose oxidase system), pore opening was blocked by cyclosporine A, but not by the free radical scavenger, ionol. In all other cases, PTP opening was blocked by both drugs. These data indicate Ca^{2+} is deleterious during hypoxia since lower [Ca^{2+}] can induce PTP and finally cell death. Supported by Russian Foundation of Basic Research (96-04-49384).

M-Pos79

CA-DEPENDENT MITOCHONDRIAL DEPOLARIZATION AS A MECHANISM FOR IRREVERSIBLE CELL INJURY. ((T. J. Delcamp, C. Dales, L. Ralenkotter and R.W. Hadley)) Univ. of Kentucky, Lexington, KY 40536.

Mitochondrial and nuclear V_m and $[Ca^{2+}]$ were studied in guinea-pig ventricular myocytes using confocal imaging and the indicators TMRE and indo-1. Mitochondrial $[Ca^{2+}]$ during normal excitation-contraction coupling was studied using line-scanning, while $[Ca^{2+}]$ during anoxia-reoxygenation injury was studied using full-frame images. Anoxia produced a modest rise in mitochondrial $[Ca^{2+}]$, but a greater rise occurred during reoxygenation. In some cells, a preferential, sustained rise in nuclear $[Ca^{2+}]$ was seen as well. Mitochondrial V_m decreased during anoxia. Reoxygenation could produce either recovery of mitochondrial V_m, or further depolarization. Maintenance of mitochondrial depolarization was predictive of cell death during reoxygenation. We hypothesize that the spike in mitochondrial $[Ca^{2+}]$ was instrumental in mediating the depolarization seen during reoxygenation. In support of this hypothesis, elevation of cytosolic $[Ca^{2+}]$ to 1 μM produced a 27 mV mitochondrial depolarization, even in well-oxygenated cells.

M-Pos80

MEASUREMENT OF MITOCHONDRIAL PHYSIOLOGY DURING CYTOSOLIC $[Ca^{2+}]$ OSCILLATIONS IN FIBROBLASTS AND NEUROBLASTOMA CELLS.
((**G.C. Sparagna**, M.-d. Wei, E.M. Goff and L.M. Loew))
University of Connecticut Health Center, Farmington, CT 06030

Recent research has suggested that mitochondrial function in many types of cells is influenced by oscillations in cytosolic free Ca^{2+} ($[Ca^{2+}]_C$), but very few of these studies have followed individual mitochondria in intact living cells. We have developed methods with confocal microscopy and fluorescent indicators that allow us to measure mitochondrial membrane potential, changes in mitochondrial redox state, and changes in intramitochondrial free calcium concentration from single mitochondria. Furthermore, we are able to measure cytosolic free calcium ($[Ca^{2+}]_C$) and thus, correlate the signals from these two intracellular compartments. Our studies were carried out in NIH-3T3 fibroblasts and differentiated NIE-115 neuroblastoma cells, where we investigated the influence of hormonally stimulated $[Ca^{2+}]_C$ oscillations on mitochondrial membrane potential, NADH concentration, and mitochondrial $[Ca^{2+}]$. We used combinations of the $[Ca^{2+}]_C$ indicators calcium green-1 and indo-1 with the membrane potential indicator TMRE, the mitochondrial $[Ca^{2+}]$ indicator dihydrorhod-2, and the autofluorescence of NADH. Quantitation of membrane potential is achieved by application of the Nernst equation to the ratio of TMRE concentration in a mitochondrion relative to the cytosol as determined by a corrected fluorescence ratio. The correction factor is obtained by convolving a computer generated model mitochondrion with the microscope's point spread function. Mitochondrial $[Ca^{2+}]$ and redox changes during the cytosolic calcium transients are determined relative to prehormone levels. (Supported by NIH Grant GM35063)

M-Pos81

RESPIRATORY AND METABOLIC EFFECTS OF cAMP BINDING TO ADENINE NUCLEOTIDE TRANSLOCASE IN ISOLATED RAT LIVER MITOCHONDRIA
((**C. Marfella**, A. Romani, and A. Scarpa)) Case Western Reserve University, Cleveland, OH 44106.

Previous experiments suggest a role for cAMP binding to isolated mitochondria and purified Adenine Nucleotide Translocase (AdNT). The effects of 200 nM cAMP on metabolism and coupled respiration were measured in rat liver mitochondria oxidizing succinate in the presence of Pi. Using polarographic recording a decrease of 18 ± 5.5% Oxygen consumption was observed when cAMP was added after 200 μM ADP (state 3 respiration). Using potentiometric recording of TPP^+ concentrations in the extramitochondrial space with a TPP^+ specific electrode, the membrane potential ($\Delta\psi$) of mitochondria, where succinate oxidation was decreased by malonate, was measured. In the presence of cAMP, the addition of 200 μM ADP causes a variable but reproducible shorter and smaller $\Delta\psi$ collapse. Under control conditions, the $\Delta\psi$ collapse induced by ADP is dramatically decreased by preincubating the F1FO ATPase with oligomycin. Under these conditions, the electrogenic activity of the AdNT is likely to be solely responsible for the small transient collapse of the $\Delta\psi$. In the presence of cAMP the duration of this transient $\Delta\psi$ collapse is decreased by 22 ± 2.9%. Consistent with these measurements, decreased transients in NADH were observed. Taken together, these observations suggest a direct role of catalytic amounts of cAMP on AdNT of rat liver mitochondria. These observed changes indicate a less electrogenic operation of the AdNT in the presence of cAMP and could be consistent with the transport of some ATP^*Mg^{2+}, rather than ATP, by the translocase. (Supported by NIH-HL 18708).

M-Pos82

LASER-INDUCED UNCOUPLING OF MITOCHONDRIAL RESPIRATION. (Boris F. Krasnikov[1] and Dmitry B. Zorov[2]) [1]International Laser Center and [2]A.N. Belozersky Institute of Physico-Chemical Biology, Moscow State University, Moscow 119899, Moscow, Russia (Spon. by H. Tedeschi).

Photodynamic therapy is widely used in the treatment of many disorders. Since the mitochondria of some cells selectively retain cationic dyes (Summerhayes et al., *Proc. Natl. Acad. Sci. USA*, 79, 5292-6, 1980), these cells can be sensitized to irradiation with light that is absorbed by these dyes. The goal of this study was to gain insight into the role of mitochondria in cell viability. Suspensions of rat liver mitochondria were treated with different rhodamine derivatives with increasing hydrophobicity (from methyl to amyl esters of unsubstituted rhodamine). At constant temperature,laser irradiation at moderate energy output of mitochondrial suspensions stained with rhodamines resulted in respiration that linearly increased with irradiating dose. The effect was reversible since respiration immediately returned to the pre-illumination rate when the light was turned off. This stimulation of respiration was insensitive to ionol and to cyclosporine A. Higher irradiation doses induced increases in respiration that were not reversible after the light was off. The data at moderate irradiation doses are interpreted as a laser-induced generation of an uncoupler in the inner mitochondrial membrane similar to "mild uncoupling" introduced by Skulachev (*Quart. Rev. Biophys.* 29, 169-202, 1996). The results are in support of an important role for mitochondria in cell viability and cellular death induced by photodynamic effects. Supported by Russian Foundation of Basic Research (grant #96-04-49384).

M-Pos83

STRUCTURE AND FUNCTION OF UNCOUPLING PROTEINS
Fleury C., Levi-Meyrueis C., Ricquier D. and **Bouillaud F.**
ceremod CNRS 9 rue Jules Hetzel 92190 MEUDON FRANCE

The uncoupling protein (UCP) is a member of the family of mitochondrial anion carriers. UCP creates a pathway that allows protons to reenter the matrix without energy conservation. UCP triggers uncoupling of mitochondria and allows mitochondrial thermogenesis to occur. UCP expression is restricted to the brown adipose tissue, a specialized thermogenic organ of mammals. UCP activity is inhibited by nucleotides and is activated by free fatty acids. Recombinant expression of the UCP in Saccharomyces cerevisiae has been obtained. The use of potential sensitive probes in flow cytometry allows the study of mitochondrial activity in living yeast cells. Mutations that increase or abolish UCP activity *in vivo* were isolated by cell sorting.

Existence of a mitochondrial carrier expressed in various tissue and 60% similar to the UCP has been suggested by systematic sequencing of cDNAs. It probably corresponds to an isoform of the UCP and accordingly the term UCP2 was proposed. cDNA cloning and sequencing of this UCP2 in mouse has been obtained (gb U69135). Expression of this carrier in Saccharomyces cerevisiae has been obtained. Comparison of the effects of both proteins on the growth rate and on the mitochondrial membrane potential *in vivo* are under investigation. According to our first results it is tempting to propose that UCP2 creates a leak accross mitochondrial inner membrane that contributes to the basal metabolic rate.

M-Pos84

CHANNELS IN MITOCHONDRIAL CARRIERS. ((**M. Klingenberg**, N. Brustovetsky, S.-G. Huang)) Institute for Physical Biochemistry, University of Munich, Goethestrasse 33, 80336 Munich, Germany

A general concept of carrier structure implies that they contain a translocation path which is gated on both sides of the binding site providing alternating access from the inside or outside. The gating is stoichiometrically coordinated with the transfer of solute molecules. Perturbance of this linkage can reversibly or transiently lead to pore types of behaviour. The width of the translocation path should be correlated to the size of the solute transporter. This can be well demonstrated in mitochondrial carriers. The ADP/ATP carrier (AAC) and the uncoupling protein (UCP) (H^+ transporter) can exhibit in single-channel patch-clamp studies high conductivities with Cl^-. Maximum conductivity for the AAC reaches 600 pS and for UCP 150 pS. In the AAC the pore formation is Ca^{++} dependent, but in UCP an inducing parameter has not yet been found. The "mega channel" in AAC is quite unspecific and slightly anion preferred, whereas in the uncoupling protein it is more anion specific (Cl^-). Both channels are inhibited by specific inhibitors of the normal transport, i.e. in AAC by ADP and bongkrekate and in UCP by GTP or ATP. However, the transport inhibitor for the AAC, carboxyatractylate, does not inhibit but even stabilizes ion pore behaviour against ADP or bongkrekate. The different conductivities relate to the great differences in the size of the solutes, ADP/ATP for AAC versus H^+/OH^- for UCP. The current/voltage relation is symmetrically linear. Strong gating occurs for the AAC pore at >160 mol/mV and for the UCP channel at >120 mV. Whereas the physiological significance of the wide Ca^{++}-induced pore in the AAC is well documented in the "mitochondrial transition pore" phenomena, the role of pore formation in UCP is unknown. In this case the wide discrepancy between Cl^- flux measurements of UCP in vesicles and in the reconstituted patch-clamp systems remain unexplained, similar as in other recently discovered carrier-channel transitions.

M-Pos85

THE HUMAN PURINERGIC RECEPTOR GENE, $P2X_4$, IS ALTERNATIVELY SPLICED. ((**D.D.K. Prasad**, Y.-X. Wang and M.I. Kotlikoff)) Department of Animal Biology, University of Pennsylvania, 3800 Spruce Street, Philadelphia, PA 19104-6046. (Spon. by M.I. Kotlikoff)

ATP acts as a fast, excitatory neurotransmitter by binding to a large family of membrane proteins, P2X receptors, that have been shown to be ligand-gated, non-selective cation channels. We report the cloning of a full length and alternatively spliced form of the human $P2X_4$ gene. Clones were identified from a human stomach cDNA library using a rat $P2X_4$ probe (Soto et al, PNAS 93:3684,1996). Sequence analysis of positive clones identified the full length cDNA, which codes for a 388-residue protein that is highly homologous (82%) to the rat gene, and an alternatively spliced cDNA. In the alternatively spliced cDNA, the 5'-untranslated region and the first 90 aminoacids in the coding region of the full-length human $P2X_4$ are replaced by a 35 amino-acid coding sequence that is highly homologous with proteins in the heat shock protein (hsp) 90 family. The open reading frames of the full length and splice variant clones were confirmed by in-vitro translation. Northern analysis indicated expression of the full length $P2X_4$ message in numerous human tissues including smooth muscle, heart, and skeletal muscle. Alternatively spliced RNAs were identified in smooth muscle and brain by RT-PCR, and confirmed in RNAse protection assays using a 740 bp antisense RNA probe that spanned the alternatively spliced and native $P2X_4$ regions. Injection of full-length, but not alternatively spliced, cRNA into *Xenopus* oocytes resulted in the expression of ATP -gated non-selective cation currents. Supported by HL45239 and HL41084.

M-Pos86

TECHNIQUES FOR IMPROVED RESOLUTION OF KINETIC DATA FROM MACROSCOPIC CURRENTS. ((**R.L. Papke**, M.M. Francis and J.S. Thinschmidt)) Univ. of Florida, Gainesville, FL 32610

Interpretation of studies of macroscopic currents with bath applications of drug can be limited by the solution exchange time of the system. Our laboratory has developed two techniques to overcome this potential limitation. In studies of the effects of a family of anabasine derivatives on α7 neuronal nAChRs expressed in *Xenopus* oocytes, it was observed that at concentrations of ACh greater than 30 μM, peak currents occurred before the concentration of agonist was maximal in the perfusion chamber. Since valid concentration-response relationships must be based on actual concentrations associated with the recorded peak responses, measurements of peak current can underestimate agonist potency at α7 receptors in our system. By plotting estimates of the actual concentrations of agonist present at the time of peak responses, we estimate roughly 5-fold higher potencies and 2-fold higher Hill slopes than are derived from conventional analyses.

In an unrelated set of experiments on $\alpha3\beta4$ neuronal nAChRs, time course of recovery from use-dependent inhibition by the ganglionic blocker bis-TMP-10 was evaluated. However, since use-dependent inhibition requires activation of the channel, measurements of total inhibition at the time of co-application of agonist with inhibitor are complicated by channel activation prior to binding of inhibitor to the open-channel site. In an attempt to control for this effect, for each application of drug, percent inhibition is calculated as the integrated area under the curve during a time course corresponding to the falling phase of the response to ACh alone. The peak of the control response to ACh alone correlates with maximal activation and therefore maximal potential use-dependent inhibition in the experimental response. In this manner, it is possible to show almost total inhibition at the time of co-application and generate a recovery rate from this point in time fitted by a single exponential. *Supported by Taiho Pharmaceuticals, NIH R01 NS3288 to RLP and NIMH NRSA MH11258 to MMF.*

M-Pos87

CATION PERMEABILITY OF A *DROSOPHILA* GABA-ACTIVATED CHLORIDE CHANNEL WITH A MUTATION IN THE EXTRACELLULAR RING. ((**Chih-Tien Wang**, Hai-Guang Zhang, Tom Rocheleau, Richard H. ffrench-Constant, and Meyer B. Jackson)) Departments of Physiology and Entomology, University of Wisconsin.

The *Drosophila* GABA receptor gene *Rdl* was expressed in *Xenopus* oocytes in order to study the conductance properties of the associated chloride channel. Asparagine 319 of this receptor lies just outside the C-terminus end of the M2 segment in a homologous position to negatively charged residues in the nicotinic receptor. In the nicotinic receptor these residues contribute to the control of cation flux by forming a ring of negative charge at the opening of the channel on the extracellular surface. We found that mutation of asparagine 319 of the GABA receptor to lysine increased the single-channel conductance for inward current from 12.1 pS to 20.2 pS. Surprisingly, this mutation also shifted the reversal potential to 25 mV, in spite of the presence of symmetrical chloride. Manipulation of the sodium and potassium concentrations on each side of the membrane of excised outside-out patches showed that the reversal potential shift was caused by cation permeability, with preferential permeation by potassium relative to sodium. Reduction of the cation concentration showed that the lysine mutant had a significant cation permeability. In contrast, the wild type channel, as well as a mutant with arginine at position 319, have very low cation permeabilities. These studies therefore identify a residue in GABA receptors that plays an important role in the selectivity of the channel for anions over cations.

M-Pos88

WHOLE-CELL CURRENT PROPERTIES OF HOMOMERIC β4L-SUBUNIT $GABA_A$ RECEPTORS. ((**S.-C. Liu**[†], L. Parent[†], R. J. Harvey[‡], M. G. Darlison[‡], E. M. Barnes, Jr.[†])) [†]Baylor College of Medicine, Houston, TX 77030, USA and [‡]Universität Hamburg, Hamburg, Germany

Expression of the β4L subunit of the chicken γ-aminobutyric acid A ($GABA_A$) receptor in *Xenopus* oocytes produced GABA-gated Cl^- currents. GABA-induced membrane currents were recorded using the two-electrode voltage-clamp technique. The maximum current of the β4L-subunit receptors elicited by 100 μM GABA was 106.5 ± 13.2 nA (n=6), while sham-injected oocytes had no GABA response. In comparison, oocytes expressing the chicken β2S subunit showed little response to the application of GABA, as reported by others for most single-subunit receptors, with a current of 4.67 ± 0.84 nA (n=6) being elicited by 100 μM GABA. The GABA dose-response curve of the homomeric β4L-subunit receptors yielded an EC_{50} and Hill coefficient of 4.82 ± 0.81 μM and 1.14 ± 0.13 (n=6), respectively. Theses β4L-subunit receptors responded to $GABA_A$ receptor modulators with the pharmacological characteristics expected for homomeric β-subunit receptors, with pentobarbital potentiating, picrotoxinin inhibiting, and diazepam not affecting the GABA-gated current. It is unlikely that endogenous polypeptides were incorporated into the β4L-subunit receptors, since similar current properties were observed in the β4L-subunit expressing oocytes incubated in the presence of actinomycin D. The homomeric β4L-subunit receptor exhibits unique properties which may be valuable for the study of the structure and function of $GABA_A$ receptor polypeptide.

Supported by NIH grants NS34253, NS11535, and HL07676.

M-Pos89

MUTATIONS IN THE CONSERVED LEUCINE OF THE M2 REGION OF HOMOMERIC ρ1 AND HETEROMERIC αβγ GABA-GATED ION CHANNELS. ((**Yongchang Chang** and David S. Weiss)) Neurobiology Research Center and Department of Physiology and Biophysics, University of Alabama at Birmingham, Birmingham, AL 35294-0021.

Previous studies have demonstrated that mutations of a conserved leucine residue of the putative pore-lining region in the nicotinic ACh receptor alters the channel's gating characteristics. In this study, we examined the gating of GABA receptors with substitutions at the homologous leucine. Experiments were conducted on the human ρ1 and rat $\alpha1\beta2\gamma2$ GABA receptors expressed in *Xenopus laevis* oocytes. In the ρ1 GABA receptor, the conserved leucine (L301) was mutated either to another hydrophobic amino acid: gly, ala, phe, ile or val, or to a hydrophilic amino acid: tyr, ser, or thr. In the $\alpha1\beta2\gamma2$ receptor, the conserved leucine was substituted with ser (αm, βm, or γm). All hydrophilic substitutions, as well as ρL301V, ρL301G and ρL301A induced a picrotoxin-sensitive whole-cell inward current even in the absence of GABA. The ρ1 holding current typically dropped in response to low concentrations of GABA, indicating that agonist binding closed the spontaneously-opening GABA receptors. The leakage currents of $\alpha1\beta2\gamma2$ mutant channels (αmβγ, αβmγ, αβγm, and αmβmγm), although not blocked by GABA, were antagonized by bicuculline and picrotoxin. These data are consistent with the idea that the residue at this position needs both proper hydrophobicity and size for the channel to gate normally. (Grant # NS35291)

M-Pos90

REDUCTION OF NMDA-EVOKED Ca^{2+} TRANSIENTS BY A MU-OPIOID RECEPTOR AGONIST IN DORSAL HORN NEURONS. ((**S.D. Hocherman** and M. Randic)) Dept. Vet. Physiol. Pharmacol., Iowa State University, Ames IA 50010.

The spinal dorsal horn is an important site for the production of antinociception by μ-receptor agonists. This effect is produced by both pre-synaptic and post-synaptic mechanisms. In order to further examine possible post-synaptic targets of opioid action, the effect of the μ-receptor agonist DAGO on Ca^{2+} transients evoked by NMDA was studied in freshly dissociated neurons from laminae I-III of the dorsal horn loaded with Fura-2 AM. The basic perfusion solution contained 0.5 μM TTX, 2 mM Ca^{2+}, no Mg^{2+} and 0-100 nM added glycine.

Co-application of DAGO (.1-10 μM) and NMDA (30 μM) resulted in a decrease of the NMDA-induced Ca^{2+} transients in a fraction of cells. The effect of DAGO was transient and repeatable. Pre-application of DAGO (2-10 min) did not seem to increase the effectiveness of DAGO. The decrease in NMDA-elicited Ca^{2+} transient was prevented by previous application of naloxone (100 μM); naloxone by itself, however, increased the NMDA transients.

NMDA-induced Ca^{2+} transients may result from entry of calcium both through NMDA receptors and voltage-dependent calcium channels (VDCC). In order to determine which of these components was being affected by DAGO, the effect of DAGO on NMDA- and K^+-induced Ca^{2+} transients were compared in the same cells. A similar degree of decrease by DAGO was observed in NMDA- and K^+-induced Ca^{2+} transients, indicating that DAGO is likely to produce a decrease in NMDA-evoked transients by reducing Ca^{2+} currents through VDCC. We further tried to isolate the effect of DAGO on calcium influx through NMDA channels by eliciting NMDA-evoked calcium transients in a solution in which Na^+ ions were substituted by NMG. No effect of DAGO was seen under this conditions. Although these results suggest that VDCC rather than NMDA channels may be modulated by DAGO in these neurons, this simple interpretation is complicated by our observation that the removal of extracellular Na^+ by substitution with NMG caused a marked increase in the NMDA-evoked Ca^{2+} response.

M-Pos91

PROPERTIES OF CALCIUM CHANNEL FORMED BY α-LATROTOXIN IN PRESYNAPTIC MEMBRANE ((**L.G.Storchak** and N.H.Himmelreich)) Palladin Institute of Biochemistry, Department of Neurochemistry, Kiev, Ukraine. (Spon. by A. Chanturiya)

α-Latrotoxin (LTX) is a high molecular weight protein with presynaptic action purified from the black widow spider venom. We studied properties of the LTX channel in rat brain synaptosomes. It was found that LTX induces an extensive and rapid Ca^{2+} uptake that is described by Michaelis-Menten kinetic. LTX is not able to enhance Na^+ and Rb^+ influxes. Mg^{2+}, Ba^{2+}, Sr^{2+} and Co^{2+} competitively inhibit the uptake of Ca^{2+}. Experiments with fluorescent dyes show that LTX-induced influx of bivalent cations depolarizes the synaptosomal plasma membrane. A rise in $[Ca^{2+}]_{in}$ leads to considerable decrease of LTX induced Ca^{2+} uptake. Using the fluorescent probe BCECF we found that a variation of the intracellular pH by +/- 0.1-0.3 has no appreciable influence on the calcium influx. However, when the pH of the external medium is lowered to 6.0 (from normal 7.16+/- 0.09), Ca^{2+} fluxes through LTX channels are inhibited. Dissipation of the proton gradient decreases LTX ability to form ionic channels without any loss of activity of the preformed channels. The toxin induced Ca^{2+} influx is strictly controlled by the level of synaptosomal metabolism; decreasing the synaptosomal ATP level inactivates the toxin induced ionic fluxes.

M-Pos92

VOLTAGE "FLIPS" CONTROLLING CALCIUM INFLUX AND VESICLE CYCLING IN THE SYNAPTIC TERMINAL OF RETINAL BIPOLAR CELLS. ((**J. Burrone** and L. Lagnado)) MRC Laboratory of Molecular Biology, Cambridge CB2 2QH, UK.

The conductances controlling the Ca^{2+} signal in the synaptic terminal of depolarizing bipolar cells from the goldfish retina were studied using permeabilized patch recording. In current-clamp mode the membrane potential (Vm) exhibited spontaneous all-or-none depolarizations from around -50 mV to -30 mV. These "flips" were associated with a rise in cytoplasmic Ca^{2+} in the terminal (measured with fura-2) and the stimulation of vesicle cycling (measured as uptake or release of FM1-43). The threshold for a flip could be defined by measuring the response to 1 pA of injected current from different holding currents and was between -40 and -45 mV, the voltage range where the L-type Ca channels localized to the terminal begin to activate. Increasing the injected current did not depolarize Vm beyond the ceiling of about -30 mV. During a flip, Vm exhibited a damped oscillation with a frequency of 50-60 Hz and initial amplitude of 3-7 mV. Depolarizing bipolar cells in the intact goldfish retina exhibit similar damped Vm oscillations in response to light (Kaneko, *J. Physiol.*, 207, 623, 1970). Flips were blocked by 10 μM nifedipine but blocking Ca-activated K channels with internal Cs^+ allowed Vm during a flip to reach 10-20 mV. Substance P (10 nM) inhibited the Ca current by 70% at potentials up to -30 mV and also blocked the generation of flips. Our results indicate that depolarizing bipolar cells can generate an all-or-none response through the action of L-type Ca channels and Ca-activated K channels in the synaptic terminal. These flips regulate transmitter release and are under the control of neuromodulators that act on Ca channels in the terminal.

M-Pos93

A NEW DECONVOLUTION METHOD FOR ESTIMATING UNITARY SYNAPTIC PARAMETERS FROM SYNAPTIC CURRENT AMPLITUDE DISTRIBUTIONS.((V.V. Uteshev*, J.W. Wells and **P.S. Pennefather**)) Faculty of Pharmacy & Dept. of Physiology, U. of Toronto, Toronto, ON., M5S 2S2.

We have developed a procedure for deconvolution of the amplitude distribution of evoked post-synaptic currents (ePSCs) and have applied it to data sets obtained by Monte-Carlo simulations or by whole-cell recordings from synaptically coupled pairs of hippocampal neurons in tissue culture. Two types of unitary evoked postsynaptic current (uePSC) amplitude distributions are considered: a skewed distribution described by a power-exponential function and a symmetrical distribution described by a Gaussian function. The procedure reduces the problem of deconvolution of ePSC amplitude distributions to the problem of obtaining a best fit of a measured ePSC amplitude histogram by an analytical expression that describe the convolution of simultaneous responses (either failures or uePSCs), in a system of equivalent and independent synapses. The information intrinsic to an ePSC amplitude histogram is not always sufficient to obtain an optimal deconvolution in which all intrinsic parameters are narrowly constrained. This problem often can be resolved by increasing information available by using more events to estimate the ePSC amplitude distribution or by fixing the failure rate using an analysis of uePSC and ePSC variance or fixing characteristics of the uePSC amplitude distributions estimated from afterdischarges of uPSCs that follow ePSCs in Sr^{2+}containing media.

M-Pos94

CLOSTRIDIUM BOTULINUM NEUROTOXINS A,B AND E INHIBIT SECRETORY ACTIVITY IN RAT MELANOTROPHS ((M Rupnik[1], TFJ Martin[2], BR DasGupta[3] and R Zorec[1]))
[1]Laboratory of Neuroendocrinology-Molecular Cell Physiology, Institute of Pathophysiology, School of Medicine, University of Ljubljana, 1000 Ljubljana, Slovenia; [2]Department of Biochemistry and [3]Department of Food Microbiology and Toxicology, University of Wisconsin, Madison, Wisconsin 53706, USA

Clostridial neurotoxins have been used as powerful tools for dissecting the machinery mediating synaptic transmission. Recently, the intracellular protein targets for most of the serotypes (A - G) of botulinum toxin were reported, which are parts of the synaptic vesicle docking/fusion complex (SNARE complex; Söllner et al., Nature, 1993, 362:318; Rothman and Warren, Curr Biol, 1994, 4:220).
To date the evidence that SNAREs (v-SNARE, synaptobrevin/VAMP; t-SNARE, SNAP-25 and syntaxin) are involved in the secretory activity of pituitary cells is missing. The aim of our study was to investigate the effects of botulinum toxin types A, B and E on Ca^{2+}-induced secretory activity of single rat melanotrophs.
The whole-cell patch-clamp was used (Zorec et al., 1991, Methods in Neurosci, 4:194) to monitor changes in membrane capacitance (C_m; a measure of membrane surface area) and to dialyse the cytosol with pipette solutions (in mM; KCl 150, $MgCl_2$ 2, HEPES 10, Na_2ATP 2, EGTA 0.5 and Ca^{2+}-saturated EGTA 3.5 to obtain 1 μM $[Ca^{2+}]_i$, pH 7.2). Cells were prepared by standard methods (Rupnik & Zorec, FEBS Letts, 1992, 303:221). Neurotoxins were microinjected (1.5 ng/μl) with Transjector 4657 (Eppendorf) 1 to 3 hours before the electrophysiological experiment. Secretory responses were measured as the rate of change in C_m (dC_m/dt) and as an increase in C_m relative to the resting membrane capacitance ($\%\Delta C_m$) 200 seconds after the start of dialysis. Results are summarized in the table below (mean ± s.e.m., (number of cells tested) ** $P < 0.001$, Student t-test).

	control (33)	BotxA (7)**	BotxB (7)**	BotxE (7)**	BotxE boil (3)
dC_m/dt [fF/s]	17.4 ± 2.4	0.8 ± 0.7	-1.3 ± 1.3	0.2 ± 0.7	16.5 ± 2.0
$\%\Delta C_m$	25.2 ± 3.4	-1.2 ± 1.1	-2.9 ± 2.3	-1.2 ± 2.3	18.5 ± 4.6

All toxin types tested completely abolished the Ca^{2+} induced secretory activity in melanotrophs. These results suggest that SNAREs (synaptobrevin, SNAP-25, syntaxin) are probably involved in the regulation of Ca^{2+} dependent secretory activity in rat melanotrophs.
The work was supported by the project J3-6027-381 by the Ministry of Science and Technology of Slovenia and Joint US-SLO project 95-471.

M-Pos95

MEASUREMENT OF NONSYNAPTIC QUANTAL TRANSMITTER RELEASE FROM SINGLE NEURONS OF BRAINSTEM SLICES. ((**Erica Jaffe***, Albert Schulte*†, Alain Marty*, and Robert H. Chow †)) *MPI für exp. Medizin, D-37075 Göttingen; †Univ. of Edinburgh Medical School, Dept. Physiol., EH8 9AG, Scotland, U.K.; MPI für biophys. Chemie, D-37077 Göttingen.

Substantia nigra (SN) neurons release dopamine from their somata and dendrites. An unresolved question is whether this nonsynaptic release occurs by exocytosis or by a nonvesicular mechanism. To address this issue, we used low-noise carbon-fiber microelectrodes in brain slices of the SN pars compacta to assay secretion from single cell bodies that had been cleared of connective tissue. Unitary amperometric events were recorded under resting conditions. The median charge of the unitary events was 3 fC. For dopamine, this is equivalent to about 9,500 molecules. Glutamate application increased the frequency of the events markedly. These results indicate that dopamine is released from the somata of substantia nigra neurons by exocytosis and that this mechanism is regulated by neuronal electrical activity. Furthermore, although for two decades carbon-fiber microelectrodes have been used to record bulk release of transmitters in brain extracellular fluid, this is the first demonstration that they can be used to record ***quantal*** monoamine secretion in brain slices, and it suggests the more general applicability of this approach to studying quantal monoamine release in the brain.

M-Pos96

CALCIUM INFLUX, BUFFERING AND EXTRUSION ASSOCIATED WITH A SINGLE ACTION POTENTIAL IN A CNS PRESYNAPTIC TERMINAL. ((**F. Helmchen**, J. G. G. Borst, B. Sakmann)) Abt. Zellphysiologie, Max-Planck-Institut für med. Forschung, D-69120 Heidelberg, Germany.

Calcium dynamics associated with a single action potential were studied quantitatively in the calyx of Held, a large presynaptic terminal in the rat brainstem. Terminals in brain slices were loaded with different concentrations of the Ca^{2+} indicators Fura-2, MagFura-2 or Calcium Orange-5N via patch pipettes. Spatially averaged Ca^{2+} signals were measured fluorometrically using a CCD camera and analyzed on the basis of a single compartment model. A single action potential led to a total Ca^{2+} influx of 0.8-1 pC, as measured using Fura-2 overload. The accessible volume of the terminal was about 0.4 pl, thus the total calcium concentration increased by 10-13 μM. The Ca^{2+}-binding ratio of the endogenous buffer was about 40, as estimated from the competition with Fura-2, indicating that 2.5% of the total calcium remain free. This is consistent with the peak increase in free calcium concentration of about 400 nM, which was measured directly with MagFura-2. The decay of the $[Ca^{2+}]_i$ transients was fast, with time constants of 100 ms at 23°C and 45 ms at 35°C, indicating Ca^{2+} extrusion rates of 400 and 900 s^{-1}, respectively. The combination of the relatively low endogenous Ca^{2+}-binding ratio and the high rate of Ca^{2+} extrusion is an efficient mechanism to rapidly remove the large Ca^{2+} load of the presynaptic terminal evoked by an action potential.

M-Pos97

Self-organization phenomena as a mechanism of postsynaptic plasticity (S.M.Korogod, **L.P.Savtchenko**, Int. Center of Molec. Physiol., Nath. Acad. Sci., 13 Nauchny, 320625 Dnepropetrovsk, Ukraine. (Spon. by R.Kado)) Simulation studies were performed in a model of thin cylinder-shaped dendrite with Na^+ and K^+ channels and with ionotropic and metabotropic glutamate receptors. The ionotropic receptors were either *NMDA*-sensitive, voltage-dependent and permeable to Ca^{2+}, Na^+, and K^+ or non-*NMDA* sensitive, voltage-independent and permeable to Na^+ and K^+. The metabotropic receptors provided *G*-protein coupled control of level of IP3 catalyzing Ca^{2+}-induced Ca^{2+} release from intracellular stores. Exchange with the stores, axial diffusion, transmembrane passive and pump currents of Ca^{2+} changed intracellular free calcium concentration $/Ca^{2+}/_i$. Tonic activation of the *NMDA*-ionotropic and metabotropic receptors could trigger self-organization of the pattern arising from initial uniform state in the form of spatially periodic $/Ca^{2+}/_i$ (hot- and cold-bands). Occurrence of the pattern and width of the bands were defined by the level of tonic *NMDA*-activation and by metabotropically controlled rate of Ca^{2+}-induced Ca^{2+} release. The band widths decreased with cell diameter, the specific membrane conductivity, and cytoplasm resistivity. This activity-induced pattern led to long-term spatially inhomogeneous change in local excitatory postsynaptic potentials (EPSPs) of NMDA synapses phasically activated with the same presynaptic intesity. The phasic EPSPs were potentiated if the synapse occurred in the hot band.

M-Pos98

MEMBRANE LATERAL PRESSURES: A PHYSICAL MECHANISM OF GENERAL ANESTHESIA ((Robert S. Cantor)) Department of Chemistry, Dartmouth College, Hanover, NH 03755

A mechanism of general anesthesia is suggested and investigated using simple statistical thermodynamic theory. Bilayers are characterized by large lateral stresses that vary with depth within the membrane. Calculations reveal that incorporation of amphiphilic solutes increases the lateral pressure near the aqueous interfaces. By what physical mechanism might this perturbation produce anesthesia? General anesthesia likely involves inhibition of the opening of the ion channel in a postsynaptic receptor. If, as seems likely, channel opening increases the protein cross-sectional area near the aqueous interface, then an increase in lateral pressure at the interface would shift the equilibrium to favor the closed state (of smaller area). Anesthetic potency is then determined by the amount of anesthetic required to increase the lateral pressure sufficiently in the interfacial region to make the free energy of opening positive. Our calculations predict the cutoff of potency for long n-alkanols and are consistent with experimental results on changes in bilayer thickness and bond order parameters. Since lateral pressures are so large, even a small (clinically relevant) concentration of anesthetics provides a sufficient change in lateral pressure to shift the free energy of opening significantly, i.e., to prevent the channel from opening. This hypothesis provides a mechanistic, thermodynamic understanding of anesthesia, as well as correlations of potency with structural and thermodynamic properties. Possible implications for other processes involving membrane proteins are discussed.

SR CALCIUM RELEASE; SPARKS AND WAVES

M-Pos99

MYOPLASMIC Mg^{2+} MODULATES THE FREQUENCY OF DISCRETE SR Ca^{2+} RELEASE EVENTS (Ca^{2+} SPARKS) IN FROG SKELETAL MUSCLE ((A. Lacampagne, M.G. Klein, K. Bagley, M.F. Schneider)) Dept. Biochem. and Mol. Biol., Univ. Maryland School of Med., Baltimore MD 21201

Ca^{2+} release events were monitored using fluo-3 and laser scanning confocal microscopy in line-scan (*x* vs *t*) mode (Klein et al, 1996, Nature, 379:455) in depolarized segments of frog skeletal muscle fibers, notched so as to allow rapid equilibration of the myofilament space with the bathing solution (5.5, 3.5 or 3.0 mM total Mg^{2+} added to 5.0 mM total ATP in an "internal" solution with 50 mM fluo-3 and no added Ca^{2+}; calculated free $[Mg^{2+}]$ = 0.65, 0.18 or 0.13 mM). The frequency of events increased reversibly from 0.02 sarcomere^{-1} s^{-1} in 0.65 mM $[Mg^{2+}]$ to 0.12 or 0.21 sarcomere^{-1} s^{-1} in 0.18 or 0.13 mM $[Mg^{2+}]$ solution, indicating a decrease in Mg^{2+} inhibition of channel opening. Addition of 0.25 mM caffeine to the 0.65 mM $[Mg^{2+}]$ solution caused a similar increase in frequency as lowering $[Mg^{2+}]$, but presumably by potentiating Ca^{2+} activation of CICR. The time course, peak amplitude and spatial extent of individual release events were independent of myoplasmic $[Mg^{2+}]$, indicating that the SR channel open time underlying the Ca^{2+} sparks is independent of myoplasmic $[Mg^{2+}]$, even though the tendency of a channel to open was strongly increased by lowering $[Mg^{2+}]$. Nifedipine (1mM) had no effect on the release events. This method of monitoring Ca^{2+} sparks demonstrates that myoplasmic $[Mg^{2+}]$ decreases the tendency of SR Ca^{2+} release channels to open in skeletal muscle fibers with the transverse tubule voltage sensors for SR Ca^{2+} release present but in the inactivated state due to prolonged fiber depolarization. Supported by NIH (R01-NS23346 and R01-AR44197).

M-Pos100

SPATIAL SPREAD OF Ca^{2+} SPARKS AT DIFFERENT SARCOMERE LENGTHS IN FROG SKELETAL MUSCLE ((A. Lacampagne, M.G. Klein, M.F. Schneider)) Dept. Biochem. and Mol. Biol., Univ. Maryland School of Medicine, Baltimore MD 21201. (Sponsored by Dr. Syamal K. Dey)

Ca^{2+} release events were monitored using fluo-3 and laser scanning confocal microscopy in line-scan mode (Klein et al, 1996, Nature, 379:455) both in briefly reprimed voltage clamped cut single fibers (Klein et al, these abstracts) and in depolarized notched segments of cut single fibers with reduced myoplasmic $[Mg^{2+}]$ (Lacampagne et al, these abstracts). Line scan images were obtained with the scan line oriented either parallel (x vs t) or perpendicular (y vs t) to the long axis of the fiber. The extent of spatial spread of a Ca^{2+} spark was quantitated as the full width at half peak along the scan line (=spatial fwhp) in the line scan image of the individual Ca^{2+} spark. Fiber sarcomere spacing was set to between 2.3 and 4.1 mm. The spatial fwhp was similar in the directions parallel or perpendicular to the myofibrils and was independent of the sarcomere spacing. Thus, sarcomeric structures (in the x dimension), myofibrillar structures (in the y dimension) and the sarcomeric and myofibrillar pattern of immobile calcium binding sites do not seem to influence the recorded spatial distribution of the fluorescence due to calcium-dye complex that is detected as the Ca^{2+} spark. Rather, the spatio-temporal distribution may be determined predominantly by diffusion of Ca^{2+}, Ca^{2+}-dye and dye. Supported by NIH (R01-NS23346 and R01-AR44197).

M-Pos101

CALCIUM-SPARKS IN FAILING HEART CELLS: MODULATION BY ISOPROTERENOL. ((A.M. Gómez, L.F. Santana, R. Altschuld, W.J. Lederer)). Depts. Physiology and Molecular Biology and Biophysics, University of Maryland School of Medicine and Medical Biotechnology Center, Baltimore, MD 21201 and Department of Medical Biochemistry, Ohio State University, Columbus, OH 43210.

Ca^{2+} sparks were studied in single cardiac myocytes isolated from rats suffering from heart failure. Cells were loaded with the fluorescent Ca^{2+} indicator fluo-3 through the patch clamp pipette. A laser scanning confocal microscopy was used to image the local Ca^{2+} release events from the SR (Ca^{2+} sparks) attributed to the opening of ryanodine receptors (RyR). The cells were controlled electrically using patch clamp methods in whole cell mode. Ca^{2+} sparks occurred spontaneously or were triggered by the opening of voltage-gated sarcolemmal L-type Ca^{2+} channels. Ca^{2+} sparks observed in the absence (Fig. 1) and presence (Fig. 2) of isoproterenol (1 μM) are shown below. The application of this adrenergic agonist increased the appearance of two kinds of Ca^{2+} sparks. (1) Ca^{2+} sparks were observed repeatedly in the same site within the heart cells without increasing the appearance of Ca^{2+} waves. (2) Ca^{2+} sparks were long lasting (see Fig. 2). Ca^{2+} transients due to the Ca^{2+} sparks are shown below the images of the Ca^{2+} sparks themselves. This adrenergic-stimulation dependent change in behavior of Ca^{2+} sparks could be observed in control cells and, with increased frequency, in failing heart cells, despite the established down-regulation of the beta-adrenergic receptors in failing heart cells.

The altered behavior is reminiscent of altered behavior of Ca^{2+} sparks following the treatment of cardiac myocytes with ryanodine and in this case may depend on phosphorylation-dependent change in the RyR gating "mode."

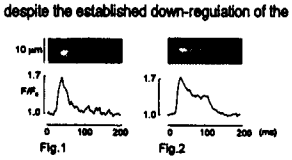

Fig.1 Fig.2

M-Pos102

Ca^{2+} SPARKS AND EC COUPLING IN PHOSPHOLAMBAN-DEFICIENT VENTRICULAR MYOCYTES. ((**L.F. Santana**, T. Shioya, *E.G. Kranias and W.J. Lederer)) Department of Physiology and Medical Biotechnology Institute, University of Maryland at Baltimore, Baltimore, MD 21201 and *Department of Pharmacology and Cell Biophysics, University of Cincinnati, Cincinnati, OH 45267. (Spon. by W.J. Lederer).

We investigated the role of phospholamban (PLB), a regulator of the SR Ca^{2+} ATPase, in cardiac EC coupling. Our experiments compared the mechanisms of global and subcellular $[Ca^{2+}]_i$ control in single ventricular myocytes from wild type (WT) and from mice lacking the PLB gene (KO). Isolated myocytes were loaded with the Ca^{2+}-sensitive fluorescent indicator fluo-3 and were examined using confocal microscopy and whole-cell voltage clamp. In KO mice, we observed that during 50 ms depolarizations $[Ca^{2+}]_i$ transients of similar amplitude decayed faster (37.5±9.74 ms; n=8) than in WT (73.42±4.9 ms;n=8) myocytes ($p<0.05$). Furthermore, the amplitude of the whole-cell $[Ca^{2+}]_i$ transient in KO was greater than in WT at all voltages examined (-30 to -60 mV; n=8). By contrast, the amplitude and voltage-dependence of the whole-cell Ca^{2+} current was similar in both, WT and KO, cells. We also detected spontaneous local SR Ca^{2+} release events, called "Ca^{2+} sparks", in WT and KO myocytes and found that Ca^{2+} sparks were nearly three-times as frequent in KO (2.41±0.67 sparks•sec^{-1}•100 μm^{-1};n=12) than in WT cells (0.88±0.2 sparks•sec^{-1}•100 μm^{-1};n=9). Finally, the amplitude (F/F_0) of spontaneous Ca^{2+} sparks in KO (1.89±0.02; n=117) was significantly higher than in WT (1.67±0.02;n=116) myocytes ($p<0.05$). The mechanisms by which KO mice differ from WT mice with respect to EC coupling mechanisms have been investigated. We have examined the roles of SR Ca^{2+} load, ryanodine receptor Ca^{2+}-sensitivity, and phosphorylation state of EC coupling proteins on Ca^{2+} sparks and $[Ca^{2+}]_i$ transients in WT and KO mice.

M-Pos103

ISOPROTERENOL CHANGES THE KINETICS OF Ca^{2+} SPARKS IN MOUSE VENTRICULAR MYOCYTES. ((L.F. Santana, A.M. Gómez, *E.G. Kranias and W.J. Lederer)) Department of Physiology and Medical Biotechnology Institute, University of Maryland at Baltimore, Baltimore, MD 21201 and *Department of Pharmacology and Cell Biophysics, University of Cincinnati, Cincinnati, OH 45267. (Spon. by L.F. Santana).

In heart, a Ca^{2+} spark results from the opening of a single ryanodine receptor (RyR) (or a few RyRs; Cheng et al. 1993. *Science* 262:740). We used Ca^{2+} sparks as a tool to investigate the effects of the β-adrenergic agonist isoproterenol (ISO) on the RyR using voltage-clamped mouse ventricular myocytes loaded with the Ca^{2+} sensitive fluorescent indicator fluo-3. We found that ISO (1 μM) increased the mean duration of Ca^{2+} sparks (but see Gómez et al. 1996. *J. Phys.* 496: 575). In the presence of ISO Ca^{2+} sparks had a longer mean time-to-peak and mean half-time-of-decay (see Fig. 1). Since phospholamban (PLB) is one the principal targets in the β-adrenergic signaling cascade we compared wild type (WT) mouse heart cells to those cells taken from animals with PLB knocked out (KO). The prolongation of the mean duration of Ca^{2+} sparks was similar in both WT and PLB-KO. We conclude that ISO affects the kinetics of the RyRs and thus Ca^{2+} sparks.

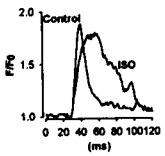

Fig. 1

M-Pos104

IMAGING OF Ca^{2+} SPARKS USING A SUPER FAST ULTRASENSITIVE CCD CAMERA. ((L.F. Santana, E.F. Etter, R.A. Tuft, K. Fogarty, F. Fay and W.J. Lederer)) Depts. Physiology and Molecular Biology and Biophysics, University of Maryland School of Medicine and Medical Biotechnology Center, Baltimore, MD 21201, Dept. Physiology, Univ. Mass. Med. Center, Worcester, MA 01605 (Spon. by T. B. Rogers).

We used rat ventricular myocytes loaded with the fluorescent Ca^{2+} indicator fluo-3 under whole cell voltage-clamp to image Ca^{2+} sparks using a wide field microscope and a very sensitive super-fast cooled CCD camera. The microscope can acquire high contrast images very quickly (R.A. Tuft et al. this meeting). Ca^{2+} sparks can be viewed in both X and Y directions using this microscope and without the enhanced contrast and intrinsic resolution of a laser-scanning confocal microscope. We are able to detect normal Ca^{2+} sparks similar to those reported previously (Cheng et al. *Science* 262:740-744, 1993). We have investigated voltage-gated Ca^{2+} sparks (Cannell et al. *Science* 268:1045-1050, 1995 and Santana et al. *Circ.Res.* 78:166-171, 1996) and Ca^{2+} sparks activating and supporting propagating waves of elevated Ca^{2+} (Cheng et al. *Am.J.Physiol.* 270:C148-C159, 1996.). This new microscope thus provides the benefits of high-speed wide field image acquisition while maintaining excellent resolution and image contrast and is now being used by us to investigate EC coupling in single cardiac myocytes.

M-Pos105

TWO-PHOTON POINT PHOTOLYSIS OF CAGED Ca^{2+}

((P. Lipp, J. Kleinle, C.Amstutz, C. Lüscher, and E.Niggli)) Dept. Physiology, University of Bern, Switzerland

Subcellular Ca^{2+} signals such as Ca^{2+} sparks and puffs play a major role in Ca^{2+} signal transduction of almost every cell type and are believed to result from clusters of ryanodine receptors (RyRs; spark) or inositol-1,4,5-trisphosphate receptors ($InsP_3Rs$; puff) in the membrane of the sarcoplasmic or endoplasmic reticulum. To investigate the biophysical properties of spatially confined Ca^{2+} transients, it is necessary to evoke such signals independently of the particular microarchitecture of the signal-transduction machinery. Therefore we investigated the possibility to generate such Ca^{2+} signals by diffraction-limited photochemical liberation of Ca^{2+} from photolabile precursors, such as DM-nitrophen or NP-EGTA. A two-photon (TP) excitation system (for photolysis of the caged compounds) was combined with a laser-scanning confocal microscope in order to follow the Ca^{2+} transients. We tuned the two-photon excitation laser system (Argon-ion pumped Ti:Sapphire) at a wavelength of 710 nm (76 MHz repetition rate; pulse duration ≈ 80 fs). The TP-laser beam was combined with the confocal pathway by a dichroic mirror that enabled us to laterally "scan" the TP-laser with respect to the confocal detection by ≈ 30 μm. Initial experiments were carried out in droplets of intracellular solution that contained either 1 mM DM-nitrophen or NP-EGTA for photolysis and 0.1 mM Fluo-3 for detection of the Ca^{2+} signal. Both caged compounds could be excited at the same wavelength and excitation caused an energy-dependent liberation of Ca^{2+}. DM-nitrophen was more effectively photolysed than NP-EGTA, presumably due to its higher TP absorbance cross-section. To test this system intracellularly, we patch-clamped cultured Hyppocampus neurones. The subcellular Ca^{2+} responses evoked by TP excitation were smoothly graded with the input energy (10 - 100 mW) and were confined to 1-20 μm. The resulting Ca^{2+} transients were remarkably dependent on the particular cell geometry (narrow dendrite vs. "infinite" cell-soma). Mathematical modelling of the Ca^{2+} transients showed that differences in the subcellular spreading can be explained by changes in the particular geometry. Therefore in Hyppocampus neurones the spatial properties of such "artifical" Ca^{2+} sparks are determined by diffusion and cell geometry. (Supported by SNF)

M-Pos106

PHYSIOLOGY OF THE HIERARCHICAL Ca^{2+}-SIGNALLING SYSTEM IN NON-EXCITABLE CELLS: SALTATORIC AND ABORTIVE Ca^{2+}-WAVES

((P.Lipp[1], E.Niggli[1], M.Berridge[2] & M. Bootman[2])) [1]Dept. Physiology, University of Bern, Switzerland; [2]The Babraham Inst. Laboratory for Molecular Signalling, Univ of Cambridge, UK (Spon. by I.C.Forster)

Application of a Ca^{2+} mobilizing hormone onto HeLa cells activates the phosphoinositide transduction pathway, resulting in a release of Ca^{2+} from the endoplasmic reticulum by inositol 1,4,5-trisphosphate receptors ($InsP_3Rs$). Rapid confocal line-scanning of Fluo3-loaded HeLa cells, revealed histamine-triggered elementary Ca^{2+} transients which underlie global Ca^{2+} signals. Both 'Ca^{2+} blips', fundamental release events arising from gating of single $InsP_3Rs$, and 'Ca^{2+} puffs', intermediate events arising from clusters of $InsP_3Rs$, were responsible for initiation of Ca^{2+} waves. Rapid application of a supramaximal histamine concentration to the HeLa cells evoked continuously propagating Ca^{2+} waves, originating from a variable number of initiation sites with a fixed subcellular location. The rate of rise of the global Ca^{2+} signal was directly proportional to the number of initiation events. Reduction of the level of feedback inherent in the intracellular Ca^{2+} signalling machinery, caused the continuous waves to attenuate, giving a saltatory propagation. Within such saltatoric waves, the underlying elementary signals (Ca^{2+} puffs), and the different steps during Ca^{2+} wave propagation (regeneration and diffusion) were evident. Threshold hormone concentrations triggered abortive Ca^{2+} waves, which remained restricted to the region of the Ca^{2+} puff(s). Spatial and temporal recruitment of Ca^{2+} blips and puffs explains variations of the amplitude and kinetics of intracellular Ca^{2+} signals, in addition to underlying global responses such as waves. We propose that this concept of a hierarchical Ca^{2+} signalling system found in non-excitable cells may be a paradigm for Ca^{2+} signal transduction, as for Ca^{2+} quarks, -sparks and -waves in cardiac muscle cells.

M-Pos107

Ca^{2+} SPARKS AND Ca^{2+} RELEASE IN TRANSGENIC MYOCYTES OVEREXPRESSING CARDIAC CALSEQUESTRIN. ((W. Wang, Y.J. Suzuki, L. Cleemann, L.R Jones* and M. Morad)) Dept. of Pharmacology, Georgetown Univ., Washington, DC 20007 and *Krannert Inst. of Cardiology, Indiana Univ., Indianapolis, IN 46202. (Spon. by J.A. DeSimone)

Calsequestrin (CSQ) is a major Ca^{2+} binding protein in the sarcoplasmic reticulum (SR) of cardiac and skeletal muscle. To examine the physiological function of CSQ during the E-C coupling process, whole cell-clamped ventricular myocytes from transgenic mice overexpressing CSQ were examined using confocal microscopy. Western blot analysis shows that these transgenic mice have 18-fold increase in ventricular CSQ level. The localized rises in cytoplasmic Ca^{2+} (Ca^{2+} sparks) and I_{Ca}-induced Ca^{2+}-release (Ca^{2+}-transients) from the SR were studied. Single myocytes were dialyzed with the Cs^+-rich internal solution containing Ca^{2+} indicator fluo-3 (1 or 2mM) in combination with different concentrations of EGTA (0, 1, 14mM). Fluorescent images were recorded using an acousto-optically steered confocal laser microscope and Ca^{2+} currents were activated by depolarizing pulses to 0mV from a holding potential of -70mV. In transgenic myocytes (n=3) dialyzed with 1mM fluo-3 & 1mM EGTA, spontaneously occurring Ca^{2+} sparks were weaker in size and intensity than those obtained from their non-transgenic littermates (n=6). In transgenic myocytes dialyzed with 1mM Fluo-3 & 14mM EGTA or 2mM Fluo-3, no sparks were detected. I_{Ca}-induced Ca^{2+}-transients were also smaller in transgenic myocytes compared to those of control cells dialyzed either with 1mM Fluo-3 & 1mM EGTA or with 0.1mM Fura-2. Since the magnitude of I_{Ca} in transgenic myocytes were found to be similar to that of control myocytes, the small magnitude of Ca^{2+}-transients may in part reflect decreased efficiency of Ca^{2+}-induced Ca^{2+} release mechanism, especially since caffeine induced-Ca^{2+} release was significantly larger in transgenic vs control myocytes. (Supported by NIH HL16152)

M-Pos108

CALCIUM SPARKS IN RODENT CARDIOMYOCYTES ARE MODULATED BY HOLDING POTENTIAL AND Ca^{2+} BUFFERS ((G. DiMassa, W. Wang, L. Cleemann and M. Morad)) Dept. of Pharm., Georgetown University Medical Center, Washington, DC 20007. (Spon. by F.N. Briggs)

Mammalian cardiomyocytes are activated mainly by release of Ca^{2+} from the sarcoplasmic reticulum (SR) by clusters of Ca^{2+}-sensitive ryanodine receptors within discrete junctional membranes. The localized nature of such releases is indicated by a) "Ca^{2+} sparks" seen through confocal microscopy and b) the persistence of Ca^{2+} signaling even when the diffusion distance of Ca^{2+} is reduced to <50 nm by dialysis of myocytes with high concentrations of Ca^{2+} buffers (Adachi-Akahane et al., 1996, J. Gen Physiol. 108). To combine these lines of inquiry we used a rapidly scanning confocal microscope (Noran, 120-240 frames/s) to measure "Ca^{2+} sparks" in rat and mouse ventricular myocytes dialyzed with 1 mM Fluo-3 and 0-20 mM EGTA. The cells were held at potentials between -50 and -120 mV where individual Ca^{2+} sparks were more clearly distinguished than during activation of the Ca^{2+} current. At more negative holding potentials Ca^{2+} sparks increased in size, and decreased in frequency. As non-fluorescent Ca^{2+} buffer concentrations increased (0, 1, 5, 14, 20 mM EGTA) the size of the sparks decreased, and were often not visualized, at 14 and 20 mM EGTA. In all cases the sparks were excluded from the nuclei, generally evolved along the sarcomere lines and lasted < 25 ms. The properties and detection of Ca^{2+} sparks were examined in detail by comparison with a computer model which simulated the duration of release, the diffusion of Ca^{2+} and buffers, the transfer from Fluo-3 to EGTA, the point spread function of the instrument and the counting statistics of detection. The results show that Ca^{2+} sparks in resting cardiomyocytes are sensitive to holding potential and can be more clearly defined by addition of 1-10 mM EGTA. (Supported by NIH HL ROI 16152).

M-Pos109

VISUALIZATION OF CALCIUM SPARKS IN HEART CELLS WITH TOTAL INTERNAL REFLECTION FLUORESCENCE MICROSCOPY (TIRF). ((**L. Cleemann** and M. Morad)) Department of Pharmacology. Georgetown University Medical Center. Washington, DC 20007.

Calcium sparks are measured with confocal fluorescence microscopy with a depth of focus ≅ 1 μm. We used TIRFM to measure Ca^{2+} sparks in superficial layers of cells where Fluo-3 was excited by Evanescence illumination (λ = 488 nm, argon ion laser), penetrating ≅ 0.2 μm up from the glass bottom of a perfusion chamber. The resulting fluorescent images (λ > 510 nm) were viewed through an upright microscope (Olympus BX50WI)) with long distance water immersion objective (LUMPlanFl, 60x, N.A. 0.9), were detected with an intensified CCD camera, acquired as individual frames on a computer, stored on video tape (sVHS, 30 frames/sec) and analyzed on a Silicon Graphics (Indy). Freshly dissociated heart cells from rat and shark were allowed to settle in the perfusion chamber and were stained with 10 μm Fluo-3 AM for 1 h. Initially the TIRF images showed only diffuse spots where the cells rested on the glass bottom. Later (>30 min.) the cells formed patchy arrays of intense fluorescence which resisted contractions and therefore were labeled "adhesions". Some streaks of light, in the general direction of the laser beam, penetrated into the fluid phase at air bubbles, imperfection in the glass surface, and, to a lesser degree, at all points of cellular contact. The background illumination resulting from this violation of the total internal reflection condition was minimized by focusing the (attenuated) laser beam to a small elliptical spot (100 μm x 200 μm). TIRF images showed only small, well defined regions within the outlines of cells seen with epi-fluorescence and bright field illumination. Within areas of adhesion, rat ventricular myocytes showed Ca^{2+} waves and Ca^{2+} sparks similar to those seen with confocal microscopy. These patterns were not seen in shark ventricular cells, which have no releasable internal Ca^{2+} stores. These results show that the use of TIRFM in isolated cardiomyocytes can measure brief, local Ca^{2+} sparks, and that these local transients depend on the presence of functional internal Ca^{2+} stores. Our data suggests that TIRFM a) produces a higher depth resolution (< 200nm) b) has a frame rate determined by the readout of the camera only. *Supported by NIH RO1 HL 16152.*

M-Pos110

SUBCELLULAR PROPERTIES OF $[Ca]_i$ TRANSIENTS IN PHOSPHOLAMBAN DEFICIENT MOUSE VENTRICULAR MYOCYTES

((J. Hüser, H. Satoh#, D.M. Bers, E.G. Kranias* & L.A. Blatter))
Dept. of Physiology, Loyola University Medical Center, Maywood, IL 60153; #Dept. of Internal Medicine, Hamamatsu University Med. School, Hamamatsu, Japan;*Dept. of Pharmacol. & Cell Biophysics, University of Cincinnati, OH 45267

Phosphorylation of the SR Ca pump regulatory protein phospholamban (PLB) is known to release its inhibitory effect on pump activity. This mechanism is believed to be a major component in the positive inotropism exerted by ß-adrenergic stimulation. We have used the Ca-sensitive fluorescent probe fluo-3/AM with laser scanning confocal microscopy to study the subcellular properties of intracellular Ca ($[Ca]_i$) transients in ventricular myocytes isolated from wild type (WT) and phospholamban knockout (PLB-KO) mice (Luo *et al., Circ. Res.* 75: 401, 1994). Comparison of the steady state twitch $[Ca]_i$ transients in WT and PLB-KO myocytes revealed no significant increase in amplitude (measured as $\Delta F/F_0$). Time constants for relaxation of the $[Ca]_i$ transient, however, were about 2 times smaller in PLB-KO cells. This acceleration of SR Ca uptake was also responsible for a marked decrease in the wavelength of $[Ca]_i$ waves in PLB-KO myocytes observed when the cell was Ca overloaded. In addition, $[Ca]_i$ waves in PLB-KO cells were more frequently aborted. Analysis of local Ca release events (Ca sparks) showed no significant difference in the amplitude. The time constants for spark relaxation were about 1.5 times smaller for PLB-KO than for WT myocytes, consistent with the idea that SR Ca uptake significantly contributes to the decay of Ca sparks. In addition, in PLB-KO myocytes a large fraction of local $[Ca]_i$ transients displaying a larger amplitude and slower relaxation could be recorded. The characteristic rest potentiation and negative staircase following the onset of electrical stimulation in WT mouse ventricular myocytes was conserved in PLB-KO cells. However, the negative staircase in PLB-KO myocytes was paralleled by increasing spatial inhomogeneities of the $[Ca]_i$ transient.

M-Pos111

INACTIVATION OF Ca^{2+} RELEASE DURING Ca^{2+} SPARKS IN RAT VENTRICULAR MYOCYTES. ((Theodore Wiesner*, Valeriy Lukyanenko and **Sandor Györke**)), Texas Tech University HSC, Lubbock, TX 79430 & *Dept. of Chemical Engineering Texas Tech University, Lubbock, TX 79409.

Termination of Ca^{2+} release during local Ca^{2+} release events (Ca^{2+} sparks) could be due to: 1) Ca^{2+} release dying off spontaneously (stochastic attrition, Stern, Biophys. J. 63: 497, 1992) or 2) inactivation/adaptation of release. To discriminate between these possibilities, we correlated the magnitude of spontaneous Ca^{2+} sparks with the rate of decay of Ca^{2+} release during the sparks. Theoretically, the rate of a stochastic decay mechanism should be very sensitive to the magnitude of the positive feedback gain that sustains the local Ca^{2+} elevation (Stern, 1992). Thus, if termination of release during Ca^{2+} sparks is due to a stochastic mechanism, an increase in the magnitude of sparks should be accompanied by a decrease in the rate of decay of release during the sparks. On the other hand, an inactivation/adaptation mechanism predicts that the rate of termination of Ca^{2+} release for large sparks will be at least as fast as termination of release for small sparks. Confocal Ca^{2+} imaging was used to measure Ca^{2+} sparks in Fluo-3 loaded isolated rat ventricular myocytes. The magnitude of the sparks was varied by changing the SR Ca^{2+} load by exposing the cells to bathing solutions containing either 1 or 10 mM $[Ca^{2+}]$. The local Ca^{2+} release flux underlying Ca^{2+} sparks was derived by adapting the method of Sipido and Wier (J. Physiol., 435: 605, 1991) to describe cell-averaged Ca^{2+} release. Our results show that in myocytes exposed to 10 mM Ca^{2+}, the magnitude of sparks was 4-fold greater then that measured in cells exposed to 1 mM Ca^{2+}. At the same time, decay of the release flux in 10 mM Ca^{2+} was at least as fast as in 1 mM Ca^{2+} (mean time constants, 10 ms vs. 11 ms). These results suggest that termination of Ca^{2+} release during Ca^{2+} sparks is not due to a stochastic mechanism, but rather to inactivation/adaptation of the Ca^{2+} release channels. (Supported by NIH HL 52620).

M-Pos112

CALCIUM MOVEMENTS IN PERFUSED WHOLE RAT HEART VIEWED WITH CONFOCAL IMAGING ((Tetsuhiro Minamikawa, Stephen Cody and **David A. Williams**)) Muscle & Cell Physiol. Lab., Dept. of Physiology, The Univ. of Melbourne, Vic., Australia.

It has been well described that intracellular calcium ($[Ca^{2+}]_i$) oscillations occur without action potentials in single cardiac cells and multicellular preparations. While in isolated cells the oscillatory Ca^{2+} transients have been directly visualised as propagated fluorescent waves using various combinations of fluorescent probes and imaging systems, in multicellular preparations they are commonly inferred from measurement of muscle tension, laser light scattering or from luminescent signals from micro- or macro-injected aequorin. Thus, spatial information about ionic events in these complex cardiac preparations has not been available to date. Moreover, it has yet to be determined whether the whole perfused heart exhibits such spontaneous Ca^{2+} oscillations, either at the cellular or subcellular level, in a steady-state.
Fluorophore loading at low temperature, confocal microscopy, and the elimination of refractive index mismatch with "bottom-less" bath designs and saline-immersible objective lenses, enabled us to image multiple $[Ca^{2+}]_i$ waves in the subepicardial mycardium of the fluo-3 loaded heart. $[Ca^{2+}]_i$ waves were sporadically seen even with perfusion of physiological $[Ca^{2+}]_o$ in a paced or arrested heart. With increase in $[Ca^{2+}]_o$ the waves became more prevalent, mutifocal, exhibited non-propagated hot-spots of spontaneous Ca^{2+} release (Ca^{2+} sparks), and an increasing fraction of waves exhibited faster propagation velocities and higher frequencies. Waves clearly propagated beyond cellular boundaries within the 3-D structures of cardiac muscle, providing the opportunity to study cell-cell communication. Caffeine in the perfusate abolished spontaneous Ca^{2+} release. This is the first direct visualisation of $[Ca^{2+}]_i$ movements in individual cells in the whole functioning heart.
Supported by the NH&MRC, Australia.

M-Pos113

SPONTANEOUS CALCIUM SPARKS IN β_1 KNOCK-OUT SKELETAL MUSCLE DEFICIENT IN DIHYDROPYRIDINE RECEPTOR SUBUNITS. (M. Conklin, P. Powers*, R. Gregg*, and R. Coronado. Department of Physiology and *Waisman Center, University of Wisconsin, Madison, WI 53706.

β_1-null cells from mice homozygous for a null mutation of the β_1 (cchb1) gene encoding the β_1 subunit of the skeletal dihydropyridine receptor do not generate Ca^{2+} transients in response to cell depolarization (Strube et al, 1996). Immunostaining of β_1-null cells indicates that β_1 is absent, α_{1S} subunit is reduced and RyR1 is present in normal amounts (Gregg et al, 1996). We used the line-scan mode in a LSCM to characterize Ca^{2+} sparks in mutant cells from intercostal muscles loaded with fluo-3. Sparks occurred repetitively at preferential locations within a given cell. Average time to peak was 63 ms, the decay time constant was 80 ms, and the fold increase in peak fluorescence intensity was 2.3. These parameters were similar to those of normal cells. Mutant sparks (n=219) had a diameter (FWHM) of 5.3 μm which was significantly larger than that of normal cells (3.9 μm). Line-scan images in mutant cells revealed symmetrical (1), left-skewed (2) or right-skewed (3) sparks. Skewed sparks were not seen in normal cells. Skewing may result from activation of RyRs in different positions within a large cluster of RyR receptors. Thus the size of the cluster of ryanodine receptors from which a spark originates may be different in normal and mutant cells. The data suggests that the expression of DHP receptor subunits determines many of the charactaristics of spontaneous Ca^{2+} sparks. Supported by NIH, NSF.

M-Pos114

RAPID SOLUTION CHANGES IN CARDIAC MYOCYTE T-TUBULES

((L.A. Blatter* and E. Niggli°)) Depts. Physiology, °University of Bern, Bern, Switzerland, *Loyola University, Chicago (spon. by A. Azzi)

Diffusion of second messengers like Ca ions across distances of tens of microns is notoriously slow. Therefore, most skeletal and cardiac myocytes have developed t-tubules to rapidly convey ec-coupling signals deep into the cell interior and to ensure subcellularly homogeneous Ca signals. However, the lumen of the t-tubules may form a compartment that has limited access to the bulk extracellular space and may therefore give rise to accumulation phenomena, even in single cell experiments. We used the lipophilic fluorescent Ca indicator Calcium-Green C-18 (C-18) to analyze the extracellular accessibility of the t-tubular lumen in isolated guinea-pig ventricular myocytes. Concentration jumps of extracellular [Ca] were applied with a rapid superfusion device while the wave-front of Ca in the t-tubules was recorded with a laser-scanning confocal microscope in the line-scan mode. After rapid increases of $[Ca]_o$ a wave-like Ca gradient traveled along the t-tubules at a velocity of 3.4 - 16.3 μm s^{-1}. In typical cardiac myocytes (120 μm * 30 μm * 15 μm) the solution change within the t-tubules was delayed by 0.63 - 2.3 s (n=6) and slowed from t1/2 = 0.9 s to 1.7 s (from F_{max} to F_{min}). This unexpectedly slow exchange of the solution within the t-tubules lasting several seconds is most likely significant during rapid solution change experiments. Furthermore, the limited access to the bulk solution may give rise to spatiall inhomogeneous accumulation and/or depletion resulting from ion fluxes across the t-tubular membrane during physiological activity. (Supported by SNF and Schweppe Foundation Chicago).

M-Pos115

TRIADIC CALCIUM RELEASE SIGNALS IN INTACT FROG SKELETAL MUSCLE FIBERS STUDIED WITH CONFOCAL MICROSCOPY ((S. Hollingworth, S.M. Baylor, L.D. Peachey* and Mingdi Zhao)). Departments of Physiology and Biology*, University of Pennsylvania, Philadelphia, PA 19104.

In cut fibers exposed to fluo-3 and activated electrically, previous confocal studies (Tsugorka et al., Science 269:1723, 1995; Klein et al., Nature 379:455, 1996) reported detection of triadic fluorescence signals with a quantized amplitude ($\Delta F/F$ at peak, ~0.3 and ~0.6 respectively). Klein et al. also reported that quantized triadic events occur frequently in resting fibers. To test if analogous signals exist in intact fibers, single fibers were injected with fluo-3 (myoplasmic concentration, 0.2-0.4 mM; 20°C) and x-t scans were acquired on a Leica TCS microscope with a Zeiss water-immersion objective (40x, 0.75na). There was little or no evidence of quantized fluorescence events in resting fibers. With fibers in TTX Ringer and activated locally by a 100-200 ms current step from an extracellular electrode, triadic signals were detected that were clearly inhomogeneous in space and time. With larger stimulations (spatially-averaged peak $\Delta F/F$ = 1-2), the triadic signals had relatively large amplitudes (peak $\Delta F/F$, up to 0.4-0.6). However, with smaller stimulations (spatially-averaged $\Delta F/F$ = 0.1-0.2), peak amplitudes were 3-4 fold smaller, thus implying that the larger signals are not elementary. Analogous experiments carried out with Oregon-Green-2 gave qualitatively similar results, although, in contrast to fluo-3, the resting fluorescence of Oregon-Green-2 is brighter at the z-line than in the middle of the sarcomere.

Supported by NIH RR-2483 (to LDP) and NS-17620 (to SMB).

M-Pos116

FURTHER LOCALIZATION OF THE PHYSIOLOGIC TRIGGER OF SKELETAL MUSCLE TYPE E-C COUPLING WITHIN THE α_1 SUBUNIT II-III LOOP OF THE DIHYDROPYRIDINE RECEPTOR (DHPR). ((R. El-Hayek[1], and N. Ikemoto[1,2])). 1, Boston Biomed. Res. Inst.; 2, Dept. Neurology, Harvard Med. Sch., Boston, MA.

Recent evidence in the literature suggests that the cytoplasmic loop linking repeats II and III of the α_1 subunit of the DHPR (II-III loop) plays a critical role in skeletal muscle e-c coupling. Among all synthetic peptides encompassing various regions of the II-III loop, only one peptide corresponding to residues Thr^{671}-Leu^{690} (peptide A) activated the RYR1 and triggered SR Ca^{2+} release (*El-Hayek et al. (1995), J. Biol. Chem. 270, 22116-22118).* We gained further evidence for the concept that peptide A region of the II-III loop represents the activating region of the skeletal muscle type e-c coupling: (i) Peptide A-induced RYR1 conformational change and SR Ca^{2+} release are tightly correlated with the high affinity peptide A binding to triads corresponding to a stoichiometry of ~ 4 moles peptide A bound to each RYR1 tetrameric unit and (ii) Peptide A activated [^{3}H]ryanodine binding to RYR1 but had no appreciable effect on the RYR2. We further localized the activating subdomain within peptide A to the predominantly positively charged decapeptide region encompassing Arg^{681}-Leu^{690} (peptide A-1). A decapeptide encompassing the cardiac counterpart of skeletal peptide A-1 had almost identical net positive charge but failed to produce any RYR1 activation. These findings indicate that the *in situ* counterpart of the Arg^{681}-Leu^{690} region of the skeletal DHPR represents the physiologic trigger of the skeletal muscle type e-c coupling. (Supported by NIH and MDA)

M-Pos117

A N *IN VITRO* MODEL OF CONTRACTION-RELAXATION COUPLING. ((N. Ikemoto[1,2], Y. Saiki[1], and R. El-Hayek[1])). 1, Boston Biomed. Res. Inst.; 2, Dept. Neurology, Harvard Med. Sch., Boston, MA.

Twitch contraction in an intact muscle cell is followed by a rapid tension decay, suggesting that the Ca^{2+} released from the SR is removed rapidly from the cytoplasm by the SR Ca^{2+} pump and by other Ca^{2+} binding proteins. The important question to be resolved is whether the two processes, SR Ca^{2+} release and the subsequent Ca^{2+} re-uptake, are operating independently or in a coupled manner. To investigate this question, we have made a preliminary effort first to devise suitable conditions for monitoring rapid release/re-uptake time courses using our triad model, and second to examine the correlation between the release and re-uptake kinetics. An abrupt increase of Ca^{2+} in the reaction solution from 0.2 μM to higher levels (≤ 1 μM) in the presence of Mg.ATP produced further Ca^{2+} uptake into the Ca^{2+}-preloaded SR moiety, as monitored in a stopped-flow fluorometric system using fluo-3 as a Ca^{2+} probe. With a partial Ca^{2+} preloading, there was no Ca^{2+}-induced Ca^{2+} release. However, the addition of increasing concentrations of low Mr (e.g. 4k) polylysine concomitantly with the Ca^{2+} jump induced first Ca^{2+} release and then Ca^{2+} re-uptake. Interestingly, the larger the magnitude of Ca^{2+} release was, the faster and larger the subsequent Ca^{2+} re-uptake became. The polylysine-induced fluorescence increase of the RyR-bound MCA (a channel-activating conformational change in the RyR) was followed by a rapid spontaneous decay which preceded Ca^{2+} re-uptake. These results suggest that the activation and inactivation of the Ca^{2+} release channel are immediately followed by the activation of the SR Ca^{2+} pump. (Supported by NIH and MDA).

CARDIAC ELECTROPHYSIOLOGY I

M-Pos118

EFFECTS OF MIBEFRADIL (Ro 40-5967) ON THE ACTION POTENTIAL OF ISOLATED VENTRICULAR MYOCYTES.
((Agnès Bénardeau & Eric A. Ertel)) F.Hoffmann-La Roche, CH-4070 Basel.

Mibefradil (Ro 40-5967) is a recently developed Ca antagonist from a new chemical class (tetralene) which, unlike diltiazem and verapamil, slows heart rate without negative inotropy. We have previously reported that mibefradil blocks T-type Ca channels more potently than L-type in guinea pig atrial cells. Because some Ca channel blockers, such as diltiazem or verapamil, can inhibit the delayed rectifier K current, we examined whether mibefradil could increase the duration of the cardiac action potential (APD) despite the inhibition of Ca currents. Action potentials (AP) were recorded in whole-cell patch-clamped guinea pig ventricular myocytes, at room T°. We find that 1 and 10 μM mibefradil dose-dependently reduces the APD 10-60% (Fig). No secondary effect appears if the drug remains applied for 30 min. In contrast, K channel blockers such as terfenadine (50 nM) and quinidine (20 μM) immediately lengthen the AP >100%. We also tested 4 metabolites of mibefradil (10 μM), which all shorten the AP although slower and more reversibly. Both amlodipine (10 μM) and Cd^{2+} (100 μM) also reduce the APD ≈60% and no additional effect is observed when mibefradil (10 μM) is applied on top of either drug. Contrary to the other Ca antagonists, mibefradil shortens the early plateau of the APs much less than the late one (Fig): this could be a consequence of the marked voltage-dependence of its block of Ca channels. In conclusion, mibefradil reduces the APD through the block of Ca channels with no evidence of K channel inhibition, suggesting that this new Ca antagonist is devoid of proarrhythmic effects.

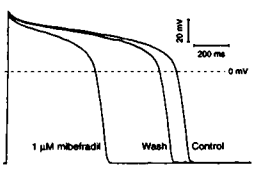

M-Pos119

MODULATION OF REPOLARIZATION BY QUINIDINE IN DIFFERENT MYOCARDIAL LAYERS IN VITRO AND IN VIVO. ((**E.P. Anyukhovsky**, E.A. Sosunov and M.R. Rosen)) Columbia University, New York, NY 10032.

We used standard microelectrode techniques to study the effects of quinidine (Q) (2.5-20 μM) on action potential duration to 90% repolarization (APD) in canine ventricular epicardial (EPI), endocardial (ENDO) and transmural (M) slabs at cycle lengths (CL) .3-4 s. Qualitatively different effects were seen in M vs ENDO and EPI. Q induced dose-dependent prolongation of APD at all CL in EPI and ENDO. In contrast, in M, the pattern of Q effect depended on CL. At Cl=.3 s APD increased dose-dependently by up to 21±5% at 20 μM. At CL=2 s APD was prolonged at 2.5 μM (by 36±9%) and with increase of [Q] this effect subsided and reversed (-17±5% at 20 μM). Experiments with E4031 (1 μM) and TTX (2 μM) suggested that APD lengthening at CL=.3 s was attributable to I_{Kr} suppression by Q, and APD shortening at long CL was due to inhibition of TTX-sensitive window current. In situ, we used plunge and surface electrodes to measure activation recovery intervals (ARI) of bipolar electrograms obtained from EPI, M and ENDO layers of canine left ventricle in conditions of AV block and ventricular pacing. Q was infused continuously so that plasma Q monotonically increased from 4.9±.3 μM (n=11) at 30 min to 23.5±4.0 μM at 3 h. At CL from .3 to 1.5 s there was no ARI gradient across the ventricular wall before and during Q infusion. At CL=.3 s Q increased ARI dose-dependently by up to 18±4% at the highest Q concentration ([Q]). At CL=1.5 s ARI were prolonged by 37±7% at 4.9±.3 μM. With increase of [Q] this effect subsided to -1±6% at the highest [Q].Thus, the effects of Q on ARI vary from prolongation to shortening depending on [Q] and CL. They are the same in all myocardial layers and follow the pattern observed in M cells (not ENDO or EPI) in vitro.

M-Pos120

ANTIARRHYTHMIC AND ELECTROPHYSIOLOGIC EFFECTS OF CHRONICALLY ADMINISTERED AMIODARONE IN ISOLATED GUINEA PIG HEARTS. ((**E.A. Sosunov**, E.P. Anyukhovsky and M.R. Rosen)) Columbia University, New York, NY 10032.

The antiarrhythmic effect of chronically administered amiodarone (Am) (80 mg/kg, IP, daily for 7 days) was examined in Langendorff perfused guinea pig hearts driven at cycle length=250 ms during 15 min of global ischemia (GI) and reperfusion. Before GI, Am prolonged the QT interval (Am,170±2 ms, n=12 vs Control (C), 150±3 ms, n=12, p<.05) whereas after 8 min of GI, QT did not differ (Am,102±4 ms vs C, 106±5 ms, p<.05). Am had no effect on arrhythmias during GI but, on reperfusion, reduced the incidence (Am, 25% vs C, 100%, p<.05) and the duration (Am, 55±47 s vs C, 519±77 s, p<.05) of ventricular fibrillation (VF). To examine the importance of QT prolongation in this model, the acute effect of the I_{kr} blocker E4031 (E) ($3x10^{-6}$M) was studied in non-Am-treated animals. Before GI, E induced QT prolongation comparable to Am (E, 166±3 ms, n=10 vs C, 148±2 ms, n=10, p<.05) which became negligible in GI (E, 100±6 ms vs C, 98±4 ms). In contrast to Am, E did not change significantly the incidence (E, 90% vs C, 100%) and the duration (E, 289±73 s vs C, 397±45 s) of VF after reperfusion. Am increased ventricular conduction time (by 12±2%, p<.05) and this effect was accentuated during GI (to 42±7%, p<.05). Am amplified 3-fold the GI induced increase in stimulation threshold. Am did not affect the upstroke of fast (Na^+-dependent) and slow (Ca^{++}-dependent) response action potentials in isolated papillary muscles. The data suggest that the antiarrhythmic activity of chronically administered Am in the present study did not depend on QT prolongation, effects on upstroke velocity of Na^+-dependent or Ca^{++}-dependent action potentials and might be due to an increase of axial resistance.

M-Pos121

EVIDENCES OF ANTAGONISM BETWEEN AMIODARONE AND T_3 ON THE K^+ CHANNEL ACTIVITIES OF CULTURED RAT CARDIOMYOCYTES. ((**W. Guo**, K. Kamiya and J. Toyama)) Dept. of Circulation, Res. Inst. Environ. Med., Nagoya Univ., Nagoya 464-01, Japan.

Effects of acute and chronic treatments with amiodarone, both in the presence and the absence of exogenous triiodothyronine (T_3), on repolarizing outward K^+ currents were investigated by patch-clamp technique in cultured newborn rat ventricular cells. Acute exposure to amiodarone dose-dependently inhibited the transient outward (I_{to}, IC_{50}=4.9 μM) and the steady-state outward (I_K, IC_{50}=6.3 μM) K^+ currents. The dose-response curve of this acute inhibitory action was unaffected by the presence of T_3. When amiodarone was applied chronically, 72-hour exposure to a low dose of the drug (1 μM) significantly decreased the current densities of I_{to} and I_K for the cells cultured in a serum-supplemented medium containing 0.12 nM T_3. In a serum-free medium without T_3, chronic amiodarone treatment revealed null effect on either I_{to} or I_K. In addition, 72-hour in-vitro treatment with T_3 enhanced the current densities of both I_{to} (EC_{50}=0.13 nM) and I_K (EC_{50}=0.33 nM). Concentration-response analysis indicated that amiodarone (1 μM) showed competitive inhibition towards the action of T_3 on I_{to} but noncompetitive inhibition towards the action of T_3 on I_K. These results suggest that different ionic mechanisms are produced by acute and long-term treatments with amiodarone. The latter showed T_3-dependent inhibition of cardiac I_{to} and I_K. When chronically administered, amiodarone may antagonize T_3 and thereby counteract its hormonal effect on K^+ channels. This implies that, at the myocyte level, antagonism of the action of thyroid hormones in K^+ channel activities may contribute to the cardiac effects of chronic amiodarone therapy.

M-Pos122

ANALYSIS OF ACTION POTENTIAL CONDUCTION AMONG CELLS OF DIFFERENT CELL TYPE WITHIN THE RABBIT ATRIOVENTRICULAR NODE. ((**David A. Golod**, Rajiv Kumar and Ronald W. Joyner)) Department of Pediatrics, Emory University, Atlanta, GA, 30322)

Action potential conduction through the Atrioventricular (AV) node involves sequential propagation from: **a**) fast-response cells which are quiescent to **b**) Transitional cells which have lower maximum dV/dt and are spontaneously active at a low rate, to **c**) slow-response cells of the central region which are spontaneously active at a higher rate. We have used a coupling clamp technique to form pairs of cells of each of these cell types to investigate the properties of action potential conduction between cells of different cell type. For the fast-response cells we have used a real-time simulation of the Luo-Rudy ventricular cell model with the size of the cell decreased by a factor of 10 to account for the much higher input resistance of atrial cells (200 MΩ) compared to ventricular cells (20 MΩ). For the transitional cells we used actual experimental recordings from cells isolated from the rabbit AV node. For the central nodal cells we used either actual experimental recordings or a real-time simulation of the Wilders *et al.* (1991) Sinoatrial nodal model for a spontaneously pacing cell. When a Transitional cell was coupled to a fast-response cell model, there were three possible outcomes, depending on the progressively increasing value of coupling conductance (G_c) which was used: **a**) continued pacing of the Transitional cell without driving of the fast-response cell, **b**) continued pacing of the Transitional cell with successful driving of the fast-response cell, or **c**) cessation of pacing of the Transitional cell. When either a real Transitional cell or a real central AV nodal cell was coupled to the nodal cell model, synchronization of spontaneous pacing occurred at very low values of G_c, with complex periodic alterations of the cycle lengths of the real cell and the model cell at values of G_c below that required for synchronization. The use of the coupling clamp technique demonstrates some of the complexity of synchronization and conduction within the rabbit AV node.

M-Pos123

EFFECTS OF ACUTE MYOCARDIAL ISCHEMIA ON EXCITABILITY AND ACTION POTENTIAL DURATION: IONIC MECHANISMS. ((**R.M. Shaw**, Y. Rudy)) Cardiac Bioelectricity Research and Training Center, Case Western Reserve University, Cleveland, OH 44106-7207.

A consequence of acute myocardial ischemia is reduced membrane excitability. However the ionic currents responsible for reduced excitability and the contribution of each of the three ischemic conditions (elevated $[K]_o$, acidosis, and anoxia) have not been elucidated. We have investigated the ionic mechanisms of steady state and post-repolarization excitability with the dynamic Luo-Rudy cell model formulated to represent these three conditions of ischemia.

Increases in extracellular potassium ($[K]_o$) had the major effect on excitability by depolarizing resting membrane potential (V_{rest}), causing reduction in sodium channel (I_{Na}) availability. Acidosis caused a $[K]_o$-independent reduction in maximum upstroke velocity, $(dV_m/dt)_{max}$. A transition from I_{Na}-dominated to calcium current, $I_{Ca(L)}$, dominated upstroke occurred, but only after sodium channels were almost fully (97%) inactivated. Incorporation of acidosis prevented transition to $I_{Ca(L)}$ -dominated upstroke by reduction of both I_{Na} and $I_{Ca(L)}$. Delayed recovery of excitability (post repolarization refractoriness) was determined by the slow recovery kinetics of I_{Na}. V_{rest} depolarization caused by elevated $[K]_o$ increased the time constant of I_{Na} recovery and of $(dV_m/dt)_{max}$ recovery from τ =10.3 ms at $[K]_o$=4.5 mM to τ=81.4 ms at $[K]_o$ =12 mM. Anoxia and acidosis had little affect on τ. Action potential shortening resulted from activation of $I_{K(ATP)}$, the ATP activated potassium current (0.6% activation caused 50% shortening of APD) and was not influenced by acidic changes of $I_{Ca(L)}$. We conclude that ischemic depression of membrane excitability and the time course of recovery are caused by elevated $[K]_o$ with additional depression by acidosis. Anoxia, even with activation of $I_{K(ATP)}$, has little direct effect on excitability.

M-Pos124

ADAPTATION OF REPOLARIZATION ACROSS THE VENTRICULAR WALL IN THE LONG QT SYNDROME ((**E.B. Caref**, M. Restivo, M. Chinushi, V. Stoyanovsky, S. John, M. Chaudry, N. El-Sherif)) VA Medical and SUNY Health Science Centers, Brooklyn, NY

A long-short sequence is a characteristic initiating feature of torsades de pointes in the Long QT Syndrome (LQTS). Adaptation of recovery was measured from activation-recovery intervals (ARI) across the left ventricular wall in the canine anthopleurin-A model of LQTS utilizing 32 transmural plunge needles, each having 8 unipolar recording sites. Restitution curves along the epicardial (EPI)-endocardial (END) axis were determined from S_2 ARI responses (S_1-S_1=1s). Figure shows dispersion of ARI at long intervals and a gradient between END and midmyocardium (M), and EPI and M. At short S_2, adaptation was greatest for M and END, but differences between M and both END and EPI remained. The electrograms show conduction block occurring at M at S_2 of 450 ms. In conclusion, although there is significant adaptation of ARI after a short cycle, dispersion still remains as a substrate for reentry.

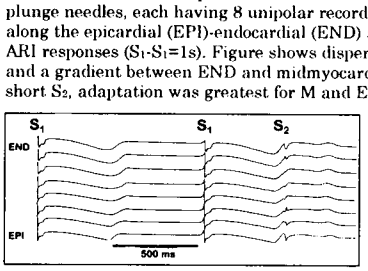

M-Pos125

CELLULAR BASIS OF PROARRHYTHMIA IN DOGS WITH CHRONIC COMPLETE ATRIOVENTRICULAR BLOCK. ((**P.G.A. Volders**, K.R. Sipido[1], A. Kulcsár, M.A. Vos, H.J.J. Wellens)) Cardiovascular Research Institute Maastricht, The Netherlands. [1]Lab of Exp. Cardiology, University of Leuven, B-3000, Belgium.

Dogs with chronic complete atrioventricular block (AVB) have an increased incidence of torsade de pointes during treatment with class-III antiarrhythmics. We have investigated the cellular basis of this proarrhythmia in single left ventricular midmyocardial myocytes (M cells) isolated from AVB and control dogs. Membrane potential (V_m) was recorded either by microelectrodes (3 mol/L KCl) along with contraction, or by patch electrodes (K^+aspartate, KCl) along with $[Ca^{2+}]_i$ (fluo-3, Ca-green-1). AVB M cell length was increased: 158±9 *versus* 143±17 μm in controls (p<0.05). Action-potential (AP) duration was larger in M cells from AVB dogs than from control dogs: at pacing cycle lengths (CL) of 0.5, 2 and 4 s APD_{95} measured 315±23, 452±71 and 507±83 ms in AVB M cells (n_{cells}=13, n_{dogs}=7) *versus* 294±28, 388±65 and 414±94 ms respectively in control cells (n_{cells}=15, n_{dogs}=5; p<0.05 for all CL). APD_{50} changed to the same extent; AP spike-and-dome configuration was the same for AVB and controls. The class-III agent almokalant (IK_r blocker; 1 μmol/L) prolonged the APD_{95} by 14, 71 and 96 % in AVB M cells *versus* 5, 14 and 24 % respectively in controls (CL of 0.5, 2 and 4 s, p<0.05 for all CL). Almokalant induced early afterdepolarizations (EAD) in 11 of 13 AVB M cells at CL of 2 and 4 s, but never at 0.5 s. In control cells EAD occurred in only 2 of 15 cells and only at CL of 4 s. EAD started at V_m of -21±7 mV with an amplitude of 10±6 mV, being similar for AVB and control M cells. These EAD did not trigger new AP. Neither the contraction signal nor $[Ca^{2+}]_i$ showed a clear increase during EAD, but relaxation was delayed. We conclude that in the dog with chronic AVB, proarrhythmia can be linked to cellular hypertrophy and AP prolongation. The AP prolongation is most likely due to a change in plateau current(s). These changes increase the susceptibility of AVB cells for class III-dependent AP prolongation and EAD formation.

M-Pos126

ACTION POTENTIAL HETEROGENEITY IN SHEEP PURKINJE CELLS: ROLE OF IONIC CURRENTS.

((**A.O. Verkerk**, A.C.G. van Ginneken, M.W. Veldkamp, L.N. Bouman)) Dept. of Physiology, University of Amsterdam, Netherlands. (Spon. by H.J. Jongsma)

Recently, we observed in free-running Purkinje fibres of the sheep two different action potential (AP) configurations. The first type had a large phase 1 repolarization and a relatively negative plateau (Fig A). The second had no or small phase 1 repolarization and a more positive plateau (Fig B). To determine which current(s) cause(s) these differences, membrane potentials and currents were studied in enzymatically isolated cells using the amphotericin perforated patch clamp technique. Like in intact fibres, the same two types of AP's were found in single Purkinje cells. Quasi steady state current (I_{ss}) and calcium current (I_{Ca}) were measured during 500 ms test pulses at various potentials from a holding potential of -40 mV. I_{ss} did not differ significantly for the two types. I_{Ca} was observed in all cells showing AP's with no or small phase 1 repolarization but just in the minority of the cells with large phase 1 repolarization. The first experiments with 4-aminopyridine showed that in the latter cell type, I_{Ca} was masked by the transient outward current (I_{to}). 500 ms depolarizing test pulses (0.2 Hz) from -80 mV to +50 mV showed that I_{to} was present in all cells with fast phase 1 repolarization but only in about 50% of the other cell type. I_{to} density in cells with small and cells with large phase 1 repolarization is 2.23±0.9 pA/pF (mean±SEM, n=5) and 10.5±3.8 pA/pF (n=9), respectively. These results suggest that the observed differences in AP's in Purkinje cells is caused by a combination of differences in I_{to} and I_{Ca} density.

M-Pos127

NORADRENALIN INDUCES ACTION POTENTIAL PROLONGATION AND EAD'S IN ISOLATED HUMAN VENTRICULAR MYOCYTES.

((**M.W. Veldkamp**, A.O. Verkerk, A.C.G. van Ginneken and L.N. Bouman)) Department of Physiology, University of Amsterdam, Amsterdam, The Netherlands.

The effects of noradrenalin (NA) on the action potential (AP) duration in ventricle appears to be species-dependent. Little is known about the effects of NA on the AP in single human ventricular myocytes. Therefore the effects of NA on AP's of human myocytes were recorded and the currents involved were investigated. Ventricular myocytes were isolated from explanted hearts from patients with end-stage heart failure, undergoing heart transplantation. AP's and membrane currents were recorded in the whole-cell configuration of the patch clamp technique. Exposure to 10^{-6} M NA resulted in a marked AP prolongation in all cells (n=7). In 2 out of 7 cells the AP duration was increased by 17%. In the other 5 cells, AP prolongation was much more pronounced and was accompanied by early after depolarizations (EAD's). Calcium current (I_{Ca}) and quasi steady state current (I_{ss}) were measured during 500 ms test pulses from a holding potential of –40 mV. In the presence of NA, I_{Ca} increased twofold from –4.7±1.1 pA/pF to –9.5±1.3 pA/pF at 0 mV (mean±SEM, n=11). Negative to –30 mV and positive to 0 mV I_{ss} was not affected, suggesting no effect of NA on the inward rectifier and delayed rectifier current. However, in the potential range from about -30 to 0 mV there was an increase in inward current from –0.34±0.04 pA/pF to –0.77±0.05 pA/pF (mean±SEM, n=5). This increase is probably due to an increase in calcium window current. The transient outward current (holding potential -80 mV) was unaffected by NA. In conclusion, an increase in I_{Ca} in the absence of changes in outward currents is responsible for the noradrenalin induced AP prolongation. The occurrence of EAD's is also likely to be due to the increase in I_{Ca}.

M-Pos128

EFFECTS OF SR INHIBITORS ON HIGH $[Ca]_o$ OR ISOPROTERENOL-INDUCED ARRHYTHMIAS AND AFTERPOTENTIALS IN ISOLATED GUINEA-PIG CARDIOMYOCYTES.

((**D. Tweedie**, S.E. Harding and K.T. MacLeod)) Cardiac Medicine, Imperial College School of Medicine at National Heart & Lung Institute, Dovehouse Street, London SW3 6LY, UK.

Effects of thapsigargin (TG, 500nM) were assessed on contraction characteristics from myocytes exposed to high $[Ca]_o$ (HC, 8 or 12mM) under current-clamp (IC) and action potential voltage-clamp (APvc). Cells exposed to HC produced large increases in contraction amplitude (+181±68%) during current-clamp and no arrhythmias, but during APvc, arrhythmias were evident. TG reduced contraction amplitude in both normal $[Ca]_o$ (NT, 1mM) and HC conditions in current-clamp (NT -73±9%, HC -74±4% vs control, respectively) and abolished all arrhythmias produced by HC during action potential voltage-clamp (5 cells). Cells exposed to certain concentrations of isoproterenol (ISO, 3-20nM) produced arrhythmias and afterpotentials when stimulated in IC, following application of 10mM caffeine all the arrhythmias and afterpotentials were abolished (6 cells). Caffeine had small effects on action potential duration (+20±12% vs control). These findings imply that high $[Ca]_o$ and isoproterenol mediated arrhythmias are sensitive to sarcoplasmic reticulum (SR) blockers and that both types of afterpotentials may be dependent upon a functional SR.

M-Pos129

ANTHOPLEURIN A CAUSES CARDIAC ELECTROGRAM FRACTIONATION FOLLOWING PREMATURE STIMULATION.

((**J.I. Vandenberg**[*], A.A. Grace[*†], M.P. Zinkin[†], M.D. Lowe[*†], R.C. Saumarez[†])) Departments of Biochemistry[*] and Medicine[†], University of Cambridge; [†]Department of Cardiological Sciences, St. George's Hospital Medical School, London, United Kingdom

Mutations in potassium and sodium channel genes underlie the congenital long QT syndrome (LQT) and thus establish a direct link between ion channel function and arrythmogenesis. LQT_3 is the result of loss of inactivation mutations of *SCN5A*. This mutation can be mimicked by the sea anemone toxin Anthopleurin A (APA) which blocks the open ⇒ inactive transition in sodium channels. Premature beats applied in a decremental pacing sequence show high-risk patients to have evidence of slowed intraventricular conduction. It has therefore been proposed that sudden death in patients with congenital LQT may relate to dispersed and discontinuous propagation of ventricular activation. We have developed an animal model of LQT_3 to specifically test this hypothesis. Ferret hearts were Langendorff-perfused with a Krebs-Henseleit HCO_3^- buffered saline at 37°C and epicardial electrograms were recorded at 8 sites from circumferentially placed platinum electrodes. Pacing was controlled by computer with the basic cycle length 600 msec and every third beat delivered prematurely with the coupling interval (S_1S_2) successively reduced by 1 msec from 350 ms to 100 ms. APA caused a dose-dependent increase in the S_1S_2 interval at which electrogram fractionation occurred (Control: 189-208 msec, n=8, 10 nM APA: 265-290 msec, n=3). Similarly, APA caused a dose-dependent increase in electrogram duration (from 5-14 msec in control to 32-41 msec in APA hearts). These data are all similar to those observed in LQT VF survivors.

M-Pos130

MYOCARDIAL CALCIUM/CALMODULIN - DEPENDENT PROTEIN KINASE II ACTIVITY IS INCREASED DURING EARLY AFTERDEPOLARIZATIONS.

((**M.E. Anderson***, A.P. Braun#, and H. Schulman#)) *Vanderbilt University, Nashville, TN 37232 and #Stanford University, Stanford, CA 94305.

Elevations in cytosolic Ca^{2+} lead to enhancement of the L-type Ca^{2+} current ($I_{Ca\text{-}L}$) in heart via the Ca^{2+}/calmodulin-dependent protein kinase II (CaMK II). CaMK II may thus act as a proarrhythmic signaling molecule for early afterdepolarizations (EADs) due to $I_{Ca\text{-}L}$. We tested the prediction that CaMK II activity should be increased in ventricular myocardium during EADs. Once activated by Ca^{2+} -bound calmodulin, CaMK II activity may become independent of Ca^{2+}/calmodulin; this Ca^{2+}- independent activity can then be used as an index of total intracellular CaMK II activation. Action potential prolongation and EADs were observed in isolated rabbit hearts following addition of clofilium (7.5 μM) to the perfusate. Inward current for EADs in this model is likely due to $I_{Ca\text{-}L}$ as EADs are rapidly terminated by the $I_{Ca\text{-}L}$ blockers nifedipine (10 μM) or Cd^{2+} (200-500 μM). Ca^{2+}- independent CaMK II activity was assayed in left ventricular homogenates and expressed as a percent of maximal Ca^{2+}/calmodulin-dependent CaMK II activity. Assays of CaMK II activity were performed after 10 min of clofilium-induced EADs (Clofilium, n=5). Addition of the selective CaMK II inhibitor KN-93 (0.5 μM) 10 min prior to clofilium prevented the appearance of EADs (Clofilium+KN-93, n=6). The control hearts were not treated with clofilium or KN-93 (Control, n=5). EADs were associated with a 37% increase in CaMK II activity over control. Our results demonstrate that activation and inhibition of CaMK II correlate with the presence of EADs, suggesting a role for CaMK II as a proarrhythmic signaling molecule.

Ca^{2+}- independent CaMK II activity (mean ± S.D.)
(% of maximal Ca^{2+}/calmodulin-dependent activity)

Clofilium	Clofilium+KN-93	Control
11.8 ± 2.2*	8.6 ± 2.4	7.5 ± 2.2

*p = 0.015 compared to both groups 2 and 3.

M-Pos131

DIFFERENTIAL SENSITIVITY OF VENTRICULAR CELL TYPES TO CLASS III ANTIARRHYTHMIC AGENTS.

((**P.C. Viswanathan**, Y. Rudy)) Cardiac Bioelectricity Research and Training Center, Case Western Reserve University, Cleveland, OH 44106-7207.

Regional differences in the electrophysiologic and pharmacologic properties of ventricular myocardium have been reported recently. The mid-myocardial M-cells are characterized by smaller density ratio of the delayed rectifier currents, I_{Ks} : I_{Kr}. We have studied the effect of Class III antiarrhythmic agents on Action Potential Duration (APD) in the three cell types: endocardial, M-cells, and epicardial cells using the theoretical Luo-Rudy model of guinea pig ventricular myocytes. We simulated the effect of drugs by selectively blocking I_{Kr} or I_{Ks}. I_{Kr} block, and not I_{Ks} block, had a greater effect in prolonging APD in the M-cells, due to smaller I_{Ks} : I_{Kr} ratio in these myocytes. At slow pacing, less than 50% block of either current caused Early Afterdepolarizations (EADs) in M-cells, but not in epicardial or endocardial cells. I_{Kr} block was also more effective in prolonging APD at slow rates (reverse rate dependence). Contrary to what has been suggested, the model predicts reverse rate dependence for IKs block as well. This prediction awaits experimental verification when specific Iks blockers are developed. In conclusion, the study demonstrates that reduced I_{Ks} : I_{Kr} density results in greater responsiveness of M-cells to Class III antiarrhythmic agents and a greater susceptibility to EADs. The results also indicate the importance of I_{Ks} in influencing the rate dependence of I_{Kr} block on APD prolongation. The nonuniformity of responses of the different cell types could introduce inhomogeneities (dispersion) of repolarization in the myocardium, thereby creating conditions for unidirectional block and reentrant arrhythmias.

M-Pos132

LYSOPHOSPHATIDYLCHOLINE DISRUPTS CELL VOLUME CONTROL IN MYOCYTES.

((M.A. Suleymanian and C.M. Baumgarten))
Dept. of Physiology, Medical College of Virginia, VCU, Richmond, VA 23298.

Lysophosphatidylcholine (LPC) accumulates during myocardial ischemia, alters ion channel and transporter function, and contributes to arrhythmogenesis. Here we report that exogenous palmitoyl (16:0) LPC also disrupts the regulation of cell volume in rabbit ventricular myocytes. Cell volume was measured by digital video microscopy and each cell served as its own control. Addition of 0.5 - 5 μM LPC(16:0) to Ca-free Tyrode solution caused a dose-dependent shrinkage of up to 7.7 ± 0.8% (5 μM). At 2 and 5 μM, shrinkage was transient; myocyte volume increased by 19.9 ± 2.0% after 10 min in 5 μM LPC. Replacement of external Na^+ with N-methyl-d-glucamine or Cl^- with methanesulfonate exacerbated cell shrinkage and largely eliminated the swelling phase. In contrast, 1 μM saxitoxin failed to abolish swelling. Swelling also was blocked by 1.8 mM Ca^{2+} and by 0.9 mM but not 0.1 mM Gd^{3+} or La^{3+}. Lysolipids (5 μM) with shorter acyl chains, capryl (10:0) LPC, and a long-chain ethanolamine lysolipid, LPE (16:0), did not alter cell volume. LPC (16:0) is known to increase membrane fluidity, and cell swelling is likely to result from Na and Cl influx. Ca, Gd, and La decrease fluidity and thereby may inhibit cell swelling. Disruption of myocyte cell volume regulation by LPC may contribute to the pathophysiology of ischemia. (Supported by NIH HL46764)

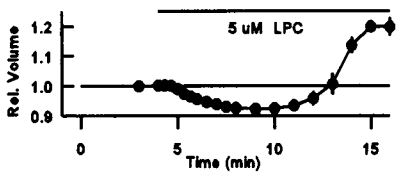

M-Pos133

IONIC BASIS OF RYANODINE'S NEGATIVE CHRONOTROPIC EFFECT ON S-A NODE PACEMAKER CELLS. ((J. Li and **R.D. Nathan**)) Department of Physiology, Texas Tech University Health Sciences Ctr., Lubbock, TX 79430.

Simultaneous recordings of electrical activity and the Indo-1 fluorescence ratio were obtained in single pacemaker cells, which were isolated from rabbit S-A node and cultured for 2 or 3 days. Ryanodine (Ry, 10 μM) decreased the amplitude of action potential-induced Ca_i^{2+} transients by 19 ± 3%, reduced the slope of the final phase of diastolic depolarization by 37 ± 3%, depolarized the take-off potential by 5 ± 1 mV, and slowed the firing rate by 32 ± 3% (n = 15; P < 0.01). Caffeine-induced Ca^{2+} release from the SR could be blocked by the same concentration of Ry. During perforated-patch whole-cell recordings, 10 μM Ry failed to alter hyperpolarization-activated or time-independent inward current in 8 pacemaker cells. Ry did, however, reduce the sum of L-type ($i_{Ca,L}$) and T-type ($i_{Ca,T}$) Ca^{2+} currents, i_{Ca} (HP = -80 mV), significantly at -30, -20 and -10 mV, in either the absence (8 cells) or presence (5 cells) of 25 μM BAPTA/AM. In contrast, $i_{Ca,L}$ was unaffected by Ry. Following rupture of the patch and almost complete rundown of $i_{Ca,L}$, Ry reduced i_{Ca} significantly at -30, -20, -10, 0 and +10 mV in 5 cells. Slowly decaying inward current tails, presumed to be Na^+-Ca^{2+} exchange current (i_{NaCa}), were abolished by either BAPTA or Ry. BAPTA also reduced the firing rate by 28 ± 4% (n = 14; P < 0.01). We conclude that Ry slows pacemaker activity by reducing both i_{NaCa} and $i_{Ca,T}$. The reduction of i_{NaCa} is indirect, due to the fall in $[Ca^{2+}]_i$, while the fall in i_{Ca} seems to be a direct effect of Ry on T-type Ca channels.

M-Pos134

TRANSIENT OUTWARD CURRENTS IN HUMAN LEFT VENTRICULAR SEPTUM DURING COMPENSATED HYPERTROPHY. ((P. Bailly, JP Bénitah, M. Mouchonière, G. Vassort and **P. Lorente**)) U390 INSERM, CHU Arnaud de Villeneuve, 34295 Montpellier, France.

A large calcium-insensitive transient outward current (I_{to}) has been recorded in various regions of the heart and seems to contribute significantly to the electrical heterogeneity of the organ and basically of the LV free wall. However, no data have been reported thus far on the distribution of I_{to} density within the LV septal wall from compensated human LV hypertrophy. Microelectrode and patch-clamp techniques were used to record action potentials and I_{to} in myocytes isolated from superficial (<3 mm depth) and deep layers (from 3 to 6 mm depth) of LV septum from patients with aortic stenosis and compensated LV hypertrophy. Subendocardial specimens were also obtained from undiseased donor hearts. In any of the superficial-subendocardial cell from diseased hearts was a macroscopic I_{to} never recorded (n=42), whereas in cells of the same location from donor hearts a typical I_{to} was clearly present with a peak density of 5.88±0.78 pA/pF at +60 mV (n=4). However, in deep layers from patients with compensated LV hypertrophy, macroscopic I_{to} was present with a peak density of 10.50±2.58 pA/pF at +60 mV (n=4). The absence of I_{to} in superficial hypertrophied septal cells was not due to a divalent cation-related shift of the current. Instead, extracellular Ca^{2+} removal induced the appearance of an I_{to}-like current mainly carried by K+ ions with a peak density of 30.7±2.6 pA/pF at +60 mV (n=29). However, its magnitude, kinetics and pharmacological characteristics did not allow identification of this current as the usual I_{to}. Both topography and pathology appear to be major modulating factors of the regional distribution of I_{to} density in human LV septum and therefore may play a prominent role in determining electrical gradients within this region.

M-Pos135

DOES MINK UNDERLIE THE DELAYED RECTIFIER K^+ CURRENT IN BULLFROG ATRIAL MYOCYTES? ((**Vicki L. Lowes**, Virginia L. Stroeher, Robert B. Clark and Wayne R. Giles)) Department of Physiology and Biophysics, University of Calgary, Calgary, Alberta, Canada. (Spon. J.A. Steele)

MinK is thought to generate the delayed rectifier K^+ current, I_K, in mammalian cardiac tissue. Bullfrog I_K, which is generated entirely by a slowly activating K^+ conductance, was chosen as a model to make a quantitative comparison of minK expressed in *Xenopus* oocytes with I_K in native tissue. The biophysical and pharmacological characteristics of I_K recorded from freshly dispersed bullfrog atrial myocytes and those of rat uterine minK expressed in *Xenopus* oocytes were compared. The steady-state voltage dependence and current-voltage relationship of I_K closely resembled those of minK. The half point of activation and slope factor were, respectively, -27.6mV and 13.3 for I_K, and -22.6mV and 15.1 for minK, and the threshold for activation of both K^+ currents was approximately -50mV. Azimilide, a class III antiarrhythmic, blocked these currents with an IC_{50} of 11.4μM (I_K) and 7.2μM (minK). The mechanism of block of both currents was also similar; the initial closed state block was followed by a smaller use-dependent component. These results strongly suggest a role for minK as part of the molecular structure encoding I_K. Attempts to identify minK in bullfrog heart were made by PCR analysis using primers targeted to conserved regions of several mammalian minK clones. In addition, total RNA blots were probed with the rat minK clone. We were unable to detect minK using either of these approaches. These results suggest that an unidentified protein which is present in bullfrog heart and is endogenous to *Xenopus* oocytes underlies this K^+ current.

M-Pos136

A COMPARISON OF REPOLARIZING K^+ CURRENTS IN RABBIT PURKINJE CELLS AND VENTRICULAR MYOCYTES. ((**J.M. Cordeiro**[a], K.W. Spitzer[b], W.R. Giles[a])) [a]Dept. of Physiology and Biophysics, University of Calgary, Calgary, Canada and [b]Nora Eccles Harrison Cardiovascular Research and Training Institute, University of Utah, Salt Lake City, U.S.A. (Spon. by A.Y.K. Wong)

Differences in action potential configuration and underlying repolarizing K^+ currents were investigated in rabbit Purkinje cells and ventricular myocytes. Electrical activity was recorded with conventional voltage clamp techniques in the whole cell configuration at 36° C. Comparison of action potential recordings at a fixed rate from these two cell types showed that Purkinje cells had a longer action potential duration (APD) and a more prominent phase 1 repolarization. Elevating $[K^+]_o$ (5.4 mM to 10.0 mM) caused APD to shorten more in Purkinje cells than ventricular myocytes; conversely, lowering $[K^+]_o$ (5.4 mM to 2.0 mM) caused a more substantial lengthening of APD in Purkinje cells than ventricular myocytes. Voltage clamp analysis revealed that I_{K1} (measured as the Ba^{++}-sensitive difference current) was much smaller in Purkinje cells than in ventricular myocytes. Addition of 4-AP (2 mM) abolished the prominent phase 1 repolarization and blocked the Ca^{++}-independent transient outward K^+ current in Purkinje cells, but had little effect on most ventricular cells. Delayed rectifier K^+ current was very small (<20 pA) in both cell types. Many of the differences in action potential waveforms in these two cell types can be accounted for by the respective densities of repolarizing K^+ currents in them.

M-Pos137

IONIC MECHANISM OF THE EFFECTS OF HYDROGEN PEROXIDE IN RAT VENTRICLAR MYOCYTES. ((**C.A. Ward** and W.R. Giles)) Dept of Physiology and Biophysics, University of Calgary, Calgary, Canada T2N 4N1. (Spon. N.M. Anderson)

Whole-cell and amphotericin-permeabilized patch clamp techniques were used to study the effects of hydrogen peroxide (H_2O_2) on action potentials and underlying ionic currents in single ventricular myocytes from adult rat hearts. Conventional whole-cell recordings failed to show any significant effects of H_2O_2 on the action potential. In contrast, when action potentials were recorded with the amphotericin perforated patch method, H_2O_2 (50-200 μM) produced a marked prolongation of action potential duration (APD). This action potential prolongation was reversed completely by tetrodotoxin (TTX; $8x10^{-6}$M). Similar results on APD were observed with anthopleura toxin ($4x10^{-7}$M), which slows inactivation of Na^+ currents. Partial inhibition of the transient outward (4-aminopyridine, 10^{-4}M) and the inward rectifier K^+ (Ba^{2+}, 10^{-5}M) currents failed to mimic the effects of H_2O_2 on action potential duration. To study the effect of H_2O_2 on Na^+ channel inactivation kinetics, experiments were performed utilizing cell-attached macropatches. H_2O_2 caused a significant enhancement of late opening events, and ensemble recordings demonstrated slowed the inactivation of Na^+ currents. The effect of H_2O_2 on APD was attenuated by the protein kinase C inhibitor bisindolylmaelimide (10^{-7}M). These results demonstrate that the action potential prolongation caused by H_2O_2 involves slowing of inactivation of the TTX-sensitive Na^+ current and suggest that this effect is mediated by protein kinase C.

M-Pos138

ROLE OF EXTERNAL Ca^{2+} IN THE MODULATION OF I_{Kr} CURRENT.

((**M-D. Drici**, Y.M. Shuba, M.Oz, M. Morad)) Dept. of Pharmacol., Georgetown Univ. Washington, DC 20007.(spon. by M. Lieberman)

The rapid component (I_{Kr}) of the delayed rectifier K^+ current (I_K) and calcium are key elements in the occurrence of complex ventricular arrhythmias known as Torsades de Pointes. The former as a main target to class III antiarrhythmic drugs prolonging the action potential, and the latter as a primordial element in the genesis of Early After Depolarizations triggering the arrhythmias. The role of intracellular calcium has been well documented in augmenting I_K but little is known about the effects of extracellular calcium ($[Ca^{2+}]_{ext}$). In order to examine this we measured, I_K tail currents in isolated whole-cell voltage clamped guinea-pig ventricular myocytes in standard Tyrode's external solution containing either 2 (control) or 5 mM $[Ca^{2+}]_{ext}$. Composition of internal solution (high EGTA, absence of cAMP) and pulse protocol (short 200 ms depolarization from holding potential -80 mV to +40 mV followed by repolarizations ranging from -60 to +20 mV with 10 mV increment) were selected to ensure predominant contribution of I_{Kr} tails to the overall K^+ tail current. Under such conditions 5 mM $[Ca^{2+}]_{ext}$ decreased significantly K^+ tail current recorded at -30 mV from 50±5 pA/pF (control) to 30±11 pA/pF. Qualitatively similar results were obtained on I_{Kr} measured in *Xenopus* oocytes expressing *HERG* gene (Sanguinetti *et al.* 1995). *HERG*-induced I_{Kr} was recorded using glass-funnel technique in external Ringer solution containing 1.8 and 5 mM of $[Ca^{2+}]_{ext}$. Increasing of extracellular Ca^{2+} from 1.8 to 5 mM resulted in a 10 to 20% inhibition of I_{Kr}. Thus, our results suggest that I_{Kr} current can be regulated by extracellular calcium.

M-Pos139

COMPLEX MODULATION OF CARDIAC I_{KS} BY PROTAMINE: A POTENTIAL MODEL FOR DIFFERENTIAL MODULATION OF SINO-ATRIAL NODE AND VENTRICULAR CURRENTS BY ENDOGENOUS PEPTIDES ((**J.J. Lippold**, G.A. Herin, and L.C. Freeman)) Kansas State University, Manhattan, KS, 66502.

We investigated the effects of the polycationic peptide protamine on I_{Ks} in guinea pig ventricular myocytes (VM) and sino-atrial node (SAN) cells using whole cell patch clamp procedures to monitor current. Protamine reduced the amplitude of I_{Ks} in both SAN and VM in a voltage-independent fashion. However the characteristics of the block were different. In SAN, tail current amplitudes measured at -40 mV following a +40 mV test pulse were decreased on average by 80% immediately after application of protamine (20 μg/mL), and by 82% after 7-10 minutes perfusion with protamine (n=4). Boltzmann analysis of isochronal activation curves revealed that reduction in the amplitude of SAN I_{Ks} was accompanied by significant gating shifts (average shift in $V_{1/2}$ = +18 mV, range = +6 to +38 mV); furthermore, a significant decrease in the slope factor *k* was observed after 7-10 minutes exposure to protamine (from 12.5±2.2 mV to 7.3±0.2 mV). Compared to SAN, steady-state block of VM I_{Ks} was lower in magnitude and slower to develop. Tail current amplitudes were decreased by only 17% immediately after application of protamine, and by only 42% after 7-10 minutes perfusion (n=6). Reduction in the amplitude of VM I_{Ks} developed without any shift in the activation curve. These data suggest the nature of protamine block of I_{Ks} may be different in SAN and ventricular regions of the heart, and the underlying mechanism(s) is complex. Furthermore, these data suggest that SAN and VM I_{Ks} may be differentially modulated by endogenous polycationic peptides such as dynorphin A-(1-13), PR-39, and eosinophil major basic protein.

M-Pos140

ELECTROPHYSIOLOGICAL EFFECTS OF THE ANTIPSYCHOTIC DRUG HALOPERIDOL ON CARDIAC K^+ CHANNELS EXPRESSED IN *XENOPUS* OOCYTES ((H. Suessbrich, R. Schoenherr, S.H. Heinemann, B. Attali, F. Lang and A. E. Busch)) Dept. of Physiology, University of Tübingen, Germany; Max-Planck-Institute, University of Jena, Germany; Dept. of Neurobiology, Weizmann Institute of Science, Israel (Spon. by E. Wöll)

The antipsychotic drug haloperidol can induce a marked QT prolongation in ECG recordings resulting in torsades de pointes, a life-threatening form of a polymorphic ventricular tachycardia. These observations pointed to effects of haloperidol on repolarizing conductances in ventricular myocytes. We therefore expressed several cloned cardiac K^+ channels, including the *h*uman *e*ther-a-go-go *r*elated *g*ene (HERG) channels, in *Xenopus* oocytes and tested them for their haloperidol sensivity. Haloperidol had only little effects on the delayed rectifier channels Kv1.1, Kv1.2, Kv1.5 and I_{sK}) the A-type channel Kv1.4, and the inward rectifier channel Kir2.1 (inhibition < 6 % at 3 μM haloperidol). In contrast, haloperidol blocked HERG channels potently with an IC_{50} value of approximately 1 μM. Reduced haloperidol, the primary metabolite of haloperidol, produced a block with an IC_{50}value of 2.6 μM. Haloperidol block was use and voltage dependent, suggesting that it binds preferentially to either open or inactivated HERG channels. As haloperidol increased the degree and rate of HERG inactivation, a binding to inactivated HERG channels is suggested. The channel mutant HERG S631A has been shown to exhibit greatly reduced C-type inactivation which occurs only at potentials greater than 0 mV. Haloperidol block of HERG S631A at 0 mV was four-fold weaker than for HERG wild-type channels. Haloperidol affinity for HERG S631A was increased four-fold at +40 mV compared to 0 mV. In summary, the data suggest that HERG channel blockade is involved in the arrhythmogenic side effects of haloperidol. The mechanism of haloperidol block involves binding to inactivated HERG channels.

M-Pos141

INHIBITION OF I_{Ks} IN GUINEA PIG CARDIAC MYOCYTES AND GUINEA PIG I_{sK} CHANNELS BY THE CHROMANOL 293B ((A.E. Busch H. Suessbrich, S. Waldegger, E. Sailer, R. Greger, H.-J. Lang, F. Lang, K.J Gibson, J.G. Maylie)) Dept. of Physiology, Universities of Tübingen and Freiburg, Germany; Dept. of Ob.Gyn., Oregon Health Sciences University. USA

The chromanol derivative 293B was previously shown to inhibit a cAMP regulated K^+ conductance in rat colon crypts. Subsequent studies on cloned K^+ channels from the rat demonstrated that 293B blocks specifically I_{sK} channels expressed in *Xenopus* oocytes, but does not affect the delayed and inward rectifier Kv1.1 and Kir2.1, respectively. In the present study, the specificity of 293B for the cardiac K^+ conductances I_{Ks} and I_{Kr}, and for the cloned guinea pig I_{sK} channel and the human HERG channel, which underly I_{Ks} and I_{Kr}, respectively, was analyzed. 293B inhibited both the slowly activating K^+ conductance I_{Ks} in cardiac myocytes and guinea pig I_{sK} channels expressed in *Xenopus* oocytes with a similar IC_{50} (2-6 μmol/l). In contrast, high concentrations of 293B had only a negligible effect on the more rapid activating I_{Kr}. Similarly, 293B exerted no effect on HERG channels expressed in *Xenopus* oocytes. Finally, 293B was also tested on the L-type Ca2+ channels both in guinea pig cardiac myocytes and recombinant channels expressed in *Xenopus* oocytes. At 10 μM 293B exerted only neglible effects on both native and recombinat Ca^{2+} currents. In summary, 293B appears to be a rather specific inhibitor of I_{Ks} and the underlying I_{sK} channels. Future studies on 293B effects on action potential duration and its antiarrhythmic properties can therefore be used to identify the physiological role of I_{Ks} in cardiac myocytes.

M-Pos142

SODIUM CYANIDE INDUCED ALTERATIONS IN DELAYED RECTIFIER CURRENT IN ATRIAL TUMOR CELLS (AT-1 CELLS).

((**Qadriyyah Debnam**, Kawonia Mull, Syeda Kabir, Mohit L. Bhattacharyya)),Department of Anatomy and Physiology, Meharry Medical College, Nashville, TN.

Atrial tumor myocytes derived from transgenic mice (AT-1 cells) maintain well-differentiated cardiac biochemical and histological phenotypes. It has been reported that the major outward current in AT-1 cells is a delayed rectifier that activates rapidly, shows inward rectification, and can be readily isolated from other currents. In these cells, we tested the effects of metabolic blockage using sodium cyanide (NaCN). Delayed rectifier type currents (I_K) were generated by stepping up to +40 mV in 10 mV steps. The rapid Na^+ current was inactivated by holding the cell at a potential of -40 mV while Ca^{2+} currents were blocked by $CdCl_2$. We noted in a few experiments that DIDS did not influence K^+ current generation restifying to the absence of any Cl^- currents. NaCN blocked I_K in dose- and time-dependent manners. At 10, 20, 30, and 40 mV, NaCN reduced the current at the end of 1 s pulse (I_{1sec}) by 17.6 ± 4.4, 24.1 ± 5.6, 28.8 ± 5.2, and 28.7 ± 5.2 %, respectively. Also, peak currents (I_{peak}) during a 4 s pulse decreased by 34.4 ± 2.8 % due to NaCN, compared to the control. The effects of NaCN were not reversible. Maximum block of I_K occurred around 20-30 mV step. The action of NaCN is irreversible. (NaCN conc. was 200-500 μM).

Supported by NIH grants GM08037 and HL07864.

M-Pos143

Kv4.2 AND Kv4.3 CONTRIBUTE TO THE Ca^{2+}-INDEPENDENT TRANSIENT OUTWARD K^+ CURRENT IN RAT VENTRICLE. ((**Céline Fiset**, Robert B. Clark, Yakhin Shimoni, and Wayne R. Giles)). Dept. of Physiology and Biophysics, University of Calgary, Calgary, Alberta, Canada. (Spon. Dr. H. Akbarali)

The hypothesis that Kv4.2 and Kv4.3 are two of the K^+ channel isoforms responsible for the Ca^{2+}-independent transient outward K^+ current (I_t) in rat ventricle was tested using whole-cell patch clamp and antisense methods. Our results show that many of the biophysical and pharmacological properties of I_t in rat ventricular myocytes closely resemble those of Kv4.2 stably expressed in mouse L-cells. 20-mer antisense phosphorothioate oligonucleotides directed against Kv4.2 and Kv4.3 mRNA were used to evaluate the contributions of these two K^+ channel isoforms to I_t in primary cultured ventricular cells obtained from 14-day old rats. The peak I_t current measured at +40mV was reduced by 53% after a 24-hour incubation period in presence of Kv4.2 antisense oligonucleotide (0.3μM) and cationic liposome (8μM). A 60% decrease in the amplitude of I_t was observed when the cells were exposed to Kv4.3 antisense oligonucleotide. To evaluate the possibility of cross-reactivity between the sequence of the Kv4.3 antisense oligonucleotide and the Kv4.2 mRNA, L-cells stably transfected with Kv4.2 were exposed to Kv4.2 or Kv4.3 antisense oligonucleotides. Peak outward K^+ current due to Kv4.2 was significantly reduced by the Kv4.2 antisense, but was unaffected by the Kv4.3 antisense. These results strongly suggest that Kv4.2 and Kv4.3 both contribute to I_t current expressed in rat ventricular myocytes.

M-Pos144

EXTRACELLULAR DIVALENT CATIONS BLOCK A MONOVALENT CATION NONSELECTIVE CONDUCTANCE IN CARDIAC MUSCLE.
((K. **Mubagwa**, M. Stengl, W. Flameng)) C.E.H.A., University of Leuven, 3000 Leuven, Belgium. (Spon. by J.B. Parys)

We studied the effect of extracellular Ca^{2+} (Ca_o) or Mg^{2+} (Mg_o) removal on resting potential (V_r) in papillary muscles, and on background conductance in ventricular myocytes. V_r was measured with 3-M KCl-filled microelectrodes in rat and guinea-pig muscles superfused with HEPES-buffered Tyrode (1.8-mM Ca_o, 0.9-mM Mg_o) at 37 °C or 22 °C. A Ca_o decrease caused depolarization (e.g., in rat: from -82±1.9 mV to -59±3.4 mV in 0.1-mM Ca_o), whereas a Ca_o increase caused hyperpolarization (to -86±2.6 mV in 9-mM Ca_o). Low-Ca_o-induced depolarization was resistant to nifedipine (3 μM) or TTX (15 μM), and high-Ca_o-induced hyperpolarization to Ba^{2+} (1 mM) or ouabain (0.1 mM). In 0-mM Ca_o, V_r was sensitive to Mg_o. Whole-cell membrane currents were measured in rat myocytes at 22 °C using ramp voltage commands (between -120 mV and +80 mV). Removal of Ca_o and Mg_o reversibly induced a current with reversal potential (E_{rev}) of -3 mV. The 0-Ca_o-induced current was completely blocked by 1.8-mM Mg_o or Sr_o, but partially by 1.8-mM Ba_o. The current was insensitive to changes of E_{Cl}, and to nifedipine (3-10 μM) or amiloride (1 mM). Its inward component disappeared in 0-mM Na_o (150-mM NMDG). These results suggest that a conductance pathway, permeable to monovalent cations but not to Cl^-, and blockable by divalent cations, exists in ventricular myocytes.

M-Pos145

RECONSTITUTION OF THE MUSCARINIC RECEPTOR, RECEPTOR KINASE AND K^+ CHANNEL IN CHO CELLS - RECEPTOR KINASE-DEPENDENT DESENSITIZATION.
((I.A. Khan, Z. Shui, H. Tsuga, T. Haga and M.R. Boyett)) University of Leeds, UK and Tokyo University, Japan

In the heart, ACh activates the muscarinic K^+ channel, but during a prolonged exposure to ACh the channel activity declines as a result of desensitization. To study the mechanism underlying desensitization to ACh, the muscarinic K^+ channel system was reconstituted into CHO cells. Cells were transfected with hm2 (receptor), GRK2 (receptor kinase), GIRK1 and CIR (the two subunits of the muscarinic K^+ channel) and GFP (green fluorescent protein). Muscarinic K^+ channel activity was recorded in cell attached patches (if the pipette contained ACh) on cells which were fluorescent. The channel showed the inward-rectification, conductance and open time characteristic of the native muscarinic K^+ channel in heart cells. In the first 3 min after attachment of an ACh-containing pipette, channel activity slowly declined (n=11), presumably as a result of desensitization to ACh, as it does in heart cells. If the receptor kinase, GRK2, was excluded, no desensitization was observed (n=7). If the cells were transfected with DN-GRK2 (mutant receptor kinase unable to phosphorylate; n=14) or m2LD (mutant receptor lacking phosphorylation sites; n=17) or both (n=11), instead of wild-type hm2 and GRK2, desensitization was greatly reduced or abolished. It is concluded that the desensitization of the muscarinic K^+ channel is the result of the phosphorylation of agonist-bound receptor by receptor kinase.
Supported by the BHF.

M-Pos146

COMPARISON OF Na/K PUMP CURRENT MEASURED BY K^+ ACTIVATION AND DHO BLOCKADE METHODS IN GUINEA PIG AND RAT VENTRICULAR MYOCYTES.
((J. Gao, R.T. Mathias, I.S. Cohen & G.J. Baldo)) Dept. of Physiology & Biophysics, SUNY at Stony Brook, NY.

The whole cell patch clamp was used to hold myocytes at -40mV in Tyrode containing 2mM [Ba^{2+}] and 1mM [Cd^{2+}], and pipette solutions with 20mM TEA^+, 100mM Cs^+ and 0mM K^+. Increasing $[K^+]_o$ from 0 to 15mM when myocytes were already bathed in saturating (1mM) dihydro-ouabain (DHO) or ouabain produced an inward shift in holding current. This shift was thought to be the inwardly-rectifying K^+ current I_{K_1} because it had similar steady-state voltage dependence and could be blocked further by additional Ba^{2+} or Cs^+. Without cardiac glycosides, 15mM K^+ induced an outward transient followed by an inward shift in holding current due to activation of Ip and I_{K_1}. Ip measured by DHO is not equal to the 15mM K^+-induced outward transient because of contamination by I_{K_1}. Using the I_{K_1} reversal potential, we estimated the intracellular [K^+] in the presence and absence of DHO to be 2.72±0.62mM (mean±S.D., n=4) and 6.52±1.52mM, respectively. This difference alters the voltage dependence of I_{K_1}, affecting the measured Ip. We conclude that Ip measured via glycoside blockade is more accurate than Ip activated by $[K^+]_o$. The K^+-activation method requires a higher $[Ba^{2+}]_o$ be used and some K^+ be included in the patch pipette solution to reduce the effect of changes in $[K^+]_i$.

Supported by grants HL54031, HL20558 and the AHA.

M-Pos147

NA/K PUMP CURRENT IN EPICARDIAL AND ENDOCARDIAL CANINE VENTRICULAR MYOCYTES.
((J. Gao, H. Yu, I.S. Cohen, R.T. Mathias, X. Sun, Y. Wang & G.J. Baldo)) Dept. of Physiology, SUNY at Stony Brook, NY.

Na/K pump current (Ip) was measured using the whole cell patch clamp technique and a saturating dose (1mM) of the cardiac glycoside dihydro-ouabain. Cells were clamped at 0mV. Pump current density in epicardial myocytes (Ip_{EPI}) was 0.63±0.13 pA/pF (mean±S.D., n=15) whereas endocardial myocyte current density (Ip_{ENDO}) was 0.29±0.07 pA/pF (n=11) with 5.4mM $[K^+]_o$ and 60mM $[Na^+]_i$ in the pipette solution. Student's t-test shows this difference is significant ($p<0.001$). Since 60mM $[Na^+]_i$ saturates the Na^+-binding sites of the Na/K pumps, the difference between Ip_{EPI} and Ip_{ENDO} is not due to changes in $[Na^+]_i$ or Na^+-affinity. Neither does K^+-affinity or K^+ accumulation account for this observation, since the same difference was observed when $[K^+]_o$ was increased to 15mM. Furthermore, DHO binding affinity is not responsible, since the same difference between Ip_{EPI} and Ip_{ENDO} was observed when DHO was increased to 2mM. The voltage dependencies of Ip_{EPI} and Ip_{ENDO} (Ip-V) obtained using a voltage ramp protocol demonstrate the ratio Ip_{ENDO}/Ip_{EPI} is constant at 0.44±0.02 (n=5). Thus Ip_{ENDO} is smaller than Ip_{EPI} at each test potential with no voltage shift between the Ip-Vs. Thus, relative to the endocardium, there appears to either be more Na/K pumps in epicardial cells or the maximal ATPase activity of the epicardial pump is higher.

Supported by grants HL54031, HL20558, HL28958 and the AHA.

M-Pos148

MODULATORS OF PKC AFFECT NA/K PUMP CURRENT IN GUINEA PIG VENTRICULAR MYOCYTES.
((J. Gao, R.T. Mathias, I.S. Cohen, X. Sun & G.J. Baldo)) Dept. of Physiology & Biophysics, SUNY at Stony Brook, NY.

Na/K pump current (Ip) was measured using the whole cell patch clamp technique and a saturating dose (1mM) of the cardiac glycoside dihydro-ouabain. The effect of the PKC activator phorbol 12-myristate 13-acetate (PMA) on Ip depends on $[Ca^{2+}]_i$. At 0.4μM, PMA has no effect on Ip at low $[Ca^{2+}]_i$ (15nM) but increases Ip by 33% at higher $[Ca^{2+}]_i$ (314nM). At 16μM PMA increases Ip by about the same amount with either high or low $[Ca^{2+}]_i$. The stimulation of Ip by PMA can be reproduced by another PKC activator, 1,2-dioctanoyl-sn-glycerol (diC_8, 25μM). Staurosporine (1-1.5μM), a potent PKC inhibitor, eliminates the effect of PMA but 4μM PKI, a specific inhibitor of protein kinase A, does not. This suggests the stimulatory effect of PMA on Ip is via PKC activation. PMA (0.4μM) has no effect on the voltage dependence of Ip at low $[Ca^{2+}]_i$. At high $[Ca^{2+}]_i$ PMA increases Ip without shifting its voltage dependence. PMA is thought to mimic the action of diacylglycerol, the natural activator of PKC. Our data suggest membrane-bound activator and free Ca^{2+}, act synergistically to activate PKC. Furthermore, PKC-mediated phosphorylation increases Na/K pump activity. This increase is not secondary to changes in $[Na^+]_i$ or pump affinity for Na^+, since our pipette contained a saturating $[Na^+]$ (60mM, Gao *et al*, 1995, J Gen. P. 106:995).

Supported by grants HL54031, HL20558 and the AHA.

M-Pos149

AN ELECTROGENIC Na^+/HCO_3^- COTRANSPORT MODULATES RESTING MEMBRANE POTENTIAL (E_m) AND ACTION POTENTIAL DURATION (APD) IN CARDIAC MYOCYTES.
((**E.A. Aiello**, H.E. Cingolani)) Centro de Investigaciones Cardiovasculares, Facultad de Medicina, La Plata, Argentina.

The Na^+/HCO_3^- cotransport regulates intracellular pH (pH_i) moving two (n=2) or three (n=3) HCO_3^- per each Na^+ across the membrane, generating a net flux of negative charges that confers electrogenic characteristics to this mechanism. An electrogenic Na^+/HCO_3^- cotransport was reported in proximal tubule, retinal glia, astrocytes, leech glia, hepatic cells, retinal pigment epithelium, and ciliary smooth muscle. However, the electrogenecity of this system is controversial in cardiac tissue. Electrically silent (J. Physiol. 458:361-384, 1992) and electrogenic (J. Mol. Cell. Cardiol. 27:231-242, 1995) cotransports were reported. In this study we used the nystatin perforated whole-cell configuration of patch clamp technique to determine the activity of the Na^+/HCO_3^- cotransport in isolated cat ventricular myocytes. Switching from HEPES to CO_2/HCO_3^- buffer hyperpolarized resting membrane potential (E_m) in 2.98±0.28 (n=5, $p<0.05$) and shortened APD to 43.3±7.7% and 30.1±4.6% of the value in HEPES (n=4,$p<0.05$), measured at 50% (APD_{50}) and 90% (APD_{90}) of repolarization, respectively. The CO_2/HCO_3^- induced hyperpolarization and APD shortening were both reversed by the anionic blocker SITS (0.1 mM) and prevented by complete replacement of extracellular Na^+ with Li^+. Quasi steady-state currents were evoked by voltage clamped ramps ranging between -130 to +30 mV during 8 seconds, from a holding potential of -70 mV. The appearence of a steady-state outward current was observed in the presence of HCO_3^-. This current increased as the driving force for HCO_3^- entry got higher. Extracellular HCO_3^- also induced a 2.89±0.57 (n=7, $p<0.05$) negative shift of reversal potential for net current, consistant with a hyperpolarization of E_m. These results allowed us to conclude that the Na^+/HCO_3^- cotransport is electrogenic and contributes to determine myocardial E_m and action potential waveform.

M-Pos150

BIFUNCTIONAL RHODAMINE-LABELED REGULATORY LIGHT CHAINS BIND TO MYOSIN HEAVY CHAINS AND PROVIDE A FRAMEWORK OF DIPOLE ORIENTATIONS IN FIBERS ((**R.E. Ferguson**[1], S.R. Martin[1], B.D. Brandmeier[1], J. Kendrick-Jones[2], R.S. Hodges[3], B.D. Sykes[3], J.E.T. Corrie[1], M. Irving[4] and D.R. Trentham[1]). [1]NIMR, London NW7 1AA, UK; [2]LMB, Hills Road, Cambridge CB2 2QH, [3]Dept. Biochemistry, U. Alberta, Edmonton T6G 2H7, Canada; [4]Randall Inst., King's College London, London WC2B 5RL, UK.

Analysis in real-time of structural changes of the regulatory domain of myosin in muscle fibers provides evidence that cross-bridges tilt during contraction (Irving *et al.*, Nature, **376**, 688-691, 1995). A more detailed description of cross-bridge movement can in principle be achieved by monitoring the movement of a framework of dipoles. To this end the interactions of several bifunctional rhodamine-labeled mutant regulatory light chains (RLC) (Corrie *et al.*, Biophys. J. **72**, Abstract this meeting, 1997) with peptides that form the RLC binding site of the myosin heavy chain (Ferguson *et al.*, J. Physiol. **487**, 161P-162P, 1995) have been studied and compared with wild-type RLC. The RLCs were also exchanged into rabbit skeletal muscle myosin subfragment 1 and the orientation and dispersion of their rhodamine absorption dipoles in subfragment 1 bound to actin filaments in stretched skeletal muscle fibers measured. Sabido-David *et al.* (Biophys. J. **72**, Abstract this meeting, 1997) compared results from this preparation with those from rhodamine-labeled RLCs directly exchanged into fibers.

M-Pos151

A NEW BIFUNCTIONAL RHODAMINE TO LABEL MUTANT REGULATORY LIGHT CHAINS OF GIZZARD MYOSIN (([1]**J.E.T. Corrie**, [1]B.D. Brandmeier, [1]J.S. Craik, [1]V.R.N. Munasinghe, [1]S. Howell, [1]D.R. Trentham and [2]J. Kendrick-Jones)) [1]Natl. Inst. Med. Res., Mill Hill, London NW7 1AA, UK; [2]Lab. Mol. Biol., Hills Road, Cambridge CB2 2QH, UK (Spon. S. Khan)

The bis(iodoacetamido)rhodamine shown has been synthesized for two-site attachment of the fluorophore to chicken gizzard myosin regulatory light chains (RLC) expressed in *E. coli*. Two mutant RLCs (D100C and A113C) have been prepared to place an additional cysteine close to the native Cys108, while in a third mutant (N104C, C108A, G115C) the native cysteine has been removed and two new cysteines introduced. 1:1 coupling of the probe and mutant RLCs was achieved in good yields. Homogeneous labeled proteins were obtained by preparative FPLC. Two-site attachment of the probe was shown by electrospray mass spectroscopy of the intact labeled RLCs and of tryptic digests, where the only fluorescent peptide was that containing the two linked cysteines. These labeled RLCs have been designed to provide probes with defined orientations relative to the light-chain region of myosin heads when exchanged into skeletal muscle fibers.

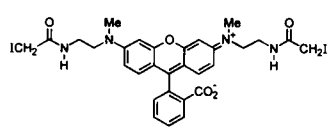

(Supported by the Medical Research Council, UK)

M-Pos152

ORIENTATION OF BIFUNCTIONAL RHODAMINE PROBES ON MYOSIN REGULATORY LIGHT CHAIN (RLC) IN RELAXED, CONTRACTING AND RIGOR MUSCLE. ((**C. Sabido-David**, *R.E. Ferguson, *B.D. Brandmeier, [$]S.C. Hopkins, [$]Y.E. Goldman, [†]J. Kendrick-Jones, R.E. Dale, *J.E.T. Corrie, *D.R. Trentham and M. Irving)). Randall Institute, King's College London, UK; *NIMR, London NW7 1AA, UK; [$]Pennsylvania Muscle Institute, Univ. of Penna., Philadelphia, USA; [†]MRC Laboratory of Molecular Biology, Cambridge, UK.

Dipole probes were introduced at defined orientations in the myosin head using chicken gizzard myosin RLC mutants labelled with a bifunctional rhodamine (BR; Corrie et al., this meeting). The 100-BR-108 (BR linking Cys100 and Cys108) dipole is roughly parallel to the long heavy-chain helix in the RLC region of the head (Rayment et al., Science, 261, 50, 1993; Xie et al., Nature, 368, 306, 1994); the 108-BR-113 and 104-BR-115 dipoles are ca. 30° apart, but both are at ca. 90° to 100-BR-108. Labelled RLCs were exchanged into single rabbit psoas fibers or myosin subfragment-1 (S-1), and dipole orientation relative to the fiber axis determined by fluorescence polarization (Ling et al., Biophys. J. 70, 1836, 1996). Mobility of each probe on the fluorescence timescale was restricted and independent of physiological state. The average angle of each dipole was more perpendicular to the fiber axis in rigor than in either relaxation or active contraction. The average angles for 100-BR-108 in active and rigor fibres differed by less than 10°, but the rotation between the two states could be much bigger if the probe crosses the 90° plane. In rigor, 104-BR-115 was the most perpendicular of the three probes; in active contraction 108-BR-113 was the most parallel. Polarization ratios from exogenous S-1 containing 100-BR-108 or 104-BR-115 and bound to actin in rigor fibers were similar to those from endogenous heads in rigor, but suggested less disorder: Supported by Wellcome Trust and MRC, UK; AR26846 and MDA, USA.

M-Pos153

MODEL-INDEPENDENT ANALYSIS OF MOBILITY AND ORIENTATION OF FLUORESCENT PROBES IN MUSCLE FIBERS ((**R.E. Dale**[1], T. Marszalek[2], S.C. Hopkins[3], M. Irving[1] and Y.E. Goldman[3])) [1]Randall Inst., King's College London, UK; [2]Institut Fizyki, UMK, Torun, Poland; [3]Penna. Muscle Inst., Univ. of Penna., Phila. PA.

Fluorescent probes typically display restricted mobility relative to the attached protein on the nanosecond time scale of the excited-state decay, which must be taken into account in determining the orientation distribution relative to the symmetry axis of the system. Assuming this mobility is rapid compared to the excited-state decay (or is monitored in nanosecond time-resolved experiments) and that motions of parallel absorption and emission dipoles are centrosymmetric about a fixed axis, S, within the protein, we show how to determine the extent of mobility of the probe dipoles and two order parameters of the angular distribution ($f(\theta s)$) of S relative to the fiber axis. In muscle fibers labeled with rhodamine, three independent polarization ratios are measured, ${}^{x}Q_{\perp} = ({}^{x}{}_{\perp}I_{\perp} - {}_{\parallel}I_{\perp}) / ({}^{x}{}_{\perp}I_{\perp} + {}_{\parallel}I_{\perp})$, ${}^{y}Q_{\perp} = ({}^{y}{}_{\perp}I_{\perp} - {}_{\parallel}I_{\perp}) / ({}^{y}{}_{\perp}I_{\perp} + {}_{\parallel}I_{\perp})$ and $Q_{\parallel} = ({}_{\parallel}I_{\parallel} - {}_{\perp}I_{\parallel}) / ({}_{\parallel}I_{\parallel} + {}_{\perp}I_{\parallel})$, where the pre- and post-subscripts for polarized fluorescence intensities (I) indicate excitation and emission polarizer axes relative to the fiber axis and the pre-superscript indicates the propagation axis of excitation beam parallel (^{x}) or perpendicular (^{y}) to the observation axis. We derive analytical expressions in terms of ${}^{x}Q_{\perp}$, ${}^{y}Q_{\perp}$ and $Q_{\parallel}$ for $\langle P_2(\cos\theta s)\rangle$, $\langle P_4(\cos\theta s)\rangle$ (average 2nd and 4th rank order coefficients of the spherical harmonic expansion of $f(\theta s)$) and $\langle P_{2T}\rangle$ (average 2nd rank order coefficient of the rapid motion relative to S). The analysis does not require assumption of a specific angular distribution for S. If the orientation of S within the protein is known for several different dipoles (Sabido-David et al., this meeting), then the protein orientation can be estimated within the fiber. Supported by NIH grant AR26846 and the MDA.

M-Pos154

CARDIAC ACTOMYOSIN RIGOR COMPLEXES. ((**O.A. Andreev**, A.L. Andreeva & J. Borejdo)) University of North Texas Health Science Center, 3500 Camp Bowie Blvd., Fort Worth, TX 76107.

We have shown previously that skeletal myosin subfragment 1 (S1) can bind one or two protomers of actin filament. These results led to a hypothesis that during muscle contraction each myosin head initially binds one and then two actins. In the present work we extended our study to a cardiac actomyosin interaction and found that cardiac S1 also could bind two actins. The interaction of cardiac S1 with F-actin was studied by EDC cross-linking, Western blot and fluorescence methods. The complexes were identified by labeling of proteins with fluorescent dyes and by Western blot. Three products with apparent molecular weights 150, 160 and 210 kDa included only actin and heavy chain of S1, and their compositions were: S1 cross-linked through 20 kDa domain to N-terminus of actin, S1 cross-linked through 50 kDa domain to N-terminus of actin and S1 cross-linked through the 20 and 50 kDa domains to two actins, respectively. Four other products with apparent molecular weights 66, 120, 185 and 235 kDa contained alkali light chain 1 (LC1). They were identified as LC1+actin, LC1+S1, LC1+actin+S1 and LC1+two actins+S1, respectively. The production of 66, 160, 185, 210 and 235 kDa complexes decreased dramatically with increase of molar ratio of S1 to actin indicating that cross-linking of LC1 and S1 through the 50 kDa domain to actin strongly depended on degree of saturation of actin filament by S1. The chemical cleavage of 185 and 235 kDa products revealed that LC1 in these complexes was cross-linked to actin. It is most likely that LC1 and 50 kDa domain of S1 cross-link to the C-terminus and N-terminus of the second actin, respectively. Fluorescence polarization measurements in cardiac and skeletal myofibrils revealed that orientation of bound cardiac S1 depended on a degree of occupation of thin filament by S1. The results demonstrated that cardiac myosin heavy and alkali light chains interacted with two actins in a similar way as the skeletal ones. Probably, the interaction of myosin head with two actins is a common feature of all myosins. Supported by NIH.

M-Pos155

CHANGES IN CONFORMATION OF ACTIN-BOUND S1 ON THE RELEASE OF ADP. ((**J. Borejdo**, M. Xiao and O.A. Andreev)) Dept of Biochem. and Molecular Biology, University of North Texas, 3500 Camp Bowie Blvd., Fort Worth, TX 76107.

It has been reported that the tail of smooth myosin subfragment-1 (S1) undergoes a large rotation upon release of ADP (Whittaker et al., Jontes et al., Nature 378, 748-753.). We reexamined this finding by comparing the conformation of the tail region of skeletal and smooth S1 bound to skeletal F-actin in the presence and in the absence of ADP. Conformation was assessed by the proximity of the tail of S1 to actin (measured by the ability of carbodiimide to form a zero-length cross-link) and by the orientation of the tail with respect to muscle axis (measured by the polarization of fluorescence of probes attached to A1 or A2). We found that when F-actin was fully saturated with skeletal or smooth S1 (prepared by Dr S. Lowey), the addition of ADP made no difference whatsoever to either the cross-linking or to the orientation. When F-actin was unsaturated with skeletal or smooth S1, the addition of ADP made no difference to the cross-linking and small difference to the orientation. The orientation of the tail of the cross-bridge in skeletal fibers was slightly different in the presence and absence of ADP. We conclude that in a physiologically important case ADP has a small effect on the conformation of the tail of S1. Supported by NIH.

M-Pos156

OBSERVATION OF TWO-STEP BINDING OF MYOSIN-S1 TO ACTIN WITH MILLI-SECOND TIME-RESOLVED ELECTRON CRYOMICROSCOPY BY SPRAYING F-ACTIN FILAMENTS ONTO GRIDS CONTAINING MYOSIN-S1 ((Matthew Walker, John Trinick, and Howard White)). Bristol University Veterinary School, Langford, Bristol BS18 7DY, UK and Dept. of Biochemistry, Eastern Virginia Medical School, Norfolk, Virginia 23507 (Spon. by Frank Lattanzio).

We have used spray-mixing and electron-cryomicroscopy to observe rapid binding of myosin-S1 to actin. Two different methods were used to observe rigor binding of myosin-S1 to actin with millisecond time-resolution. In the initial experiments droplets ~0.5 micron in size containing myosin-S1 were sprayed onto a grid layered with a film of f-actin less than 0.1 micron thick. We have subsequently done experiments in which the f-actin is sprayed onto grids containing a thin film of myosin-S1. Although the actin filaments are broken into shorter filaments (0.2 to 0.3 microns) by the shear forces involved in droplet formation, the sprayed filaments are long enough to observe myosin-S1 binding to them. In both cases the grid is then frozen by plunging into liquid ethane. Control of the size distribution and density of the spray is obtained by regulating the liquid input to the sprayer using a syringe pump driven by a micro-stepping motor. Times of 5-10 msec are obtained by freezing the grid just after it passes through the spray. For longer reaction times the grid is stopped between spraying and freezing. In micrographs of samples frozen 5-10 ms after mixing, most of the S1 bound to the actin (either by spraying S1 onto actin or actin onto S1) is disordered. The appearance of the bound S1 is similar to that observed during steady-state ATP hydrolysis (Walker et al, Biophys. J. 66, 1563-1572) and a few milliseconds after spraying grids containing actomyosin-S1 with ATP (Walker et al, Biophys. J. 68, 87s-91s). After longer delays more of the S1 is bound to actin with a similar appearance to the steady state rigor conformation observed in the absence of ATP. The time course observed here by cryo-electronmicroscopy is similar to that observed by solution kinetic measurements of myosin-S1 binding to pyrene-actin. This work is supported by AR40964 and MRC (UK).

M-Pos157

A COMPARISON OF THE RATE CONSTANTS OF THE ATP CLEAVAGE AND PHOSPHATE RELEASE STEPS FROM ASSOCIATED FAST SKELETAL, CARDIAC AND SMOOTH ACTOMYOSINS USING A NOVEL FLUORESCENT PHOSPHATE PROBE. ((Martin R. Webb, Betty Belknap and Howard D. White)) National Institute for Medical Research, Mill Hill, London, NW7 1AA, UK and Dept. of Biochemistry, Eastern Virginia Medical School, Norfolk Va. 23507.

We have measured the kinetics of phosphate (Pi) release during a single turnover of actomyosin ATP hydrolysis using double mixing stopped-flow fluorescence at very low ionic strength or in the presence of polyethyleneglycol to promote association of the actomyosin-S1. Myosin-S1 and ATP are mixed and incubated for several seconds to allow ATP to bind to myosin and generate a steady-state mixture of M-ATP and M-ADP-Pi. The steady state intermediates are then mixed with rabbit skeletal actin. The kinetics of Pi release are measured using a fluorescent probe for Pi, based on a phosphate binding protein (Brune et al. Biochemistry 33, 8262, 1994). The kinetics of Pi release for all three actomyosin-S1s are biphasic. At saturating actin, there is a correlation between the amplitude of the fast phase and the size of the Pi burst in the absence of actin: the size of this phase corresponds to the M-ADP-Pi formed during the first mix and the kinetics of the phase is Pi release from AM-ADP-Pi. The slow phase corresponds to the amount of M-ATP present after the initial mix and measures the rate of the cleavage step on associated actomyosin. We had previously shown that for rabbit skeletal myosin-S1 at 20° C, the rate of the Pi release step, 70 +/- 5 s^{-1}, is 20 times larger than the cleavage step. (Webb and White, Biophys. J. 70, 40a, 1996). The rates of the Pi release step decreases to 20 +/- 4 s^{-1} for porcine ventricular myosin-S1 and 4 +/- 1 s^{-1} for turkey gizzard myosin-S1(without the phosphorylatable light chain). The rate constants of the slow phase of the Pi release (measuring the associated cleavage steps) are 1.5 s^{-1} for porcine ventricular and 0.5 s^{-1} for turkey gizzard myosin-S1. This work was supported by the MRC and NIH (HL41776, and AR40964).

M-Pos158

KINETIC DISSECTION OF THE EFFECT OF SIZE AND CHARGE OF THE 50K/20K JUNCTION REGION ON THE ENZYMATIC ACTIVITY OF MYOSIN. ((**Marcus Furch**, Michael A. Geeves[1], and Dietmar J. Manstein)) Max-Planck-Institut für Medizinische Forschung, Jahnstr. 29, D-69120 Heidelberg and [1]Max-Planck-Institut für Molekulare Physiologie, Postfach 102664, D-44026 Dortmund, Germany

Structural and functional studies have shown that the flexible, positively charged loop connecting the 50K and 20K domains of myosin (loop 2) interacts with actin residues D1, E2, E3, D4, D24, D25, E99 and E100. This contact is thought to constitute the "weak" interaction between actin and myosin identified from studies of the kinetics and energetics of the purified proteins in solution. The actin-activated (Mg^{2+}) ATPase activities of chimaeric myosins containing substitutions of the loop2 region were shown to correlate strictly with those of the myosins from which the loop2 regions were derived (Uyeda *et al.*, 1994). We were interested in extending these studies to dissect the relative importance of changes to the charge and length of loop2. For this purpose we used the lower eukaryote *Dictyostelium discoideum* as host for the production of recombinant myosin motors. Mutant myosin motors carrying inserts of one to six positively charged GKK-repeats or uncharged GNN-repeats were produced. High synthesis levels were obtained for each mutant motor domain; between 0.5 and 2 mg of homogeneous, functional protein per g of cells was obtained after purification.

The introduction of positively charged GKK-motifs has a clear effect on the actin-activated (Mg^{2+}) ATPase activities of the recombinant motors. In particular, the rate of binding to actin is increased whilst the dissociation rate constant for the actomyosin complex is reduced. These results are consistent with a model in which the initial recognition between the two proteins and the association equilibrium constant of the actomyosin complex is mainly determined by electrostatic forces.

Uyeda, T.Q.P., K.M. Ruppel, and J.A. Spudich. 1994. Enzymatic activities correlate with chimaeric substitutions at the actin-binding face of myosin. *Nature*. 368: 567-569.

M-Pos159

ATP-INDUCED STRUCTURAL INTERMEDIATES OF THE MYOSIN HEAD, DETECTED BY A SPIN LABEL AT CYS 707, ARE NOT MODIFIED BY ACTIN BINDING. ((John Matta, Josh E. Baker, Jack Grinband, David D. Thomas)) University of Minnesota, Minneapolis, MN

We have used EPR to monitor the rotational dynamics of a spin label (IASL) attached to Cys 707 (SH1) on the myosin head (S1). EPR of this spin label resolves three structural states of the ATPase cycle, each characterized by different spin-label mobilities: M (strong-binding state, no probe mobility), M* (weak-binding, moderate mobility), and M** (weak-binding, high mobility). In a contracting muscle fiber, all three states are observed, but only the two mobile (weak-binding) states are observed in relaxed fibers or in S1 + ATP in solution. To determine the effects of actin binding on these structural states, we performed EPR on actin (A) + IASL-S1 (M) + nucleotide (N), measured the fraction of bound heads, and obtained the spectrum of the ternary complex (A•M•N) in the steady state. In the presence of ATP, only the weak-binding states (M* and M**) were observed, with the conformations and their population distribution indistinguishable from those observed in the absence of actin. In contrast, the spectrum of IASL-S1 + ADP (strong-binding) was substantially altered by actin. We conclude that (1) the myosin structures present in the weak-binding states A•M*•ATP and A•M**•ADP•P are the same as those observed in the absence of actin, (2) actin does not significantly perturb the equilibrium constant for ATP hydrolysis, (3) the strong-binding state is not significantly populated in the presence of saturating ATP in solution, and (4) the strong-binding state is perturbed by actin.

M-Pos160

A SIMPLE GRAPHICAL PROCEDURE FOR QUANTIFYING ALKYLATION OF MYOSIN'S SH1 AND SH2 ((**L. Xie**, W. X. Li, V. A. Barnett*, M. Schoenberg)) LPB, NIAMS, NIH, Bethesda, MD 20892 and *Dept. of Physiology, Univ. of Minnesota Medical School, MN55455.

Based upon previous assertions about the effect of alkylation of SH1 and SH2 on the myosin high-salt calcium and EDTA ATPase, we developed a simple graphical procedure for obtaining the fractional labeling of SH1 and SH2 after treatment of myosin with alkylating agents. The procedure provides values for N, X and Z where N is the ratio of calcium ATPase activity with label only at SH1 to that without label, X is the fraction of heads with label solely at SH1, and Z is the fraction at both SH1 and SH2. The procedure was tested by applying it to two previously studied compounds, IASL and FDNB, and then was used to determine a protocol for maximizing the extent of labeling of SH1 alone by N-phenylmaleimide, a previously unstudied compound. In agreement with previous results, we found IASL and FDNB specifically alkylated SH1 without alkylating SH2. A long period treatment (about one day) with 0.5 M IASL resulted in nearly 100% of SH1 alkylated with very little alkylation of SH2. A 240 min treatment with 20 μM FDNB gave 80% labeling at SH1 without obvious modification at SH2. Although N-phenylmaleimide is less specific for SH1 than IASL and FDNB, ~80% of SH1 sites could be alkylated before significant alkylation on SH2. The value of N was 15.7 for IASL, 7.1 for FDNB and 5.5 for N-phenylmaleimide. Our simple graphical evaluation method should be useful for future studies concerned with the effect of these two important cysteines on the function of myosin.

M-Pos161

NPM-REACTED MYOSIN CROSSBRIDGES CAN BIND STRONGLY TO ACTIN. ((**S. Xu**, L. C. Yu and M. Schoenberg)) LPB, NIAMS, NIH, Bethesda, MD 20892.

Previous mechanical studies of NPM-modified fibers done in the presence of 2 mM Mg^{2+} showed relaxed-like behavior in the absence of ATP. In agreement, the 2-dimensional X-ray diffraction pattern in the same solution also is relaxed-like. However, both the 2-D diffraction pattern and the fiber stiffness turn rigor-like when EDTA replaces Mg^{2+} in the ATP-free solution. Ap5A/glucose/hexokinase added to the nominally ATP-free, Mg-containing solution also leads to rigor-like behavior. This suggests that the difference between relaxed and rigor-like behavior is not due solely to ± Mg^{2+}, but more likely due to ± MgATP. This is the first demonstration that NPM-reacted crossbridges, which do not hydrolyze ATP in the steady state, can undergo the weakly- to strongly-binding conformational change. This, in turn suggests that the nucleotide-driven weakly- to strongly-binding conformational change in the contractile cycle is a step distinct from the hydrolysis step, and that one can block the latter, without the former. The data also suggest that NPM-reacted crossbridges show a one-to-one correspondence between strength of actin binding and the presence or absence of nucleotide.

M-Pos162

MYOSIN SUBFRAGMENT-1 MODIFIED WITH NPM OR pPDM DOES NOT HYDROLYZE ATP BUT WILL BIND STRONGLY TO F-ACTIN IF ATP CONCENTRATION IS SUFFICIENTLY LOW ((L. Xie, W. X. Li, M. Schoenberg)) LPB, NIAMS, NIH, Bethesda, MD 20892. (Spon. by S. V. Smith)

Myosin subfragment-1 was labeled with NPM in the presence of ATP or with pPDM in the presence of ADP at 4°C, conditions which favor labeling of both Cys-707 (SH1) and Cys-697 (SH2). Unlabeled S-1 was removed by sedimentation with a small amount of F-actin. The modified protein in the supernatant was then thoroughly dialyzed. The myosin high-salt EDTA and calcium ATPase activity of the isolated S-1 was close to zero, suggesting nearly complete modification of SH1 and SH2. At 100 mM ionic strength, the NPM-reacted S-1 bound to F-actin in the absence of ATP with a binding constant of ~$3*10^6$ M^{-1}. At high ATP concentration, the binding constant was ~$5*10^3$ M^{-1}. The K_d for ATP dissociation of the actomyosin was ~2 μM. The binding of pPDM-reacted S-1 to F-actin in the absence of ATP was weaker than that of NPM-reacted S-1 but was stronger than reported previously. Like for NPM-reacted S-1, ATP dissociated pPDM-reacted S-1 from F-actin. Much work remains, but our preliminary data suggest, in apparent conflict with previously-published data, that the binding of NPM- or pPDM-reacted S-1 is ATP-sensitive and can be quite strong at very low ATP concentrations.

M-Pos163

CROSSLINKING STUDY OF NUCLEOTIDE AND ACTIN EFFECTS ON THE SH_1-SH_2 HELIX IN S1.
((Lisa K. Nitao and Emil Reisler)) Dept. of Chemistry and Biochemistry and The Molecular Biology Institute, UCLA, Los Angeles, CA 90095.

Previous biochemical studies have shown that the SH_1 and SH_2 groups on myosin subfragment 1 (S1) can be crosslinked in the presence of nucleotides by using reagents of different crosslinking lengths. Because in the structure of S1 the SH_1-SH_2 sequence has been identified as an α helix (Rayment et al., Science, 261:50 (1993)), the crosslinking results could be indicative of helix melting, bending, or increased flexibility in the presence of nucleotides. Nucleotide and actin-induced changes in this region were examined in this study by monitoring the crosslinking of SH_1 and SH_2 with m-PDM, o-PDM, and p-PDM in the presence of actin or nucleotides. The protocol adopted in these experiments was to modify SH_1 with one of the reagents, remove excess reagent on spin columns, and then monitor the crosslinking via changes in the Ca ATPase activity of S1. For m-PDM, MgADP increased the rate of crosslinking ~3-fold. For o-PDM, both MgADP and MgATPγS increased the rate ~3-4 -fold. For p-PDM, the rate without nucleotide was higher than for m-PDM and o-PDM (~4-5 -fold). In the presence of nucleotides, the increase was ~15-fold for MgADP while that for MgATPγS was ~50-fold. Actin appeared to have no effect on any of the crosslinking reactions (in the absence of nucleotides). These results are interpreted in terms of nucleotide enhanced bending and/or flexibility in the SH_1-SH_2 helix.

M-Pos164

MOLECULAR MODELING OF ACTOMYOSIN. THE 265kD EDC CROSS-LINKED COMPLEX OF 2 ACTINS WITH S1. ((J. Shi and P. Dreizen)) Physiology & Biophysics, SUNY Brooklyn, Brooklyn, NY.

Initial formation of acto-S1 crossbridges involves electrostatic interactions between actin 1-4 and S1 heavy chain in 20kD-50kD junction (near 640-642) or 50kD lower domain (near 572-574). These sites are identified as 170 and 180kD bands, respectively, on SDS electrophoresis following EDC cross-linking. A 265kD complex is also found under appropriate conditions (Borejdo et al, 1992; Bonafe & Chaussepied, 1995), and results from interactions of S1 with 2 adjacent actin monomers at the same sites as in binary A-S1 complexes. We have attempted molecular modeling of the ternary complex. The complex can not be formed using a molecular model for Actin(1-4)-S1(626-647), based upon the Rayment model, because S1 is too far from the N-terminus of the lower actin. We then used a molecular model for Actin(1-4)-S1(570-573), in which S1 is moved ~5Å toward lower actin. The ternary complex was refined by molecular dynamics and energy minimization, keeping the 2-actin S1 complex rigid except for the flexible S1 loop (627-646) and modeling to get optimal side-chain interactions between Lys640-Asp1 and Lys641-Glu4. Some lysine side-chains appear stretched, but this could be relieved by several Å additional shift of S1 toward lower actin. The differences between the 180kD and 265kD models and the Rayment model are too large to be accounted for by dynamic movement of individual side-chains, but are consistent with conformational variants, related to the extent of S1 packing on actin filaments, or to sequential changes during strong cross-bridge binding.

M-Pos165

INTRAMOLECULAR CROSS-LINKING OF LYSINE RESIDUES IN F-ACTIN INHIBITS FILAMENT MOVEMENTS IN ACTOMYOSIN CROSS-BRIDGE CYCLE. ((J. Feng and P. Dreizen)) Physiology & Biophysics, SUNY Brooklyn, NY 11203.

Reaction of glutaraldehyde-actin with myosin S1 in presence of MgATP eliminates *in vitro* motility, although acto-S1 ATPase remains high (Prochniewicz & Yanagida, 1990), suggesting that actin flexibility has a role in actomyosin motility. Glutaraldehyde induces inter- and intramolecular cross-linking of lysines at different polymeric distances, so that interpretation is difficult. We have explored the effect using actomyosin-MgATP in a PEP backup system, with simultaneous measurements of turbidity and P_i produced. In control acto-myosin-ATP, turbidity rises in the first 6 minutes, while ATPase is constant and before depleting ATP. The turbidity change reflects rearrangement of actin and myosin filaments during cross-bridge cycling, and provides a simple model for filament motility. Using glutaraldehyde-treated F-actin and myosin-MgATP, turbidity does not increase and ATPase actually rises, confirming that glutaraldehyde-actin does not support filament rearrangement, although actomyosin ATPase is active. F-actin was next modified by bis-imidoester reagents, which cross-link pairs of lysine ε-amino groups at different spacer distances. SDS gel electrophoresis shows that the cross-links are predominantly intramolecular. Increasing spacer distance from 3Å to 11Å is accompanied by progressive loss of the turbidity change, although actomyosin ATPase remains constant. Thus, intramolecular cross-linking of lysine residues about 11Å apart in actin appears to blockade dynamic changes in the actin subdomains which are involved in motility during cross-bridge cycling.

M-Pos166

THE BINDING OF F-ACTIN TO 6-[FLUORESCEIN-5(&6)-CARBOXAMIDO]-HEXANOIC ACID MODIFIED SKELETAL MYOSIN SUBFRAGMENT-1 ((K. Tarng and J.M. Chalovich)) Department of Biochemistry, School of Medicine, East Carolina University, Greenville, NC 27858

The helix-turn-helix motif of residues 516-558 of the S1 heavy chain is thought to contribute to the strong hydrophobic interaction with actin subdomain-1 (Rayment et al., Science 261, 58-65, 1993). Kassab et al. reported that Lys 553, within this region, can be specifically labelled with 6-[fluorescein-5(&6)-carboxamido]-hexanoic acid (Biochem. 34, 1995, 9500-9507). This probe was found to undergo a decrease in fluorescence upon binding to actin. We have investigated the possible usefulness of this probe in monitoring interactions between S1 and actin. The binding of ATP to modified S1 (S1*) causes a 15% decrease in the fluorescence. The rate of the fluorescence change upon binding to ATP is similar to the burst rate as measured by Trp fluorescence. Therefore the environment of Lys 553 is sensitive to ATP hydrolysis and modification of this residue is relatively benign. The addition of actin to the S1*-ATP complex resulted in a very rapid increase in fluorescence. Upon mixing rigor S1* with an excess of actin at 19 mM ionic strength, there is a 15% decrease in fluorescence which appears to be a biexponential process. The plot of k_{obs} against total free protein concentration is hyperbolic confirming several earlier reports that the binding occurs in at least 2 steps. However, the fluorescence amplitude for actin binding becomes very small when the ionic strength is raised to 100 mM. As the ionic strength is raised above 100 mM, there is a small increase in fluorescence upon mixing S1* with actin. The binding of S1* to the complex of actin and pyrenyl-labelled tropomyosin (tropomyosin*) was also examined. The fluorescence of both the S1* and tropomyosin* decreased with the same apparent rate constant. The probe on Lys 553 of S1 reports similar events to the probe on Cys 374 of actin during the interaction of S1 and actin in rigor. However, the Lys 553 reporter group is most useful at low ionic strength.

M-Pos167

ATP TURNOVER BY SINGLE HEAVY MEROMYOSIN TRACKS.
((P.B.Conibear and C.R. Bagshaw)) Department of Biochemistry, University of Leicester, Leicester LE1 7RH, U.K.

In order to quantitate the coupling between ATPase activity and filament sliding in actomyosin *in vitro* motility assays, it is desirable to measure these parameters simultaneously at the single filament level. Previously we have used fluorescence microscopy to monitor ATP turnover at the level of isolated myosin filaments, containing about 2000 heads/μm, immobilised on the surface of a flow cell using rhodamine and fluorescein ATP analogs (Conibear & Bagshaw (1996) FEBS Lett. 380 13-16). In order to reduce the head density to match more closely that of the actin (380 monomers/μm), we are now using HMM tracks laid down from decorated filaments. To increase detection sensitivity, tracks were visualised with 1 μM Cy3-EDA-ATP, which showed an increased emission on binding to myosin. Total internal reflection fluorescence (TIRF) microscopy was used to suppress the excitation of free nucleotide. The excitation light from a 50 mW YAG laser (532 nm) was introduced by multiple reflections along a Spectrosil slide via a coupling prism. We have monitored Cy3-EDA-ATP turnover by displacement with an excess of ATP initiated by flash photolysis of caged-ATP using a Xenon flash lamp. Kinetic analysis yields a rate constant similar to that expected for myosin in solution (0.15 s^{-1} at 30° C). In separate assays, we have used flash photolysis to initiate sliding of short actin filaments (<1 μm) along 10 μm HMM tracks. Work is in progress to monitor Cy3-EDA-ATP turnover and BODIPY-labelled actin sliding simultaneously, in order to measure the number of myosin heads in a track which undergo an actin-activated cycle.

Supported by the Wellcome Trust

M-Pos168

INTERACTIONS BETWEEN THE TWO HEADS OF HMM IN BINDING TO ACTIN. ((**Paul Conibear** & Michael Geeves.)) Dept. Biochemistry University of Leicester UK & Max Planck Institute for Molecular Physiology, 44137 Dortmund Germany.

The two heads of HMM appear to be independent in the binding and hydrolysis of ATP yet there is evidence that the two heads interact when binding to a single actin filament. Using pyrene labelled actin we have examined the binding of the two heads of HMM to actin in the presence and absence of ADP. In the absence of ADP both heads bind very tightly to actin and quench the fluroescance of the pyrene label suggesting that both heads are in the R-state. In the presence of ADP or ADP +Pi + BDM the quenching of pyrene fluorescence is much smaller for HMM than for S1 suggesting some inhibition of the formation of two R-states. Modelling the data suggests the following scheme. The first head of HMM binds in a similar fashion to S1. If the first head is in the A-state the second cannot bind actin significantly (i.e. in the presence of ATP). If however the first head is in the R-state, then the second head can form the A-state with little inhibition and the data are consistent with an effective actin concentration of 60 μM for the second head. However the equillibrium constant for the isomerisation of the second head to the R-state is reduced by a factor of 5 compared to the equivalent isomerisation for an unconstranied head (i.e. S1). This model suggests that for rapidly shortening fast skeletal muscle only single headed binding is possible but some two-headed binding will occur under isometric conditions.

M-Pos169

Ca^{2+} ACTIVATION AND CROSS-BRIDGE-MEDIATED ACTIVATION OF THE CARDIAC THIN FILAMENT: A COMPARISON OF SARCOMERE LENGTH DEPENDENCE. ((**Stephen H. Smith**, Yipeng Wang, and Franklin Fuchs)) Dept. Cell Biology and Physiology, University of Pittsburgh Sch. Med., Pittsburgh, PA 15261

Recent work in this laboratory has suggested that the length-dependence of Ca^{2+} sensitivity in cardiac muscle is related to the cooperative effects of cross-bridge attachment to actin (Wang and Fuchs, 1995). It is proposed that the access of cross-bridges for actin is reduced at short sarcomere length. Evidence in support of this proposal is presented, for the rigor state, based on assay of K^+-activated myosin ATPase activity. Given the key role postulated for the cross-bridges we have compared the length-dependence of Ca^{2+} activated force with the length-dependence of cross-bridge-mediated activation of the thin filament. To determine the latter skinned bovine cardiac muscle fibers immersed in a relaxing solution (5mM MgATP, pCa > 8) were exposed to solutions with progressively lower [MgATP] and force was measured (Metzger, 1995). Comparing sarcomere length 1.7-1.8μm and 2.3-2.4μm the Ca^{2+} sensitivity differed by ~ 0.25 pCa units. However there was no detectable effect of a sarcomere length on cross-bridge mediated thin filament activation. This difference may reflect the different degrees of cooperativity of the two modes of thin filament activation.

M-Pos170

MANIPULATION AND NANOMETER MEASUREMENT OF A SINGLE MOTOR PROTEIN MOLECULE CAPTURED DIRECTLY BY A SCANNING PROBE. ((**K.Kitamura***, M.Tokunaga+, A.Iwane*, K.Saito+ and T.Yanagida*+)) *Dept. Biophys. Engineering, Osaka Univ. and +Yanagida Biomotron Project, ERATO, JST, Osaka, Japan.

The experimental apparatus was built on a refined total internal reflection microscope to directly visualized single fluorophores (Nature, 374, 555-, 1995). Myosin subfragment-1(S1) was fluorescently labeled and biotinylated without loosing its function by exchanging its light chain for a fluorescently-labeled and biotinylated one (Iwane et al. in this meeting). Monitoring a single S1 molecule on the surface of a cover slip, it was captured directly onto the tip of a fine ZnO whisker probe, which could be scanned in three dimensions with the nanometer accuracy, by using a biotin-avidin system. When the S1 captured on the probe was brought into contact with the actin filaments fixed on the cover slip in the presence of ATP(1μM), the S1 caused a displacement of ~40nm and a force of ~1pN at a probe stiffness of 0.02pN/nm.

This technique can be extended to measure the intermolecular forces between biomolecules, controlling the gap between the two molecules with the nanometer accuracy. This is called "Intermolecular force scanning microscopy" (Aoki et al. in this meeting).

M-Pos171

Orientation dependent displacements by single one-headed myosin molecules in a synthetic myosin filament ((**H. Tanaka***, A. Ishijima+, M. Honda*, K. Saito+, T. Yanagida*+)) *Dept. Biophys. Engineering, Osaka Univ. and +Yanagida Biomotron project, ERATO, JST

Very sparse myosin-rod cofilaments 5-7μm long were made by slowly mixing one-headed myosin prepared by papain digestion with rod at the molar ratio of 1 to 400, in which 3-4 myosin heads were expected to be contained. This number was confirmed by single molecule imaging microscopy. The displacements by a single myosin molecule were measured at a various angles between actin and myosin filaments by dual laser trapping nanometry. The trap stiffness was 0.04pN/nm. [ATP],1μM. Temp., 20°C.

The displacement was ~15nm at <10°(near correct orientation) and decreased to ~5nm at 70-80°. When the angle was further increased to 130-140°, the displacement was ~5nm, and surprisingly the displacement increased to ~10nm at 170-180°. Similar results were obtained for native two-headed myosin.

Conclusion: 1)the displacement by a myosin head greatly depends on its orientation relative to the actin filament; 2)the unitary step size of a myosin head correctly oriented is 15nm or the unitary step size is 5nm but a head can undergo sequential multiple power strokes during one ATP cycle near the correct orientation, 3)the displacements by a single one-headed myosin are similar to those of a single two-headed one.

M-Pos172

MYOSIN SUBFRAGMENT-1 (S1) IS FULLY EQUIPPED WITH FACTORS ESSENTIAL FOR MOTOR FUNCTION AS WELL AS NATIVE MYOSIN. ((**A. Iwane***, K. Kitamura*, M. Tokunaga†, and T. Yanagida*†)) *Dept. Biophys.Engineering, Osaka Univ.and †Yanagida Biomotoron Project, ERATO, JST, Osaka, Japan (Spon. by Y. Maeda)

The sliding velocity of actin filaments propelled by chicken skeletal myosin subfragment-1 (S1) was measured when its tail end was specifically bound to the glass surface in order to minimize the damage caused to the molecule upon interaction with the surface. For specific binding, a regulatory light chain non-covalently bound to the end of S1 distal from a globular catalytic domain, containing the nucleotide and actin binding sites, was replaced by a recombinant fusion protein of biotin-dependent transcarboxylase (BDTC) and chicken gizzard smooth muscle regulatory light chain (cgmRLC). The BDTC-cgmRLC of S1 was then attached to the glass surface using a biotin-avidin system. The velocity of actin filaments caused by S1 bound to the surface in this manner was 6.8+/-0.6 μm/sec at 29 °C,which was 3.5-fold larger than that (1.9+/-0.3 μm/sec) when bound directly to the surface as in previous studies, but similar to that caused by native chicken skeletal myosin (6.5+/-0.6 μm/sec). The actin-activated Mg-ATPase activity was similar to that of S1 before S1 was exchanged for BDTC-cgmRLC. The results show that S1 fully contains factors essential for motor function as well as native myosin.

M-Pos173

MYOFIBRILLAR ATPase : IDENTIFICATION OF THE STEPS INVOLVED IN TRYPTOPHAN FLUORESCENCE CHANGE. ((R. Stehle, F. Travers and T. Barman)) INSERM U 128, CNRS, 34033 Montpellier Cedex 1, France.

On mixing rabbit psoas myofibrils with ATP, there is a tryptophan fluorescence change (White, 1985, *J. Biol.Chem 260*, 982). Working with myofibrils by stopped flow is difficult but by optimizing their preparation we obtained the kinetics of the change. We attribute these to reaction steps as determined by chemical sampling techniques (using [γ-^{32}P]ATP and quenching by acid or by cold ATP in a rapid flow quench apparatus). To enable temporal resolution, experiments were performed in 40% ethylene glycol at 4°C, μ = 0.16M, pH 7.4. By **flow quench** we obtained : k_2/K_1 = 0.11 $\mu M^{-1}s^{-1}$ (or 0.10 $\mu M^{-1}s^{-1}$), $k_{+3} + k_{-3}$ 3.4 s^{-1} (or 3.2 s^{-1}), and K_3 = 1.7 (or 2.0) with (or without) Ca^{2+}.

$$\text{(A)M} \underset{K1}{\rightleftharpoons} \text{(A)M.ATP} \xrightarrow{k_2} \text{(A)M*.ATP} \underset{k_{-3}}{\overset{k_{+3}}{\rightleftharpoons}} \text{(A)M**.ADP.Pi}$$

By **fluorescence stopped flow**, at low [ATP] (<30 μM) the signal increased exponentially with an amplitude of 5–6 % of the total. The rate constant, attributed to the limiting ATP binding kinetics, was linearly dependent on the [ATP], giving a slope of 0.12 $s^{-1}\mu M^{-1}$ similar to k_2/K_1 obtained by flow quench. At higher [ATP] (> 60 μM), the fluorescence increase showed a second slower phase contributing about 50% to the total increase.This second rate constant was independent of [ATP] and is attributed to the cleavage step with a value equal to the $k_{+3} + k_{-3}$ obtained by flow quench. This shows that the fluorescence of myofibrils increases by 3 % when the ATP becomes tightly bound in (A)M*ATP and a further 3% when (A)M.ADP.Pi is formed. (Supported by EU and NATO).

M-Pos174

SINGLE MOLECULE ENERGY TRANSDUCTION.

((C.VEIGEL, D.C.S.WHITE AND J.E.MOLLOY)) Department of Biology, University of York, York, YO1 5DD, U.K.

We have built an optical tweezers transducer (Molloy *et al.* 1994, 1995) using the three bead configuration of Finer *et al.* (1994) to measure displacements and forces produced by the interaction of rabbit skeletal HMM and S1 with actin. The forces F in our previous studies were 1-2pN and the mean displacements d were 5nm which gives an average work (assuming linear elasticity) of $\frac{1}{2}F \cdot d = 5$pNnm. This is close to thermal energy but much less than ΔG for ATP, which would be about 50pNnm per ATP under the experimental conditions. Possible reasons for this discrepency are (i) that the work per mechanical event equals $\frac{1}{2}kT$ and multiple events are required per ATP to maintain the overall efficiency (ii) that the forces and displacements are underestimated in our measurements. In order to test these possibilities we have (i) measured the stiffness of the [bead-actin filament-bead] unit in order to measure series compliance introduced by the [bead-actin filament] attachment, (ii) determined the [ATP] dependence of the life time of the attachments. Tight coupling (one ATP molecule per mechanical cycle) requires that the rate constant for detachment, determined from the distributions of attached life times, be related to [ATP] by first order Michaelis-Menten kinetics. Our experiments with HMM suggest 1.4 ATP per mechanical crossbridge cycle. We found series compliance to be 0.3-0.4pN/nm, much greater than the trap stiffness used in the displacement measurements. This means that the displacements have to be corrected by only 5-10%. However, the series compliance in the [bead-actin filament] attachment is close to the stiffness measured during crossbridge attachment. The stiffness measured during crossbridge attachment (0.3pN/nm) should be considered as a lower limit for the stiffness of the strongly attached crossbridge itself.

M-Pos175

NOVEL LYSINE SPIN LABEL FOR MODIFICATION OF MYOSIN HEAD

((B. Bauman, T Kalai, K. Hideg, E. A. Fajer, A. Powell and P. Fajer)) , Inst. Molecular Biophysics, NHMFL, Florida State University, Tallahassee, FL 32306 and Central Research Laboratory, Chemistry, Univ. of Pecs, Hungary H-7643

The reactive lysine residue at the interface of the catalytic and regulatory domains of myosin heads presents an interesting vantage point for investigation of conformational changes accompanying force generation. Previous attempts to label this site with isothiocyanate, activated succinimide esters or mixed esters resulted in weak immobilization of the spin label (38 Gauss splitting), preventing their use for either orientation or protein dynamics studies. A novel spin label with imidazolide as a functional group was found to be strongly immobilized when bound to S1 with a splitting of 65.4 Gauss. We are currently evaluating its potential for studying actomyosin interactions in solution and in muscle fibers.

M-Pos176

LC2-PHOSPHORYLATION INDUCED STRUCTURAL CHANGES AT LC1 STUDIED BY FLUORESCENCE QUENCHING AND ENERGY TRANSFER.

((Bishow Adhikari, Yin Jianlin[#], Brett Hambly[#], and Piotr Fajer)) Inst. of Mol. Biophys., Biol. Sci. and NHMFL, Florida State University; and [#]University of Sydney, Sydney, Australia.

LC2-phosphorylation has regulatory and modulatory functions depending on muscle type. In smooth muscle, it is required for regulation; in skeletal muscle, it performs a modulatory role. While modulation may be achieved entirely by electrostatic interactions within LC2 and the heavy chain or between the LC2 region and thick filament backbone, the regulatory mechanism relies on communication between LC2 and the motor domain. To determine whether structural changes are transmitted to LC1 upon LC2 phosphorylation, we have performed dynamic fluorescence quenching experiments of rabbit skeletal myosin labeled with AEDANS at Cys-177 of LC1. Acrylamide was used as the collisional quencher, and the myosin was phosphorylated (up to 80%) by Ca^{2+}-CaM activated MLCK (*generous gift of Dr. J. Stull*) and dephosphorylated (to $\leq$ 20% LC2-P) by alkaline phosphatase. LC2 phosphorylation was accompanied with an ~1.5-2-fold increase in K_{sv}, suggesting that phosphorylation leads to a more open conformation (dynamically more accessible to the solvent) of the fluorophore attached at the Cys-177 of LC1. The change in the solvent accessibility at LC1 was not accompanied by large changes in the distance ($\leq$ 2%) between the two light chains, as determined by the relative efficiency of energy transfer between Cys-154 of LC2 and Cys-177 of LC1 with a IAEDANS and IAF donor-acceptor pair.

M-Pos177

THE *IN VITRO* ANALYSIS OF AN ACTIN MUTATION, *E93K*, OF *DROSOPHILA MELANOGASTER*. ((**A. Razzaq**, J.E. Molloy, D.C.S. White and J.C. Sparrow)) Department of Biology, University of York, Heslington, York Y01 5YW, United Kingdom.

We have used *in vitro* assays for motility and force (optical tweezers) to investigate the interaction of a *Drosophila melanogaster* actin mutant, *E93K*, with wild type myosin (rabbit HMM). This mutation alters a region that is thought to participate in the secondary binding of actin to myosin. Although *E93K* actin filaments bind to a rabbit skeletal muscle HMM surface in rigor, they dissociate from the surface under standard motility assay conditions (25mM KCl, 2mM ATP, 4mM $MgCl_2$, 25mM Imidazole, 1mM EGTA, pH 7.4, Γ=53mM, 23°C). At lower ionic strength (as before but 10mM KCl, Γ=38mM) *E93K* filaments remained bound to the surface and exhibited sliding at a 50% reduced velocity (1.34±0.2μm/s) to WT (2.69±0.3μm/s). Optical trap measurements of the forces and displacements generated by single *E93K* actin with single rabbit HMM molecules revealed that although the working-stroke size (5.5nm) was the same as WT, the force produced was reduced by 25%. These results suggest that the lower *in vitro* sliding velocity of *E93K* is not a consequence of a reduced working-stroke size under unloaded conditions. Moreover, the observed force reduction favours the proposal that increased *E93K* crossbridge compliance, under the partially loaded conditions of the motility assay, leads to a diminished power stroke displacement and subsequent filament velocity.

M-Pos178

THE RATE OF CROSSBRIDGE DETACHMENT IS REDUCED IN HYPOTHYROID RAT MYOCARDIUM. ((T. Wannenburg, P. P. de Tombe)) Section on Cardiology, Bowman Gray School of Medicine, Winston-Salem, NC 27157 and Dept. Physiology & Biophysics, University of Illinois at Chicago, Chicago, IL 60612.

The development of hypothyroidism in rats induces a shift to a slower cardiac MHC isoform. We therefore tested the hypothesis that the rate of crossbridge detachment is reduced in hypothyroid rat myocardium. Rats were rendered hypothyroid by the administration of propylthiouracil (PTU) for a minimum of 6 weeks. We determined the relationship between steady state force development and the rate of ATP consumption at 20°C in skinned cardiac trabeculae from PTU treated animals and controls. Passive sarcomere length was measured by laser diffraction and set to 2.2 μm. ATP consumption was measured using a fluorescent system coupled to the oxidation of NADH. We found that the slope of the force - ATPase relation (bottom left) was reduced from 7.5 ± 0.7 pmol mN^{-1} mm^{-1} s^{-1} in controls (n = 9), to 4.0 ± 0.8 pmol mN^{-1} mm^{-1} s^{-1} (n = 11) in the PTU group (mean ± sem, $p < 0.05$). The maximum forces developed were not significantly different at 59.6 ± 8 mN mm^{-2} (PTU) and 56.0 ± 9 mN mm^{-2} (controls), and there did not appear to be a significant effect on calcium sensitivity (bottom right). These results suggest that the rate of crossbridge detachment is reduced in hypothyroid rat myocardium.

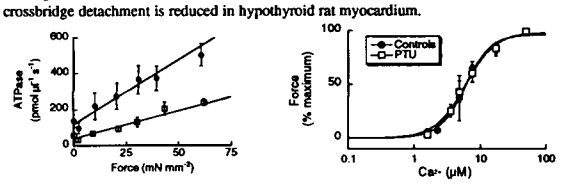

M-Pos179

DELETION OF AN INTERNAL REGION OF TROPOMYOSIN PREVENTS THIN FILAMENT ACTIVATION. ((**C. Landis**, A. Bobkova, E. Homsher, L. S. Tobacman)) University of Iowa, Iowa City, IA 52242

A recombinant tropomyosin (ASTmΔ234) missing 3 of tropomyosin's (Tm) 7 putative actin binding sites has properties suggesting the deleted region is crucial for thin filament activation. Control Ala-SerTm and Ala-SerTmΔ234 were modified on the 5' end to mimic acetylated Tm. Although Tm residues Q49-V167 are missing in the deletion mutant, neither its overall affinity for actin, nor its initial affinity for a bare actin filament is diminished more than a factor of 2. When ASTm or ASTmΔ234 and troponin (Tn) are added in equimolar amounts in the absence of Ca^{2+} the association constants are similar (ASTmΔ234 K_{app}=2.58 μM^{-1} and ASTm K_{app}=2.22 μM^{-1}). Both binding curves shift in the same way upon the addition of Ca^{2+} (ASTmΔ234 K_{app}=1.76 μM^{-1} and ASTm K_{app}=1.34 μM^{-1}). Conversely, ASTmΔ234 abolishes Ca^{2+} regulation of the thin filament. It inhibits both myosin S-1 MgATPase rates and in vitro motility, regardless of whether Tn is present. MgATPase rates for ASTmΔ234 plus Tn remain low upon the addition of Ca^{2+} unlike ASTm which has a 20 fold increase. Motility assays show when 100 nM of ASTmΔ234 is added no movement is observed nor is this reversed by the addition of Tn plus Ca^{2+}. Notably, although myosin S-1 increased ASTm binding to actin 100 fold no such effect is seen for the deletion Tm. This suggests that the deleted region is important for stabilizing the myosin- induced "on" state of the thin filament.

M-Pos180

ROLE OF RESIDUE 311 IN ACTIN-TROPOMYOSIN INTERACTION: *IN VITRO* MOTILITY STUDY USING YEAST ACTIN MUTANT *E311A/R312A*. ((**Jack H. Gerson***, Elena Bubkova[§], Earl Homsher[§], and Emil Reisler*))
*Molec. Biol. Inst., UCLA, Los Angeles, Ca 90095; [§]Dept. of Physiol., UCLA, Los Angeles, CA 90024.

In their atomic model of the actin-tropomyosin complex, Lorenz, *et al.* list the actin residues that are likely involved in electrostatic interactions with tropomyosin (Tm). We have investigated the role in such interactions of actin residue D311 (E311 in yeast), which is predicted to have a high binding energy contribution to actin-Tm interactions, using the yeast actin mutant *E311A/R312A* in the *in vitro* motility assays. *Wt* yeast actin, like skeletal α-actin, is fully regulated when complexed with Tm and troponin (Tn) in the pCa range of 8 to 5, making yeast actin a suitable model for the study of regulation. Structure-function comparisons of the *wt* and *E311A/R312A* actins, including CD, acto-S1 ATPase, and binding assays show no significant differences between them, while polymerization studies indicate a slightly faster reaction rate for the mutant. In the absence of regulatory proteins, our motility results reveal no appreciable difference in sliding speed between the two actins. However, with Tm and Tn present, the mutation increases both the sliding speed and the number of moving filaments at all tested pCa's. This results in an effective shift to the left of the pCa curve by approximately 0.75 pCa units. *In vitro* motilities of actin-Tm complexes were determined over a wide range of HMM for both the *wt* and mutant actins. Actin motility was inhibited at low, and potentiated at high, HMM concentrations. This correlates with previous solution studies results of acto-S1 ATPase activities in the presence of Tm. The *E311A/R312A* actin was more dramatically affected by Tm than the *wt* actin at both low and high HMM concentrations.

M-Pos181

THE USE OF pPDM-HMM AND MICRONEEDLES TO MEASURE pN FORCES EXERTED BY MYOSIN HEADS ON SINGLE REGULATED THIN FILAMENTS. ((D. Lee, A. Bobkova, L.S. Tobacman*, and E. Homsher)) Physiol. Dept., Med. Sch., UCLA, Los Angles, CA 90095, * Dept. of Int. Med., Univ.Iowa, Iowa City, IA 52242.

We used two methods to estimate the force exerted by heavy meromyosin (HMM) heads pulling on actin thin filaments in *in vitro* motility assays. In the first, N,N'p-phenylenedimaleimide-treated HMM (pPDM-HMM) was added to a motility surface coated with untreated HMM. The sliding speed of the thin filaments was inversely proprotional to the amount of pPDM-HMM added, presumably because weak binding of the pPDM-HMM to the thin filaments exerted a load on them. Addition of [Pi] up to 20 mM had no effect on sliding speed in the absence of pPDM-HMM, but [Pi] did reduce the amount of pPDM-HMM needed to halt filament sliding by ca. 25% per decade increase in [Pi]. This behavior is similar to the [Pi] induced reduction in isometric force seen in isolated muscle fibers. When the Ile79Asn TnT mutant protein, associated with the presence of familial myocardial hypertrophy, replaced the native TnT in the Tn complex of regulated filaments, the filament sliding speed increased from 4 μm/s to 6.5 μm/s (Lin, et al, *JCI.* 97:1-8, 1996). However, the sliding speed decreased more steeply with added pPDM-HMM and fell to zero at a pPDM-HMM concentration 20% less than that needed in the presence of native Tn/Tm. This implies that the presence of the mutant TnT reduces cardiac muscle's ability to generate force. The second method is to attach fluorescently labeled thin filaments to a very fine and compliant glass microneedle and bring the filaments into contact with an HMM covered surface. The thin filament then slides over the surface, bends the microneedle, and is halted by the microneedle's restoring force, which is proportional to the microneedle deflection. The force needed to halt unregulated thin filaments was >10 pN/μm of thin filament in contact with the surface. We are currently comparing the force exerted on thin filaments containing native regulatory proteins to those containing the Ile79Asn TnT mutant to test the conclusion that isometric force exerted on the thin filaments is reduced in the presence of the TnT mutant protein. (Supported by NIH grants AR 30988 (EH) and HL 38834 (LST)).

M-Pos182

TRANSGENIC (TG) MOUSE HEARTS WITH A SHIFT IN THE POPULATION OF TROPOMYOSIN (TM) ISOFORMS OR POINT MUTATIONS OF α–TM SHOW ALTERED MYOFILAMENT SENSITIVITY TO CA^{2+}. ((B.M. Wolska*, C. Evans*, K. Palmiter*, M. Muthuchamy*, J. Oehlenschlager*, D. Wieczorek*, R.J Solaro*)) *University of Illinois at Chicago College of Medicine, Chicago, IL 60612, *University of Cincinnati College of Medicine, Cincinnati, OH 45267.

We studied myofilaments from nontransgenic mouse hearts that express α-Tm (NTG), and from hearts overexpressing either α-Tm (Tgα Tm), β-Tm (Tgβ Tm), or a mutant α-Tm (Tgα Tm (Asp175Asn)) linked to familial hypertrophic cardiomyopathy (FHC). We found no significant difference in myofilament Ca^{2+} sensitivity between TG-α-Tm and NTG mice. Transgene expression was driven by the murine α-myosin heavy chain promotor. Myofilaments from TG-β-Tm mice showed a significant increase in sensitivity to Ca^{2+} compared to NTG mice at pH 7.0 (Δ pCa_{50} = 0.13), but not at pH 6.5. TG-β-Tm myofilaments demonstrated the same dependence of Δ pCa_{50} on sarcomer length (1.8, 2.0 and 2.4μm) as NTG mice. Myofilaments from TG-α-Tm(Asp175Asn) mouse hearts which expressed a high copy number of the transgene demonstarated a significant increase in myofilament Ca^{2+} sensitivity (Δ pCa_{50} = 0.11) compared to NTG mice. TG-α-Tm(Asp175Asn) mice which expressed a low copy number of the transgene did not show a shift in pCa_{50}. These results indicate that Tm may be involved in acidosis altered regulation of myocardial contractility. Asp 175 appears to be important in Ca^{2+} sensitivity of myofilaments. A high proportion of α-Tm (Asp175Asn) in the myocardium, as occurs in FHC patients, may contribute to altered cardiac function.

M-Pos183

PROTEIN KINASE C MEDIATED PHOSPHORYLATION IN DIABETES ((**A.Malhotra**, D.Reich, A.Nakouzi, V.Sanghi, D.L.Geenen and P.M.Buttrick)) Cardiology, Albert Einstein College of Medicine, Bronx, NY 10461.

To explore a possible role for protein kinase C (PKC) mediated phosphorylation of myofibrillar proteins in diabetic cardiomyopathy we characterized the cellular distribution of the major PKC isoforms in cardiocytes isolated from diabetic rats and determined patterns of phosphorylation of the major regulatory proteins, including troponin I (TnI). Female rats (200-225g) were made diabetic with a single injection of streptozotocin and myocardiocytes were isolated and studied 3-4 weeks later. In non-diabetic animals, 75% of the PKC ϵ isoform was located in the cytosol and 25% was particulate whereas in diabetics, 51% was cytosolic and 49% was particulate ($p<0.05$). PKC δ, the other major PKC isoform seen in adult cardiocytes, did not show a change in translocation pattern. In parallel, TnI phosphorylation was five-fold increased in cardiocytes isolated from the hearts of diabetic animals relative to control animals ($p<0.01$). The change in PKC ϵ distribution and in TnI phosphorylation in diabetics was analogous to that seen with angiotensin II treatment and was completely prevented both by rendering the animals euglycemic with insulin or with concomitant treatment with a specific angiotensin type I receptor (AT1) antagonist. Since PKC phosphorylation of troponin I has been associated with a loss of calcium sensitivity of intact myofibrils, these data suggest that angiotensin II receptor-mediated activation of PKC may play a role in the contractile dysfunction seen in chronic diabetics.

M-Pos184

DISPARATE FLUORESCENE OF IAANS ATTCHED TO Cys84 AND Cys35 OF cTnC IN CARDIAC TROPONIN ((**W.J. Dong**[†], C.-K. Wang[‡], A. M. Gordon[‡] and H. C. Cheung[†])) [†]D. Biochem., Univ. Alabama at Birmingham, Birmingham, AL 35294; and [‡]D. Physio. & Biophys., Univ. Washington, Seattle, WA 89195

Monocysteine mutants cTnC(C35S) and cTnC(C84S) from cardiac muscle were labeled with the fluorescent probe IAANS at Cys84 and Cys35, respectively. The labeled proteins were studied by a variety of steady-state and time-resolved fluorescence methods. In the absence of divalent cation, the fluorescence of the attached IAANS indicated an exposed environment at Cys35 and a relatively less exposed environment at Cys84. The binding of Ca^{2+} to the single regulatory site elicited a large enhancement of the emission of IAANS attached to Cys84, but only marginal fluorescence changes of the probe at Cys35. However, upon reconstitution with cTnI or cTnI plus TnT, the fluorescence of IAANS-Cys84 in apo binary complex of troponin was spectrally similar to that observed with the Ca^{2+}-loaded uncomplexed cTnC. Only small changes in the fluorescence of IAANS-Cys84 were observed when the regulatory site in reconstituted troponin was saturated. The exposed Cys35 of the uncomplexed cTnC mutant became considerably less exposed and less polar when the mutant was incorporated into apo troponin. In contrast to the Cys84 site, saturation of the regulatory site II by Ca^{2+} in reconstituted troponin resulted in a large change in the fluorescence of IAANS attached to Cys35. These results suggest involvement of the inactive loop I in the trigger mechanism in cardiac muscle. The fluorescence of the probe at both Cys84 and Cys35 was sensitive to phosphorylation of cTnI, and this sensitivity was observed in both apo and Ca^{2+}-loaded states. (Supported by NIH Grants AR31239 and HL52558)

M-Pos185

KINETICS OF Ca^{2+} BINDING TO THE REGULATORY SITE OF TROPONIN FROM CARDIAC MUSCLE ((**W.J. Dong**†, C.-K. Wang‡, A. M. Gordon‡ and H. C. Cheung†)) †D. Biochem., Univ. Alabama at Birmingham, Birmingham, AL 35294; and ‡D Physio. & Biophys., Univ. Washington, Seattle, WA 89195

The kinetics of the interaction between Ca^{2+} and the binary cTnC•cTnI complexe and fully reconstituted troponin from cardiac muscle was studied at 4.0 °C. This was done by measuring the rates of Ca^{2+}-mediated fluorescence changes of a monocysteine mutant cTnC(C84S) labelled with the probe IAANS at Cys35. In the presence of Mg^{2+}, the binding kinetics of binary complex was resolved into two phases with negative amplitude (decreasing intensity). The rate of the fast phase increased with $[Ca^{2+}]$, reaching a maximum of about 34 s^{-1}, and that of the slow phase was 5 s^{-1} and not sensitive to Ca^{2+}. The dissociation kinetics was determined with chelators to displace bound Ca^{2+}, and the kinetic transient was resolved into two phases with positive amplitude (increasing fluorescence), ~23 s^{-1} and ~4 s^{-1}. Essentially the same kinetic parameters were obtained with reconstituted troponin. These results yielded an apparent second-order rate constant of 5.9 x 10^7 $M^{-1}s^{-1}$ for Ca^{2+} binding and are consistent with the previously proposed three-step mechanism (Dong et al., (1996) JBC 271:688). The binding rate constant for the complex is much smaller than the value previously obtained for isolated cTnC. While phosphorylation of cTnI by protein kinase A increased the apparent dissociation rate of Ca^{2+} from the complex, it decreased the apparent second-order binding rate constant. The overall effect of cTnI phosphorylation is a 5-fold decrease of the overall equilibrium constant. (Supported by NIH Grants AR31239 and HL52558).

M-Pos186

CONFORMATIONAL AND FUNCTIONAL CHANGES OF TROPONIN T MODULATED BY THE STRUCTURE OF THE NH_2-TERMINAL VARIABLE REGION. ((**J.-P. Jin**, O. Ogut, and J. Wang)) Dept. Physiology and Biophysics, Case Western Reserve Univ., Cleveland, Ohio 44106 and Dept. Medical Biochemistry, Univ. of Calgary, Calgary, Canada T2N 4N1

Troponin T (TnT) is expressed as multiple isoforms from three different genes through alternative mRNA splicing of three variable regions in the polypeptide chain. A large to small, acidic to basic TnT isoform switch has been demonstrated during both cardiac and skeletal muscle development, generated mainly by alternative splicing of the functionally unclear NH_2-terminal variable region. By applying a metal-binding cluster (Tx) found in the NH_2-terminal region of chicken fast skeletal muscle TnT, we have developed a metal-induced TnT conformational transition model to investigate the structure-function relationships of TnT isoforms and their variable regions. In addition to increased NH_2-terminal α-helical contents induced by the binding of transition metal ions to the Tx segment, Zn^{2+}-binding property and monoclonal antibody epitopic analyses demonstrated potential conformational relationships between the NH_2-terminal variable region and other domains of intact TnT molecule. Solid-phase protein-binding assays have established that Zn^{2+} binding to the Tx cluster induced epitopic structure changes in this segment and further affected TnT's association with tropomyosin. The results suggest that metal-induced structural changes in the NH_2-terminal region may reconfigure the overall conformation of intact TnT through structural relationships between the NH_2-terminal variable region and other domains of TnT. Accordingly, the developmental and muscle type-specific NH_2-terminal structure of TnT isoforms may modulate the regulation of muscle contraction. (Supported by the Medical Research Council and Heart and Stroke Foundation of Canada and the Case Western Reserve University School of Medicine)

M-Pos187

GENOMIC STRUCTURE OF MOUSE SLOW SKELETAL MUSCLE TROPONIN T GENE IMPLIES A PROTOTYPE PRIMARY STRUCTURE OF TROPONIN T, A MUSCLE REGULATORY PROTEIN WITH MULTIPLE MUSCLE TYPE-SPECIFIC AND DEVELOPMENTAL ISOFORMS. ((**A. Chen**, Q.-Q. Huang, and J.-P. Jin)) Dept. Physiology and Biophysics, Case Western Reserve Univ., Cleveland, Ohio 44106 and Dept. Medical Biochemistry, Univ. of Calgary, Calgary, Canada T2N 4N1 (Spon. by T.T. Egelhoff)

Troponin T (TnT) participates in the Ca^{2+}-regulation of striated muscle contraction. Three different TnT genes have been identified in vertebrates and alternative mRNA splicing generates multiple isoforms from each gene. The primary structure and expression regulation of cardiac and fast skeletal muscle TnTs (cTnT and fTnT) have been demonstrated in many species. In contrast, less is known for the expression and structure of slow skeletal muscle TnT (sTnT). We have cloned and sequenced mouse genomic DNA containing the entire sTnT gene. The results demonstrate a potentially prototype TnT gene that contains fewer alternatively spliced exons compared to the fTnT and cTnT genes of the same species. A single exon homologous to the cTnT exon 15 and the embryonic-dominant fTnT exon 17 is present in the sTnT gene, corresponding to the alternatively spliced COOH-terminal variable region of the fTnT gene. Only two exons are found in the mouse sTnT NH_2-terminal variable region in contrast to 6 alternatively spliced exons in the fTnT gene. The sTnT gene expression is regulated differently from the fTnT gene and preliminary results have shown that sTnT is the predominant TnT expressed in cultured myotubes. The structure and expression features of sTnT gene provides a useful system to investigate the structure-function relationship of TnT isoforms as well as muscle-specific gene expression during muscle differentiation and development. (Supported by the MRC and Heart and Stroke Foundation of Canada, and the Case Western Reserve University)

M-Pos188

TROPONIN T DIVERSITY AND FUNCTION IN *C. ELEGANS* ((T.StC. Allen, K. McArdle, E. Polyak, and E.A. Bucher)) Dept of Cell and Developmental Biology, U. of PA, Philadelphia, PA 19104-6058

To understand the biological roles of troponin T (TnT) in striated muscle, we are studying the diversity and expression patterns of TnT isoforms in *C. elegans*, as well as the consequences of mutations in one of these isoforms. Four isoforms have been detected: TnT-1, encoded by the gene *mup-2* (mutations in this gene cause defects in muscle positioning); TnT-2, by the gene *TnT-2*; and splice variants TnT-3a and TnT-3b, both by the gene *TnT-3*. The four isoforms have a long, invertebrate-specific, C-terminal tail flanking a leucine zipper motif conserved in all known TnTs. Sequence variations among the four arise because of deletions in the N-terminal hypervariable region (corresponding to a.a. ~10-~60 of rabbit fast skeletal αTnT) and in the C-terminal tail. Expression of each is developmentally regulated and tissue specific.

Two mutations in the TnT-1 gene have been isolated. One is a premature stop at codon 94 and is believed null; the other truncates the C-terminal tail. Both give indistinguishable mutant phenotypes (defects in sarcomeric organization, muscle positioning, and muscle contraction); however, the mutant phenotype of the latter is observed only at temperatures >~18°C (Myers *et al. J. Cell Biol.* **132**: 1061-1077). The aberrant contractions caused by TnT-1 mutations contrast to the flaccid paralysis observed with animals mutant for a sarcolemmal voltage-gated Ca channel or for troponin C (TnC). The heat-sensitive TnT-1 mutation failed to relieve the flaccid paralysis caused by Ca channel and TnC mutations in animals doubly homozygous for the TnT-1 mutation and for either Ca channel mutation or TnC mutation. Thus, aberrant contractions resulting from mutation of TnT-1 appear to require a regulatory system competent to bind Ca^{2+} and disinhibit force production.

M-Pos189

EFFECTS OF GENETICALLY ENGINEERED $BTnC_2$ IN WHICH SITES II AND IV ARE INACTIVATED ON SKINNED MYOFIBRILLAR BUNDLES FROM THE BARNACLE (*B.nubilus*) ((*†C.C. Ashley, *L.D. Allhouse,*T. Miller, *G. Guzman and *J.D. Potter)) *Univ. Lab. Of Physiology, Oxford, OX1 3PT, UK, †Friday Harbor Labs, University of Washington WA 98250, *Molecular and Cellular Pharmacology, University of Miami Medical School, Miami, FL 33101.

Recombinant $BTnC_2$ ($rBTnC_2$) containing mutations at both Ca^{2+} binding sites II and IV (rBTnC2-4-) was studied in native TnC depleted muscle fibres. Previous studies have suggested that only sites II and IV bind calcium in $BTnC_2$ (Collins *et al.* Biochem. 30:702 (1991); Ashley *et al.* J.Muscle Res.12:532 (1991)). The mutant lacking both sites II and IV was prepared by rendering the calcium binding site inactive by insertion of an ALA for an ASP residue in the X co-ordinating position of each of the calcium binding loops. Myofibrillar bundles (120μm diam.) were prepared under mineral oil. Native TnC was extracted with either 10mM orthovanadate or 2mM EDTA (Ashley *et al.* Biophys.J. 70:A380 (1996)). Subsequent exposure (2 mg/ml, I = 0.15 M, 20°C, 30 min) to rBTnC2-4- and with reconstitution either in the presence or absence of calcium failed to regulate force, but blocked the regulation by $rBTnC_2$ (wild type). These results suggest that calcium binding to the two calcium-specific sites (II and IV) in $BTnC_2$ is not required to bring about an interaction between $BTnC_2$ and BTnI. Since this interaction requires magnesium, there may be additional magnesium-specific binding sites present.

M-Pos190

ISOFORMS OF TROPONIN-I IN SALMON MYOTOMAL MUSCLE. ((D.M. Jackman and **D.H. Heeley**)), Department of Biochemistry, Memorial University, St. John's, NF, Canada A1B 3X9.

Three full length troponin-I (Tn-I) clones (33G9, 29C12 & 35E12) were isolated from a cDNA library prepared from Atlantic salmon fry whole myotomal muscle (age = 10 weeks post hatch). Based on the distribution of substitutions, most of which are N-terminally located, the isoforms probably arise from separate genes. In all three sequences the second Pro contained within the minimum inhibitory peptide region (G-K-F-K-R-P-P-L-R-R-V-R) of other Tn-Is is substituted for Ala. In addition, the second amino acid (A.A) within this region has been deleted in 33G9 & 35E12. Two of the clones (33G9 & 35E12) are predicted to consist of 172 A.As and two are predicted to be basic (33G9 & 29C12, which contains 180 A.As). The pI of 35E12 is predicted to be non basic. Other selected features are: 33G9 (1 x Y, 1 x W), 29C12 (4 x Y, 2 x W, 4 x C) & 35E12 (1 x Y, 1 x W, 1 x C). Since, cysteine was not detected in Tn-I isolated from mature fast myotomal muscle and N-terminal sequencing of a fast Tn-I peptic fragment yielded a sequence that matched residues 41-51 of 33G9, 33G9 is concluded to be present in adult fish. However, a unique sequence was obtained from mature slow myotomal Tn-I. One possibility is that developmental forms of Tn-I are synthesised in the swimming muscles of salmonid fish.

M-Pos191

INTER-SUBUNIT PHOTOCROSSLINKING OF SINGLE CYS MUTANT TROPONIN I IN BINARY AND TERNARY COMPLEXES. ((**Y. Luo**, Y. Qian, J.-L. Wu, T. Tao and J. Gergely)) Muscle Res. Group, Boston Biomed. Res. Inst.; Depts of BCMP and Neurology, Harvard Med. Sch.; and Neurology Service, Mass. Gen. Hosp., Boston, MA 02114.

To study the spatial relations among three troponin (Tn) subunits, TnI, TnC and TnT, the photocrosslinker benzophenone-4-iodoacetamide was attached to the single cysteine of TnI mutants at positions 6, 48, 89, 104, 133 or 179. In the binary complex TnI•TnC, cross-linking took place with all mutants in the presence of Ca^{2+}, with differences in the yield and Ca^{2+} sensitivity. The highest yield was found for Cys6 with little Ca^{2+} sensitivity. This suggests crosslinking with the C-terminal portion of TnC, which would be consistent with the proposed antiparallel arrangement of TnC and TnI and with the structural, rather than regulatory, role assigned to the C-terminal portion of TnC. Crosslinking between Cys104, in the inhibitory region of TnI, and TnC resulted in a multicomponent band on SDS PAGE that was sharpened by Ca^{2+}. This suggests mobility in the inhibitory region which is reduced by Ca^{2+}. For the other mutants Ca^{2+} binding enhanced crosslink formation in comparison with that in the Mg^{2+} state. In the ternary complex, cross-linking to TnT was significant only for Cys89 and Cys48 with essentially no Ca^{2+} sensitivity. For these two mutants, the cross-linking to TnC was reduced, whereas for the other mutants it was enhanced by TnT. Thus it appears that the interactions between TnI and TnT are largely confined to residues 40 - 90 of TnI while the interactions between TnI and TnC are more extensive. The conformation of the 40 - 90 segment is altered upon binding to TnT so that its contact with TnC is decreased. However, for almost all other parts of TnI, TnT seems to strenthen TnI's contact with TnC. Finally, in the Ca^{2+} state, TnT further sharpened the crosslinked TnI104-TnC multi-band into a single strong band, manifesting the Ca^{2+} dependence of the flexibility of the inhibitory region. The flexibility and its reduction by Ca^{2+} may point to its role in the transmission of the effect of Ca^{2+} binding to the regulatory sites in TnC. (Supported by NIH HL-05949 and AR-21673)

M-Pos192

THE CONFORMATION OF TROPONIN-I STUDIED BY CHYMOTRYPTIC DIGESTION
((T. Tao, **B.-J. Gong** and J. Gergely)) Muscle Research Group, Boston Biomedical Research Institute, Boston, MA 02114

Troponin-I (TnI) is the inhibitory subunit of the striated muscle regulatory protein troponin (Tn). We have used limited proteolysis to probe the conformation of TnI in complexes with other thin filament proteins, with and without Ca^{2+}. When free TnI (M_r=21k) was treated with chymotrypsin (enzyme:TnI wt ratio 1:500, 25°C for ~10 min) two fragments were produced with molecular masses of 11.56 and 9.53 kDa as determined by mass spectrometry. N-terminal sequencing revealed that the 11.56 kDa fragment is blocked at the N-terminus, and that the 9.53 kDa fragment begins at Asp101 or Lys107 in the so-called inhibitory region (residues 96-116) of TnI. Both the digestion pattern and the rate of digestion remained unchanged when TnI was complexed with troponin-C (TnC). Digestion of the ternary Tn complex fluorescently labeled at Cys133 of TnI produced a fluorescent fragment of apparent M_r≅16k. The N-terminus of this fragment is blocked, indicating that the digestion site(s) is C-terminal to Cys133. Mass spectrometry of a partially purified fraction yielded a molecular mass of 16.95 kDa for this fragment. Neither the patterns nor the rates of digestion were Ca^{2+}-dependent for the binary and ternary complexes. When the digestion was carried out on the reconstituted thin filament composed of labeled Tn, tropomyosin and actin, the same 16.95 kDa fragment was produced both with or without Ca^{2+}. However, the rate of digestion was significantly reduced in the absence of Ca^{2+}. These results indicate: 1) The inhibitory region of TnI is particularly sensitive to proteolysis, perhaps because it is highly exposed and/or flexible. 2) The presence of TnC has no effect on the susceptibility of this region to proteolysis. 3) The additional presence of troponin-T protects this region from proteolysis, while exposing a site closer to the C-terminus, most likely at Leu140. 4) The conformation at the Leu140 site is not Ca^{2+}-dependent for the ternary Tn complex. 5) For the thin filament, on the other hand, this site becomes more resistant to proteolysis in the absence of Ca^{2+}, presumably owing to the interaction between the C-terminal region of TnI and actin. (Supported by HL05949 and AR21673)

M-Pos193

PATHWAYS OF COMMUNICATION BETWEEN CARDIAC TROPONIN I AND TROPONIN C DURING ACIDOSIS AND TNI PHOSPHORYLATION BY PROTEIN KINASE A
((**X.-L. Ding**, E.H. Sonnenblick & J. Gulati)) The Molecular Physiology Laboratory, Division of Cardiology, Albert Einstein College of Medicine, Bronx, NY 10461

It is known that both acidosis and phosphorylation of the N-terminal serines 23 and 24 of cardiac TnI by cAMP-dependent protein kinase (PKA) reduce Ca^{2+}-sensitivity of tension development. The pathways of communication of these effects were investigated presently in rat cardiotrabeculae. The studies were made with cTnC/sTnC exchange, as well as the N-fragment mutants of sTnC (and cTnC) comprising amino acids 1-84 (Akella et al., Biophys. J. 70, A259, 1996). On skinned cardiotrabeculae, the PKA-induced cTnI phosphorylation produced a rightward shift of 0.14±0.02 in pCa-force relation. This effect was the same whether the endogenous cTnI was phosphorylated with treatment of the trabeculae with PKA or whether isolated cTnI was phosphorylated separately and substituted into the trabeculae. The shift was increased to 0.27±0.04 at acidotic pH6.2 ($P<0.01$). The influence of cTnI phosphorylation was independent of cTnC/sTnC isoforms. However, the effect of cTnI phosphorylation was eliminated with sTnC N-fragment at pH7. These findings indicate most directly that the effect of the phosphorylation of serines 23 and 24 of cTnI is communicated to the TnC trigger domain from the N-terminal of cTnI through the C-domain of TnC. At pH6.2, the effects of acidosis and phosphorylation both were still manifest with the sTnC N-fragment, suggesting the existence of alternate pathways as well for the transmissions of these signals from cTnI to the N-terminus of TnC.

M-Pos194

THE mini-N TRIGGER FRAGMENT (RESIDUES 1-84) OF SKELETAL MUSCLE TROPONIN C: UNCOUPLING OF BINDING FROM FUNCTION
((**Arvind Babu Akella**, Hong Su and Jag Gulati))
Cardiology Division, Albert Einstein College of Medicine, Bronx, NY

We have previously shown that a *mini-N* fragment of rabbit sTnC comprising sites I and II can trigger force development with Ca in TnC-extracted skinned fibers. In efforts to elucidate the molecular basis of the contraction switch in skeletal muscle, the properties of this fragment are further characterized, and we find that the presence of the hydrophobic sequence ^{78}MMVRQMK^{84} is critical for function. A fragment designed with 77 residues, deleting ^{78}MMVRQMK^{84} indicates total loss of contractile function in the fiber. To determine how many *mini-N* molecules occupied each TnC-slot, the protein was radiolabelled with ^{125}I and its uptake in the fiber measured. The stoichiometry (mini-N:TnI) was found as 1:1. A striking finding was that the *mini-N* could be loaded in the fiber even in the absence of Ca, indicating that the pertinent hydrophobic patch was exposed in the fragment even in the apo state. However, the force development still required Ca, indicating that binding step of the trigger domain of TnC to TnI can be uncoupled from the overall activation of the contraction switch. The results show that Ca-binding to the sites I and II of sTnC regulates multiple dissociable events in the trigger mechanism. *[Supported by NIAMS/NIH]*

M-Pos195

N-TERMINAL DELETION OF CARDIAC TROPONIN T REDUCES FORCE BUT DOES NOT ALTER Ca^{2+}-SENSITIVITY OR CO-OPERATIVITY IN SKINNED RAT CARDIAC FIBERS. ((**M. Chandra**, J. J. Kim and R. J. Solaro)) Dept. of Physiology and Biophysics, University of Illinois at Chicago, Chicago, IL 60612.

The most striking difference between cardiac troponin TnT (cTnT) and skeletal troponin T (sTnT) from various species is that the cardiac isoform has an extended amino terminus, which is rich in negatively charged amino acids. To investigate the functional significance of this negatively charged amino terminal region in cTnT, we have isolated and purified a mutant form of adult rat cTnT (77-289) in which amino acids 1-76 were deleted. We exchanged the native troponin complex in skinned rat cardiac fiber bundles with the cTnT species by adding either full length cTnT or cTnT (77-289) in large excess. In the absence of cTnI-cTnC, the Ca^{2+}-independent force developed by fibers reconstituted with cTnT (77-289) was considerably less (30% of the initial force) than that observed for the full length cTnT (68% of the initial force). In the presence of cTnI-cTnC, the Ca^{2+}-dependent force observed was also less for cTnT (77-289) when compared with full length cTnT (46% and 72%, respectively). Interestingly, in both cases no significant changes in Ca^{2+}-sensitivity (pCa) or co-operativity (n) were observed. These results are summarised as follows : **1)** unextracted fiber, pCa=5.75 (± 0.03), n=3.17 (± 0.61) ; **2)** full length cTnT, pCa=5.71 (± 0.04), n=2.10 (± 0.40) ; **3)** cTnT (77-289), pCa=5.74 (± 0.04), n=2.34 (± 0.24). Our observations agree with the results of Pan et.al (*J.B.C.* **266**;12432, 1991), who showed that deletion of 1-46 amino acids of rabbit fast sTnT decreased the Ca^{2+}-regulated maximal ATPase activity with no alterations in both Ca^{2+}-sensitivity and co-operativity. Their observations were made under conditions where cross-bridge mediated changes in the thin filament co-operativity were negligible. Even in cardiac muscle, in which cross-bridge mediated activation is more prominent (Metzger, J.M. *Biophys. J.* **68**;1430, 1995), N-terminal deletion of cTnT reduces force with no changes in Ca^{2+}-sensitivity or co-operativity.

M-Pos196

THE C-TERMINUS OF CARDIAC TROPONIN I IS REQUIRED FOR FULL INHIBITORY ACTIVITY AND Ca^{2+}-SENSITIVITY OF RAT MYOFIBRILS.
((**H.M. Rarick**, R.J. Solaro, and A.F. Martin)) Dept. Physiology & Biophysics, University of Illinois at Chicago, Chicago, IL 60612

The C-terminus of troponin I is known to be important in myofilament Ca^{2+}-regulation in skeletal muscle. We examined the role of C-terminal domains of cardiac TnI (cTnI) by generating three C-terminal deletion mutants. Wild-type cTnI (WT-cTnI; cardiac mouse) and mutants, $cTnI_{1\text{-}199}$ (missing 12 residues), $cTnI_{1\text{-}188}$ (missing 23 residues) $cTnI_{1\text{-}151}$ (missing 60 residues), were expressed in *E.coli* and purified. The inhibitory ability of the cTnI mutants was examined in myofibrils from which cTnI-cTnC was extracted by exchanging endogenous cardiac troponin with exogenous cTnT. When cTnI and cTnC were extracted from rat cardiac myofibrils by excess cTnT, the Ca^{2+}-sensitivity of the myofibrils was lost. Addition of increasing amounts of exogenous WT-cTnI or $cTnI_{1\text{-}199}$ to cTnT-extracted myofibrils (pCa 8) caused a dose-dependent inhibition to 25% of maximum ATPase activity obtained at pCa 4.875. However, $cTnI_{1\text{-}188}$ and $cTnI_{1\text{-}151}$ only inhibited to 40% and 60% of maximum ATPase activity, respectively. Next, we formed a complex of WT-cTnI or each mutant with cTnC, reconstituted the complex into the cTnT-extracted myofibrils, and measured the Mg^{2+}ATPase activity as a function of pCa. We found that the $cTnI_{1\text{-}188}$/cTnC complex only partially restored Ca^{2+}-sensitivity and the $cTnI_{1\text{-}151}$/cTnC complex could **not** restore any Ca^{2+}-sensitivity. Each cTnI C-terminal deletion mutant bound to cTnC as shown by gel filtration and urea-PAGE analysis and co-sedimented with actin. These results indicate that in cardiac TnI, residues 152-188 (C-terminal to the inhibitory region) are required for full inhibitory activity and Ca^{2+}-sensitivity.

M-Pos197

STRUCTURAL ELEMENTS OF THE COOH-TERMINAL REGION OF TROPONIN-T INVOLVED IN THE REGULATION OF SKELETAL MUSCLE CONTRACTION

((Thomas Panavelil, Georgianna Guzman, Michelle Jones, [§]Bo-Sheng Pan, Danuta Szczesna and James D. Potter)) Dept. Mol. & Cell. Pharmacology, Univ. of Miami, School of Medicine, Miami FL 33136; [§]Merck Research Laboratories, West Point PA 19486.

The COOH-terminus of TnT is expressed as two isoforms, α and β, by a mutually exclusive splicing of the two 3' mini exons of the gene. We have shown previously (Pan & Potter, *J.Biol.Chem.*, 267, 1992) that the type of Ca^{2+}-specific site dependent interaction between TnC and the COOH-terminus of TnT depends on which isoform (α or β) of TnT is present. In another study we also demonstrated (Potter *et al.*, *J. Biol.Chem.*, 270, 1995) the importance of this same Ca^{2+} dependent TnC·TnT interaction in the potentiation of actomyosin ATPase. Both results suggested that this TnC·TnT interaction is important in the Ca^{2+} regulation of contraction. In the present study, recombinant full length TnTs corresponding to the α and β isoforms and three COOH-terminal deletion mutants (δ_1, δ_2, δ_3) were used to displace troponin (T-I-C) complex from rabbit skeletal myofibrils (Shiraishi and Yamamoto, *J. Biochem.*, 115, 1994). TnT-treated (Tn-depleted) myofibrils were then reconstituted with the TnC·TnI complex. We found that the Ca^{2+} sensitivity of myofibrillar ATPase activity was gradually shifted towards higher [Ca^{2+}] following the incorporation of TnTα, TnTβ, or TnTδ_1 (lacking the α/β-region of variability), respectively. We also found that the degree of the ATPase activity potentiation was similar for TnTα and TnTβ, but lower for TnTδ_1. These results demonstrate that the COOH-terminus of TnT contains sequence elements that contribute to the Ca^{2+} sensitivity and potentiation of myofibrillar ATPase activity and play an important role in the Ca^{2+} regulation of skeletal muscle contraction.

M-Pos198

EFFECTS OF TROPONIN I (TnI) ON ACTIN S1 ATPASE AND S1 BINDING KINETICS IN THE ABSENCE AND PRESENCE OF RABBIT SKELETAL TROPOMYOSIN (Tm) AND TROPONIN (Tn).

((**S. S. Lehrer**, M. Chai, & M. A. Geeves)) Boston Biomedical Research Institute, Boston, MA & Max Planck Institute for Molecular Physiology, Dortmund, Germany.

Previous studies have indicated that TnI inhibits actin.S1 and actin.Tm S1 ATPase. To investigate this mechanism we monitored the TnI dependence of the S1 ATPase for actin, actin.Tm and actin.Tm.Tn ± Ca^{2+} at moderate levels of actin activation (5 μM actin, 2-9 μM S1, 1.1 μM Tm, 2 μM Tn in 36 mM NaCl, 6 mM $MgCl_2$, 3 mM ATP, 10 mM Hepes, pH 7.5, 25°). TnI inhibited the ATPase to S1 background levels for all filaments. The apparent K_I for TnI was 6.7 and 5.8 X 10^6 M^{-1} for actin.Tm and actin.Tm.Tn+Ca^{2+}respectively, and the binding stoichiometry, n, was 0.14 TnI/actin in both cases. For actin.Tm.Tn+Ca^{2+}, SDS gels showed that at saturation, extrinsic and intrinsic TnI, Tm, TnT and TnC were still bound to actin. For actin and actin.Tm.Tn-Ca^{2+}, K_I≈2 X 10^6 M^{-1} and n≈1 TnI/actin. The observed rate constant, k_{on}, of 5 μM pyrene-actin binding to 1 μM S1, was also dependent on TnI. k_{on} decreased 3X at saturating TnI for actin.Tm and actin.Tm.Tn+Ca^{2+} and on removing Ca^{2+} from actin.Tm.Tn. Partial saturation of actin and actin.Tm.Tn-Ca^{2+} with TnI also caused a decrease in k_{on}. These data indicate that: 1) TnI is sufficient to inhibit ATPase and S1 binding to actin.Tm. TnC and TnT are not necessary; 2) Ca^{2+} dissociates intrinsic TnI from an actin.Tm site but the TnI remains bound to actin.Tm.Tn, since extrinsic TnI binds without interference and without dissociation of TnC and TnT; 3) TnI inhibits actin.Tm and actin.Tm.Tn+Ca^{2+} S1 ATPase by both inhibiting the closed/open (off/on) Tm transition and the rate of binding of S1 with actin; 4) TnI inhibits actin S1 ATPase by inhibiting the S1 binding rate.

(Supported by NIH HL 22461 & NATO).

KINESIN

M-Pos199

STATISTICAL KINETICS OF PROCESSIVE MECHANOENZYMES

((**M.J. Schnitzer** and S.M. Block)) Princeton University, Princeton, NJ 08544.

Motility studies of individual processive motor proteins, such as kinesin, afford a novel approach to biochemical kinetics. In traditional kinetic studies, reaction rates are determined from bulk measurements of proteins in solution, and fluctuations in rates chiefly reflect sources of instrumental or other noise. In contrast, fluctuations in single-molecule rates directly reflect the underlying stochastic behavior of the enzyme. Fluctuation analysis of processive motors relies on the randomness parameter, *r*, a measure of the temporal irregularity in the enzyme pathway (Svoboda et al., *Proc. Nat. Acad. Sci. USA.* **91:** 11782, 1994). Measurements of *r* are robust: they are comparatively immune to thermal and instrumental noise, and can be performed even when individual enzymatic cycles are not discerned. The randomness parameter provides an estimate of the number of rate-limiting steps in the biochemical pathway, and can therefore be used to provide constraints on proposed mechanisms. Using published biochemical data and reaction pathways for kinesin, we predict *r* as a function of ATP concentration. We are also using optical trapping interferometry of beads driven by single molecules of kinesin (Svoboda et al., *Nature* **365**: 721, 1993) to determine *r* as a function of ATP concentration. Such determinations address important questions about mechanochemical coupling, such as how many ATP molecules are hydrolyzed for a given advance along the substrate.

M-Pos200

A SPECTROSCOPIC PROBE ON A MICROTUBULE MOTOR PROTEIN.

((**N. Naber**, E. Pate, and R. Cook.)) Dept. of Biochemistry, & Biophysics, Cardiovascular Research Institute, University of California, San Francisco, CA 94143 and Dept. Math., WSU.

To investigate conformational changes in the motor protein, ncd, we have attached an MSL-ESR probe to Cys-670 of the ncd motor domain. Spin labeling is highly specific; >95% of the label is at Cys-670. Reaction with a 1:1 MSL-ncd labeling ratio goes to completion in < 3 min., 0°C. Labeling does not affect ncd function as monitored by either the microtubule activated, ncd ATPase or the binding to microtubules. The probe is partially imobilized with respect to ncd in the absence of microtubules. Binding to microtubules results in a significant increase in the fraction of immobilized probes. Superposition of the motor domain, crystal structures of ncd and myosin subfragment-1 reveals that the labeled cysteine is in a region which corresponds to the helix containing the two reactive sulphydrals in myosin, and is ~10 Å from the junction of the ncd neck and the ncd motor domain. We conclude that the binding of ncd to microtubules results in a conformational change near the motor domain - neck junction and may be involved in the working powerstroke. This is clearly different from myosin, where EPR probes on the reactive sulphydrals have failed to detect any conformational change in myosin upon binding to actin. This is the first successful attempt to employ EPR spectroscopy to monitor conformational changes in a non-myosin, motor protein. (Supported by HL32145 and a grant from the MDA)

M-Pos201

THEORETICAL FORMALISM FOR SINGLE KINESIN MOTILITY

((Yi-der Chen)) NIDDK, NIH, Bethesda, MD 20892-0520

Single kinesin molecules have been shown to be able to move submacroscopic particles (latex beads) unidirectionally on microtubules using the free energy of ATP hydrolysis. Exactly how the chemical free energy of the hydrolysis reaction is converted into mechanical energy in kinesin is not clear. Recently, we have shown (Phys. Rev. Lett. 77, 194 (1996)) that an enzymatic Brownian particle can use the free energy of the reaction it catalyzes to move unidirectionally on a periodic electric potential field, if the enzyme can oscillate between charged and uncharged states during the catalysis reaction. We showed that, although the model is not directly applicable to the kinesin-microtubule system where the existence of a periodic electric field on a microtubule is not very likely, the formalism or the theoretical calculation procedure can be extended to systems where the force and the movement are generated by the attachment and detachment of the motor (the so-called "cross-bridge" model). In this study, the application of the formalism to the calculation of movements of single-kinesin powered beads on a microtubule is discussed based on the biochemical kinetic information obtained in solution studies. Both one-head and two-head kinesin molecules are investigated.

M-Pos202

KINETIC STUDY OF THE MUTANT OF HUMAN KINESIN K560 G234A

((Y. Z. Ma and E. W. Taylor)) Dept. of Mol. Gen., University of Chicago, Chicago, IL 60637.

K560 G234A was prepared from E. Coli strain using plasmid provided by R. Vale. Gly234 is believed to interact with γ-phosphate of ATP (Kull et al. Nature 380: 550-555, 1996). We have compared the kinetic properties of the K560 G234A with wild type K560. The binding of mant-ATP and mant-ADP gave an increase in fluorescence which fitted a single exponential term while K560 gave an increase followed by a decrease phase. The apparent second order rate constants for nucleotide binding are similar to that for K560 but the maximum rate constants are two times larger for the mutant compared to wild type. The ATP hydrolysis step does not show a Pi burst. The rate of ATP hydrolysis is 0.002 s^{-1} and is activated to 0.038 s^{-1} by microtubules. The corresponding values for K560 are 8 s^{-1} and 70 s^{-1} respectively. The rate constant of mant-ADP release is about 1 s^{-1} in the absence of microtubules. Microtubules increase the rate constant of mant-ADP release to 6 s^{-1} for one head without changing the rate constant of mant-ADP release from the other head. K560 G234A binds to microtubules strongly and does not dissociate in the presence of ATP and ADP. The results indicate that Gly234 is critical for the hydrolysis of ATP, for transmission of the conformational changes between the nucleotide and microtubule binding sites and for the interaction of the two heads when bound to microtubules.

M-Pos203

Atomic Resolution Model of the Kinesin Power Stroke. ((W. Wriggers and K. Schulten)) Beckman Institute and Department of Physics, UIUC, Urbana, IL 61801.

The discovery and dispensation of the crystal structure of the kinesin motor domain [Kull et al., Nature 380:550 (1996)] has made it possible to study the mechanochemical coupling of this smallest known motor protein by computer simulations. Kull et al. crystallized the ADP-bound motor at pH 4.6. The structural ramifications of this low pH and the conformation of ATP-kinesin are not known. However, the structure of the head domain of the kinesin-like motor ncd, crystallized at pH 7 [Sablin et al., Nature 380:555 (1996)], and motility experiments of kinesin mutants (Fletterick and Vale, pers. comm.) permit a knowledge-based prediction of ADP- and ATP-kinesin structures at neutral pH. We have searched for candidate structures in conformational space using *simulated annealing* molecular dynamics simulation protocols. The resulting structures suggest a three-step scenario for the conversion of ATP hydrolysis into action: (1) a sensing mechanism for the additional gamma phosphate of ATP involving two "salt-bridge switches" (residues 96/231/190 and 199/203/236), followed by (2) an observed transfer of the conformational changes to the microtubule binding site, and, finally, (3) changes in protein-microtubule interactions which we project to result in a 10^{0}-rotation of the ATP-kinesin head relative to ADP-kinesin. We compare our model to recent low-resolution electronmicroscopy data which confirm a nucleotide-dependent orientation of the kinesin motor domain bound to a microtubule [Hirose et al., Nature 376:277 (1995)].

M-Pos204

MOTILITY OF SINGLE-HEADED KINESIN ((W.O. Hancock and J. Howard)) Dept. of Physiology and Biophysics, Box 357290, University of Washington, Seattle, WA 98195.

Kinesin molecules move for many microns along microtubules without dissociating. We hypothesize that this processive movement requires coordination between the two heads of the kinesin dimer. To test this hypothesis we have examined the motility of a single-headed kinesin heterodimer that retains the native rod and tail domains. The Drosophila kinesin heavy chain gene is co-expressed in bacteria with a decapitated gene that contains a C-terminal hexa-His tag. Single-headed heterodimers are purified by Ni column chromatography followed by sucrose density gradient centrifugation. Using the microtubule gliding assay, we observe two differences between single-headed and wild-type kinesin. First, at high motor density single-headed kinesin moves microtubules slower (0.12 (0.012 s.d.) μm/s) than the wild-type control (0.53 (0.10 s.d.) μm/s). Second, we observe a decrease in the rate at which microtubules land and move along the surface, a measurement of both microtubule affinity and processivity. Over a range of motor densities, single-headed kinesin requires a 10-fold greater surface density to achieve wild-type microtubule landing rates. These results demonstrate that single headed kinesin molecules are functional, but that coordination of the two heads of a kinesin dimer is likely essential for processivity and movement at wild-type speeds. Supported by MDA (W.O.H.) and NIH AR40593 (J.H.).

M-Pos205

KINETIC STUDIES OF MICROTUBULE-DIMERIC NCD ATPase. (E. Pechatnikova and E.W. Taylor). University of Chicago, Chicago, IL. 60637.

Kinetic mechanism of microtubule-dimeric ncd (Mt-MC1) complex were studied. The MC1 motor domain, residues 209-700, was prepared from BL21(DE3) cells using plasmid pGEX, provided by Y.Y. Toyoshima. The protein is dimeric, based on gel filtration and equilibrium ultracentrifugation. Bound nucleotide was removed from Mt-MC1 complex by the treatment with apyrase. The apparent second order rate constants for mantATP and mantADP binding (k^a), the maximum rate of the binding step, the phosphate burst and the rate of mantADP dissociation for the reaction of MC1-mantADP complex with Mt were measured (24°C). The maximum steady-state rate is 1±0.2 s^{-1}.

Substrate	k^a $M^{-1}s^{-1}$	Maximum rate (s^{-1})	Burst (s^{-1})	ADP dissociation by Mt (s^{-1})
mantATP	$2x10^6$	110	23-27	
mantADP	$0.2x10^6$	600		1.4 (+ATP)

The rate of ADP release from MC1 in the absence of microtubules is 0.001 s^{-1}, which is three times faster than from the ncd monomer. Microtubules at saturating concentration released only 30% to 40% of bound mantADP from MC1 with the rate of 2 s^{-1}; the rate of mantADP release from the second head of MC1 by ATP is equal 0.6 s^{-1}. The binding of MC1 to microtubules in the presence of ADP is strong (K^d Mt-MC1 [ADP]=1.75 μM (Mt)). The rate constant for ADP release, mantATP binding and the steady-state maximum rate are approximately 3 to 4 times smaller, compared to monomer, while the rate of mantADP binding is three times larger.

M-Pos206

STRUCTURE/FUNCTION ANALYSIS OF KINESIN IN DROSOPHILA.
((K. Stupka, D. Rose, and W.M. Saxton)) Department of Biology, Indiana University, Bloomington, IN 47405.

Kinesin is a motor protein that translocates along microtubules utilizing energy generated by ATP hydrolysis. To understand how kinesin heavy chain (KHC) interacts with microtubules, we are taking a combined genetic, molecular, and biochemical approach in *Drosophila*. We have generated 40 *Khc* mutations that affect the function of kinesin in vivo, causing lethality when combined with a *Khc* deficiency. The relative severities of these mutations have been determined based on the timing of lethality during development. Sequence analysis has thus far identified 3 nonsense and 10 missense mutations in the mechanochemical head domain, 2 nonsense and 1 missense mutation in coil two of the stalk, and 1 missense mutation in the tail. We are beginning to analyze the effects of some of the missense mutations on the behavior of the head domain in vitro. Two mutations lying in a portion of KHC thought to interact with microtubules have been cloned into a bacterial expression system for in vitro biochemical analysis. One mutation, which causes a severe in vivo phenotype, changes an amino acid that is identical in all members of the kinesin superfamily. The other mutation, which causes a relatively mild phenotype, changes an amino acid that is identical in 1/3 of the members of the kinesin superfamily. We hope to present the results of in vitro biochemical tests of the mutant proteins. (K.S. is supported by the American Heart Association, Indiana Affiliate)

M-Pos207

LOAD-DEPENDENCE OF KINESIN'S BEHAVIOR IN THE FORCE FIELD OF AN OPTICAL TRAP ((C. M. Coppin and R. D. Vale)) Howard Hughes Medical Institute, University of California, San Francisco, CA. 94143

The motility of kinesin and its affinity for microtubules is known to be influenced by the exertion of an external load. The motor stalls and eventually dissociates from its microtubule under an opposing load of ~5 pN (Hunt et al., 1994; Meyhöfer and Howard, 1995; Svoboda and Block, 1994). However, while moving away from the center of an optical trap (which functions as a spring) kinesin frequently dissociates before reaching the stall load. This behavior was investigated with an in vitro motility assay using a high-resolution optical trapping microscope (Coppin et al., 1996). The mean pre-stall dissociation load initially increases steeply as a function of trap stiffness and then abruptly levels off above a critical stiffness of ~0.03 pN/nm. This behavior is consistent with the results of Monte Carlo simulations based on a model incorporating a short-lived dissociable state in which both heads are weakly bound. In this minimal model, the load-dependence of the dissociation rate is due to the distortion of the binding potential energy by the presence of the parabolic potential energy of the trap. The behavior of kinesin under a "pushing" (microtubule plus-end directed) load was also investigated by repositioning the center of the trap in front of the motor as soon as it started walking. The motor continued to walk forward stepwise and underwent occasional dissociations, exhibiting a behavior similar to that observed under a minus-end directed load. However, no stalling was observed, even under loads exceeding 5 pN. A force-velocity curve for plus-end directed loads is in preparation.

Coppin et al. (1996). *Proc. Natl. Acad. Sci. (USA)* 93, 1913-1917.
Hunt et al. (1994). *Biophys. J.* 67, 766-781.
Meyhöfer, E., and Howard, J. (1995). *Proc. Natl. Acad. Sci. USA* 92, 574-578.
Svoboda, K., and Block, S. M. (1994). *Cell* 77, 773-784.

M-Pos208

ALTERNATING SITE COOPERATIVITY LEADS TO PROCESSIVITY OF DIMERIC KINESIN ((M.L. Moyer[1], S.P. Gilbert[2], and K.A. Johnson[1])) Biochemistry & Molecular Biology[1], Pennsylvania State University, University Park, PA 16802 and Biological Sciences[2], University of Pittsburgh, Pittsburgh, PA 15260.

The observation that single molecules of kinesin can move several micrometers along a microtubule (MT) has lead to the designation of kinesin as a processive enzyme. Previous studies have defined the mechanistic basis of this phenomenon and show that processive ATP hydrolysis is established in part by ordered release of the kinesin motor domains from the MT followed by immediate and rapid rebinding of kinesin to the MT (Gilbert *et al.*, 1995 *Nature* 373,671). Recent stopped-flow studies have focused on the binding kinetics of dimeric K401 and monomeric K341 to the MT. The results show that binding of the two heads of K401 to the MT leads to biphasic ADP release. Evidence for alternating site cooperativity is presented whereby ATP binding to one kinesin site stimulates the release of ADP from the second site. Results of studies of ATP binding to K401 and the MT-K401 complex are consistent with coordination of the ATPase cycles. It is the coordination of the ATPase cycles of dimeric kinesin that establishes the interactions of the motor domains with the MT resulting in processive translocation. Supported by NIH GM 26726 to KAJ, U. of Pitt. to SPG, NIH Predoctoral Fellowship to MLM.

M-Pos209

COOPERATIVE BINDING OF KINESIN MOLECULES TO A MICROTUBULE IN THE PRESENCE OF ATP ((Etsuko Muto[1] and Toshio Yanagida[2])) [1]Yanagida Biomotron Project, ERATO, JST and [2]Dept. of Biophys. Engineering, Osaka University, Osaka, Japan. (Spon. By K. Hirose)

To examine whether kinesin molecules bind cooperatively to a microtubule, we have measured the binding of kinesin-coated fluorescent beads (0.2 μm in diameter) to a microtubule (15-20 μm) in the presence of ATP under an optical microscope. The binding occurred preferentially in the vicinity of a kinesin-bead which had been already moving along the microtubule. The rate of binding was approximately 2 beads/μm microtubule/min in the vicinity of the moving bead (within $\pm$2.5 μm range). This was significantly larger than that outside of this area (0.7 beads/μm microtubule /min). This enhanced binding was independent of the position of the microtubule. When a kinesin-coated bead occasionally stuck on the microtubule, similar enhanced binding was observed in the vicinity of the stuck bead. Our results, therefore, showed that the affinity of kinesin for a microtubule was higher in the vicinity of a moving/stuck bead. This implies that kinesin binding makes a kind of active field in the long range of a microtubule to increase its affinity for other kinesin.

M-Pos210

DETACHMENT OF SINGLE KINESIN MOLECULES FROM MICROTUBULES INDUCED BY THE PHOTOLYSIS OF CAGED ADP. ((H. Higuchi and T. Yanagida)) Biomotron project, ERATO, JST and Dept. Biophys. Engineering, Osaka, Japan.

To relate the transients of force and displacement by single kinesin molecules with the elementary steps of the ATPase cycle, recently we determined the rate constant of ATP binding and the rate of force generation of single kinesin molecules using laser trapping nanometry combined with laser photolysis of caged ATP (Higuchi et al. 1996). Here, we determined the detachment rate of single kinesin molecules from microtubules after photolysis of caged ADP. Single kinesin molecules bound to beads were brought into contact with microtubules in the presence of caged ADP but no ATP (rigor), and were stretched to produce the passive force of 2-8 pN. Kinesins detached from microtubules at various time lags after the photorelease of 0.1 mM ADP. Time lags at a histogram fitted a single exponential curve with a decay time of ~200 ms, indicating that the detachment occurred by a single step reaction with the rate constant of ~5 /s. These results suggest that either head of a kinesin which binds to microtubule in rigor detached from a microtubule by a single step reaction or the two heads detached cooperatively from it.

M-Pos211

MOVEMENTS OF TRUNCATED KINESIN FRAGMENTS WITH A SHORT OR AN ARTIFICIAL FLEXIBLE NECK.

(**Yuichi Inoue**[#], Sayuri Morimoto[*], Atsuko Iwane[#], Yoko Y.Toyoshima[§], Hideo Higuchi[*] and Toshio Yanagida[#§*]) [#]Dept. Biophys & Engineering, Osaka Univ, Osaka. [§]Medical School, Osaka Univ, Osaka. [§]Dept. Life Science,Tokyo Univ, Tokyo. [*]Yanagida Biomotron project, ERATO, JRDC, Osaka, Japan.

To investigate the role of the neck domain of kinesin, we performed high resolution measurements of the movements and forces produced by kinesin fragments that have different neck domains by using optical trapping nanometry. We made four types of recombinant fragments of *Drosophila* kinesin with different neck sizes(K340, K351 and K411) and with a short neck consisting of artificial 11 amino acids sequence,-Leu-Gly-Pro-Gly-Gly-Gly-His-Arg-Lys-Cys-Phe, that would form a flexible chain (K340-chain).

Truncated kinesin fragments with a short neck of ~ 11 a.a.(K351) showed rapid movement (800 nm/s) and 8 nm steps as well as recombinant fragments with the full length of neck domain (K411) and native kinesins. Kinesin fragments lacking this region (K340), however, showed very slow movements (< 50 nm/s), suggesting the importance of the neck domain of 341 - 351 a.a.. Replacement of the short neck domain by an artificial 11 amino acid sequence that was expected to form a flexible random chain(K340-chain) recovered the normal fast (> 700 nm/s) and stepwise movements. Thus, the results suggest that the neck domain acts as a flexible joint rather than as a rigid lever arm as have been believed in the case of myosin.

MEMBRANE TRANSPORT - Na/Ca EXCHANGE

M-Pos212

THE ENDOGENOUS XIP REGION REGULATES THE CARDIAC Na^+-Ca^{2+} EXCHANGER (NCX1). ((S. **Matsuoka**[1], D.A. Nicoll[2], Z. He[2] and K.D. Philipson[2])) Dept. Physiol., Kyoto University, Kyoto 606-01, Japan[1] and Cardiovascular Research Laboratories, UCLA, LA, CA 90095[2].

The cardiac sarcolemmal Na^+-Ca^{2+} exchanger is modulated by two interacting regulatory mechanisms, Na^+-dependent inactivation and activation by Ca^{2+}. A segment of the exchanger, the endogenous XIP region, has been proposed to be involved in regulation, as a peptide with the sequence of this region potently inhibits exchange activity. To test this hypothesis, nine XIP region mutants were expressed in *Xenopus* oocytes, and studied by inside-out giant membrane patches. In the wild type, the outward Na^+-Ca^{2+} exchange current is initiated by bath (intracellular) application of Na^+ but then partially decays (Na^+-dependent inactivation). XIP-region mutants were grouped in two phenotypes. The inactivation was accelerated in group 1, and completely eliminated in group 2. Cytoplasmic Ca^{2+} (0.1~10 μM) augmented the outward current and suppressed the Na^+-dependent inactivation in both the wild type and group 1 XIP-region mutants. However, the apparent affinity of the group 1 XIP-region mutants for regulatory Ca^{2+} was decreased. The outward current of both group 1 and 2 XIP-region mutants responded to removal and to reapplication of 1 μM Ca^{2+} with a significantly reduced half-time compared to the wild type. We conclude that the endogenous XIP region is important in regulation of the exchange function through both the Na^+-dependent inactivation and Ca^{2+} activation.

M-Pos213

TEMPERATURE DEPENDENCE OF MYOCARDIAL CA EXCHANGE. ((**F.D. Marengo**, S.Y. Wang & G.A. Langer)) Cardiovascular Research Labs, UCLA School of Medicine, Los Angeles, CA 90024-1760.

Cellular Ca content and distribution is regulated by various systems -i.e. sarcoplasmic reticulum Ca ATPase, sarcolemmal Na/Ca exchange (NaxCa) and mitochondria. These systems are critically dependent on temperature. The purpose of this work is to study the effect of temperature on cellular Ca compartmentation and its exchange characteristics in intact functional neonatal cultured myocytes. The NaxCa mediated Ca exchange (Ca_{NaxCa}), including its sarcoplasmic reticulum (SR) and sarcolemmal (SL) contributions, is measured with isotopic and gas-dissection techniques for membrane isolation. Mitochondrial Ca and the La displaceable pool were studied with on-line isotopic technique. The major findings are: 1)The amount of Ca exchanged through Ca_{NaxCa} is dependent on temperature (Q10~1.6, between 17-37°C). 2)This dependency is explained by an increment in the contribution of SR-Ca to Ca_{NaxCa}. 3)A fraction of SR which does not exchange through Ca_{NaxCa} at low temperatures can be mobilized by caffeine. This caffeine sensitive fraction is reduced as temperature is increased and is no longer measurable as a separate entity at 37°C. 4)If we consider the data of items 2 and 3 together, SR content would be temperature dependent with a Q10=1.5. 5)A La displaceable pool, which represents over 66% of the total exchangeable Ca increases in the range of 22 to 33°C with a Q10 of 1.25 which is consistent with a distribution of 70% SL-bound and 30% SR-derived (Post and Langer, 1992a). 6)The rate constant for the mitochondrial Ca component increases by 60% from 22 to 37°C, but Ca content in this organelle is not modified over this temperature range. (Supported by NIH, Laubisch and Castera Funds)

M-Pos214

ANTISENSE KNOCK DOWN OF Na/Ca EXCHANGE ALTERS PHYSIOLOGICAL RESPONSES OF CULTURED ARTERIAL MYOCYTES. ((M.K. Slodzinski and M.P. Blaustein)) Physiol. Dept, U. of Md. Med. Sch., Baltimore, MD 21201

Antisense oligodeoxynucleotides (AS-oligos) targeted to the Na/Ca exchanger (NCX) inhibit Na_o-dependent (NCX-mediated) Ca^{2+} influx in primary cultured rat mesenteric artery myocytes (*AJP* 269:C1340, 1995). We now show AS-oligo knock down of NCX mediated Ca^{2+} efflux. Myocytes were cultured for 7 days with or without oligos. Digital imaging of fura-2 loaded cells was then used to measure the cytosolic free Ca^{2+} concentration ($[Ca^{2+}]_{cyt}$). Cells were superfused with Na_o,Ca-free media containing 0.25 mM $LaCl_3$ to block Ca^{2+} extrusion via the plasma membrane Ca^{2+} pump (PMCA). Caffeine (CAF) and cyclopiazonic acid (CPA) were added to raise $[Ca^{2+}]_{cyt}$ by unloading the SR. Restoring Na_o speeded the decline of $[Ca^{2+}]_{cyt}$ 70-fold in control cells (no oligos), and in scrambled (NS-) oligo and sense oligo treated cells, but only 7-fold in AS-oligo treated cells. AS-oligo knock down was reversed by incubating AS-oligo treated cells in normal media for 5 days: the Na_o-dependent fall in $[Ca^{2+}]_{cyt}$ in recovered cells was not different from controls. When La^{3+} was washed out, to reactivate the PMCA, in the presence of CPA and CAF and absence of external Na^+, the rate of $[Ca^{2+}]_{cyt}$ decline was greatly speeded up in AS-oligo as well as NS-oligo treated cells and controls. Thus, AS oligos do not affect the PMCA. When serotonin (5-HT, in physiological solution) was applied repeatedly, at short (3 min) intervals, the peak of the Ca^{2+} transient declined with successive applications. This decline was significantly smaller in AS-oligo treated cells than in control and NS-oligo treated cells. Also, $[Ca^{2+}]_{cyt}$ recovery after the peak was slower in AS-oligo treated cells than in control and NS-oligo treated cells. When 5-HT was applied repeatedly in Na-free media, the responses of control and NS-oligo treated cells were similar to those of AS-oligo treated cells. These data show that selective knock down of NCX inhibits Na^+-dependent Ca^{2+} efflux as well as influx, and alters the responses of arterial myocytes to a physiological agonist. Clearly, NCX plays a physiological role in arterial myocyte Ca^{2+} homeostasis.

M-Pos215

GENISTEIN INHIBITS Na^+/Ca^{2+} EXCHANGE ACTIVITY OF CULTURED RAT CORTICAL NEURONS ((C. Wang, L. Yu, N. Davis, R.A. Colvin)) Neurobiological Program, Biological Sciences Department, Ohio University College of Osteopathic Medicine, Athens, OH 45701

Rat cortical neurons from E-18 rats were dissociated and plated on polyethyleneimene coated 6-well plates with addition of 10μM Ara-C to inhibit glial cell proliferation. Na^+/Ca^{2+} exchange was studied using cells cultured for 3 or 9 days. Neurons were incubated with sodium loading buffer (137mM NaCl, 1mM ouabain, 25μM nystatin, 2mM $MgCl_2$, 10mM HEPES) for 10 minutes on ice. Na^+/Ca^{2+} exchange was initiated by incubating Na^+ loaded neurons at 37°C with 137mM choline chloride, 0.1mM EGTA, 0.55mM $CaCO_3$, 10mM HEPES, and 0.83μCi/ml $^{45}Ca^{2+}$ ($[Ca^{2+}]_{free}$=257μM). The exchange was terminated by addition of 500mM $LaCl_3$ in HEPES buffer. Cellular Ca^{2+} content increased rapidly during the first minute of the reaction, and thereafter maintained a stable plateau. A nearly two fold increase in Ca^{2+} uptake was seen when comparing 3 day and 9 day cultures. Western blot analysis also showed a two fold increase in Na^+/Ca^{2+} exchanger (NCX1) protein levels as cells matured in culture. However, when mRNAs from cultured neurons were extracted and hybridized with probes for NCX1, NCX2 and NCX3 isoforms, there was no difference in steady state mRNA levels as the cells matured. To study the effect of genistein, a specific tyrosine kinase inhibitor, cells were incubated with 200μM genistein (in 1% DMSO) for 1 hour before the incubation with sodium loading buffer. There was a significant decrease of Ca^{2+} uptake in genistein treated neurons (control: 4.632±0.342 nmol/mg protein/15min, n=8; genistein: 2.674±0.178 nmol/mg protein/15min, n=9, mean±S.E. P<0.05). Daidzein, an inactive analog of genistein and phorbol myristate acetate (PMA), a PKC activator were without effect. The results suggest that as cells mature in culture, Na^+/Ca^{2+} exchange protein stability is increased, perhaps by post-translational modification or subcellular sequestration. Further, since genistein inhibits tyrosine kinase, a cytosolic and/or membranous protein tyrosine phosphatase may be responsible for dephosphorylation of proteins leading to the decrease in Na^+/Ca^{2+} exchange activity. This suggests that a tyrosine phosphatase inhibitor should block the effect of genistein.

M-Pos216

TRANSPORT AND REGULATION OF THE CARDIAC Na^+-Ca^{2+} EXCHANGER, NCX1: COMPARISON BETWEEN Ca^{2+} and Ba^{2+}. ((M. Trac, M. Hnatowich, A. Omelchenko, and L.V. Hryshko)) Inst. Cardiovasc. Sci., St. Boniface Gen. Hosp. Res. Ctr., Univ. Manitoba, Winnipeg, Canada, R2H 2A6.

The effects of substituting Ba^{2+} for Ca^{2+} were examined on transport and regulatory properties of the cloned cardiac Na^+-Ca^{2+} exchanger, NCX1, expressed in *Xenopus* oocytes. Inward and outward exchange currents were measured using the giant excised patch technique. For inward current measurements, substantial Na^+-Ca^{2+} exchange currents were observed, whereas Na^+-Ba^{2+} exchange currents were barely detectable. Similarly, outward currents were greatly reduced when pipettes contained Ba^{2+} rather than Ca^{2+}. These decreases in forward and reverse exchange current were not due to failure of Ba^{2+} to activate the exchanger at the high affinity regulatory Ca^{2+} binding site. Ba^{2+} is capable of activating Na^+-Ca^{2+} exchange current, albeit with lower affinity (K_D ~ 10 μM vs 0.3 μM for Ca^{2+}) and efficiency (50 % of Ca^{2+}-activated currents). Ba^{2+} was also much less efficient at alleviating Na_i^+-induced inactivation, compared to Ca^{2+}. Among the manifold consequences to cardiac muscle during Ba^{2+} replacement of Ca^{2+}, changes in exchange function alone would appear adequate to account for contractile failure. (Supported by grants from MRC and HSF.)

M-Pos217

INTERACTION OF NA-CA EXCHANGE INHIBITORY PEPTIDE (XIP) WITH ITS PUTATIVE PEPTIDE BINDING SITE PEPTIDE HOMOLOG. ((C.C. Hale, E.N. Peletskaya, S. Bliler, and T.P. Quinn)), Depts. of Vet. Biomedical Sciences and Biochemistry and the Dalton Cardiovascular Research Center, University of Missouri, Columbia, MO 65211. (Spon. by M.J. Rovetto)

The exchange inhibitory peptide (XIP; RRLLFYKYVYKRYRAGKQRG) corresponds to residues 219-238 of the cardiac sodium-calcium exchange (NCX) protein. Sequence analysis of XIP affinity column purified proteolyzed bovine cardiac sarcolemmal (SL) protein fragments identified a negatively charged region from cytoplasmic loop f (residues 444-455) as a potential XIP binding site. A peptide homologous to this region (IDDDIFEEDEN) binds XIP in a cross-linking/probe-transfer reaction using APDP (Pierce) while an equally negatively charged control peptide (GEDDDDDECGEE) homologous to NCX loop f residues 732-743, did not. In other studies, FITC-labeled XIP fluorescence was quenched by peptide IDDDIFEEDEN. Fluorescence titration data gave an estimated Kd ≈ 1 μM (low μM range) for the FITC-XIP/peptide IDDDIFEEDEN interaction. FITC-XIP titration with the control peptide GEDDDDDECGEE demonstrated nonspecific binding. The results suggest a specific interaction between XIP and the putative XIP binding site peptide homolog IDDDIFEEDEN. The nature of this interaction is unclear and remains a question for further research. (supported by AHA (CCH), AHA-Missouri Affiliate (CCH), and DOE DEFG02-93ER61661 (TPQ)).

M-Pos218

ANIONIC PLASMALOGENS STIMULATE CARDIAC SODIUM-CALCIUM EXCHANGE. ((C.C. Hale, E.G. Ebeling, and D.A. Ford)) Dept. Vet. Biomedical Sciences, Dalton Cardiovascular Research Center, University of Missouri, Columbia MO 65211 and Dept Biochemistry and Molecular Biology, St. Louis University, St. Louis, MO 63104.

While plasmalogens are the predominant phospholipid (PL) subtype in the cardiac myocyte sarcolemma (SL) membrane and primary degradation targets during ischemia, their physiological role and effect on transport proteins is not well understood. In the present study, we reconstituted sodium-calcium exchange (NCX) from bovine cardiac SL vesicles into proteoliposomes composed of plasmalogen and/or diacyl phospholipids subclasses. Reconstituted NCX activity was 10-fold higher in plasmalogen-containing proteoliposomes over diacyl-containing proteoliposomes. Moreover in mixed PL proteoliposomes, NCX activity increased as a function of the plasmalogen/diacyl composition ratio. Addition of the anionic PL phosphatidylserine, increased NCX activity regardless of the PL composition. The role anionic PL have on NCX activity was further evidenced in proteoliposomes composed entirely of plasmenylcholine or phosphatidylcholine both of which had relatively low NCX activity. Following treatment with phospholipase D (PLD), which generates the anionic phosphatidate-PL counterpart, these preparations were stimulated 7-fold and 2-fold respectively. We conclude that NCX activity is higher in the presence of plasmalogen PL over diacyl PL. While anionic PL stimulate NCX transport regardless of PL subtype, the greatest anion effect is in the presence of plasmalogens. (supported by the AHA (CCH), AHA-Missouri Affiliate (CCH), NIH 42665 (DAF), NIH 03316 (DAF).

M-Pos219

STRUCTURE-FUNCTION STUDIES OF Calx, THE Na^+-Ca^{2+} EXCHANGER FROM *DROSOPHILA*, REVEAL CONSERVATION OF REGULATORY SITES. ((C. Dyck, J. Buchko, M. Hnatowich, M. Trac, and L.V. Hryshko)) Inst. Cardiovasc. Sci., St. Boniface Gen. Hosp. Res. Ctr., Univ. Manitoba, Winnipeg, Canada, R2H 2A6.

Structure-function studies of NCX1 have identified protein regions involved in the Na_i^+ and Ca_i^{2+} regulatory processes. The high affinity Ca_i^{2+} binding site for Ca_i^{2+} regulation has been identified and the importance of the XIP region in Na_i^+ regulation has been demonstrated (Philipson et al., NYAS, 779:20-28, 1996). The generality of these findings for other exchangers has yet to be established. In this study, we have examined these putative regulatory regions in Calx, the Na^+-Ca^{2+} exchanger from *Drosophila*. Calx is inhibited by regulatory Ca^{2+}, unlike all previously characterized Na^+-Ca^{2+} exchangers. Analogous mutations in the high affinity regulatory Ca_i^{2+} binding site predictably alter the response to regulatory Ca_i^{2+}. Similarly, analogous mutations in the XIP region of Calx lead to an acceleration or elimination of the Na_i^+-induced inactivation mechanism. Thus, despite opposite responses to regulatory Ca^{2+}, both the Ca^{2+} binding site and XIP region serve similar functional roles. As the high affinity regulatory Ca_i^{2+} binding site and the XIP region show substantial similarity for all identified Na^+-Ca^{2+} exchangers (e.g. NCX1, NCX2, NCX3, Calx), these results imply that similar structure-function relations for these regions may also exist. (Supported by grants from MRC and HSF).

M-Pos220

Na^+-ALKALINE EARTH METAL EXCHANGE BY Calx, THE Na^+-Ca^{2+} EXCHANGER FROM *DROSOPHILA*: DETERMINATION OF KINETIC CHARACTERISTICS. ((**A. Omelchenko**, M. Trac, M. Hnatowich, and L.V. Hryshko)). Inst. Cardiovasc. Sci., St. Boniface Gen. Hosp. Res. Ctr., Univ. Manitoba, Winnipeg, Canada, R2H 2A6.

The ability of alkaline earth metals (Me^{2+}) to substitute for Ca^{2+} in Na^+-Ca^{2+} exchange has been investigated for Calx expressed in *Xenopus* oocytes. Outward currents from giant excised patches were measured under conditions where pipette Me^{2+} exchanges for cytoplasmic Na^+. To analyze and compare current characteristics between different patches, the general solution to the eight state consecutive exchange model has been modified by incorporating a Na_i^+-dependent inactivation step (Hilgemann et al. J Gen Physiol, 1992), as well as an assumption of non-instantaneous equilibria for ion binding. Theoretical analysis of the Na_i^+-dependent inactivation process enables kinetic information to be obtained and provides a satisfactory account for the observed experimental differences between Me^{2+}. Our results show a Me^{2+} rank order of $Ca^{2+} \approx Sr^{2+} > Ba^{2+}$ for: i) the current decay (during inactivation) rate constant, ii) the current recovery (from inactivation) rate constant, and iii) the half-maximal Na_i^+ concentration to produce peak currents. In contrast, the half-maximal Na_i^+ concentration to produce steady state currents was equal for Me^{2+}. The calculated ratio of maximal turnover rates (v) for Me^{2+} were $v_{Ca} : v_{Sr} : v_{Ba} : v_{Mg}$ = 8.5 : 8 : 1.8 : 1. (Supported by grants from MRC and HSF).

M-Pos221

CALCIUM INFLUX MEDIATED BY THE SODIUM-CALCIUM EXCHANGER IS INHIBITED BY CALYCULIN A. ((**M. Condrescu**, Y. Fang and J. P. Reeves)) Department of Physiology, UMDNJ-NJ Medical School, Newark, NJ 07103.

Calyculin A (CA; 100 nM), an inhibitor of protein phosphatases 1 and 2A, reduced Ca or Ba influx mediated by the expressed Na/Ca exchanger in transfected CHO cells that were loaded with Na by treatment with ouabain or gramicidin. Inhibition of exchange activity required 10 min of treatment with CA (IC_{50} 15 nM) and was partially alleviated by the presence of the protein kinase inhibitor K252a (1 μM). Okadaic acid (1 μM), a more selective inhibitor of protein phosphatase 2A, did not inhibit exchange activity. CA also inhibited Ca or Ba influx in cells expressing a mutant exchanger missing most of the exchanger's central hyrophilic domain. Remarkably, CA treatment did not inhibit Na-dependent Ca efflux. Treatment with CA (10 min), but not okadaic acid, produced a dramatic breakdown in the cytoskeletal filament systems for vimentin, actin and tubulin which was partially alleviated by K252a. Treatment with cytochalasin D or nocodazole disrupted the actin and tubulin networks, but neither agent, alone or in combination, mimicked the effects of CA. We speculatively suggest that the effects of CA on exchange activity are induced by hyperphosphorylation of intermediate filament proteins and a breakdown in intermediate filament integrity.

M-Pos222

HYPEROSMOLARITY STIMULATES SODIUM-CALCIUM EXCHANGE ACTIVITY IN TRANSFECTED CHO CELLS. ((**Y. Fang**, M. Condrescu and J. P. Reeves)) Department of Physiology, UMDNJ-NJ Medical School, Newark, NJ 07103.

Ba influx via the expressed Na/Ca exchanger was measured (fura-2) in transfected CHO cells treated with (a) ionomycin (0.3 μM) to deplete intracellular Ca stores and (b) gramicidin (1 μM) to equalize Na concentrations across the cell membrane. At 5 mM or 24 mM Na, Ba influx was stimulated by addition of 500 mM mannitol; mannitol had no effect on Ba influx in the absence of Na, or in vector-transfected control cells. Stimulation of exchange activity was observed at the earliest times examined after mannitol addition (10 s) but declined after 2 min. Mannitol increased $[Ca]_i$ slightly; pretreating cells with EGTA-AM abolished the increase in $[Ca]_i$ and reduced, but did not eliminate, the stimulation of Ba influx. Mannitol also accelerated exchange activity in cells expressing a deletion mutant of the exchanger missing most of the central hydrophilic domain, but the degree of stimulation was reduced compared to the wild-type exchanger. Stimulation of exchange activity by hyperosmolarity was not inhibited by treating cells with agents which disrupt the actin and tubulin filament systems (cytochalasin D, nocodazole), or by protein kinase inhibitors (K252a, genistein). We conclude that hyperosmolarity accelerates exchange activity, in part by increasing $[Ca]_i$ and in part by an unknown mechanism.

M-Pos223

REGULATION OF SODIUM-DEPENDENT BARIUM INFLUX BY CYTOSOLIC CALCIUM IN TRANSFECTED CHO CELLS EXPRESSING THE CARDIAC SODIUM-CALCIUM EXCHANGER ((Y. Fang and **J. P. Reeves**)) Department of Physiology, UMDNJ-NJ Medical School, Newark, NJ 07103

Transfected CHO cells expressing the bovine Na/Ca exchanger (CK1.4 cells) were loaded with fura-2 and pretreated under Ca-free conditions with (a) ionomycin (0.3 μM), to release Ca from intracellular stores, and (b) gramicidin (1 μM), to equalize Na concentrations across the plasma membrane. Under these conditions, Ba influx was completely dependent upon the presence of Na and was therefore mediated by the Na/Ca exchanger; Ba influx in vector-transfected control cells was negligible and was unaffected by Na. Introducing EGTA into the cytosol by pretreating the cells under Ca-free conditions with 50 μM EGTA-AM for 3 min after fura-2 loading reduced cytosolic $[Ca]$ from 50 nM to near zero levels. This treatment inhibited, but did not completely block, Na-dependent Ba influx in cells expressing the wild-type exchanger. In cells expressing a Ca-insensitive deletion mutant of the exchanger, EGTA loading did not inhibit Na-dependent Ba influx. Preincubating CK1.4 cells with 0.1-0.3 mM $CaCl_2$ increased $[Ca]_i$ to 50-150 nM and accelerated Na-dependent Ba influx in proportion to the increase in $[Ca]_i$. We conclude that Na/Ca exchange activity under these conditions is partially independent of $[Ca]_i$ and can be further activated at low $[Ca]_i$ values.

M-Pos224

PKA REGULATION OF SODIUM-CALCIUM EXCHANGER ACTIVITY ON DIFFERENT NCX1 SPLICED ISOFORMS. ((**S.He**, A.Ruknudin, S.Luo, D.H.Schulze)) Department of Microbiology and Immunology. University of Maryland at Baltimore, Baltimore,MD 21201

Na^+/Ca^{2+} exchanger, NCX1, is an important membrane protein that regulates intracellular calcium level, and has been shown to undergo alternative splicing in the C-terminus of the intracellular loop of the protein. We previously demonstrated that splicing of NCX1 was achieved by using six exons (A to F) in which A and B are mutually exclusive, and the rest (C to F) are cassette-type exons which are expressed in a tissue restricted manner. For example, neuron and astrocyte, two main cell types in rat brain, have preference for NCX1 isoform utilization. Neurons predominantly express A isoforms (AD and ADF) while astrocytes predominantly express B isoforms (BDEF, BDF and BD). We cloned the full length rat NCX1 and engineered different isoforms using restriction enzyme sites: ACDEF, BD, and alternative splicing regionless (no ACDEF, named as ASRL). Same amount of in vitro synthesized cRNA of different isoforms was injected into Xenopus oocytes and Na-dependent Ca^{45} influx was measured to study the Na^+/Ca^{2+} exchanger activity while all three isoforms showed similar Ca^{45} influx activity. Since this alternatively spliced region contains potential PKA substrate motifs, we studied the activation of PKA on Ca^{45} influx. Surprisingly, PKA activation in Xenopus oocytes upregulates ACDEF by 30-50% and does not affect BD or ASRL. The specific effect of PKA activation on ACDEF can be blocked by preincubating Xenopus oocytes with KT5720, a specific PKA inhibitor. We conclude that PKA activation can upregulate calcium transport activity of the cardiac NCX1 isoform (ACDEF) in a unique manner that differs from the other isoforms studied.

M-Pos225

DELETION OF THE ALTERNATIVELY SPLICED REGION OF THE Na^+/Ca^{2+} EXCHANGER, NCX1, REDUCES FUNCTIONAL ACTIVITY. ((**S.Luo**[1], C.F.Neubauer[1], A.Ruknudin[1,2], S.He[1], W.J.Lederer[2,3], D.H.Schulze[1])) University of Maryland, Departments of Microbiology and Immunology[1], Physiology[2],Biophysics and Molecular Biology[3], Baltimore, MD 21201

The Na^+/Ca^{2+} exchanger, (NCX1), which regulates the level of intracellular Ca^{2+} particularly in heart cells, is present at different levels in most tissues. The Na^+/Ca^{2+} exchanger protein differs in structure in various tissues in a restricted region of the intracellular loop and these differences depend on the splicing of 6 germline encoded exons. Others have demonstrated that when most of the intracellular loop is removed, little change in the amount of exchange function is noted but the regulation by intracellular ions is lost. To further investigate the alternatively spliced region (ASR) of NCX1, we studied both the human cardiac isoform (exons ACDEF) and a deletion mutant lacking the ASR. Both of these constructs contain a VSV epitope-tag onto the C terminus of the open reading frame. These two constructs were transfected in the mammalian cell lines (HeLa and NIH3T3 cells) and function was analyzed using Ca^{2+} imaging of single cells using confocal microscopy. Transfected cells were loaded with the Ca^{2+} indicator, Fluo-3, and increase in $[Ca^{2+}]_i$ was used as a measure of Na^+/Ca^{2+} exchange function when external Na^+ was changed. The amount of increase in $[Ca^{2+}]_i$ measured was dependent on the Na^+ gradient and was blocked by Ni^{2+} We noticed repeatedly, cells expressing exchanger without the ASR demonstrated nearly a 50% decrease in the levels of Na^+/Ca^{2+} exchanger activity. To further study this phenomenon, we transfected 293HEK cells with either the cardiac isoform of the human Na^+/Ca^{2+} exchanger or the ASR deletion construct and studied $^{45}Ca^{2+}$ flux. We show that Ca influx in the ASR deletion construct transfected into 293HEK cells show a 25-30% decrease in Na-dependent Ca flux when compared to the cardiac isoform. These data were normalized to the total amount of transfected exchanger protein using the VSV epitope-tag. These results suggest that the alternatively spliced region may play a critical role in the normal functioning of the Na^+/Ca^{2+} exchanger.

M-Pos226

POSSIBLE DIRECT REGULATION OF CARDIAC Na,Ca EXCHANGE BY PIP_2.
((D.W. Hilgemann[a], S.Feng[a], K.D. Philipson [#], D.A. Nicoll[#], J.P. Reeves[+], and M. Condrescu[+])), Depts. of Physiology; [a]UTSW,Dallas, TX, 75235; [+] UMDNJ, Newark, NJ, 07103; [#] UCLA, Los Angeles, CA. 90095.

Activation of cardiac Na,Ca exchange by cytoplasmic ATP may reflect the production of PIP_2 (Hilgemann & Ball, Science 273,956,1996). As new evidence, PIP2 antibodies reverse rapidly the stimulatory effect of ATP in giant cardiac membrane patches. Normal reversal of the ATP effect, thought to reflect PLC activity, is greatly accelerated by certain hydrophobic agents (e.g. 1 mM extracellular valproic acid) which can mimic effects of membrane stretch (not tolerated by giant patches) on stretch-activated ion channels. With such agents, or high $[Ca^{2+}]_i$, the stimulatory effect of ATP is transitory and usually cannot be repeated, suggesting depletion of phosphatidylinositols from the membrane. ATP effects are obtained only rarely in NCX1-expressing Xenopus oocyte patches, although exchange current is strongly activated by PIP_2. In contrast, large stimulatory effects of ATP are obtained in patches from BHK cells stably transfected with NCX1 (exchange current densities; >5-fold greater than cardiac patches). Mutation studies suggest that the autoinhibitory 'XIP' exchanger domain could be a PIP2 receptor; deletion of positively charged amino acids in the XIP region, and their substitution for alanine, alters regulatory properties of the exchanger and its sensitivity to ATP and PIP_2.

M-Pos227

FUNCTIONAL COMPARISON OF THREE DIFFERENT ISOFORMS OF THE SODIUM-CALCIUM EXCHANGER (NCX1, NCX2, NCX3).
((**B. Linck**, Z. Qiu, D.W. Hilgemann, K.D. Philipson))
UCLA, Los Angeles, CA 90095-1760. (Spons. by K.D. Philipson)

The Na^+-Ca^{2+}-exchanger (NCX) is an integral membrane protein of the sarcolemma, which regulates intracellular Ca^{2+} levels. The cardiac isoform (NCX1) is well characterized, whereas less is known about the recently cloned isoforms NCX2 and NCX3. To test whether the exchanger isoforms have different functional characteristics, we studied the Na^+_i-dependent $^{45}Ca^{2+}$ uptake in BHK cells stably transfected with either NCX1, NCX2 or NCX3 and in membrane vesicles prepared from transfected cells. We also measured outward exchange currents in giant (half-cell) membrane patches from transfected cells. In cells, the Ca_o^{2+} dependency of $^{45}Ca^{2+}$ uptake gave Vmax values of 20, 16 and 18 nmol/mg prot/min and Km values of 280, 350 and 360 µM for NCX1, NCX2, and NCX3, respectively. Na^+_o inhibited Ca^{2+} uptake with $K_{1/2}$ values of about 14 mM (NCX1), 11 mM (NCX2) and 15 mM (NCX3). In membrane vesicles, the responses to extravesicular Ca^{2+} and Na^+ were similar for NCX1, NCX2, and NCX3 with a Ca^{2+} affinity at the intracellular surface of about 12 µM and a $K_{1/2}$ for inhibition by external Na^+ of 8 mM. Furthermore, the responses to valinomycin, chymotrypsin, XIP and pH were comparable in NCX1, NCX2 and NCX3. In giant patches, results for NCX1 were indistinguishable from results with cardiac myocytes, including stimulatory effects of ATP. Previously described features of NCX2 were verified (e.g., decreased inactivation), and no striking functional differences between NCX1 and NCX3 were noted. Thus, in general, NCX1, NCX2, and NCX3 have similar kinetic properties.

M-Pos228

THE ACTIVITY OF RETINAL NA:CA,K EXCHANGER EXPRESSED IN 293 CELLS
((A. Navangione*, N.Gabellini*, E. Carafoli* and G. Rispoli*))
*Dipartimento di Biologia, Sez. Fisiologia Generale, Via Borsari 46, Ferrara, Italy 44100, *Dipartimento di Biochimica, via Trieste 75, Padova, Italy 35121.

The retinal Na:Ca,K exchanger cDNA (Reiländer et al., EMBO J., 11, 1689-1695, 1992) was transiently expressed in HEK293 cell by transfection with plasmid DNA co-precipitated with Ca-phosphate. The correct targeting of the expressed protein to the plasma membrane was confirmed by immunocytochemistry. The activity of the expressed exchanger was assessed by whole cell voltage clamp recording. It was not possible to record the forward exchange mode, since the intracellular Ca concentration (Ca_i) necessary to promote an appreciable forward current was lethal to the cell. The reverse exchange current (12 ± 2 pA) was measured upon intracellular perfusion with Na (153 mM) and bathing the cell in Ca (Ca_o, 1 mM) and K_o (20 mM). As expected, the exchange current was abolished by removing Ca_o or by increasing Na_o to null the Na gradient. Surprisingly, the exchange current was almost unaffected by the removal of K_o. This result was at variance with the large decrease in exchange activity (72%) observed with the exchanger reconstituted in lipid vesicles (Reiländer et al., 1992), when increasing K_o (from 25 to 100 mM) in the presence of 50 mM Na_o, 50 mM K_i and 4 mM Ca_i. However, such a large activity decrease was not expected theoretically under the above conditions. In fact, only a 40% exchange current decrease was observed in isolated rod outer segments upon increasing K^+_o from 0 to 120 mM. The difference in K sensitivity between the exchanger expressed in 293 cells and that in the retina might be due to the incorrect folding, or post-transcriptional modification of the expressed protein or to the requirement of an accessory protein that could be present in the rod outer segment.

M-Pos229

A NOVEL 13 kD CYTOPLASMIC SOLUBLE PROTEIN IS REQUIRED FOR THE NUCLEOTIDE (MgATP) MODULATION OF THE Na/Ca EXCHANGE IN SQUID NERVE FIBERS.
((**R. DiPolo**[1,3] G. Berberian[2,3]. D. Delgado[1]. H. Rojas[1] and L. Beaugé[2,3])). IVIC, Caracas Venezuela[1]. Instituto M.y. M Ferreyra, Córdoba Argentina[2] and The Marine Biological Laboratory[3], Woods Hole MA. USA.

As it happens with some preparations, in squid axons nucleotide (MgATP) regulation of the Na/Ca exchange is lost after plasma membrane vesicle isolation. This has been a significant obstacle in the biochemical characterization of the MgATP effect. An important clue in solving this long standing puzzle is presented in this work by showing that prolonged intracellular dialysis of squid axons produces a complete run down of the MgATP effect. Here we report that a soluble cytoplasmic factor (SCF) isolated from fresh squid axoplasm and/or squid brain, reconstitutes the MgATP stimulation of the Na-gradient dependent ^{45}Ca uptake in squid optic nerve membrane vesicles. Partial purification of this factor uncovers the presence of a novel 13 kD soluble cytoplasmic protein (SCPr) which, when microinjected in ATP de-regulated dialyzed squid axons, completely restores the MgATP stimulation of Na_o-dependent Ca efflux. We propose that in the squid preparation this SCPr constitutes the link between the nucleotide and the target effector: the Na/Ca exchanger itself, or other plasma membrane structures which may secondarily interact with the exchanger. (Aided by Grants from NSF IBN9631107. CONICIT. S1-2651. CONICET BID-PID 1053.

M-Pos230

VOLTAGE-DEPENDENCE OF THE VARIOUS MODES OF EXCHANGE MEDIATED BY THE REGULATED AND DEREGULATED Na/Ca EXCHANGER IN MUSCLE CELLS.
((J. Tie, S. Ajaga, R. Espinosa-Tanguma, J. DeSantiago and H. Rasgado-Flores)). Dept. Physiology and Biophysics. FUHS/The Chicago Medical School. North Chicago Il 60064.

The Na/Ca exchanger plays an essential role in the physiology of muscle cells. This exchanger: 1) has a stoichiometry of $3Na^+$:1 Ca^{2+}; 2) can operate as Na/Ca, Ca/Ca or Na/Na modes of exchange; 3) requires intracellular Ca^{2+} (Ca_i) to operate in any of its modes; 5) is activated by intracellular ATP; and 4) when exposed to α-chymotrypsin, becomes de-regulated, i.e., its Ca_i-requirement and ATP activation are removed. Considerable controversy exists regarding the voltage-sensitivity of the various modes of exchange mediated by the Na/Ca exchanger. Clarification of this issue could be provided by measuring the ionic fluxes mediated by the exchanger under voltage-clamp conditions. Internally perfused barnacle muscle cells offer this opportunity. Using this preparation, we have found that: i) α-chymotrypsin treatment inverts the voltage sensitivity of the Ca/Ca mode of exchange, i.e., before the treatment, depolarization decreases Ca/Ca exchange while the converse is observed following the treatment; ii) Na/Na exchange is voltage-insensitive regardless if the exchanger is activated with α-chymotrypsin or Ca_i; iii) external Na^+ (Na_o)-dependent Ca^{2+} efflux is inhibited by depolarization when the exchanger is activated by Ca_i but it is insensitive to voltage when it is activated by the protease; and iv) external Ca^{2+} (Ca_o)-dependent Na^+ efflux is independent of voltage when the exchanger is activated with Ca_i but becomes promoted by depolarization when it is activated by α-chymotrypsin. To explain these results we postulate that the exchanger possesses three intrinsic negative charges, that ionic efflux translocation is rate-limiting, and that treatment with α-chymotrypsin removes this rate-limiting step. Thus, when the exchanger is activated by Ca_i and mediates Na^+ efflux (i.e., Na/Na exchange and Ca_o-dependent Na^+ efflux) the exchange is voltage-insensitive. However, when the exchanger is activated by Ca_i and mediates Ca^{2+} efflux (i.e., Ca/Ca exchange or Na_o-dependent Ca^{2+} efflux) depolarization inhibits the exchange. After α-chymotrypsin treatment the rate limiting step becomes the ionic translocation from the extracellular space to the intracellular space. Thus, Ca influx (i.e., Ca/Ca exchange or Ca_o-dependent Na^+ efflux) is activated by depolarization. On the other hand, when the exchanger mediates Na^+ influx (i.e., Na/Na exchange and Na_o-dependent Ca^{2+} efflux) the exchange is voltage-insensitive.

M-Pos231

CHARACTERIZATION OF RAT BRAIN NCKX2, A SECOND Na/Ca,K EXCHANGER.
((J. Lytton, M. Tsoi, K.-H. Rhee, D. Bungard and S.-L. Lee)) Department of Medical Biochemistry, University of Calgary, Calgary, Alberta, Canada, T2N 4N1.

We have recently described the cloning of a novel Na/Ca,K exchanger from rat brain (NCKX2). Transcripts for this molecule are about 11 kb in length and expressed almost exclusively in the brain. The protein encoded by this cDNA is 670 amino acids long with a molecular weight of about 75 kDa. NCKX2 is 45% identical overall to the Na/Ca,K exchanger from bovine retinal rods (NCKX1). Within the hydrophobic domains the identity is much higher (75%), although neither the amino-terminal extracellular loop nor the central cytosolic loop share much similarity. A "tag" for the FLAG epitope was introduced into the extracellular loop of NCKX2, and the resulting construct expressed transiently in HEK293 cells. Immunoblots show a doublet of bands at about 80 kDa suggesting post-translational processing via signal peptide cleavage and/or glycosylation. Immunofluorescent analysis of the transfected cells demonstrates strong labeling at the cell surface. The function of the expressed NCKX2 protein was assessed by digital imaging of fura-2 loaded transfected cells. A perfusion switch from normal saline buffer (containing 145 mM NaCl and 5 mM KCl) to a Na-free KCl buffer causes a large increase in $[Ca]_i$ which returns to baseline following a switch back to saline buffer. Switching to a Na-free LiCl buffer results in no change in $[Ca]_i$. A subsequent switch to a Na-free LiCl buffer containing 5 mM KCl results again in an increase in $[Ca]_i$. These data indicate that NCKX2 indeed encodes a K-dependent Na/Ca exchanger.

M-Pos232

DISTRIBUTION OF Na^+/Ca^{2+} EXCHANGER IN HYPERTOPHIC AND FAILING RAT CARDIAC MYOCYTES.

((K.W. Dilly[1,2], A.M. Gómez[1,2], C.F. Neubauer[1,2], D.H. Schulze[3], R. Altschuld[4] and W.J. Lederer[1,2])) Departments of [1]Physiology, [2]Molecular Biology & Biophysics, [3]Microbiology & Immunology. University of Maryland at Baltimore, Baltimore. MD. 21201. [4]Department of Medical Biochemistry,Ohio State University, Columbus, OH. 43210. USA.

Changes in the $[Ca^{2+}]_i$ transient in hypertrophic and failing hearts have been reported in human cardiac myocytes and animal models. Levels of Ca^{2+} ATPase (mRNA) are decreased in cardiac hypertrophy and failure (Arai et al. (1993) Circ. Res. 72:463-469, De la Bastie et al (1990). Circ. Res. 66:554-564). This is consistent with a reduction in sarcoplasmic reticulum (SR) Ca^{2+} uptake that is implied by the prolonged $[Ca^{2+}]_i$ transient.

We were interested in investigating whether any compensatory mechanisms arise in hypertrophied and failing heart cells that may affect the kinetics of the $[Ca^{2+}]_i$ transient. Since the Na^+/Ca^{2+} exchanger and the Ca^{2+} ATPase are the two major transport proteins responsible for the falling phase of the $[Ca^{2+}]_i$ transient, we examined the distribution of the Na^+/Ca^{2+} exchanger protein in these pathological cells. We used a laser scanning confocal microscope to examine the immunolocalisation of the Na^+/Ca^{2+} exchanger as well as other proteins associated with EC coupling. Cardiac myocytes isolated from hypertrophic, failing and age matched control rat hearts were examined. All cells examined revealed Na^+/Ca^{2+} exchanger distribution along the T-tubules (at the Z-lines), along the external sarcolemma membrane and at the intercalated disks (Kieval et al. (1992) Am.J.Physiol. 263 C545-550). Our early findings indicate that, compared to control cells, hypertrophic and failing myocytes show an increase in Na^+/Ca^{2+} exchanger at the external SL membrane. There is a gradient of increasing Na^+/Ca^{2+} exchanger along the T-tubules from the center of the cell towards the surface. In contrast, dihydropyridine and ryanodine receptors appear to remain more evenly distributed along the T-tubular membrane and on the SL surface. The increasing levels of Na^+/Ca^{2+} exchanger (as mRNA and protein) seen in failing human hearts (Studer et al. (1994) Circ. Res. 75:443-453) suggests that increased Na^+/Ca^{2+} exchanger on the surface of the cells we examined may reflect a net increase in total Na^+/Ca^{2+} protein rather than a simple re-distribution. The specific functional untility of the higher levels of Na^+/Ca^{2+} exchanger at the surface of the cardiac myocytes is being investigated.

M-Pos233

REGULATION OF Na-Ca EXCHANGER EXPRESSION IN VASCULAR SMOOTH MUSCLE

((X.-F. Li and J. Lytton)) Department of Medical Biochemistry, University of Calgary, Calgary, Alberta, Canada T2N 4N1 (Spon. by R.D. Loutzenhiser)

Previous work in our laboratory has demonstrated that NCX1 (the predominant Na-Ca exchanger gene) transcripts in rat brain (Br), heart (Ht) and kidney cortex (Kc) each contain unique sequences in the untranslated region at their 5' end. These regions have been mapped to three separate exons, and thus it appears expression of NCX1 is controlled by independent promoters in different tissues. In the present study, regulation of tissue-specific NCX1 transcript expression was examined in vascular smooth muscle cells by Northern blot analysis. Both Br- and Ht-containing transcripts are expressed in cultured rat aortic smooth muscle cells (RASMC), although the Br-type predominates. Cultured confluent RASMC were treated with 0.1% fetal bovine serum (FBS) for 24 hours, and then with 100 nM angiotensin II (Ang II), 15% FBS, 10 nM dexamethasone (Dex), 25 mM KCl, or 10 nM Dex plus 15% FBS. The level of Br-type transcript was increased by KCl, reduced by Dex and not affected by angiotensin II or FBS alone. FBS, however, reversed the Dex-induced reduction. The level of Ht-type transcript, on the other hand, was increased by Ang II or by Dex plus FBS, but was not affected by Dex, FBS or 25 mM KCl alone. Our data clearly indicate that NCX1 Ht- and Br-type transcripts are regulated differently. (Supported by HSFC to XFL, AHFMR and MRC to JL)

M-Pos234

SODIUM-CALCIUM EXCHANGE IN GUINEA-PIG, MARMOSET AND HUMAN CARDIAC CELLS

((A. R. Wright, S. A. Rees, S. E. Harding*, and T. Powell)) University Laboratory of Physiology, Parks Road, Oxford, UK. * NHLI, Imperial College, London, UK.

The guinea-pig is much used in cardiac cellular electrophysiology because of the similarity between its ventricular action potential and that of human. There are, however, significant differences in the expression and function of the underlying ion channels and transporters. We have investigated Na^+-Ca^{2+} exchange current ($I_{Na,Ca}$) in cardiac myocytes from guinea-pig, marmoset (*Callithrix jacchus*, a lesser primate) and human. Whole cell current was recorded using an external solution containing 72 mM Na^+ & 2 mM Ca^{2+}, and an internal solution containing 12.3 mM Na^+ and 300 nM free Ca^{2+}. A holding potential of -90 mV was used, and current was recorded during a voltage ramp. Exchanger slope conductance ($g_{Na,Ca}$) was measured in the 0 to -20 mV range. Membrane capacitance (C_M) was measured by integrating the transient current response to a voltage step. Recordings were made at 31-34°C.

Myocyte source	$g_{Na,Ca}$	$E_{Na,Ca}$	C_M	$g_{Na,Ca}/C_M$
Guinea-pig ventricle	4.2±0.6 nS (92)	-77±1 mV (92)	112±7 pF (25)	45±3 pS/pF (25)
Guinea-pig atrium	1.5±0.2 nS (17)	-76±3 mV (17)	32±2 pF (17)	45±4 pS/pF (17)
Marmoset ventricle	1.9±0.2 nS (16)	-73±2 mV (16)	115±9 pF (39)	19±4 pS/pF (14)*
Human ventricle	2.7±0.6 nS (12)	-78±3 mV (12)	246±33 pF (8)	11±3 pS/pF (8)*

*: $p<0.05$ vs. guinea-pig ventricle

$g_{Na,Ca}$ was greater in guinea-pig ventricular cells than in atrial cells, but the normalised exchanger conductance ($g_{Na,Ca}/C_M$) was not significantly different. In healthy adult marmoset ventricular cells, $g_{Na,Ca}/C_M$ was markedly smaller than in guinea-pig. Human ventricular cells from failing hearts had a larger C_M than guinea-pig or marmoset ventricular cells. Human $g_{Na,Ca}/C_M$ was significantly smaller than that of guinea-pig, but was not significantly different to that of marmoset. This raises the issues of whether $I_{Na,Ca}$ is generally smaller in primate cells than in guinea-pig, and of whether Na^+-Ca^{2+} exchange density in diseased human tissue might be similar to that in healthy tissue.

M-Pos235

PHENYLEPHRINE INCREASES SODIUM-CALCIUM EXCHANGE CURRENT IN RAT VENTRICULAR MYOCYTES.

((M. Stengl, K. Mubagwa, E. Carmeliet and W. Flameng)) CEHA, KU Leuven, Belgium

We have investigated the effect of the alpha-adrenergic agonist phenylephrine (PE) on the sodium-calcium exchange (NCX) current in rat ventricular myocytes. The NCX current was measured at 22°C as the whole-cell current induced by extracellular sodium, while blocking Ca^{2+} current by nifedipine, K^+ currents by extracellular Ba^{2+} and intracellular TEA, Na^+ current by a holding potential of -30 mV and sodium pump current by 0 extracellular K^+ or by ouabain. Either ramp or square voltage clamp pulses were employed. Under these experimental conditions, applying external Na^+ induced a current, which was further increased by PE. PE (80 µM) reversibly increased the current by up to 20-25% of control at all tested membrane potentials (e.g. from 0.18±0.047 to 0.22±0.056 pA/pF at -50 mV) both above and below the reversal potential. The reversal potential (+6.54±9.59 mV), which corresponded with the theoretical reversal potential calculated for NCX current under our ionic conditions (0 mV), was not changed in the presence of PE. The effect of PE was resistant to propranolol (3 µM). Applying PE, when Li^+ was substituted for Na^+, did not stimulate the current. Our data indicate that PE stimulates the NCX current in intact rat ventricular myocytes.

M-Pos236

LOCALIZATION OF A FUNCTIONALLY IMPORTANT RESIDUE (Asn 101) IN THE Na/Ca EXCHANGER

((D.A. Nicoll, A.E. Doering, J.N. Weiss and K.D. Philipson)) UCLA Cardiovascular Research Labs, Los Angeles, CA 90095.

A mutant of the cardiac Na/Ca exchanger was constructed with Cys replacing Asn at residue 101 (N101C), modeled to be at the cytoplasmic side of the membrane between transmembrane segments 1 and 2. Mutant Na/Ca exchange activity was characterized and the effects of various membrane-permeable and -impermeable sulfhydryl-modification reagents were measured to determine the location of N101 and what role it plays in exchanger function. The membrane permeable reagent NEM inhibits exchange activity (measured as ^{45}Ca uptake in oocytes expressing the mutant protein) by 91%. Iodoacetamide and iodoacetate do not affect exchanger activity directly; but iodoacetamide, which is membrane permeable, blocks the NEM effect while iodoacetate, which is membrane impermeable, does not. Membrane impermeable reagent MTSET does not affect mutant activity when applied extracellularly, but blocks activity 65% when injected into the oocyte. None of these reagents have any effect on wild-type exchanger activity. These data place N101 on the cytoplasmic side of the membrane. Na/Ca exchange current of N101C was measured under voltage clamp in the giant excised patch, and the inhibitory effect of NEM was confirmed. Inhibition was relieved or prevented (depending on the protocol) by 15 sec exposure to chymotrypsin. Interestingly, the mutant showed very little secondary regulation by cytoplasmic sodium and calcium, so N101 is important for these regulatory effects. Since the cytoplasmic loop of the Na/Ca exchange protein is essential for secondary regulation, we speculate that N101 may function as a binding site for a portion of the loop or may play an essential role in a conformational change involving the loop. Further investigation of the interaction of NEM with mutant N101C, the sensitivity of this interaction to chymotrypsin, and the relevance of these phenomena to the secondary regulatory effects of sodium and calcium is in progress.

M-Pos237

EVIDENCE FOR A ROLE OF Na^+-Ca^{2+} EXCHANGE CURRENTS IN BOTH FORWARD AND REVERSE MODES DURING THE ACTION POTENTIAL IN CANINE VENTRICULAR CELLS.

((G.R. Li, H. Sun and S. Nattel)) Montreal Heart Institute, Montreal, QC, Canada

Reverse-mode Na^+-Ca^{2+} exchange has been reported to play an important role in triggering SR Ca^{2+} release in cardiac cells. However, evidence is lacking for reverse-mode Na^+-Ca^{2+} exchange current ($I_{Na,Ca}$) detected during the AP. To evaluate this, cells were studied at 36 °C with whole-cell patch clamp technique. APs were recorded with current clamp mode. Membrane currents were recorded by voltage clamping with the AP recorded in control. $I_{Na,Ca}$ was defined by subtracting currents before and after $[Na^+]_o$ substitution by Li^+. We found that $I_{Na,Ca}$ was biphasic during the AP, with a transient early outward component followed by a long-lasting, gradually decaying inward component (Fig). The outward $I_{Na,Ca}$ peak was larger (389±157 pA) than inward component (-219±29 pA), while $I_{Na,Ca}$ was smaller for the outward (4.1±1.1 pC) than the inward component (-20.3± 3.2 pC, n=6). APD was reversibly reduced by 40.5±3.1% (n=5, $p<0.01$) after $[Na^+]_o$ replacement by Li^+. Our results provide the first evidence for outward $I_{Na,Ca}$ activated by reverse mode Na^+-Ca^{2+} exchange during the AP, while the inward $I_{Na,Ca}$ induced by the forward mode may play an important role in maintaining APD.

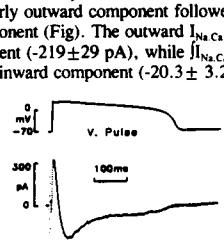

M-Pos238

ACTION POTENTIAL VOLTAGE CLAMP OF Na-Ca EXCHANGE CURRENT: AGE-DEPENDENT CHANGES IN RABBIT VENTRICLE.

((**P.S. Haddock**, M. Artman and W.A. Coetzee)) Departments of Pediatrics, Physiology and Neuroscience, NYU Medical Center, New York, NY 10016.

Previous studies, in which identical voltage clamp waveforms were used in different age groups, suggest enhanced Na-Ca exchange current (I_{NaCa}) in the newborn compared with the adult. However, the increase in action potential duration (APD) which occurs postnatally, may promote Ca^{2+} influx via the Na-Ca exchanger and thus compensate for the postnatal decline in Na-Ca exchange expression in the mature heart. To examine this possibility, we measured I_{NaCa} in rabbit myocytes from different age groups, with age-appropriate action potentials (AP) as command waveforms. APs were recorded at 34°C using the perforated-patch technique from ventricular myocytes isolated from the hearts of newborn (1-8 day) and adult rabbits. APD_{90} increased from 160±15 (1 day old;n=25) to 268±22ms in adults (n=25,p<0.05;see figure). Despite the shorter AP, outward I_{NaCa} was high at birth and fell significantly during the post-natal period (1 day: 0.4±0.06, adult : 0.04±0.01 pC/pF; n=15-20, p<0.05, see figure). Similarly, Ca^{2+} extrusion via inward I_{NaCa} also declined after birth (1 day: -0.3±0.02, adult: -0.08±0.02 pC/pF; n= 12-20, p<0.05,see figure).I_{NaCa} elicited contraction in 1-11 day old myocytes (1 day: 4.8±0.58% resting length), but was unable to evoke contraction in adults. We conclude that, despite a relatively short APD_{90}, I_{NaCa} is greater in the newborn, and declines postnatally, even though APD_{90} lengthens.

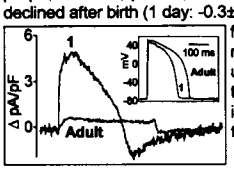

M-Pos239

EXPRESSION OF CALCIUM TRANSPORT PROTEINS DURING ISCHEMIA AND REPERFUSION IN RABBIT HEARTS IN VIVO.

((**Malcolm M. Bersohn** and Cecil R. Carmack)) Veterans Affairs Medical Center and University of California, Los Angeles, CA 90073

We investigated the effects of coronary occlusion and reperfusion in the open-chest rabbit on the expression of the sarcolemmal sodium-calcium exchanger (NCX1), the sarcoplasmic reticulum Ca-ATPase (SERCA2) and calcium release channel (CRC), along with heat-shock protein (HSP70). A large branch of the circumflex artery was occluded for 30 minutes, 60 minutes, or 60 minutes followed by 30 minutes reperfusion. Tissue from the ischemic zone was compared to control tissue from the same heart. We quantitated mRNA levels in Northern blots of total RNA, and all data were normalized for GAPDH mRNA levels in each extract. Results are expressed as the fraction of the control value for the same heart (Mean ± SE, n=6-7).

	30 min ischemia	60 min ischemia	60 isch. 30 reperfuse
NCX1	91 ± 12%	50 ± 11%	88 ± 12%
SERCA2		48 ± 10%	72 ± 13%
CRC		58 ± 14%	88 ± 11%
HSP70	112 ± 12%	170 ± 37%	809 ± 316%

One hour of ischemia causes a significant reduction in the expression of 3 major Ca transport proteins while HSP70 expression increases moderately. Thirty minutes of reperfusion leads to recovery of Ca transporter mRNA levels while HSP70 levels are greatly increased, suggesting a regulated transcriptional response to the stress of ischemia and reperfusion.

MEMBRANE STRUCTURES

M-Pos240

TRANSIENT CONFINEMENT OF GPI-ANCHORED PROTEINS BY GLYCOLIPID MEMBRANE DOMAINS.

((**E.D. Sheets** and K. Jacobson)) Departments of Chemistry and Cell Biology & Anatomy, University of North Carolina, Chapel Hill NC 27599.

Movements of membrane components can be followed with nanometer precision by using the microscopy-based technique of single particle tracking (SPT). The trajectories from 6.6 s observation periods are classified into four modes of transport—fast random diffusion, slow random diffusion, confined diffusion and a fraction of molecules that are stationary on this time scale. The latter three categories exhibit highly anomalous diffusion, whereas the rapidly diffusing class undergoes normal Brownian motion. We used SPT to assay the movements of Thy-1, a glycosylphosphatidylinositol (GPI) anchored protein, on the surfaces of C3H fibroblasts and found that 37% of Thy-1 undergo confined diffusion to regions ~315 nm in diameter. Longer observations showed that Thy-1 is confined for ~8 s durations and that no Thy-1 molecules remain completely stationary, suggesting that molecules can switch between modes of transport. Because results of recent biochemical analyses of detergent inextractable cell lysates suggested that GPI-anchored proteins are associated with glycosphingolipid (GSL) domains, we assayed the movements of GM1, a representative GSL. We find that GM1 behaves similarly to Thy-1; that is, 35% of GM1 undergo confined diffusion to ~400 nm diameter domains. However, only 16% of fluorescein phosphatidylethanolamine (which had been incorporated into the plasma membrane) experience confined diffusion, suggesting that phospholipids may be excluded from domains containing GPI-anchored proteins and GSLs. The effects of cholesterol- or glycosphingolipid-depletion on the movements of Thy-1 and GM1 were also assayed by SPT. These results intimate that the lipid milieu plays a dominant role in restricting the movements of GPI-anchored proteins. Supported by NIH grant 41402.

M-Pos241

HOW ADAPTATION TO DIFFERENT NITROGEN SOURCES CHANGES THE POLYPEPTIDE COMPOSITION OF THE *SYNECHOCOCCUS* PCC 7942 CYTOPLASMIC MEMBRANE.

((**M. Zinovieva**, C. Fresneau and B. Arrio)) University Paris-XI, LBM URA 1116 CNRS, Orsay 91405, FRANCE.

Changes in nitrogen sources have been shown to modify the cytoplasmic membrane protein composition. Several years ago, a NO_3^--dependent 47 kDa polypeptide was described in *Synechococcus* cytoplasmic membrane. By use of SDS-PAGE polypeptide analysis we found that another 126 kDa polypeptide existed in the cytoplasmic membrane of *Synechococcus* PCC 7942 cells grown in the presence of NO_3^-. The presence of NH_4^+ led to the disappearance of this protein. The amount of 126 kDa polypeptide was inversely related to the NO_3^- concentration. Transfer of NH_4^+-grown cells to a medium containing NO_3^-, as the sole nitrogen source, induced the appearance of both polypeptides. Up to 12 hours, increase in polypeptides was similar at $NaNO_3$ concentration of 2 mM and 175 mM, which are the extreme concentrations for these cells. Later, the 2 mM $NaNO_3$ concentration resulted in higher levels of the polypeptides. Similar effects were observed for 2 mM and 15 mM of $NaNO_2$. The modifications in protein composition were independent of Na^+. The change in the protein composition exerted an influence on the number of electrostatic charges at the membrane surface resulting in electrophoretic mobility variations, as measured by laser Doppler electrophoresis. The study of the cytoplasmic membrane electrophoretic mobility in the absence and in the presence of various salts showed the binding of NO_3^-. It was more pronounced in the membranes from the cells grown at low NO_3^-. The data obtained suggest that composition of surrounding medium may regulate the affinity of transport system(s) to nitrate.

M-Pos242

DOCOSAHEXAENOIC ACID (DHA)-INDUCED EXFOLIATED VESICLES ARISE FROM DISTINCT PLASMA MEMBRANE DOMAINS.

((**E. Eugene Williams**, William Stillwell and Laura J. Jenski)) Dept. of Biology, Indiana University-Purdue University at Indianapolis, Indianapolis IN 46202

Cell membranes are organized into poorly understood patchworks of lipid and protein known as membrane domains. We isolated and analyzed membrane vesicles shed from the surface of a murine leukemia cell line (T27A) in order to determine whether these structures represent random regions of the plasma membrane or instead are derived from distinct domains which could be used to assess domain structure and composition. From the fluorescence depolarization of diphenylhexatriene-derived membrane probes, we found the released vesicles (EVs) were significantly more ordered than the parent plasma membrane (PM), indicating distinct, and thus non-random, compositions. When cells were cultured in medium enriched with DHA, a membrane component known to induce domain formation in artificial membranes, the PM was unaffected while EV order was significantly reduced. EVs from DHA-cultured cells contained 5 times more DHA than the PM fraction and than EV and PM from untreated cells. Eighty percent of the shed DHA was found in the form of a single molecular species, *sn*-1 steroyl, *sn*-2 DHA-phosphatidylethanolamine (PE). EVs were also found to contain elevated levels of cholesterol. These combined results were unexpected since cholesterol interacts unfavorably with both DHA and PE. The incompatibility of the observed membrane components suggest there may be two or more separate populations of EVs. We conclude that EVs from this cell line represent membrane domains, and that T27A cells regulate membrane DHA content and structure by forming and then shedding these domains.

M-Pos243

DIFFUSION AND ITS RESTRICTION IN AXONS AND DENDRITES OF DEVELOPING HIPPOCAMPAL NEURONS

((**A. Pralle**, E.-L. Florin, C. Dotti and J.K.H. Hörber)) *Cell Biophysics, European Molecular Biology Laboratory, D-69117 Heidelberg, Germany*

Mature neurons exhibit highly specialized plasma membrane areas, including an axonal and a somatodendritic surface. So far it is not clearly understood how this polarisation is established and maintained. A current hypothesis is that site-directed insertion of membrane proteins establishes the membrane polarisation. To maintain the distinct membrane area the diffusion of the constituents must be restricted.

We investigate the variations of the diffusion of membrane components in different functional areas. Experiments are performed on cells throughout the various developmental stages of neuronal cells to study the changes of diffusion during the establishment of the polarisation. Using single-particle tracking methods we analyse the free diffusion of lipids in the axonal and somato-dendritic plasma membrane to determine the flow of membrane along the growing axon and to locallize areas of reduced or blocked diffusion. Additionally experiments with an optical trap are performed to investigate the nature of the obstacles to diffusion.